

RENEWABLE FEEDSTOCKS FOR THE PRODUCTION OF CHEMICALS

Joseph J. Bozell
National Renewable Energy Laboratory
1617 Cole Boulevard
Golden, CO 80401

Keywords: renewables to chemicals, biomass

INTRODUCTION

Many similarities exist between biomass and crude oil when compared as chemical feedstocks. Both begin as complex multicomponent mixtures. Both must be fractionated into more easily managed building blocks before conversion to products. Both require methodology for the transformation of these building blocks into useful derivatives. Biomass differs from crude oil in that it offers a *renewable* and *sustainable* source of carbon in the form of polymeric (cellulose, starch, lignin, hemicellulose, protein) and monomeric (carbohydrates, oils, amino acids, plant extractives) components. These materials could be used to supply both direct replacements for existing petrochemical raw materials and new building blocks for chemical production. Renewables could become much more important over the next 20 years should recent projections on oil production prove correct.¹

Renewable carbon is produced at a huge rate in the biosphere; about 77×10^9 tons is fixed annually, an amount that has led several projections to conclude that biomass could supply almost all domestic organic chemical needs.² Cellulose alone has an annual production of about 100×10^9 tons.³ Since 7-8% of crude oil consumption in the U. S. is used for chemicals production, incorporation of biomass as a raw material could also result in important global environmental benefits associated with a decrease in crude oil use.⁴ Moreover, the infrastructure for a biomass to chemicals industry is already starting to emerge. Currently, almost 30 billion lb/yr of chemical products are made from or contain some type of renewable component.⁵ However, the large majority of these products use renewables with little or no conversion of the structures originally found in nature. Selective and efficient separation and transformation technology for renewables significantly lags that for petrochemicals thus limiting the amount of discrete chemicals produced from biomass. Research at the National Renewable Energy Laboratory (NREL) is directed toward developing the tools necessary to make biomass as valuable a feedstock for chemicals production as crude oil.⁶

ADVANTAGES AND DISADVANTAGES OF BIOMASS AS A CHEMICAL FEEDSTOCK

The rationale for using biomass as a chemical feedstock is illustrated by several important advantages it exhibits when compared to petrochemicals.

- A huge array of diverse materials, frequently stereochemically and enantiomerically defined, is available from biomass giving the user many new structural features to exploit.
- Many products of the chemical industry are oxygenated. There are few general ways to add oxygen to crude oil derived hydrocarbons, and many of them require the use of toxic reagents in stoichiometric amounts resulting in severe waste disposal problems.⁷ Biomass is already highly oxygenated, and could be used to avoid problems with oxidation.
- Increased use of biomass would extend the lifetime of diminishing crude oil supplies.^{8,9}
- The use of biomass could be a way to mitigate the buildup of CO_2 in the atmosphere because the use of biomass as a feedstock results in no net increase in atmospheric CO_2 content.¹⁰
- A chemicals industry incorporating a significant percentage of renewable materials is secure because the feedstock supplies are domestic.
- Biomass is a more flexible feedstock than is crude oil. Crude oil is formed and its composition set by geological forces. With the advent of genetic engineering, the tailoring of certain plants to produce high levels of specific chemicals is possible.

However, several disadvantages have also been described.

- Existing economic circumstances are an important issue. A renewables based industry must be compared to the existing petrochemical industry because the products from both serve the same marketplace. The petrochemical industry

is huge and highly efficient in all stages of operation. Much of its capital investment is paid off. The mechanisms and operation of its processes are well understood and give single products of high purity. The biomass industry is still developing processes that possess these features.

- Many of the biomass sources being considered as chemical feedstocks have traditionally been used as sources of food. The justification for diverting part of this resource to chemical production has been questioned. Biomass also requires space to grow, and the environmental impact of large scale biomass plantations has been examined.^{11,12}
- Biomass is necessarily seasonal, leading to peaks and valleys in the supply of feedstock. The chemical producer using biomass needs a regular day to day supply, and must be assured that the material used at the beginning of the year will be the same quality as that used at the end of the year.
- The wide range of materials that comprise biomass could be a detriment if new processes need to be developed for each feedstock. The building blocks extracted from biomass are foreign to traditional chemical producers and must be demonstrated to function similarly to existing building blocks.

BIOMASS VS. PETROCHEMICAL REFINING

Conversion technology for biomass lags significantly behind that for petrochemicals leading to a divergence of the two industries and an understanding of the economic differences. The number of products from the petrochemical industry is much greater, and the variety of possible routes to a given product is more diverse than for biomass. To illustrate the effect of conversion technology differences, consider how biomass usually fits in the context of petrochemical refining (Figure 1).¹³

The top half of Figure 1 is an abbreviated schematic of the petrochemical industry. Refining proceeds from naturally occurring, but nonrenewable resources such as coal, oil, or natural gas, through the simplest building blocks that can be extracted, to primary chemicals, and finally, to the many products and intermediates made by the chemical industry. Conversion processes for the petrochemical refinery are nicely self-contained, and move smoothly in a "horizontal" sense (as Figure 1 is drawn) from raw materials to products.

A similar diagram can be prepared starting from renewable feedstocks (bottom half of Figure 1). The flow of materials is exactly analogous to a petrochemical refinery. The indigenous resources are lignocellulosics, grains, sugar crops, oil crops, etc., from which one again extracts smaller building blocks, and converts them into a slate of intermediates and products. However, the biomass refinery has fewer "horizontal" processes available to it for the selective conversion of biomass to chemicals. Typically, renewable raw materials proceed only a short distance horizontally (for example, from lignocellulosics to cellulose), and then move in a vertical manner to place a biomass derived building block into the petrochemical realm, i. e., components available from biomass are converted into hydrocarbons (e.g., glucose might be converted to benzene or similar). The remaining horizontal movement to end products is then carried out in the petrochemical refinery.

There is some sense to this approach. It is direct; one simply develops technology to convert renewables into building blocks already recognized by the chemical industry. The infrastructure is in place, and the technology is well developed to make these building blocks into products of importance.

This most common use of renewables (structural duplication of existing petrochemical products) is known as *direct substitution*. However, given the current supply and cost scenarios for crude oil, this use for biomass is almost always less economically favorable because of the additional chemical manipulations necessary to make biomass building blocks replicate existing petrochemical building blocks. The lack of a wide range of useful synthetic techniques unique for transforming renewables results in an uneconomical force fit of a new feedstock into an existing industry. An alternative approach known as *indirect substitution* results in a much greater "horizontal" movement through the biomass refinery. The key to this approach is a recognition that the best opportunities for use of biomass result from duplicating *properties* of existing petrochemicals rather than *structures*.

For several years, we have been studying the new synthetic methodology necessary to make indirect substitution practical and use the unique structural features and physical properties inherent in biomass derived feedstocks. We are investigating materials that can be obtained easily and in high yield from renewable feedstocks, how they are efficiently converted to new products, and determining how the properties of these new products resemble those of petrochemical derivatives.

SEPARATION: CLEAN FRACTIONATION OF LIGNOCELLULOSICS

The processes outlined in Figure 1 indicate that an efficient separation of renewable feedstocks into their individual components is necessary. To address this issue, we have developed a new refining process for wood, known as Clean Fractionation.¹⁴ This process is carried out by treating wood with a ternary mixture of methyl isobutyl ketone (MIBK), ethanol, and water, present in proportions to maintain a single phase at all temperatures of the separation process (Figure 2). The process selectively separates the wood components by dissolving the lignin and hemicellulose. The cellulose is obtained as a solid while the soluble component is further fractionated by adding H₂O, resulting in a phase separation. The lignin is found in the organic phase and can be isolated by solvent evaporation. The hemicellulose is obtained as a dilute aqueous solution.

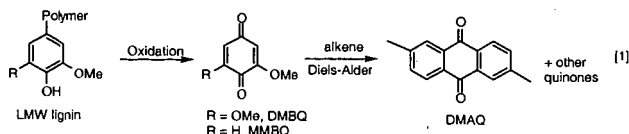
This process provides several benefits not realized by conventional wood separation technology. The single phase nature of the solution allows greater control over the lignin isolation step, and more complete lignin removal during the fractionation. At the completion of the run, the organic phase containing the lignin remains homogeneous even after phase separation. Since the solvent mixture remains as a single phase until additional water or MIBK is added, the lignin isolation step is more controlled and minimizes aggregation of lignin particles and redeposition on the cellulose.

This process offers a direct analogy to the petroleum refining process in that it efficiently converts wood into its individual constituents. Greater than 95-98% of the cellulose present in the starting feedstock is isolated after fractionation with little cross-contamination by other components. In addition, the process is self-contained, and much more environmentally friendly when compared to existing separation (kraft or sulfite) processes. Up to 99% of the solvents used for separation can be recovered and recycled resulting in reduction of downstream environmental processing of effluent. The cellulose is also more easily purified using environmentally benign processing (chlorine free bleaching) than cellulose from other wood fractionation processes.

We have investigated the use of each of these components for the production of chemicals. Some components are obtained from the Clean Fractionation process, while others are obtained from other sources. Results of these studies are described in the following sections.

LIGNIN CONVERSION: PREPARATION OF PULPING CATALYSTS

Antraquinone (AQ) is a well known additive in the pulp and paper industry. AQ improves the performance of alkaline pulping operations while protecting the cellulose product from degradation reactions that normally occur. However, AQ is not widely used by the pulp and paper industry because of cost. We developed a process for the synthesis of an AQ-containing catalyst mixture (equation 1).¹⁵



This process is an excellent example of indirect substitution. The process starts from lignin, and through a two step chemical process yields a mixture of quinones, including dimethylantraquinone. This new catalyst mixture has been demonstrated to promote pulping at least as effectively as AQ itself. In certain instances, we have observed the activity of the catalyst mixture to be 2 times as high as AQ. Pulp prepared with the catalyst exhibits properties equivalent to pulp produced using conventional methodology. The process could also address the economic issues of AQ. If certain yield and performance targets are met, this process would be one of the least expensive methods for catalyst production known.

However, a single technical issue still exists in the first step of the process, oxidation of the lignin. While the oxidation occurs, its yield is, as yet, too low to make the overall process economically viable. Success in the first step requires that the polymeric lignin starting material, which is a heterogeneous mixture of dozens of different substructural units, be converted efficiently into a *single* material using a *single* reagent. Solution of this problem would complete the list of requirements

necessary for positioning this process as a new, commercially viable approach to pulping catalysts.

CELLULOSE CONVERSION: LEVULINIC ACID AS A PLATFORM CHEMICAL

A huge amount of waste cellulose is produced annually in the U. S. as paper sludge in pulping operations or as waste paper delivered to landfills. Several years ago, a process was developed by Biofine Corporation to convert this cellulose into levulinic acid (LA, 4-oxopentanoic acid), a material that can be used as a "platform chemical." Platform chemicals are materials that currently may have only a small market, but could be expanded to a large market if other chemicals could be produced from the platform. For a platform to be successful, it must be made cheaply enough so that its derivatives are also inexpensive. LA from the Biofine process is projected to cost as little as \$0.04 - \$0.10/lb depending on the scale of the operation. We have investigated the use of this inexpensive LA for the production of two derivatives: methyltetrahydrofuran (MTHF), a fuel additive with a huge potential market, and delta-amino levulinic acid (DALA) a broad spectrum herbicide/pesticide with a projected market of 200 - 400 million pounds/year. Our results indicate that both derivatives can be produced efficiently from LA.

A new catalytic process for MTHF production developed under this project by workers at the Pacific Northwest National Laboratory gives a 49% mass yield (66% of theoretical) in a single step. Mass yields as high as 60% (81% theoretical) are obtained with improved reactor systems. In addition, a three step process for the conversion of LA to DALA that is a significant improvement over known approaches to DALA has been developed. Each DALA process step proceeds in high (>80%) yield and affords DALA (as the hydrochloride salt) in greater than 99% purity, giving a process that is a significant improvement over other reported DALA syntheses¹⁶ and could be commercially viable.

HEMICELLULOSE CONVERSION: ISOLATION OF XYLOSE AND ARABINOSE FROM CORN FIBER FOR POLYOLS PRODUCTION

Corn fiber is an exceedingly abundant (annual production of 10 billion pounds) and inexpensive renewable feedstock available as a byproduct of the corn wet milling industry. The most abundant component is hemicellulose, which makes up about 60% of the weight of the corn fiber.¹⁷ Xylose and arabinose make up about 60-70% of the weight of the hemicellulose¹⁸ and represent an enormous potential feedstock stream for the production of chemicals. The key to the use of corn fiber as a source of xylose and arabinose is the ability to cleanly separate those materials from the remaining components in the fiber. The literature reports several methods for corn fiber fractionation using both acidic and basic media.¹⁹ However, none give an effective selectivity for the desired C5 sugars.

We have developed a separation for corn fiber that gives a stream enriched with xylose and arabinose. While this fraction is probably not yet of sufficient purity for use in chemicals production, the process has significantly reduced the number of components in the original corn fiber. The process employed exhibits mass balances typically around 75 - 85%; select runs are as high as 90%. The process achieves an isolation of C5 sugars in 30-35% yield as a dilute aqueous solution; select runs have given sugar yields as high as 40%, corresponding to recovery of almost 90% of the C5 sugars present in corn fiber. We observe that some of the sugars are still present in an oligosaccharide form, and it is important to note that our yields assume that the oligosaccharide component is all C5 sugar. Evidence has been obtained to support this assumption. If the sugar solution is further hydrolyzed after isolation, the oligosaccharide component disappears while the xylose/arabinose concentration increases. More recent work has resulted in a significant improvement in the amount of monomeric C5 sugar isolated.

The first product targets intended for manufacture from these sugars have also been identified. New catalytic transformations being carried out in partnership with Michigan State University indicates that these sugars can be selectively transformed into C2 and C3 fragments (i. e., ethylene glycol and propylene glycol).

CONCLUSIONS

These transformations of lignin, cellulose, and hemicellulose demonstrate how renewables can be used as starting templates for chemical synthesis. In considering ways to increase the use of renewables for production of chemicals, new techniques in organic synthesis, environmentally friendly processing, and catalysis, will be of great importance. Combining the use of renewable materials as sources of chemical

feedstocks with new technology will lead to processes as efficient as those currently used for the conversion of petrochemicals.

ACKNOWLEDGEMENTS

This work was supported by the U. S. Department of Energy, Office of Industrial Technologies.

REFERENCES

1. Kerr, R. A., *Science*, 1998, 281, 1128.
2. (a) Goheen, D. W., *J. Chem. Ed.*, 1981, 58, 544; (b) Kovaly, K. A., *Chemtech*, 1982, 487; (c) Kleinhans, W., *Zuckerindustrie*, 1988, 113, 939; (d) Kennedy, J. F. and Melo, E. H. M., *Brit. Polym. J.*, 1990, 23, 193.
3. These numbers correspond to the production of 171×10^9 total tons of biomass, and assumes that biomass is 45% carbon; "Kirk-Othmer Encyclopedia of Chemical Technology", 4th ed., John Wiley, New York, Volume 12, p. 16 (1994); Goldstein, I. S., editor, "Organic Chemicals from Biomass", CRC Press, Boca Raton, FL, Chapter 1, (1981).
4. The energy used in manufacturing all chemicals is split about 50/50 between operating energy and contained feedstock energy, about 2.7 quads (2.7×10^{15} btu) each. Of that 2.7 quads, about 37% or 1.0 quads is used in the manufacture of organic chemicals. This corresponds to 0.48×10^6 bbl oil equivalent/day, a significant number. "U. S. Chemical Industry Statistical Handbook", Chemical Manufacturers Association, Washington, D. C., (1993).
5. Production and use information for renewables is available from several sources: Chemical Marketing Reporter; Chemical and Engineering News; U.S. Department of Commerce, "U.S. Industrial Outlook," Washington, D.C.; Chemical Week; Chemical Economics Handbook (SRI International); Situation and Outlook Reports published by Economic Research Service, USDA; Leeper, S., Ward, T. and Andrews, G., "Production of Organic Chemicals Via Bioconversion: A Review of the Potential, INEL Report (1991); Bozell, J. and Landucci, R., "Alternative Feedstocks Program Technical and Economic Assessment: Thermal/chemical and Bioprocessing Components" (1993); Webster, L.C., "Environmentally Benign Production of Commodity Chemicals Through Biotechnology: Recent Progress and Future Potential" (1994); Morris, D. and Ahmed, I., "The Carbohydrate Economy", Institute for Local Self-Reliance, Washington, D.C., (1992).
6. (a) Bozell, J. J., Hoberg, J. O., and Dimmel, D. R., *Tetrahedron Lett.*, 1998, 39, 2261; (b) Bozell, J. J., Hoberg, J. O., Claffey, D., Hames, B. R. and Dimmel, D. R. in "Green Chemistry: Frontiers in Benign Chemical Synthesis and Processing" Anastas, P. T.; Williamson, T., eds. Oxford University Press (1998); (c) Bozell, J. J., Hames, B. R. and Dimmel, D.R., *J. Org. Chem.*, 1995, 60, 2398; (d) Hoberg, J. O. and Bozell, J. J., *Tetrahedron Lett.*, 1995, 36, 6831; (e) Dimmel, D. R., Pan, X. and Bozell, J. J., *J. Wood Chem. Tech.*, 1996, 16, 205.
7. Haines, A. H., "Methods for the Oxidation of Organic Compounds", Academic Press, New York (1985, 1988).
8. The Royal Dutch/Shell group has developed several scenarios for the impact of biomass on chemicals and fuel production. One scenario projects a biomass market in the first half of the 21st century of \$150 billion/year, with up to 30% of worldwide chemical and fuel needs supplied by renewable feedstocks in the same time period. (a) "The Evolution of the World's Energy System", Group External Affairs, Shell International Limited, SIL Shell Centre, London, SE1 7NA; (b) Romm, J. J. and Curtis, C. R., *Atlantic Monthly*, 1996, 277, (4), 57.
9. The concept of "diminishing supplies" is subjective. During the oil crises of the 1970s, projections concluded that oil prices would be about \$100/barrel by the late 20th century. On the contrary, crude oil is probably at record low levels (about \$10 - \$12/barrel). A recent projection by the International Energy Authority predicts that the price of oil (in 1993 dollars) will rise only to \$28/barrel by 2050. See Hall, D. O., and House, J. I., *Sol. Energy Mater. Sol. Cells*, 1995, 38, 521.
10. This statement presumes that the CO₂ contained in standing trees, debris, and soil is not released and that consumed biomass is replaced by fresh plantings, i.e., the system must be sustainable. See Harmon, M. E., Ferrell, W. K., and Franklin, J. F., *Science*, 1990, 247, 699.
11. Cook, J. H., Beyea, J. and Keeler, K. H., *Annu. Rev. Energy Environ.*, 1991, 16, 401.
12. The issue becomes more acute when biomass is considered as a feedstock for fuel as well as chemical production. If biomass is considered fuel source, a huge amount of land might be needed. An estimated 130×10^6 hectares of land would be necessary to supply the United States with transportation fuel alone,¹¹ an area equal to that used for farming in 1988.
13. After Lipinsky, E. S., *Science*, 1981, 212, 1465.
14. Black, S., Hames, B. R. and Myers, M., U. S. Patent 5730837, to the Midwest Research Institute.

15. (a) Dimmel, D. R., Althen, E., Savidakis, M., Courchene, C. Bozell, J. J., *Tappi J.*, 1998, in press; (b) Bozell, J. J., Dimmel, D. R. and Power, A. J., *Ind. Uses Agricultural Mat., Situation and Outlook Report*, 1994, 27; (c) Dimmel, D. R. and Bozell, J. J., *Tappi J.*, 1991, (5), 239.
16. (a) Benedikt, E. and Köst, H.-P., *Z. Naturforsch., B: Anorg. Chem. Org. Chem.*, 1986, 41 B(12), 1593; (b) Wang, J. and Scott, A. I., *Tetrahedron Lett.*, 1997, 38, 739; (c) Cottier, L., Descotes, L., Eymard, L., Rapp, K., *Synthesis*, 1995, 303; (d) Matsumura, Y., Takeshima, Y., Okita, H., *Bull. Chem. Soc. Jpn.*, 1994, 67, 304; (e) Wynn, R. W. and Corwin, A. H., *J. Org. Chem.*, 1950, 15, 203.
17. Anderson, J. W. and Bridges, S. R., *Am. J. Clin. Nutr.*, 1988, 47, 440.
18. (a) Sugawara, M., Benno, Y., Koyasu, E., Takeuchi, M., and Mitsuoka, T. *Agric. Biol. Chem.*, 1991, 55, 565; (b) Leathers, T. D. and Gupta, S. C., *Appl. Biochem. Biotech.*, 1996, 59, 337; (c) Wolf, M. J., MacMasters, M. M., Cannon, J. A., Rosewall, E. C., and Rist, C. E., *Cereal Chem.*, 1953, 30, 451; (d) Hooper, F. E., *Ind. Eng. Chem.*, 1942, 34, 728; (e) Fly, A. D., Czarnecki-Maulden, G. L., Fahey, Jr., G. C., and Titgemeyer, E.C., *J. Nutr.*, 1996, 126, 308.
19. (a) Hojilla-Evangelista, M. P., Svendsen, L. K. and Johnson, L. A., "Proceedings of the Corn Utilization Conference VI", St. Louis, (1996); (b) Mistry, A. H. and Eckhoff, S. R., *Cereal Chem.*, 1992, 69, 202; (c) Mistry, A. H. and Eckhoff, S. R., *Cereal Chem.*, 1992, 69, 82; (d) Moniruzzaman, M., Dale, B. E., Hespell, R. B. and Bothast, R. J., *Appl. Biochem. Biotechnol.*, 1997, 67, 113; (e) Hespell, R. B., O'Bryan, P. J., Moniruzzaman, M. and Bothast, R. J., *Appl. Biochem. Biotechnol.*, 1997, 62, 87; (f) Doner, L. W. and Hicks, K. B., *Cereal Chem.*, 1997, 74, 176; (g) Grohmann, K. and Bothast, R. J., *Process Biochem. (Oxford)*, 1997, 32, 405; (h) Dien, B. S., Hespell, R. B., Ingram, L. O. and Bothast, R. J.; *World J. Microbiol. Biotechnol.*, 1997, 13, 619; (i) Asghari, A., Bothast, R. J., Doran, J. B. and Ingram, L. O., *J. Ind. Microbiol.*, 1996, 16, 42; (j) Ladisch, M. R., *Proc. Sugar Process. Res. Conf.*, 1986, 152; (k) Anderson, N. E. and Clydesdale, F. M., *J. Food Prot.*, 1980, 43, 760-762; (l) Heller, S. N., Rivers, J. M. and Hackler, L. R., *J. Food Sci.*, 1977, 42, 436-439; (m) Garleb, K. A., Fahey, Jr., G. C., Lewis, S. M., Kerley, M. S. and Montgomery, L., *J. Anim. Sci.*, 1988, 66, 2650-2652; (n) Robertson, J. B. and Van Soest, P. J. in "The Analysis of Dietary Fiber" (James, W. P. T. and Theander, O., eds.) pp. 123-158, Marcel Dekker, New York, 1981.

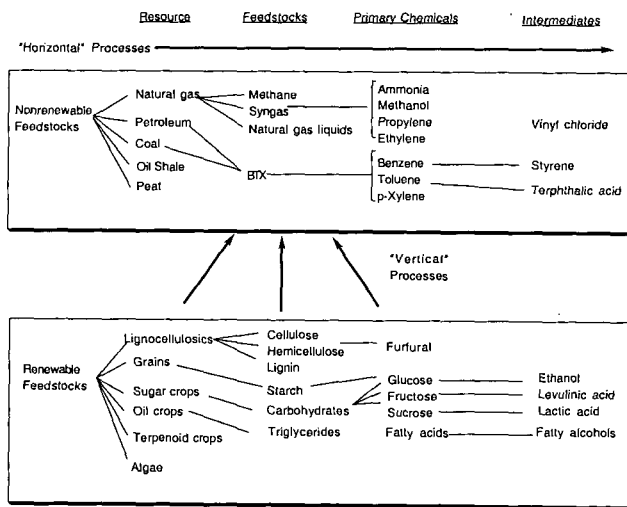


Figure 1 - Comparison of Petrochemical and Biomass Refining

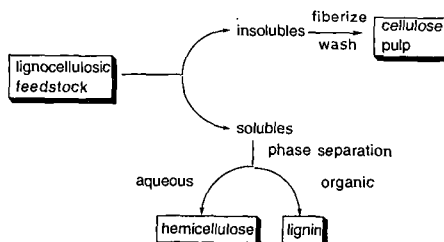


Figure 2 - Schematic of the Clean Fractionation Process

CHEMICALS FROM BIOMASS VIA THE CONVERTECH SYSTEM

Edward S. Lipinsky
Innovative Thinking, Inc.
Worthington, Ohio

Ian Bywater and Ken Scott
Convertech Group Limited
Christchurch, New Zealand

KEYWORDS: lignocellulose, steam processing, biomass

ABSTRACT

Biomass is suspended in steam which acts as a mobile carrier in the Convertech System. The lignocellulose complex is disrupted so that hemicellulose can be separated from Cellulig. Cellulig can be converted into panelboard materials. Cellulig™ also can be further separated into low-MW cellulose and partly depolymerized lignin. The hemicellulose can be converted into furfural or lactic acid, if the starting material is a hardwood or grass. The low-MW cellulose is suitable for conversion into cellulose acetate which has prospects as a degradable polymer. The ethanol-soluble lignin can be used as an extender for phenolic resins. Additional opportunities will be discussed.

INTRODUCTION

Steam is a highly desirable reactant to use in processing biomass. It is environmentally benign, cheap, has excellent thermal properties, and can be easily removed by condensation or as a gas phase. Therefore, steam processing has a long history. Important milestones in this history include the following events. Mason developed the Masonite process and hardboard products in 1926 [1]. DeLong modified the Masonite gun and the processing conditions to disrupt and fractionate lignocellulose in a batch process [2]. Marschessault elucidated the chemistry of this steam explosion process [3]. Brown and Bender invented the Stake Technology continuous steam explosion process [4]. These three events occurred between about 1975 and 1983.

In 1989, Scott conceived the Convertech System which is a continuous steam processing technology in which the biomass particles are suspended in steam. Rafferty's patent that was assigned to Convertech was the first public disclosure [5]. This paper focuses on the Convertech System which has not yet received much attention in this country.

DISCUSSION

Convertech System

The Convertech process uses steam hydrolysis to achieve a breakdown of the biomass into its chemical constituents (in particular, cellulose, lignin, volatiles, and sugars derived from hemicellulose). The main hydrolysis, chemical extraction and drying operations are carried out in a series of five continuously operated modules (Figure 1). Depending upon the nature of the lignocellulose, it is shredded or milled and fed into the plant as a stream of small particles.

The technology includes an interlock which is a rotating valve used to transfer in a continuous fashion the fine biomass material between the different pressure zones [6]. It is this device that makes possible the efficient cascading of heat and hydrolysis.

Steam is the sole medium used to transport the particles through each module, conduct the hydrolysis and chemical extraction operations, and carry out the drying. This contributes to making the process simple, robust, and clean while minimizing corrosion from strong acids.

The major technical differences between the Convertech System and steam explosion processes include focus on energy recycling and use of suspended solids. Convertech's current emphasis is on separation of hemicellulose from lignocellulose and production of a low-moisture product. Steam explosion processes usually separate lignin from lignocellulose.

Materials and Chemical Opportunities

Processing of lignocellulose can provide a spectrum of products that include fuels, food products, animal feeds, materials for particle board products, and chemicals. In the chemicals area, there are

many alternative opportunities. Figures 2 and 3 are provided to summarize just the chemical opportunities.

Commercialization remains a problem for the Converttech System and for other systems that are based on steam treatment. If there are so many opportunities, why is there a problem? We believe that the answer may be that the diversity of potential products is a blessing but also a curse. Commercialization depends on focus on relatively short term goals, not on the entire spectrum. Therefore the following discussion pertains only to a few opportunities that may be relatively easy to implement. Once established, many other latent opportunities will be realizable.

Furfural from Hemicellulose

Acid digestion of hemicellulose in hardwoods and grasses (e.g., corn stover and bagasse) results in furfural. The Converttech process extracts and depolymerizes hemicellulose early in its sequence of operations so that this solution can be converted into furfural.

Furfural is used mostly for production of furfuryl alcohol. Furfuryl alcohol is used to make foundry core resins and coatings that are highly resistant to chemicals and heat. Furfural is also a source of tetrahydrofuran which is a powerful solvent and a source of chemicals for making urethanes and nylon polymers. Furfural also has considerable prospects as a binder for wood products (see below).

Cellulig

After removal of hemicellulose from lignocellulose, the resulting solid is a mixture of low molecular weight (low MW) cellulose and low MW lignin. This fibrous mixture is dried in the final module of the Converttech System (Figure 1). Thus, Cellulig is ready to be converted into a high density fiberboard for use as a construction material. This strong material does not need synthetic binders to make an attractive product. Enhancement of Cellulig's natural binder with furfuryl alcohol polymers results in super-strong materials that are interpenetrating polymers. Such products are the logical outcome of the Converttech System and may well be the basis for its initial success.

Cellulose

Although initial success may come from Cellulig products, there are additional opportunities that emerge as soon as this mixture of cellulose and lignin becomes readily available. Separation of Cellulig into its two constituents is easily accomplished with such volatile solvents as ethanol, methanol, or acetone (Figure 2). One result is a low MW cellulose that is chemically quite reactive and relatively pure.

There are two attractive uses for this cellulose: production of cellulose acetate and production of glucose oligomers.

Cellulose Acetate

Cellulose reacts with acetic anhydride to produce new grades of cellulose acetate [7] that were expected to be less strong but more easily degradable than are conventional grades of cellulose acetate. Actually, cellulose acetate is surprisingly slow to degrade because the standard plasticizers for this material are also stabilizers that inhibit hydrolysis. Recent advances in additives that enhance the degradability of cellulose acetate render degradable cellulose acetate a more attractive product [8]. The degradability and low cost of a properly plasticized Converttech cellulose acetate could lead to large markets.

Glucose Oligomers

The Superconcentrated HCl Process [9] provides a water-soluble product that is a mixture of glucose and glucose oligomers with degrees of polymerization of about 2 to 6 glucose units. The process was developed as a source of glucose and ethanol. However, it deserves to be evaluated for its potential for other uses that have higher potential value. An example is production of alkyl glucosides by reaction with methanol, ethanol, or other alcohols. The HCl catalyst for glucoside production is contained in the initial oligomer product.

Hydrolysis of the glucose oligomers described above is an alternative to direct hydrolysis of starch or cellulose to manufacture glucose. Glucose is a key chemical intermediate, in addition to its uses in food products (Figure 3).

Lignin

Utilization of the cellulose content of Cellulig would intensify the search for lignin uses to consume this by-product. The lignin that results from Convertech processing is not similar to that which results from kraft pulping or sulfite pulping. It does resemble "steam explosion lignin". That is, it is soluble in ethanol or acetone and does not contain any sulfur. It is low in molecular weight and more reactive than conventional lignins.

If available at low price, Convertech lignin may be desirable to use as an extender-type ingredient in many compositions. For example, epoxy resins are frequently extended with coal tar products ("coal tar epoxies"). Convertech lignin may compete quite well in such a market. Reactive extenders can be used in some phenolic resins.

If cellulose markets become large, still larger lignin markets must be sought. The high energy value of lignin makes it attractive as a fuel for gas turbine power generation or diesel fuel.

CONCLUSIONS

The Convertech System has great potential for enabling the conversion of lignocellulose into materials and chemicals. Realization of this great potential for commodity chemicals production depends on site-specific situations and/or soaring fossil fuel prices and/or serious action on global warming issues.

Developers of this type of technology have special problems in commercializing their processes. They need to be prepared for huge demand at an unknown future time. However, they must devote their current efforts to programs that do not require that petroleum prices rise or carbon taxes to be enacted for success to occur. Therefore, at present, prospects appear better for manufacture of reconstituted wood products that could use Cellulig as the feedstock, with furfural as a chemical coproduct. Development of other chemicals and fuels via the Convertech System need to be driven by the relevant end-use sectors.

REFERENCES

1. Mason, W.H., U.S. Patent 1,578,609 (1926).
2. Delong, E.A., Can. Patent 1,096,374 (1980).
3. Marschessault, R.H., et.al., in Wood and Agricultural Residues; Soltes, E.J., Ed.; Academic Press: New York, 1983; p. 401-413.
4. Brown, D.B., U.S. Patent 4,186,658; Brown, D.B., and Bender, R., U.S. Patent 4,211,163 (1978).
5. Rafferty, A.J., U.S. Patent 5,454,911 (1995).
6. Scott, K.E., U.S. Patent 5,819,992 (1998).
7. Marchessault, R.H., in Steam Explosion Techniques; Focher, B., et.al., Eds.; Gordon and Breach: Philadelphia, 1991; p. 10.
8. Lipinsky, E.S., and Sinclair, R.G., W.O. 9,220,738 (1992).
9. Goldstein, I.S., and Easter, J.M., TAPPI 75, 135-140 (1992).

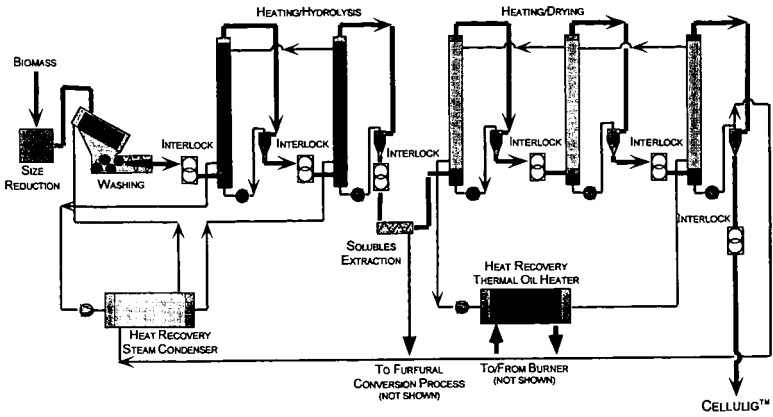


Figure 1. Converttech Flow Diagram

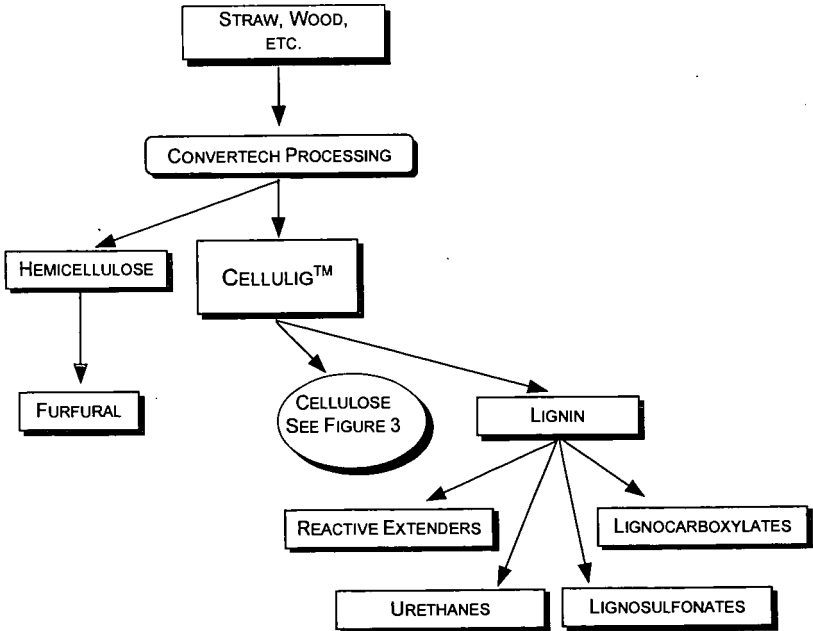


Figure 2. Lignocellulose Processing for Chemicals by Converttech Process

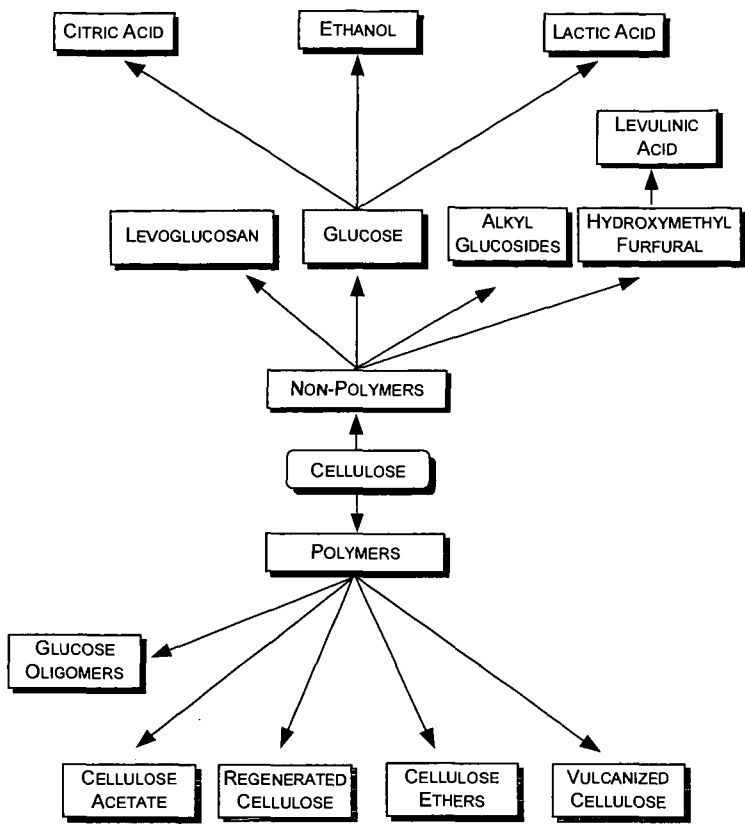


Figure 3. Chemicals from Converttech Cellulose

NOVEL IMMOBILIZED-BIOCATALYST BIOREACTORS FOR PRODUCTION OF FUELS AND CHEMICALS

Brian H. Davison, and Nhuan P. Nghiem
Oak Ridge National Laboratory, Oak Ridge TN 37831-6226

ABSTRACT

There are known biocatalytic pathways to produce many common fuels and petrochemicals. These biocatalysts can be either enzymes or living microorganisms. The challenge is to produce these fuels and chemicals efficiently and economically. Critical parameters include feedstock costs, yield, rate and downstream processing. Here we will examine several immobilized biocatalyst reactor designs that will increase overall rates. We will also discuss extractive bioreactors designed to decrease downstream separation cost by directly removing the dilute inhibitory products. Illustrative examples tested at ORNL will include ethanol production, extractive fermentation to butanol, and nonaqueous enzymatic bioconversions.

Keywords: Ethanol, bioreactors, non-aqueous biocatalysis.

INTRODUCTION

Bioconversion processes utilize a biocatalyst (microorganism, enzyme, or other active fraction) to enhance the conversion of a feed material or substrate to a useful product in a controlled environment. It is particularly desirable for such a system to have high volumetric productivity with maximum concentration and yield of the product. Continuous operation with good process control is also desirable. At least two subcomponents need to be considered: the production of the bioreagent and the bioconversion reactor itself.

Most bioconversion processes utilize a soluble substrate in an aqueous solution and produce a product that is also soluble in the aqueous phase. However, the substrate can be a solid, such as cellulose or starch or even gases, such as syngas or methane. Similarly, the products can be solids, liquids, or gases. The reaction medium can be an aqueous solution, a moist gas, or even an organic liquid in contact with the biocatalytic component. An efficient biocatalyst system must be available in a bioreactor configuration that optimizes interphase contact, mass transport, and conversion kinetics.

Characteristics of an advanced bioreactor should include, if possible, a high concentration of the biocatalyst, continuous operation, and excellent contact between the reacting components. Many bioreactor configurations have been proposed and are listed in Table 1. Ethanol production has been carried out in many of the bioreactors and the volumetric productivity for each is also shown. The literature values (1,2) indicate that cell retention can provide substantial increases in productivity. The conventional bioreactor system today is a large stirred tank operating in the batch mode usually with microorganisms or enzymes in aqueous suspension as the biocatalyst. Downtime between batches can decrease the overall productivity of these processes. However most of the productivity gains are from the high levels of biocatalyst possible in retained systems. Retaining and "reusing" the biocatalyst will also decrease the costs due to the enzyme or microbe itself and may be essential for an economic process.

There are a variety of methods to retain the biocatalyst within the system. Here we will divide the discussion of novel systems between aqueous based immobilized-cell systems and nontraditional nonaqueous biocatalytic system (3). Serious consideration is now being given to the use of biocatalytic systems in or in contact with nonaqueous media. These primarily include organic solvents and supercritical liquids (4). However, reactor concepts for these systems are only now being developed. A discussion of aqueous based cell retention systems tested at ORNL will be followed by nonaqueous systems using solvents or vapors.

Table 1. Ethanol production in various bioreactors.
[Productivities were at >95% conversion (1,2)]

Reactor	Productivity ($\text{g L}^{-1} \text{h}^{-1}$)
Batch	1.8-2.5
CSTR	6-8
Batch w/cell recycle	6-7
CSTRs in series	10
CSTR w/cell recycle	10-15
Hollow fiber	15-30
Immobilized-cell CSTR	10-20
Immobilized-cell packed column	10-50
Immobilized-cell fluidized-bed	20-100

AQUEOUS-PHASE RETAINED BIOCATALYSTS

One method to retain microbes in a continuous process is cell recycle using centrifugation or membrane. However, an alternative to a conventional CSTR with cell recycle is the use of retained biocatalysts by immobilization onto integral parts of the reactor or by immobilization into or onto solid particles that will be kept in the bioreactor even at high flow rates. Two primary approaches can be used: 1) adsorption or attachment of the biocatalyst to external or internal surfaces of the solid phase; or 2) encapsulation of the biocatalyst within the particulate matrix or media (5). This can result in a very high concentration of the biocatalyst that does not wash out of the bioreactor. Here the biocatalyst production step becomes a separate process for the production of large amounts of biomass or enzymes. Although the retained-cell concept can be used in stirred tanks, it is even more effective when used in columnar bioreactors.

Many commodity chemicals can be produced by fermentation. Research at ORNL has emphasized those systems that operate continuously with high volumetric productivity, which are most promising. Columnar bioreactors with retained biocatalysts have been particularly attractive, and three of these reactors are now described and compared with other systems.

ETHANOL PRODUCTION IN A FLUIDIZED-BED BIOREACTOR

In prior efforts at ORNL, immobilized *Zymomonas mobilis* was used in FBRs for high productivity and conversion production of ethanol (6). The bacteria were immobilized within small uniform gel beads (~1-mm diam.) at cell loadings of up to 50 g dry wt/L. Conversion and productivity were measured under a variety of conditions, feedstocks, flow rates, and column sizes (up to 8 ft tall). Volumetric productivities of 50 to 100 g ethanol L⁻¹ h⁻¹ have been achieved with residual glucose concentrations of <0.1%. The biocatalyst beads have been shown to remain active for over 2 months. This technology has several advantages over conventional batch technology. Immobilization increases volumetric productivity by increasing cell density. The use of beads of near 1-mm diam. minimizes the effect of mass transfer resistances. Fluidization allows for good interphase mass transfer and the release of large volumes of coproduct CO₂. The columnar operation allows multistage operation and localizes the high inhibitory product concentrations to the top of the reactor. This would allow a much smaller reactor with smaller capital costs to be used for the same alcohol output. Another advantage of this FBR was the operation without asepsis. A major advantage was the improved ethanol yield per gram dextrose of 0.49 g/g or >97% of the theoretical stoichiometric limit of *Z. mobilis* compared to a yield of 0.45 to 0.47 g/g for yeast. Under current economic conditions, the raw materials (i.e., dextrose from corn or other sources) are the largest single part of the cost; therefore, even a small but consistent increase in the yield can result in appreciable savings over the expected FBR operating lifetime of months.

Recently this concept was extended to a combined process with two concurrent reactions. The production of ethanol from industrial dry-milled cornstarch was studied in a laboratory-scale fluidized-bed bioreactor using immobilized biocatalysts. (7) Saccharification and fermentation were carried out either simultaneously or separately (see Figure 1). Simultaneous saccharification and fermentation (SSF) experiments were performed using small, uniform κ-carrageenan beads (1.5 to 2.5 mm in diameter) of co-immobilized glucoamylase and *Z. mobilis*. Dextrin feeds obtained by the hydrolysis of 15% dry-milled cornstarch were pumped through the bioreactor at residence times of 1.5 to 4 h. Single-pass conversion of dextrins ranged from 54 to 89%, and ethanol concentrations of 23 to 36 g/L were obtained at volumetric productivities of 9 to 15 g L⁻¹ h⁻¹. Very low levels of glucose were observed in the reactor, indicating that saccharification was the rate-limiting step. In separate hydrolysis and fermentation (SHF) experiments, dextrin feed solutions of 150 to 160 g/L were first pumped through an immobilized-glucoamylase packed column. At 55°C and a residence time of 1 h, greater than 95% conversion was obtained, giving product streams of 162 to 172 g glucose/L. These streams were then pumped through the fluidized-bed bioreactor containing immobilized *Z. mobilis*. At a residence time of 2 h, 94% conversion and ethanol concentration of 70 g/L were achieved, resulting in an overall process productivity of 23 g L⁻¹ h⁻¹. At residence times of 1.5 and 1 h, conversions of 75 and 76%, ethanol concentrations of 49 and 47 g/L, and overall process productivities of 19 and 25 g L⁻¹ h⁻¹, respectively, were achieved.

EXTRACTIVE FERMENTATIONS WITH IMMOBILIZED CELLS

Many commercial organic acids and solvents, such as acetic, citric, lactic, and succinic acids, can be produced by fermentation (8). All are produced in relatively dilute form due to their high level of inhibition of the microorganism. This inhibition is due to both the chemical itself and the lowered pH from acid production. Improvements in rate have been observed using various means of cell retention including cell recycle, membranes, and immobilization. (9, 10) Several processes have been proposed to remove the inhibitory product from the ongoing fermentation. (11) The key advantages suggested for extractive bioconversion are higher feed concentrations leading to less process wastes and reduced product recovery costs compared to those of distillation. Possibilities for in situ product removal include pervaporation, the use of

hollow-fiber reactors, and the use of solid adsorbents as well as the use of an immiscible extractive solvent. Key issues are the extractant toxicity and capacity as well as the actual contacting scheme devised and its operability. Adsorption has been proposed in various forms to remove the acids from the broth. This has included direct addition into the batch STR (with problems of attrition and power); passing a broth recycle stream through a side adsorbent bed; and a direct addition and removal of the adsorbent to a fluidized bed of immobilized biocatalysts.(12)

This biparticle FBR has been tested for simultaneous fermentation and separation of lactic acid. (13) The bioreactor is a fluidized bed of immobilized *Lactobacillus delbreuckii*. Another solid phase of denser sorbent particles (a polyvinyl pyridine resin) was added to this fluidized bed. These sorbent particles fell through the bed, absorbed the product, and were removed. In test fermentations, the addition of the sorbent enhanced the fermentation and moderated the fall of the pH. The biparticle FBR utilizing immobilized microorganisms and adsorbent particles has been shown to enhance the productivity of lactic acid to $7 \text{ g L}^{-1} \text{ h}^{-1}$ – a sixteenfold increase over a control batch fermentation in this nonoptimized system. Regeneration of the sorbent allowed significant concentration of the product.

Most studies of extractive acetone-butanol fermentation have been performed in a batch reactor (14) with free cells. An immobilized-cell FBR with a cocurrent immiscible liquid extractant(15) demonstrated a significant 50 to 90% increase in butanol production rate and yield in a nonoptimized extractive FBR system compared to the nonextractive FBR. The extractant oleyl alcohol removed most of the butanol from the aqueous phase during an active fermentation in a fluidized bed with immobilized *C. acetobutylicum* for the acetone-butanol fermentation. Under continuous, steady-state operation, the butanol yield increased to 0.3 g/g with a productivity of $1.8 \text{ g L}^{-1} \text{ h}^{-1}$ when butanol was removed in this manner.

NONAQUEOUS BIOCATALYSIS

Enzymatic reactions in a nonaqueous phase offer a number of advantages over traditional aqueous based processes, including elimination of undesirable side reactions, more favorable thermodynamic equilibria and simplified product recovery. Most nonaqueous biocatalysis has been performed with placing the enzyme in an organic solvent. The enzyme may be insoluble in the solvent. Many proteins precipitate and are inactivated by solvents and so may require modification to increase their solubility and activity. Hydrophobic groups such as polyethylene glycol can be chemically added to the protein to increase its solubility while retaining catalytic activity (16).

Surprisingly, "dry" enzymes can also retain catalytic activity directly to vapors. In this case the enzyme or biocatalyst is a "solid" catalyst on which the enzyme binds and reacts. Bench scale reactors were operated in continuous recycle and single pass modes using immobilized porcine lipase to catalyze gas-phase esterification of ethyl alcohol with two carboxylic acids (acetic acid and propionic acid). (17) Order of magnitude rate increases (over uncatalyzed reactions) in conversion were achieved. Product concentrations ranged from 0.1 to 0.5 mM in air and were strongly affected by substrate concentration and acid induced enzyme inactivation. We have continued these efforts with tranesterification reactions.

CONCLUSIONS

Immobilized-biocatalysts have been demonstrated to be a valuable class of advanced bioreactors for aqueous fermentations. They provide continuous operation, high biocatalyst concentrations, and good interphase mass transfer; thus resulting in higher productivity and often improved product yields. The improved yields may be due to the cell retention by immobilization, which allows less substrate to go to the production of more biocatalyst and thus more can go to product. This has been shown in four configurations here, two including in situ product removal. Nonaqueous systems may offer certain advantages and efforts to develop immobilized biocatalyst systems are just beginning. Further effort is still needed to scale-up and commercialize these attractive designs.

REFERENCES

1. Godia, F., Casas, C., and Sola, C. *Process Biochem.* **22**, 43-48 (1987)
2. Maiorella, B. L., p. 861-914 in: Moo-Young, M., (ed.), **Comprehensive Biotechnology**, vol. 3. Pergamon, New York (1986).
3. Davison, B. H., J. W. Barton, and G. Petersen, *Biotechnol. Prog.* **13**:512-518 (1997).
4. Laane, C., Tramper, J., and Lilly, M.D., eds., **Biocatalysis in Organic Media**, (1987).
5. Scott, C. D., *Enzyme Microb. Technol.* **9**, 66-73 (1987).
6. Davison, B.H. and C. D. Scott, *Appl. Biochem. Biotechnol. Symp.*, **18**, 19-34 (1988).
7. Krishnan, M.S., N.P. Nghiem and B.H. Davison, *Appl. Biochem. Biotechnol.* (in press, 1999).
8. Wise, D.L., ed., **Organic Chemicals From Biomass**, Benjamin/Cummings Publ. (1983).

9. Vickroy, T. B., p. 761-776 in: Moo-Young, M., (ed.), **Comprehensive Biotechnology**, vol. 3. Pergamon, New York. (1985).
10. Ghose, T. K., and A. Bhadra, p. 701-727 in: Moo-Young, M., (ed.), **Comprehensive Biotechnology**, vol. 3. Pergamon, New York (1985).
11. **Extractive Bioconversions**, B. Mattiasson and O. Holst, eds., Marcel Dekker, Inc., New York. (1991).
12. Davison, B. H., and J. E. Thompson, *Appl. Biochem. Biotechnol.* **34/35**, 431-439 (1992).
13. Kaufman, E. N., S. p. Cooper, M. K. Budner, and G. R. Richardson, *Appl. Biochem. Biotechnol.* **57/58**, 503-515 (1996).
14. Ishii, S., Masahito, T., and Kobayashi, T., *J. Chem. Eng. Japan* **18**, 125-130 (1985).
15. Davison, B. H., and Thompson, J. E., *Appl. Biochem. Biotechnol.* **39/40**, 415-26 (1993).
16. Woodward, C. A., and E. N. Kaufman, *Biotechnol. Bioeng.* **52**, 423-428 (1996).
17. Barton, J. W., E. K. Reed, and B. H. Davison, *Biotechnol. Techniq.* **11**, 747-750 (1997).

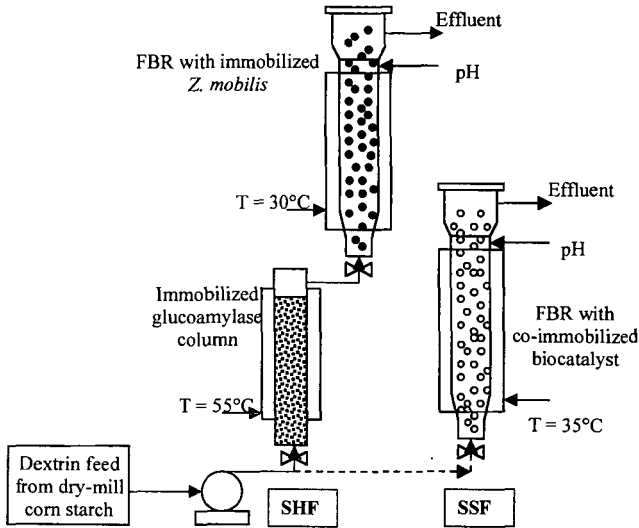


Figure 1. Process schemes for direct fermentation of starch into ethanol via immobilized cells. SHF is separate hydrolysis and fermentation, SSF is simultaneous fermentation and separation.

COMPARISON OF STEAM AND HOT LIQUID WATER PRETREATMENTS FOR THE BIOCONVERSION OF LIGNOCELLULOSICS TO ETHANOL

Deborah E. Schulman, Stephen Allen, Joe Lichwa, and Michael J. Antal Jr.

Hawaii Natural Energy Institute, University of Hawaii at Manoa, Honolulu, HI 96822

Mark Laser and Lee Lynd, Thayer School of Engineering, Dartmouth College, 8000 Cummings Hall, Hanover, NH 03755

INTRODUCTION

In order for lignocellulosic substrates to be made biologically available to microorganisms, which convert them to ethanol, these materials must first be pretreated. Since pretreatment is one of the most costly steps in ethanol production, accounting for 33% of total processing cost according to a base case design by the National Renewable Energy Laboratory (NREL - Lynd, et. al., 1996), it has been widely investigated. The bulk of pretreatment research has focused on acid and steam pretreatment of the lignocellulose. However, these methods may pose difficulties associated with material recovery, inhibitor formation, and waste disposal.

Successful pretreatment methods are known to disrupt cells and open the lignocellulose matrix (Kallavus and Gravitis, 1995), increasing pore volume (Gretlein and Converse, 1991; Thompson et. al. 1992) and available surface area (Thompson et. al. 1992). There is also a correlation between hemicellulose solubility and pretreatment effectiveness. Lignin is chemically modified during pretreatment. It has a melting temperature lower than typical pretreatment temperatures and does not return to its initial state (Torget et. al., 1991; Ooshima, et. al., 1990). High hydrogen ion concentrations accelerate sugar degradation (Leesomboon, 1988 & Antal et. al., 1991) and maintaining neutral pHs has been shown to improve pentosan recoveries (Weil et. al. 1998).

Water seems to be an important contributor to the pretreatment process. Due to the increased disproportionation of water at high temperatures, water lowers the pH of the reaction environment. The ion product concentration of liquid water at 220 °C is 10^{-11} and results in a pH of 5.6 compared to 7.0 the pH of water at 25°C (Marshall & Franck, 1981). Hydrolytic reactions cleave glycosidic linkages in hemicellulose and lignin. There is also evidence for the elementary bimolecular cleavage of the ether bond by water at 225°C (Xu et. al. 1997). Additionally, water lowers the softening point of lignin (Goring, 1963). Hemicellulose is deacetylated by water (Bouchard, et. al., 1991) and both lignin and hemicellulose are depolymerised by water (Bobbleter and Concini, 1979 and Chua and Wayman, 1979).

The use of water at elevated temperature and pressure to fractionate biomass into its constituents was first employed in the 1930s (Aronovsky and Gortner, 1930). Recently, however, it has received renewed recognition as a possible pretreatment for ethanol production (Bobbleter and Concini, 1979, van Walsum et. al. 1996, & Weil et. al. 1998). Mok and Antal (1992) were able to completely remove hemicellulose from hardwoods and herbaceous material, without significant degradation. More recently, pretreatment with hot liquid water at 220°C and up to 2 minutes has been shown to be extremely effective for both fractionation and bioconversion (Allen et. al. 1996 and Van Walsum et. al. 1996).

A complete mechanistic understanding as to why pretreatment is effective at rendering lignocellulose amenable to enzymatic attack has remained illusive. Due to this uncertainty empirical evidence is used for process optimization. Pretreatment effectiveness and cost can be rated based upon several metrics. These include reactivity, pentosan recovery, inhibitor formation, solubilization, feed particle size reduction, materials of equipment construction, and residues. However, care must be taken to identify factors that might increase costs down the line.

In this paper we focus on the effectiveness of pretreatment methods as measured by their solubilization, pentosan recoveries, inhibitor formation, and solids concentration. Solubilization is a measure of fractionation of recalcitrant crystalline cellulose from the less ordered hemicellulose and lignin, which more readily enters the liquid fraction. Greater solubilization results in more accessible pore areas in the lignocellulosic residue (LCR) for bioconversion (Weil et. al., 1994), and separates out the hemicellulose and lignin. Under pretreatment conditions, which typically produce reactive cellulose, xylose is easily degraded. Thus, it is not surprising that many pretreatment methods degrade xylose. For example, xylose recoveries with steam pretreatment are at best 65% (Heitz et. al. 1991). Technology has recently become available which allows for bioconversion of pentosan sugars to ethanol. In order for enzymatic bioconversion of biomass to ethanol to be economically competitive with acid processes and gasoline, it is necessary to get the most from the feed and thus xylose recovery is an extremely important factor along with a minimization of hydrolyzate inhibition products. Therefore, an understanding of inhibitor formation and an optimization of conditions designed to reduce their formation are necessary. Furfural, a breakdown product of xylose, is a known inhibitor of cellulase enzymes. It can be used as a measure of inhibitor formation. Many of the products formed by xylose degradation are cellulose inhibitors. Therefore furfural is a good gauge of the amount of inhibitors. Solids concentration is important because dilute process streams are undesirable, increasing process costs.

The results of steam pretreatment (SP) and hot water pretreatment (HLWP) liquid are presented in this paper of sugarcane bagasse. These pretreatment techniques were compared on the basis of metrics including pentosan recovery, hydrolyzate inhibitor formation, and solubilization. Emphasis was placed on understanding the inherent chemical differences between the techniques.

MATERIALS AND METHODS

Sugarcane bagasse was used as a representative feedstock in order to compare SP and HLWP techniques. A custom-built aqueous fractionation device was employed which could pretreat up to 1 kg of biomass (50 % moisture) as a batch using hot liquid water, steam or both. Details of the reactor appear in Allen et. al. (1998). Pretreatment by HLW was preceded by a 20-50s steam preheat of the material in order that latent heat could be used to arrive at the desired temperatures and high transient temperatures could be avoided. Timing began after addition of the water was completed for HLWP and after the desired temperature was attained for SP. After the reaction the LCR was rinsed with cold water and this fluid, the flush, was collected. Feed material was pretreated with both techniques for 2-5 minutes at 220 °C.

The analytical procedures used to characterize the feed material, lignocellulosic residues and liquid products are also described in Allen et. al. 1998 and are based on NREL's Ethanol Project LAP 002 & 014 (Ruiz and Ehrman, 1996). The amount of solubilized material present in the extract was determined by evaporating duplicate aliquots (20 to 25 g each) to dryness (1 d @ 105 °C).

RESULTS AND DISCUSSION

Results of experiments, comparing aqueous fractionation of sugarcane bagasse with steam and HLW appear in Table I. All experiments were performed at 220°C with 2 and 5-minute reaction times.

Approximately 35% solubilization was achieved for a 2-minute reaction time with both pretreatment modes. These values are not as high as those obtained by Allen et al. (1996) for HLW (50%), but higher than the 30% solubilization achieved with steam pretreatment by Jollez et al. (1994). For a reaction time of 5 minutes, solubilization increased for HLWP (44%), but decreased for SP. The decrease in solubilization with time associated with SP can be attributed to the formation of insoluble breakdown products (tars and resins) from solubilized xylose. This hypothesis is supported by the observation of a dark, tar-like sticky coating, which was soluble in acetone, and coated the lignocellulosic residue (LCR) for the 5-minute steam experiment. In the chemistry of xylose breakdown, under the conditions being employed, there are many higher order reactions, which are not well understood, but which result in resin formation (Leesomboon, 1988).

Significantly higher solids concentration were achieved with SP as compared to pretreatment with HLW. These experiments did not focus on achieving high solids concentration and with optimization, higher solids concentrations could be achieved for HLW, however, due to the nature of the techniques, these values will never approach those achievable with SP. It is therefore unclear whether, in analyzing these experiments we are looking at SP versus HLW or high solids versus low solids aqueous pretreatment. A low solids concentration can result in increased costs associated with both the energy requirements to heat the greater amount of required water and to process a dilute extract.

From the xylose recovery data, it is apparent that xylose degradation is occurring. In all cases, xylose recovery decreases with increasing time (figure 1). This is understandable, since an increase in time gives more time for the formation of products, which turn around and attack the parent via higher order reactions. For both reaction times, SP results in lower xylose recoveries and more inhibition product formation (table 2). Furfural concentration increases with decreasing pentosan recovery and increasing time (figure2). Its yield from xylose breakdown is approximately 20-30 mol % at 250 °C (Antal et. al., 1991). Therefore, it is not expected to account for all lost xylose, but does indicate degradation and inhibitor formation.

With HLWP, the LCR is immersed in water. Therefore, when the hemicellulose is solubilized it will dissolve in the extract liquid. Since water has a lower boiling point than dissolved products of hemicellulose, the vapor above the mixture should be mostly water and, as observed, most of the solubilized hemicellulose was recovered in the extract. In SP, in order for this material to be collected as extract, it must either enter the vapor phase and condense or dissolve in the steam condensate, which condenses on the LCR and reactor walls and drips down. This is the reason that after SP experiments, the flush contains most of the dissolved hemicellulose products. This statement does not hold true for furfural and acetic acid since they have low vaporization temperatures, 162°C and 118°C respectively, and can easily enter the vapor phase and recondense to form extract.

SP solubilized material is more likely to enter the vapor phase than in HLWP because it is extremely concentrated in the liquid phase. This can lead to decreased recoveries associated with recondensation and vapor losses. If steam, containing dissolved xylose oligomers and its breakdown products, is released from the reactor, these compounds may be lost with the steam.

As furfural enriched steam cools, the possibility of loss of vapor phase products due to recondensation on the reactor and tank walls is increased.

Another reason for the xylose losses associated with steam pretreatment is losses associated with the formation of breakdown products. With SP, pentosan recovery, hydrolyzate inhibition and solubilization are interdependent. As xylose is broken down, inhibition products are formed. This leads to decreases in xylose recoveries and solubilization, since as the products are formed soluble xylose is converted into insoluble resins, which are difficult to analyze and detect. The material balances reinforce this concept, since they indicate limited xylose loss. As mentioned earlier, resins were visible on the LCR and if the yield of furfural from xylose is 20-30 mol %, degradation is significant in SP.

In aqueous chemistry, the water acts as a buffer. All products, which dissolve in the water, are diluted. This will affect the pH of the reaction, since acetic acid is present due to deacetylation of hemicellulose and lactic and formic acids are present, as a result of xylose degradation. In steam pretreatment, where there is a very small amount of condensed liquid on the surface of reacting material, acids will be concentrated in this liquid phase, resulting in a high $[H^+]$ concentration. This concentration influences xylose breakdown, since acid catalyzes the xylose breakdown reaction. Leesomboon (1988) found that reaction rate, for a given time and temperature, depends solely on $[H^+]$ concentration.

CONCLUSIONS

Results indicate that HLWP performed better than SP on the basis of sugar recovery, hydrolyzate inhibitor formation and solubilization. Explanations, accounting for these differences are related to the different thermochemical conditions, which the feed material encounters. These conditions can lead to vapor losses, losses associated with recondensation, and carbohydrate breakdown. Additionally, shorter reaction times resulted in less xylose degradation and furfural formation. SP performed better on the basis of solids concentration.

ACKNOWLEDGEMENTS

This work is supported by the Consortium for Plant Biotechnology and Research (grant # OR-22072-65) and the National Renewable Energy Laboratory (grant # XXE-8-17099-01). The authors would like to thank Dr. Charles Wyman and BCI for their interest and support.

REFERENCES

- Allen, S.G.; Kam L.C.; Zemann A.J.; Antal M.J. Fractionation of Sugar Cane with Hot, Compressed Liquid Water. *Ind. Eng. Chem. Res.*, **1996**, *35*, 2709.
- Allen, S.G.; Lichwa, J.; Antal, M.J. Renewable Resources Research Laboratory Analytical Procedure. Hawaii Natural Energy Institute, **1998**.
- Antal, M.J.; Leesomboon, T.; Mok, W.S.; Richards G.N. Mechanisms of Formation of 2-furfuraldehyde from D-xylose. *Carbohydrate Research*, **1991**, *217*, 71.
- Aronovsky, S.I.; Gortner, R.A. The Cooking Process. I. The Role of Water in the Cooking of Wood. *Ind. Eng. Chem.* **1930**, *22*, 264.
- Bobleter, O.; Concini, R. Degradation of Poplar Lignin by Hydrothermal Treatment. *Cell. Chem Technol.* **1979**, *13*, 583.
- Bouchard, J.; Nguyen, T.S.; Chornet, E.; Overend, R.P. Analytical Methodology for Biomass Pretreatment. Part 2: Characterization of the Filtrates and Cumulative Distribution as a Function of Treatment Severity. *Biores. Technol.* **1991**, *36*, 121.
- Chua, M.G.S.; Wayman, M. Characterization of Autohydrolysis Aspen (*P. Tremuloides*) Lignins. 1. Composition and Molecular Weight Distribution of Extracted Autohydrolysis Lignin. *Can. J. Chem.* **1979**, *57*, 2603.
- Goring, D.A.I. Thermal Softening of Lignin, Hemicellulose, and Cellulose. *Pulp Pap. Mag. Can.* **1963**, *64*, T517.
- Grethlein, H.E.; Converse A.O. Common Aspects of Acid Prehydrolysis and Steam Explosion for Pretreating Wood. *Bioresource Technology*, **1991**, *36*, 77.
- Heitz, M.; Capek-Menard, E.; Koerberle, P.G.; Gange, J.; Chornet, E.; Overend, R.P.; Taylor, J.D.; Yu, E. Fractionation of *Populus tremuloides* at the Pilot Plant Scale: Optimization of Steam Pretreatment Conditions using the STAKE II Technology. *Biores. Technol.* **1991**, *35*, 23.
- Kallavus, U.; Gravitis, J. A Comparative Investigation of the Ultrastructure of Steam Exploded Wood with Light, Scanning, and Electron Microscopy. *Holzforschung*, **1995**, *49*, 182.
- Leesomboon, T. A Study of Catalytic Reaction Chemistry of Five and Six Carbon Sugars in Near Critical Water. **1988**, Masters Thesis, University of Hawaii at Manoa.
- Lynd, L.; Elander, R.T.; Wyman, C.E. Likely Features and Costs of Mature Biomass Ethanol Technology. *Appl. Biochem. Biotechnol.* **1996**, *57/58*, 741.
- Marshall, W.L.; Franck E.U. Ion Product of water Substance, 0 - 1000 °C, 1-10,000 Bars - New International Formulation and Its Background. *J. Phys. Chem. Ref. Data*, **1981**, *10*, 295.
- Mok, W. S-L.; Antal, M.J. Jr. Uncatalyzed Solvolysis of Whole Biomass Hemicellulose by Hot Compressed Liquid Water. *Ind. Eng. Chem. Res.* **1992**, *31*, 1157.

- Ooshima, H.; Burns, D.S.; Converse, A.O. Adsorption of Cellulase from *Trichoderma reesi* on Cellulose and Lignocellulosic Residue in Wood Pretreatment by Dilute Sulfuric Acid with Explosive Decompression. *Biotechnol. Bioeng.*, **1990**, *36*, 446.
- Jollez, P.; Chomet, E.; Overend, R.P. Steam-Aqueous Fractionation of Sugar Cane Bagasse: An Optimization study of Process Conditions at the Pilot Plant Level. In *Advances in Thermochemical Biomass Conversion*; Bridgwater, A.V., Ed.; Chapman & Hall Publishers: 1994; Vol. 2, pp 1659-1669.
- Ruiz, R.; Ehrman, T. NREL Ethanol Project: Chemical Analysis and Testing, Laboratory Analytical Procedure; Determination of Carbohydrates in Biomass by HPLC and Dilute Acid Hydrolysis Procedure of Total Sugars in the Liquid Fraction of Process Samples, **1996**, LAP-002 and LAP-014.
- Thompson, D.N.; Chen H.C.; Grethlein, H.E. Comparison of Pretreatment Methods on the Basis of Available Surface Area. *Biores. Technol.*, **1992**, *39*, 155.
- Target, R.; Walter, P.; Himmel, M.; Grohmann, K. Dilute Sulfuric Acid Pretreatment of Corn Residues and Short Rotation Woody Crops. *Appl. Biochem. Biotechnol.*, **1991**, *28/29*, 75.
- van Walsum, G.P.; Allen, S.G.; Spencer, M.J.; Laser, M.S.; Antal, M.J. Jr.; Lynd, L.R. Conversion of Lignocellulosics Pretreated with Liquid Hot Water to Ethanol. *Appl. Biochem. Biotech.* **1996**, *57/58*, 157.
- Weil, J.; Westgate, P.; Kohlmann, K.; Ladisch, M.R. Cellulose Pretreatments of Lignocellulosic Substrates. *Enzyme Microbiology and Technol.* **1994**, *16*, 1002.
- Weil, J.R.; Sarikaya, A.; Rau, S.-L.; Goetz, J.; Ladisch, C.M.; Brewer, M.; Hendrickson, R.; Ladisch, M.R. Pretreatment of Corn Fiber by Pressure Cooking in Water. *Appl. Biochem. Biotech.* **1998**, *73*, 1.
- Xu, X.; Antal, M.J. Jr.; Anderson, D.G.M. Mechanism and Temperature-Dependent Kinetics of the Dehydration of *tert*-Butyl Alcohol in Hot Compressed Liquid Water. *Ind. Eng. Chem. Res.*, **1997**, *36*, 23.

Table 1: Summary of experimental results

Reaction Medium	Time min.	Solids	Glucose	Xylose	Solubilization	Material
		Concentration ¹ %	Recovery %	Recovery %	%	Balance %
Steam	2	18.3	98	48	35	87
	5	34.3	104	25	20	86
Hot Liquid Wat	2	2.4	103	83	36	97
	5	1.4	98	68	43	91

¹Solids concentration is the mass of dry feed material expressed as a percentage of the total liquid in which it is immersed (extract + LCR moisture).

²Solubilization is calculated as dry LCR/ dry feed x 100

Table 2: Carbohydrate recoveries and degradation product formation

Reaction Medium	Time (min.)	Glucose Recovery (%)	Xylose Recovery (%)	Furfural (g/g Feed Xylose)
Steam Experiments				
Extract ¹	2	0	0	5
Flush ²		4	36	0
LCR ³		93	12	
Extract	5	0	0	5
Flush		1	5	12
LCR		103	21	
Hot Liquid Water				
Extract	2	3	63	3
Flush		0	5	0
LCR		100	15	
Extract	5	3	58	4
Flush		0	2	0
LCR		95	8	

¹ Extract - the liquid which is collected out of the bottom of the reactor after an experiment

² Flush - the cold water with which the hot LCR is rinsed after the reaction.

³ LCR - lignocellulosic residue, the material which remains as a solid after pretreatment.

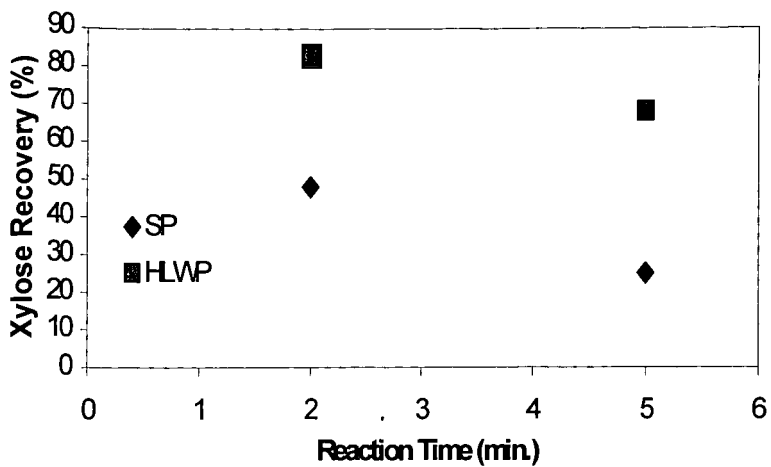


Figure 1: Xylose recovery as a function of reaction time.

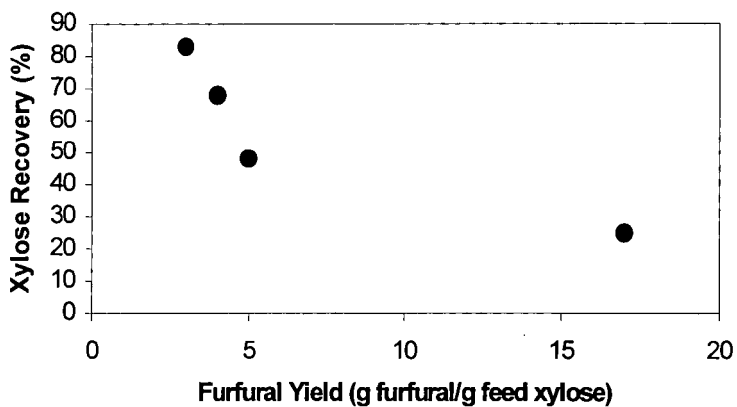


Figure 2: Xylose recovery as a function of furfural formation.

CHEMICAL CONVERSION OF BIOMASS POLYSACCHARIDES TO LIQUID HYDROCARBON FUELS AND CHEMICALS

J. Michael Robinson,* Estefani Banuelos, Wendell C. Barber, Caroline E. Burgess, Chhan Chau, Anita A. Chesser, Merry H. Garrett, Cynthia H. Goodwin, Preston L. Holland, Bruce O. Horne, Laura D. Marrufo, Eric J. Mechalke, Jeremy R. Rashidi, Brandon D. Reynolds, Teresa E. Rogers, Ernie H. Sanchez, Jose S. Villarreal

Chemistry Department, The University of Texas of the Permian Basin
Odessa, TX 79762

Keywords: biomass fractionation, liquid hydrocarbon fuels, oxygenate fuel additives

INTRODUCTION

Biomass has been traditionally converted to liquid fuels by either 1) fermentation or 2) pyrolysis methods. Modern improvements to these classical processes are many in number but do not essentially change the type of product resulting from these two vastly different sets of reaction conditions. While ethanol production by fermentation has become more efficient, it is still limited to a 67% yield due to the loss of one-third (1/3) of the available carbon as carbon dioxide gas. Pyrolytic reactions also lose carbon as gases and char but may achieve about 80% carbon conversion.¹ While most pyrochemical processes usually require nearly dry feedstock, the Shell Hydrothermal Upgrading (HTU) process requires a 3:1 ratio of water to biomass.² However, HTU produces only 50% biocrude which still contains 10-15% oxygen. Obviously, there remains a need for a variety of fuels from many sources, especially conventional liquid fuels for transportation purposes. To resolve this fuel problem and to use a renewable resource, a strategy was selected to prepare valuable liquid hydrocarbons from biomass by a new *chemical* process.

Our initial goal was to develop an efficient multistep chemical process for the conversion of the principle components of biomass, cellulose and hemicellulose, into hydrocarbon fuels. We envisioned the use of selective reduction reactions to allow for 100% carbon conversion by keeping the carbon chain intact. Furthermore, if initial reactions could be conducted in an aqueous medium, then the use of wet feedstock would be possible. Overall, a six-carbon sugar polymer like cellulose would afford a single pure 6-carbon hydrocarbon product such as hexene or hexane. This is precisely what we have developed, a novel *chemical* process.³

RESULTS AND DISCUSSION

Our use of the term *chemical* implies mild conditions, i.e., boiling aqueous solutions at atmospheric pressure and with chemical catalyst systems rather than enzymes. This chemical process consists of multiple reactions, the first two of which occur in water. **Scheme I** comprises a brief summary of the main reaction steps that achieve the strategic objectives of the organic portion of the process. For simplicity in this abstract, Scheme I only shows the reaction path of a 6-carbon carbohydrate as in cellulose or starch.

Step 1 is a reductive depolymerization of carbohydrate biopolymers. Cellulose (or starch) is simultaneously hydrolyzed in dilute acid and catalytically hydrogenated to glucitol (commonly named sorbitol) in near quantitative yields.⁴ Hemicellulose is similarly converted into 5-carbon polyols (e.g., xylitol), sorbitol, and some gluconic acids. Lignin, if present, is simply removed by filtration or centrifugation after the reaction. While the acid is mild, the highly selective ruthenium catalyst is only active at about the temperature shown. Thus, Step 1 uniquely provides the polyols required for the next reaction and simultaneously provides a facile separation of lignin.⁵ However, the ruthenium is easily deactivated by ambient oxygen in these batch laboratory reactions and thus does not recycle well for subsequent reactions. Collaboration is being sought to study various alloys that might be more suitable for this important biomass fractionation reaction. Alternatively, starch obtained from commercial (com) processes gives a pure 6-carbon source and commercial sorbitol is thus also directly available commercially using stable nickel catalysts.

Step 2 of the process is the key reaction: the *chemical* conversion of polyhydric alcohols to liquid hydrocarbons by reduction with hydriodic acid. The major part of the reduction occurs in this step: five hydroxyl groups of sorbitol undergo reduction. Our strategy to overcome the physical problems of insoluble solids forming during this step was to use homogeneous chemical agents that concomitantly reduce I₂ to regenerate HI.⁶ If the I₂ reacts quickly, it does not interfere with the polyol reduction reaction. Such use met with the unexpected results of simultaneous alkene formation and oligomerization. Considerable effort has been extended toward identifying the various oligomerization products and the variables that control their formation.

Thus in Step 2, polyhydric alcohols such as sorbitol are reduced essentially quantitatively to a mixture of halocarbon and hydrocarbon compounds by reaction with hydriodic acid (HI) and a phosphorous type reducing agent, either phosphorous acid (H_3PO_3) or hypophosphorous acid (H_3PO_2). The reaction occurs in boiling aqueous solution at atmospheric pressure for about 1-2 hour. Reaction conditions can be varied to give on one extreme about 99% 2-iodohexane and on the other extreme about 86% hydrocarbons with the remainder being halocarbons. The immiscible products are simply removed as a separate phase from the water solution. So Step 2 provides a highly reduced C_6 compound and descending amounts of C_{12} , C_{18} , and C_{24} hydrocarbons. These groups represent fuels in the range of gasoline, kerosene, diesel, and fuel oil, respectively. Each hydrocarbon group is a mixture of alkene and cycloalkane isomers. The higher homologues typically contain at least one ring. An example structure for the $C_{12}H_{22}$ isomers (1,2,4-trimethyl-3-propylcyclohexene, MW = 166) is shown in Scheme I. Sizable amounts of substituted decalins (two rings) also are present. The mixture of isomers in each group depresses the melting point and helps the fuel remain liquid.

In contrast, we found that Step 2 products such as these do not form from glucose; it must first be reduced to sorbitol. Nor do such products form on treatment of wood directly with HI.⁷ In fact, certain Canadian authors found that H_3PO_2 greatly "suppresses the yield of oil products." Products obtained from glucose reactions in this manner are complex mixtures of high molecular weight oils and tars containing significant amounts of oxygen and iodine. We are presently revisiting these glucose reactions with new techniques for the production of small, valuable chemicals rather than fuels.

Step 3 might be considered a cleanup reaction in that all of the remaining halocarbons in mixtures from Step 2 are subsequently converted to alkenes by an elimination reaction with caustic (NaOH or KOH) in boiling alcohol. Vast differences in boiling points of hexene (68 °C) from the other higher mass hydrocarbons, 200 °C and 300 °C, allow facile separation by distillation of the final mixture. The elimination of HI (Step 3) by KOH produces KI as insoluble by-product. KI is then recycled to KOH and HI (1-3 M solutions) by electrochemical means using an Aqualytics bipolar cellstack.⁸ This electrochemical regeneration have been studied on a pilot scale in our labs and determined very efficient. Details will be presented.

Hydrocarbon fractions distilled immediately after Step 3 contained traces of iodine (15-250 ppm). However, further lowering of the iodine content is desired for two reasons: (1) potential corrosion due to the HI produced upon combustion and (2) potentially expensive iodine resource impact costs. Therefore one additional polishing reaction, **Step 4**, was added. The hydrocarbons are simply refluxed with powdered zinc for 0.5 hour and all traces of iodine are removed. There are several optional steps to produce chemicals and solvents from hexene, one of which the catalytic hydrogenation of hexene to furnish hexane, an important large volume industrial solvent for seed oil extractions and polymer reactions.

Physical values, H/C ratio, and octane numbers are shown for these fuels and compared to conventional liquid fuels. 2-Hexene, for example, has an Octane No. of 87, density of 0.75, and a H/C ratio of 2, all ideal for gasoline except that for other reasons alkenes are not desired in a gasoline fuel. The C_{12} hydrocarbons have several desirable properties (less volatile, highly branched, cyclic, partially unsaturated, and a H/C ratio of 1.83). This group of isomers is deemed most suitable as a narrow boiling point range jet turbine fuel. Indeed, this C_{12} mixture has a high density of 0.84 and a bp range of about 190-210 °C, similar to the values of kerosene, but structurally too branched to make a standard (linear alkane) diesel fuel. The C_{18} and C_{24} isomer mixtures fit into a fuel oil range unless cracked in a conventional refinery manner into smaller hydrocarbons. These hydrocarbon products have high thermal values (43 MJ/kg) relative to ethanol (26.8 MJ/kg) or pyrolysis oils (Shell HTU ~ 36 MJ/kg) resulting from traditional methods of biomass conversions.

Reactions of hemicellulose required two additional models: xylose and gluconic acid. Xylose reactions yield pentene and oligomer hydrocarbons in a similar manner as shown in Scheme 1 by first making xylitol. Mixtures of xylitol and sorbitol give the expected cross oligomers with the exception of little C_{10} . However, gluconic acid is not reduced to a polyol but is directly reacted with the reducing HI to afford lactones such as 4-ethylbutyrolactone as major products (75%) along with some iodohexanoic acids. The value of these stable lactones as potential oxygenate fuel additives is under study. Hexanols and other oxygenates such as TAME and THME are also available from biomass via this chemical process.

SUMMARY AND ECONOMIC PROJECTION

This multistep *chemical* process for reduction of biomass to liquid hydrocarbon fuels is the first of its kind. It stands in sharp contrast to other research areas that follow classical lines of bio- (fermentation) or thermal (pyrolysis) conversion. In fact, uncoupling the reduction process to a series of mild selective chemical reactions was the key to the problem of obtaining high valued liquids from biomass. As a result, economic advantages abound. One particular advantage of this *chemical* process is that both Step 1 and Step 2 reactions take place in water as solvent, which allows the use of wet biomass. The water immiscible organic products of Step 2 simply coalesce as an upper layer facilitating their separation by mere decantation. Another benefit of the process is that the cyclic alkene dimers and trimers produced directly in Step 2 actually require less reduction, 10% and 13%, respectively, than hexene. These oligomeric hydrocarbons also do not require base treatment and subsequent reagent regeneration costs as do the haloalkanes. Step 2 is highly tunable, which allows a choice of products. Each simple reaction step is driven to essentially quantitative yield resulting in the same high yield for the entire process.

While we may only use hydrogen in Step 1, and in optional steps, it is convenient at this time to estimate the total costs of reduction based on a typical price for hydrogen. Using a hydrogen cost of \$0.40/lb and a cost range of \$10 to \$40/ton for biomass (dry weight basis) containing 75% holocellulose, then total feedstock and reduction costs might be estimated as \$0.37 to \$0.54 per gallon for hexene. Similarly, the C₁₂ and C₁₈ isomers range from \$0.34 to \$0.51/gal. However, there are other costs associated with this multiple step process that will definitely contribute to overall process economics. Establishment of accurate economics is a continuing process and will be discussed. Safe distillation and recovery of concentrated HI with saleable by-product phosphoric acid has been achieved. However, methods of coupled reductions that complement HI other than the use of phosphorous acid(s) have also been discovered. Industrial support is therefore being solicited to complete these studies and file several more patents. Total costs depend upon the exact steps, reagents, products, and precisely by which method of regeneration of HI from incipient I₂ is employed. It is likely that the high quality, high value products available *via* this process are today more economically attractive for their chemical (solvent) value, fuel additive (oxygenate) value, and as advanced jet fuels.

REFERENCES

1. Soltes, E.J. "Of Biomass, Pyrolysis, and Liquids Therefrom", Ch. 1 in ACS Symposium Series #376 "Pyrolysis Oils From Biomass; Producing, Analyzing, and Upgrading" Soltes, E.J. and Milne, T.A., Editors, American Chemical Society, Washington, D.C., 1988.
2. Naber, J.E.; Goudriaan, F.; Louter, A.S. "Further Development and Commercialization of the Shell Hydrothermal Upgrading Process for Biomass Liquefaction", 3rd Biomass Conference of the Americas [Proc.], 1997, 1651.
3. Robinson, J.M. "Process for Producing Hydrocarbon Fuels", U.S. Patent No. 5,516,960, May 14, 1996.
4. Sharkov, V.I. "Production of Polyhydric Alcohols from Wood Polysaccharides," *Angew. Chem. I.E.E.* 1963, 2, 405.
5. Robinson, J.M.; Burgess, C.E.; Mandal, H.D.; Brasher, C.D.; O'Hara, K.; Holland, P.L. "Unique Fractionation of Biomass to Polyols Provides Inexpensive Feedstock for Liquid Fuels Process," 212th American Chemical Society National Meeting, Orlando, FL, Aug. 26-30, 1996, FUEL Abstract # 90.
6. Foster, L.S.; Nahas, H.G., Jr. "Hydriodic Acid: Regeneration of Oxidized Solutions," *Inorg. Synth.*, Vol. 2, 210, W.C. Fernelius, Ed., 1946.
7. Cooper, D.; Douglas, M.; Ali, O.; Afrashtehfar, S.; Ng, D.; Cooke, N. "A Low Pressure-Low Temperature Process for the Conversion of Wood to Liquid Fuels and Chemicals Using Hydrogen Iodide" *Canadian Bioenergy R&D Semin. [Proc.]* 5th, 1984, 455.
8. Mani, K.N. "Electrodialysis Water Splitting Technology," Aquatech Systems Report, Allied Signal, Inc., Warren, NJ, 1990.

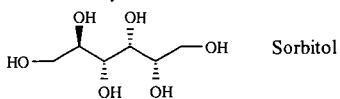
ACKNOWLEDGMENT

This research has been supported by UTPB; the Robert A. Welch Foundation (Texas); the National Renewable Energy Laboratory (NREL); and the U.S. Department of Energy, Basic Energy Sciences, Advanced Research Projects. Special thanks are extended to Dr. Norman Hackerman, President Emeritus of Rice University and Chairman of the Welch Foundation, as well as to Dan Tyndall and Dr. Tom Milne at NREL who have been particular helpful. Many other students have participated in the research and development of this process over the span of several years. Their assistance is greatly appreciated.

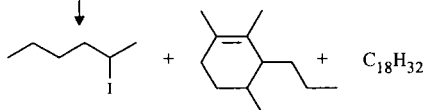
Biomass to Hexene :

Biomass: Cellulose + Hemicellulose + Lignin

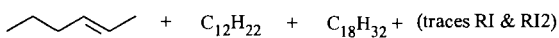
Step 1 94% \downarrow H^+/H_2O , Ru/ H_2 (600 psi), 1 hr 165°



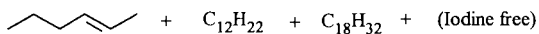
Step 2 100% \downarrow HI/ H_3PO_3 , 117°, 2 hr



Step 3 100% \downarrow NaOH/ROH heat 1 hr



Step 4 \downarrow Zn/heat



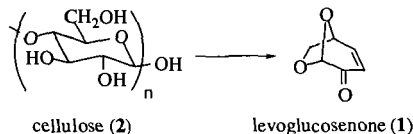
A CONVENIENT PROCEDURE FOR THE PREPARATION OF LEVOGLUCOSENONE FROM CELLULOSE AND THE CONVERSION OF LEVOGLUCOSENONE TO NOVEL CHIRAL DERIVATIVES

Walter S. Trahanovsky, Chen Wang, Jason M. Ochaoda, and Synthia Chang, Department of Chemistry, Iowa State University, Ames, Iowa 50011-3111

Key words: biomass, cellulose, levoglucosenone

INTRODUCTION

The preparation of levoglucosenone (**1**) by the pyrolysis of cellulose (**2**) under acidic conditions



has been reported recently.¹ In general, the procedures involve separating a slightly volatile liquid pyrolysate from a mixture of solids followed by purification of the liquid pyrolysate. Normally, 2-5% of pure levoglucosenone (**1**) is obtained.¹

The potential of levoglucosenone (**1**) for use in organic synthesis is exceedingly high. It is a relatively small (six carbon atoms), enantiomerically pure, rigid molecule with several important functional groups including a ketone group, a double bond conjugated with the ketone, a protected aldehyde, and two protected hydroxyl groups.¹

We have found a convenient method for converting cellulose (**2**) to levoglucosenone (**1**) in >10% yield. This procedure as well as methods to convert levoglucosenone (**1**) into potentially useful chiral derivatives is presented.

EXPERIMENTAL

In some runs cellulose (**2**) was acidified by the following pretreatment. A quantity of 20 g of cellulose (**2**), 600 mg of phosphoric acid, and enough methanol to cover the cellulose (**2**) were added to a round bottom flask and allowed to stand at room temperature for 1 h. The methanol was then removed on a rotary evaporatory under reduced pressure.

Cellulose (**2**) and soy oil were added to a round bottom flask containing a magnetic stirring bar. If the cellulose (**2**) had not been acidified by the pretreatment, an acid was also added to the flask. The flask was connected to a vacuum distillation apparatus and the pressure was lowered to 15-30 mm Hg. The reaction mixture was heated with stirring to ca. 300 °C. Within seconds levoglucosenone (**1**), water, and charcoal began to form and the water and levoglucosenone (**1**) distilled from the mixture and were condensed.

Yields of levoglucosenone (**1**) were determined by gas chromatography using a standard (octyl alcohol) or by direct weighing.

RESULTS AND DISCUSSION

Preparation of levoglucosenone (**1**).

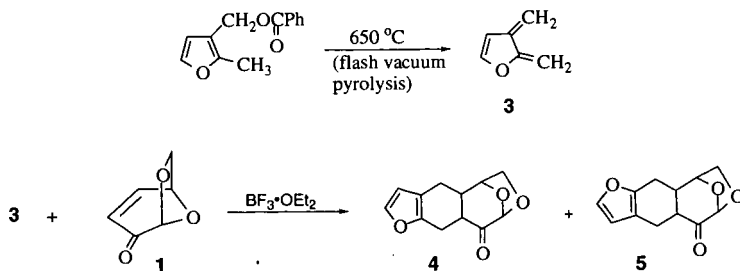
The yield of levoglucosenone (**1**) as a function of the temperature, the ratio of cellulose to soy oil, and the type of acid was studied. It was found that the highest yields (> 10%) of levoglucosenone (**1**) were obtained by using a 1:3 ratio of [cellulose (**2**):soy oil] and a temperature of 300 °C. It was found that preacidification was not necessary: phosphoric acid could be added directly to the reaction mixture.

Conversion of levoglucosenone (**1**) to chiral derivatives.

Levoglucosenone (**1**) was converted to several derivatives which were fully characterized by infrared, mass, and ¹H and ¹³C NMR spectroscopy.

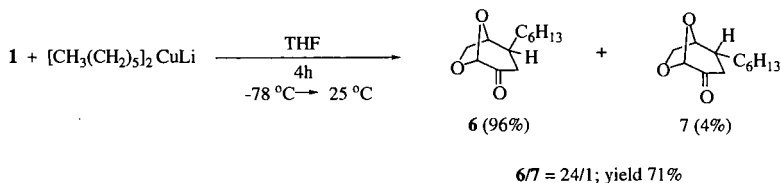
Diels-Alder reaction with the furan-based o-quinodimethane.

The preparation of (3) has been reported.²



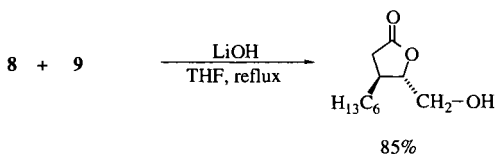
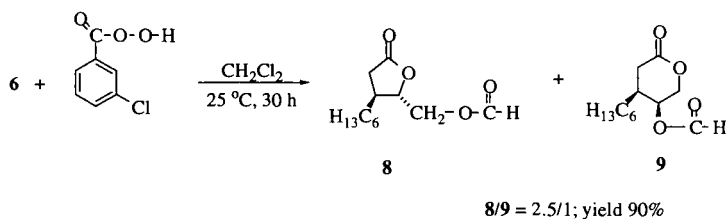
Conjugate addition of hexyl cuprate.

This procedure was based on that reported by Yamada et. al.³ The addition of pentyl cuprate to levoglucosenone (1) has been reported.⁴



Baeyer-Villiger oxidation of 6, the hexyl cuprate adduct of levoglucosenone.

This procedure was based on that reported by Murry et. al.⁵ The Baeyer-Villiger oxidation of the pentyl derivative, using different reagents, has been reported.⁴



ACKNOWLEDGEMENTS

We thank the Iowa Energy Center for generous financial support.

REFERENCES

1. (a) Witczak, Zbigniew J.; editor. *Levoglucosenone and Levoglucosans Chemistry and Applications*, Frontiers in Biomedicine and Biotechnology, Vol. 2, ATL Press, Inc., Science Publishers, Mount Prospect, IL, U.S.A., 1994. (b) see specifically Christophe Morin in ref. 1a, p. 17-21.
2. Trahanovsky, W. S.; Cassady, T. J.; and Woods, T. L. *J. Am. Chem. Soc.*, **1981**, *103*, 6691.
3. Yamamoto, K.; Ogura, H.; Jukuta, J.; Inone, H.; Hamada, K.; Sugiyama, Y.; Yamada, S. *J. Org. Chem.*, **1998**, *63*, 4449.
4. Ebata, T.; Koseki, K.; Okano, K.; and Matsushita, H.; in ref. 1a, p. 59-72.
5. Sosnowski, J. J.; Danaher, E. B.; Murry, R. K., Jr. *J. Org. Chem.*, **1985**, *50*, 2759.

FLASH PYROLYSIS OF BIOMASS SUBMITTED TO A CONCENTRATED RADIATION. APPLICATION TO THE STUDY OF THE PRIMARY STEPS OF CELLULOSE THERMAL DECOMPOSITION

Jacques LEDE * and Olivier BOUTIN
Laboratoire des Sciences du Génie Chimique (CNRS-ENSIC-INPL)
1, rue Grandville - BP 451 - 54001 NANCY Cedex (FRANCE)

* Author for correspondence - Tel. +33 (0)3.83.17.52.40 - Fax. +33 (0)3.83.32.29.75
e-mail : lede@ensic.u-nancy.fr

Keywords : Solar thermochemistry ; Cellulose ; Pyrolysis

ABSTRACT

Concentrated radiation and more specifically concentrated solar energy can be used to drive thermochemical processes. Several types of chemical systems can be considered, aiming at the production of chemical energy carriers or the processing of chemical commodities. The solar thermochemical conversion of carbonaceous materials is one of the most often suggested option. In addition, concentrated light can be also used as a very efficient laboratory device for studying basic kinetic pathways in very clean conditions, as for example the primary steps of the biomass thermal degradation. The present paper describes the first results of experiments where small samples of cellulose are submitted to short flashes of a concentrated radiation provided by an image furnace. The observation of the surface after the reaction, as well as the HPLC analysis of the products bring evidence that the reaction passes through the intermediate of short life time liquid species. Thanks to a mathematical model taking into account the heat transfer limitations, it is possible to derive kinetic data that are compared to the results of the literature. In addition to these chemical results, the paper points out the importance of the optical properties of cellulose with respect to the efficiency of the sunlight absorption.

INTRODUCTION

Concentrated radiation can be used to drive endothermal chemical reactions under controllable and very clean conditions of high heat flux densities. It is for example the case with concentrated solar energy that can be obtained through different devices like solar towers, dish concentrators, solar furnaces, ... The available powers range from a few kW to several MW according to the facilities. The aim of the first part of this paper is to briefly mention the main different domains of solar chemical reactions presently studied all over the world mainly in the framework of the SolarPACES program (1). Special emphasis will be given to the conversion of carbonaceous materials like biomass. All these studies are made in the context of search of new sources of renewable energies for a futur optimal protection of environment. The second part of the paper will show that concentrated radiation (obtained from a solar simulator) can be also used for studying the fundamental aspects of biomass thermal degradation. First results concerning the primary steps of cellulose pyrolysis will be given and compared to mathematical models.

SOLAR THERMOCHEMISTRY AND SOLAR THERMOCHEMICAL PROCESSES

The first aim of the activities developed all over the world is the production of energy carriers : solar energy is converted into chemical fuels which can be stored for long times and transported over long distances. In addition, solar energy can also assist in the processing of high temperature chemical commodities. Among the chemical systems which are the most extensively studied are :

- The solar reforming of natural gas with the production of syngas
- The solar thermochemical storage of solar energy relying on the dissociation of ammonia
- The solar thermal production of H₂. This can be done through the direct and very high temperature splitting of water or through thermochemical cycles based for example on the dissociation of metal oxides (like ZnO).
- The solar processing of specific chemical commodities like fullerenes, nanomaterials, ...
- The solar thermochemical conversion of biomass attracts also much attention since many years for several reasons (2). There are many ways of biomass thermal upgrading : gasification ; slow and fast pyrolysis ; ... leading to a great number of possible interesting products (gases, charcoal, bio oils, ...) with many potential utilisations (fuels, electricity, chemicals, ...). The corresponding solar assisted processes bring the advantages to upgrade the totality of the biomass feedstock and to design 100 % renewable plants with no use of fossil fuels, O₂ or air (gasification). The emissions are reduced and respect the natural cycle of carbon.

All these processes cannot be developed with the only knowledge of the chemical systems involved. They need to optimize the solar reactor where they are driven. Among the problems to be solved are: to maintain clean the window through which the solar radiation enters into the reactor ; to adapt the reactor to the nature of the solar facility (vertical or horizontal axis ; at the

ground or at the top of a tower ; ...); to be able to operate in transient conditions ; ... In addition, the optical properties of the absorbing solid reactants must be well known. Some failures in solar biomass conversion can be explained by the fact that some of its components are not perfectly absorbing materials. It has been for example recently shown that cellulose may reflect up to 80 % of the incident radiation and that it behaves also as a semi transparent material, meaning that important fractions of the radiation may cross the sample without any absorption (3).

CONCENTRATED RADIATION: A TOOL FOR STUDYING THE FUNDAMENTALS OF BIOMASS PYROLYSIS.

A very great number of papers have been and continue to be published in the field of biomass thermochemical conversion. The aim of many of them is to derive kinetic models. However, these models are often valid for the unique device where they have been determined. It is the reason why there still exist many disagreements and also controversies (4). For example, it is not well understood if the vapours formed in cellulose fast pyrolysis are formed directly from a solid phase or through intermediate "active" liquid species.

Concentrated radiations can be available in very clean conditions of very high heat flux densities and during well controlled times. The following section will show that these conditions can be favourably used for a better understanding of the primary steps of cellulose thermal degradation.

Experimental measurements

The concentrated radiation is provided by an image furnace reproducing, at the laboratory scale, the conditions of a solar furnace. Its principle has been previously described in details (5). It relies on the use of a high power Xenon lamp located at the first focus of a first elliptical mirror, the second focus of which being adjusted at the same location as the second focus of a second elliptical mirror. The image of the arc of the lamp is then formed at its first focus, where the chemical tests on cellulose samples are performed. The available flux can be adjusted through the use of several diaphragms. A system of pendulum allows also to irradiate the samples during known times (as low as a few milliseconds). The cellulose samples subjected to the flashes of light may be under the form of a thin layer deposited on a glass surface or of small pressed cylinders. In that case, the sample is settled inside a transparent glass vessel feeded by argon, at the exit of which is placed a glass wool filter trapping the aerosols and condensibles. Several measurements can be performed:

- Observation of the surface of the irradiated sample with a microscope, after the flash.
- Measurements of mass balances (mass loss of the sample and mass increase of the filter).
- Analysis by HPLC of the products remaining on the sample and trapped on the filter.
- Analysis of the gases leaving the filter by GC.

Experimental results

With available heat flux densities close to 10^7 W m^{-2} , a film of cellulose of $450 \pm 50 \mu\text{m}$ thickness completely disappears in about one second. The reaction does not produce measurable quantities of char. No reaction is visible for flashes lower than about 0.2 second. For intermediate durations of the irradiation, it is possible to microscopically observe the surface of the sample after cooling: the fibrillar structure of initial cellulose has disappeared with blunting of the contours as during a phase change. In the same time, agglomerations occur with the formation of large networks. This behaviour precedes the formation of vapours for longer times of flashes. Undoubtedly, these observations show that gases and vapours are formed only after cellulose has passed through short life time liquid intermediate species. Notice that if these species are liquid at the reaction temperature, they are solid at room temperature. These solid products are 100 % water soluble.

In similar experimental conditions but with pressed pellets of cellulose, these same intermediate species are observed. After a given time of flash, steady state conditions are reached. They correspond to a constant superficial thickness of the layer of liquid species (a few hundred of microns) and in the same time, to a linear increase of the weight of the products trapped on the filter, as the flash time increases. These experiments do not produce noticeable fractions of char. The mass balances are verified with accuracies of about 80 %. The remaining fraction is probably due to untrapped vapours (probably water) and to the formation of light gases. Their analysis is under investigation by gas chromatography but their fraction seems to be very low (less than a few %). These last measurements are difficult because of the high dilution of the gases in argon and also of the very short duration of each experiment.

The HPLC analysis of the aqueous solution of the intermediate species as well as of the products trapped on the filter are also under investigation. They reveal the presence of relatively few peaks compared to the analysis of the more usual bio oils derived from flash pyrolysis. The composition of the intermediate species is independant of the time of flash. The products trapped on the filter have increasing fractions of low molecular masses products when the time of irradiation increases. Most of the known peaks correspond to molecules

(oligoanhydrosaccharides) resulting directly from the depolymerization of the cellulose polymer. The intermediate liquid species contain high fractions of molecules with degrees of polymerization higher than 3 while the trapped products contain noticeable fractions of levoglucosan and cellulosan mainly for long flash times experiments.

Theoretical

In addition to these experiments it is possible to build models representing the thermal decomposition of cellulose. They rely on heat and mass balances at the level of a solid sample submitted to a given external available heat flux density and undergoing an endothermal chemical reaction occurring in competition with internal heat transfer resistances. The reaction is supposed to give rise to liquid species remaining on the sample and disappearing by a secondary reaction giving vapour species leaving the surface without any mass transfer resistance.

The model relying on the thin film experiences correspond to a first approximation to the so-called chemical regime : constant sample temperature (no gradient) and reaction controlled by chemistry. The phenomena occur in transient conditions. The pressed thick pellet experiments correspond to the so called ablation regime : after a short time, steady state conditions are reached the reaction occurring near and inside a thin superficial layer, while the heart of the pellet is at room temperature.

The agreement between these 2 models and the two different types of experiments is good, assuming that the rate constants for the 2 processes (cellulose \rightarrow intermediate species \rightarrow vapours) are those usually chosen in association with the Broido Shafizadeh kinetic pathway (4). However the comparison strongly depends upon the values of the thermophysical properties of cellulose and of the liquid species (thermal conductivity ; mass density ; heat capacity) as well as of their optical characteristics (emissivity ; absorptivity ; reflectivity) that will have to be more accurately measured in the future.

CONCLUSION - DISCUSSION

Concentrated radiation (ex. concentrated solar energy) can be used to drive thermochemical reactions for the preparation of energy carriers and/or of chemical commodities. It is for example the case for the solar upgrading of biomass. The high qualities of a concentrated radiation can also be used as a laboratory tool for studying the primary steps of biomass thermal degradation. The experiments described have been favourably performed in very reproducible conditions with a solar simulator (image furnace) and with cellulose samples. They show that if it is well known that lignin passes through a liquid phase, it is also the case for cellulose. In spite of many previous experimental and theoretical evidences, this phenomenon continued to be questioned (4) and even rejected (6). The results presented in this paper show that in conditions of high heat flux densities, the existence of intermediate liquid species resulting from the partial depolymerization of cellulose cannot be ignored and that a simple model of the cellulose \rightarrow vapours type does not represent the reality. Notice that if these liquids play important and favorable roles in ablative pyrolysis (7,8) they can also create problems in entrained flow reactors where they can lead to agglomerations between the particles and finally increase the risks of clogging.

The liquid intermediate species observed in the present work can be compared to the "active cellulose" postulated in the Broido Shafizadeh model, even if these authors had few chances to observe a liquid phase during their low temperature experiments. Anyway, such a kinetic pathway associated to the often used and accepted rate constants allows to favourably predict our results. This agreement is observed thanks to mathematical models derived in the two extreme situations of the chemical and ablation regimes. However, our works show the necessity to better determine the thermophysical properties of cellulose and of its products of depolymerization.

ACKNOWLEDGEMENTS

The authors want to thank ADEME (under the framework of AGRICE: contract n° 96 01 048) and CNRS-ECODEV for their financial support.

REFERENCES

1. Grasse W. SolarPACES Annual Report 1997. DLR (Köln, Germany, May 1998)
2. Lédé J., Accepted for publication in Solar Energy.
3. Boutin O., Lédé J., Olalde G., Ferrière A. 9th Int. Symp. SolarPACES, Solar thermal concentrating Technologies. Odeillo, Font Romeu, France (June 1998)
4. Lédé J., Diebold J.P., Peacocke G.V.C., Piskorz J., Developments in Thermochemical Biomass Conversion, 1997, Bridgwater A.V. and Boocock D.G.B. (eds.), Blackie Academic and Professional, London, pp. 27-42
5. Boutin O., Ferrer M., Lédé J., J. Anal. Appl. Pyrolysis, 1998, 47, pp. 13-31

6. Varhegyi G. Jakob E., Antal M.J., Energy and Fuels, 1994, 8, n° 6, pp. 1345-1352
7. Lédé J., Li H.Z., Villermaux J., ACS Symp. Series 376, Pyrolysis Oils from Biomass, Producing, Analyzing and Upgrading, Soltes J. and Milne T.A. (Eds.), 1988, Washington D.C., pp. 66-78
8. Lédé J., Verzaro F., Antoine B., Villermaux J., Chem. Eng. Proc., 1986, 20, pp. 309-317

BACK TO THE FUTURE: HYDROGEN PRODUCTION, NOW AND THEN

Catherine E. Gregoire Padró
National Renewable Energy Laboratory
1617 Cole Blvd.
Golden, CO 80401

Keywords: hydrogen production; carbon sequestration; sustainable energy systems

ABSTRACT

The availability of a reliable and cost-effective supply of hydrogen will be essential in the development of the so-called Hydrogen Economy. Whereas most hydrogen is now produced from steam reforming of natural gas, renewable and sustainable resources will be the sources of choice. Getting from the current production paradigm to this idyllic future will require a transitional phase that exploits our abundant fossil resources in new ways, and challenges our sustainable technologies to reduce costs and improve efficiency and convenience. This paper discusses the current state of fossil-based and sustainable hydrogen production technologies and proposes innovative approaches to this Hydrogen Economy in a carbon-constrained world.

INTRODUCTION

In the future, our energy systems will need to be renewable and sustainable, efficient and cost-effective, convenient and safe. Hydrogen has been proposed as the perfect fuel for this future energy system. Produced from water and sunlight in nearly inexhaustible quantities, hydrogen could supply the energy needs of all sectors of the economy. But, the technologies needed for the Hydrogen Economy are not technically mature or are too costly to compete with other energy forms.

In its Hydrogen Program, the U. S. Department of Energy (DOE) conducts R&D for the development of safe, cost-effective hydrogen production technologies that support and foster the transition to the Hydrogen Economy. Although the long-term focus is on renewable technologies, the introduction of hydrogen into the transportation and utility sectors will require the availability of inexpensive hydrogen - most likely relying on fossil fuels such as natural gas, coal, and oil.

A HOLY WAR FOR HYDROGEN ?

Hydrogen Economy purists frequently express dismay at the notion of using fossil fuels to produce hydrogen in the transition to a hydrogen-based energy system. The argument focuses on the "contamination" of the hydrogen utopia - where hydrogen produces no pollution in the production, storage, transportation, and use cycles. Producing "unholy" hydrogen from fossil fuels results in the production of anthropogenic CO₂, which cannot be (easily) recycled to produce more fuel. We should note that carbon emissions are not necessarily evil - CO₂ produced in a biomass-based hydrogen system is recycled in the biomass growth phase, and results in net zero (within a few percent) CO₂ emissions [1].

But we are faced with economic realities - hydrogen is pretty cheap when produced in large steam methane reformers, and may be even cheaper when produced by gasification of coal. Renewable-based technologies are not ready for commercialization, and face significant economic hurdles when they do get there. And it will not do us much good to develop these renewable production technologies if there are no viable end uses for our "holy" hydrogen. Pragmatists look to fossil fuels as stepping stones to the future, providing hydrogen at reasonable costs for the evolving end users. That doesn't mean we cannot improve upon today's technologies to provide the cleanest hydrogen possible. The DOE Hydrogen Program is dedicated to developing improved production technologies that can provide fossil-based hydrogen in the near-term at competitive prices, and renewable-based hydrogen in the mid- and long-term.

NEAR-TERM FOSSIL-BASED HYDROGEN PRODUCTION TECHNOLOGIES

The production of hydrogen from fossil fuels, particularly natural gas, is an integral part of the DOE Hydrogen Program strategy to introduce hydrogen into the transportation and utility energy sectors. This strategy includes reducing the cost of conventional and

innovative hydrogen production processes that rely on cheap fossil feedstocks to improve the economics of hydrogen use. The Program supports a number of projects that rely on improvements to existing processes, resulting in reduced costs and improved emissions.

Air Products and Chemicals is investigating a modification to the conventional steam methane reforming process that includes incorporation of a CO₂ adsorbent in the reforming reaction to remove CO₂ from the product stream [2]. This "upset" to the reaction equilibrium drives the reforming reaction ($\text{CH}_4 + 2\text{H}_2\text{O} = [\text{CO} + \text{CO}_2] + 4\text{H}_2$) to produce additional hydrogen at lower temperatures than conventional reformers. The cost of hydrogen is expected to be 25-30% lower with this process, primarily due to reduced capital equipment costs and reduced operating costs. In addition, the adsorption of the CO₂ in the reforming stage results in a high-purity CO₂ stream from the adsorbent regeneration step. This has interesting implications in a carbon-constrained world, discussed later.

The Program supports the development of a compact plasma reformer for hydrocarbon fuel reforming for industrial, distributed utility, and vehicular refueling applications. The Massachusetts Institute of Technology is examining the potential of the plasma reforming process to perform the reforming and water-gas shift in a single reactor [3]. Improvements to the process are expected to result in a reduction in specific energy consumption.

In a project cosponsored by the Hydrogen Program and the Office of Fossil Energy, Air Products and Chemicals is developing a ceramic membrane reactor for the simultaneous separation of oxygen from air and the partial oxidation of methane. If successful, this process could result in improved production of hydrogen and/or synthesis gas compared to standard reformers.

MID-TERM RENEWABLE HYDROGEN PRODUCTION TECHNOLOGIES

Thermal processing of plant material (biomass) is similar to the processing of fossil fuels, with a number of the down-stream unit operations being essentially the same for both feedstocks. Hydrogen Program R&D focuses on the processing units that are feedstock-dependent, leveraging the vast database of experience available on the common unit operations. Using agricultural residues and wastes, or biomass specifically grown for energy uses, hydrogen can be produced using a variety of processes, including pyrolysis and gasification. These systems offer the opportunity to produce hydrogen from renewable resources in the mid-term (5-10 years).

Biomass pyrolysis produces a liquid product (bio-oil) that, like petroleum, contains a wide spectrum of components that can be separated into valuable chemicals and fuels. Unlike petroleum, bio-oil contains a significant number of highly reactive oxygenated components derived mainly from constitutive carbohydrates and lignin. These components can be transformed into a variety of products, including hydrogen. Catalytic steam reforming of the bio-oil or selected fractions is possible, using Ni-based catalysts that are similar to those used in steam methane reforming. By using high heat transfer rates and appropriate reactor configurations that facilitate contact with the catalyst, the formation of undesirable carbonaceous deposits (char) can be minimized. At the National Renewable Energy Laboratory (NREL) and the Jet Propulsion Laboratory, research and modeling are underway to develop processing technologies that take advantage of the wide spectrum of components in the bio-oil, and address reactivity and reactor design issues [4,5]. Evaluation of co-product strategies indicates that high value chemicals, such as phenolic resins, can be economically produced in conjunction with hydrogen [6].

One of the significant differences between solid fossil fuels (coal) and biomass is the moisture content (and affinity to moisture). Biomass is typically 50 weight percent (wt%) moisture (as received), requiring drying of the feed to about 15 wt% moisture for efficient and sustained operation in typical pyrolysis and gasification operations. However, in a supercritical water gasification process under development at the Hawaii Natural Energy Institute (HNEI) at the University of Hawaii, feed drying is not required, thus providing an opportunity to reduce equipment and operating costs. There are tradeoffs: particle size reduction requirements are more severe for this process (~1 mm) than for other biomass gasification and pyrolysis processes (~1 cm). A slurry containing approximately 15 wt% biomass is pumped at high pressure (>22 MPa, the critical pressure of water) into a reactor, where hydrothermolysis occurs. Increasing the temperature to ~700°C in the presence of catalysts results in the reforming of the hydrolysis products. Catalysts have been identified that are suitable for the steam reforming operation [7]. HNEI, Combustion Systems Inc., and General Atomics are investigating appropriate slurry compositions,

reactor configurations, and operating parameters for supercritical water gasification of wet biomass.

LONG-TERM RENEWABLE HYDROGEN PRODUCTION TECHNOLOGIES

The use of solar energy to split water into oxygen and hydrogen is an attractive means to directly convert solar energy to chemical energy. Biological, chemical, and electrochemical systems are being investigated within DOE as long-term (>10 years), high-risk, high-payoff technologies for the sustainable production of hydrogen.

Biological Systems

In nature, algae absorb light and utilize water and CO₂ to produce cell mass and oxygen. A complex model referred to as the "Z-scheme" has been identified to describe the charge separation and electron transfer steps associated with this process that ultimately drives photosynthesis. A number of enzymatic side pathways that can also accept electrons have been identified. Of interest is a class of enzymes known as hydrogenases that can combine protons and electrons obtained from the water oxidation process to release molecular hydrogen. These algal hydrogenases are quickly deactivated by oxygen. Researchers have identified mutant algal strains that evolve hydrogen at a rate that is 4 times that of the wild type, and are 3-4 times more oxygen tolerant [8,9].

Photosynthetic organisms also contain light harvesting, chlorophyll-protein complexes that effectively concentrate light and funnel energy for photosynthesis. These antenna complexes also dissipate excess incident sunlight as a protective mechanism. The amount of chlorophyll antennae in each cell is directly related to the amount of "shading" experienced by subsequent layers of microorganisms in a mass culture. In a recent set of experiments, researchers have observed that green alga grown under high light intensities exhibit lower pigment content and a highly truncated chlorophyll antennae size. These cells showed photosynthetic productivity (on a per chlorophyll basis) that was 6-7 times greater than the normally pigmented cells [10], a phenomenon that could lead to significant improvements in the efficiency of hydrogen production on a surface-area basis.

These technical challenges are being addressed by a team of scientists from Oak Ridge National Laboratory (ORNL), the University of California Berkeley, and NREL. Various reactor designs are under development for photobiological hydrogen production processes (single-stage vs two-stage, single organism vs dual organism). At HNEL, a new, potentially low cost, outdoor tubular photobioreactor is under development to test a sustainable system for the production of hydrogen [11].

In addition to the photosynthetic production of hydrogen from water, the Program supports the development of systems to convert CO (found in synthesis gas) to hydrogen via the so-called water-gas shift reaction ($\text{CO} + \text{H}_2\text{O} = \text{CO}_2 + \text{H}_2$). This reaction is essential to the widely-used commercial methane reforming process for the production of hydrogen. In the industrial process in use today, high-temperature (450°C) and low-temperature (230°C) shift reactors are required to increase the overall hydrogen production efficiency and to reduce the CO content to acceptable levels. In this project, microorganisms isolated from nature are used to reduce the level of CO to below detectable levels (0.1 ppm) at temperatures of around 25-50°C in a single reactor [12,13]. This process, under development at NREL, has significant potential to improve the economics of hydrogen production when combined with the thermal processing of biomass or other carbon-containing feeds.

Photochemical Systems

Among the technologies that have been investigated, photocatalytic water splitting systems using relatively inexpensive, durable, and nontoxic semiconductor photocatalysts show promise. Supported catalysts such as Pt-RuO₂/TiO₂ have sufficient band gaps for water splitting, although the current rate of hydrogen production from these systems is too low for commercial processes. Modifications to the system are required to address issues such as the narrow range of solar wavelengths absorbed by TiO₂, the efficiency of subsequent catalytic steps for formation of hydrogen and oxygen, and the need for high surface areas. Binding of catalyst complexes that absorb light in the visible range to the TiO₂ should improve the absorption characteristics. Aerogels of TiO₂ as a semiconductor support for the photocatalysts have potential for addressing reaction efficiency and surface area issues. The University of Oklahoma is investigating these systems.

The Florida Solar Energy Center, in conjunction with the University of Geneva, is investigating tandem/dual bed photosystems using sol/gel-deposited WO_3 films as the oxygen-evolving photocatalyst, rather than TiO_2 . In this configuration, the dispersion containing the wider band gap photocatalyst must have minimal light scattering losses so that the lower band gap photocatalyst behind it can also be illuminated.

Photoelectrochemical Systems

Multijunction cell technology developed by the PV industry is being used for photoelectrochemical (PEC) light harvesting systems that generate sufficient voltage to split water and are stable in a water/electrolyte environment. The cascade structure of these devices results in greater utilization of the solar spectrum, resulting in the highest theoretical efficiency for any photoconversion device. In order to develop cost effective systems, a number of technical challenges must be overcome. These include identification and characterization of semiconductors with appropriate band gaps; development of techniques for preparation and application of transparent catalytic coatings; evaluation of effects of pH, ionic strength, and solution composition on semiconductor energetics and stability, and on catalyst properties; and development of novel PV/PEC system designs. NREL's approach to solving these challenges is to use the most efficient semiconductor materials available, consistent with the energy requirements for a water splitting system that is stable in an aqueous environment. To date, a PV/PEC water splitting system with a solar-to-hydrogen efficiency of 12.4% (lower heating value, LHV) using concentrated light, has operated for over 20 hours at 11 suns [14]. HNEI is pursuing a low-cost amorphous silicon-based tandem cell design with appropriate stability and performance, and is developing protective coatings and effective catalysts. An outdoor test of the a-Si cells resulted in a solar-to-hydrogen efficiency of 7.8% LHV under natural sunlight [15].

THE ROLE OF HYDROGEN IN A CARBON-CONSTRAINED WORLD

After basking in a week of temperatures in the 70's in December in the Denver area while Russia is gripped in the worst early winter cold spell this century, one begins to wonder if perhaps all those "Chicken Little" environmentalists might be on to something. Concerns about global climate change are increasing around the world, and industries are beginning to address the economic impacts of environmentally-sound energy consumption.

Decarbonization of fossil fuels is proposed as a "quick fix" to increased energy consumption in a carbon-constrained world. Removal of carbon from fossil fuels prior to use in energy production is likely to be far less costly than attempting to remove CO_2 from dispersed sources. If fossil fuels are converted to hydrogen in a central facility, the collection of CO_2 (or elemental carbon, depending on the process) is relatively simple compared to collecting CO_2 from every fossil-fuel-consuming vehicle on the road.

Technical barriers exist. For steam methane reforming (the predominant hydrogen production technology in use today), collection of CO_2 from the hydrogen purification step will require process and operation changes that could impact overall energy efficiency and therefore cost. CO_2 disposal or sequestration, in a manner that keeps the greenhouse gas out of the atmosphere for a significant period of time (perhaps 100+ years), is the subject of numerous research projects throughout the world. Environmental effects of deep ocean disposal on marine life and water quality (pH in particular) have yet to be determined. Security of aquifer disposal is also uncertain. In addition, the use of hydrogen as a transportation fuel would require development of efficient delivery, dispensing, and on-board storage processes. Use of hydrogen in power production will require continued improvements in fuel cells and gas turbines.

CONCLUSIONS

The production of hydrogen, from fossil fuels or from renewables, is only one part of the equation. Significant changes in our fuel infrastructure are required to address the use of this clean fuel. Codes and standards for the safe use of hydrogen are under development, and must be implemented to ensure the safety of the public. As with any new fuel or technology, education is essential. The DOE Hydrogen Program continues to support the development of technologies that will enable the transition to a clean and sustainable Hydrogen Economy, with emphasis on technical viability, environmental friendliness, and economic competitiveness.

REFERENCES

- [1] Mann, M.K., and P.L. Spath, 1997, "Life Cycle Assessment of a Biomass Gasification Combined-Cycle Power System," NREL/TP-430-23076.
- [2] Hufton, J., S. Mayorga, T. Gaffney, S. Nataraj, M. Roa, and S. Sircar, 1998 "Sorption Enhanced Reaction Process (SERP) for the Production of Hydrogen," Proceedings of the 1998 U.S. DOE Hydrogen Program Review, NREL/CP-570-25315, 695-706.
- [3] Bromberg, L., D. Cohn, A. Robinovich, and N. Alexeev, 1998, "Plasma Catalytic Reforming of Methane," Proceedings of the 1998 U.S. DOE Hydrogen Program Review, NREL/CP-570-25315, 627-638.
- [4] Wang, D., S. Czernik, and E. Chornet, 1998, "Production of Hydrogen from Biomass by Catalytic Steam Reforming of Fast Pyrolysis Oil," *Energy & Fuels*, 12 (1), 19-24.
- [5] Miller, R.S. and J. Bellan, 1997, "A Generalized Biomass Pyrolysis Model Based on Superimposed Cellulose, Hemicellulose and Lignin Kinetics," *Comb. Sci. and Techn.*, 126, 97-137.
- [6] Wang, D., S. Czernik, D. Montane, M.K. Mann, and E. Chornet, 1997, "Hydrogen Production via Catalytic Steam Reforming of Fast Pyrolysis Oil Fractions," Proceedings of the Third Biomass Conference of the Americas, Montreal, 845-854.
- [7] Matsunaga, Y., X. Xu, and M.J. Antal, 1997, "Gasification Characteristics of an Activated Carbon in Supercritical Water," *Carbon*, 35, 819-824.
- [8] Ghirardi, M.L., R.K. Togasaki, and M. Seibert, 1997, "Oxygen Sensitivity of Algal Hydrogen Production," *Appl. Biochem. Biotechnol.*, 63-65, 141-151.
- [9] Seibert, M., T. Flynn, D. Benson, E. Tracy, and M. Ghirardi, 1998, "Development of Selection/Screening Procedures for Rapid Identification of Hydrogen-Producing Algal Mutants with Increased Oxygen Tolerance," International Conference on Biological Hydrogen Production, Plenum, NY, in press.
- [10] Melis, A., J. Neidhardt, I. Baroli, and J.R. Benemann, 1998, "Maximizing Photosynthetic Productivity and Light Utilization in Microalgal by Minimizing the Light-Harvesting Chlorophyll Antenna Size of the Photosystems," International Conference on Biological Hydrogen Production, Plenum, NY, in press.
- [11] Szyper, J.P., B.A. Yoza, J.R. Benemann, M.R. Tredici, and O.R. Zaborsky, 1998, "Internal Gas Exchange Photobioreactor: Development and Testing in Hawaii," International Conference on Biological Hydrogen Production, Plenum, NY, in press.
- [12] Maness, P.-C. and P.F. Weaver, 1997, "Variant O₂-Resistant Hydrogenase from Photosynthetic Bacteria Oxidizing CO," Proceedings of the Fifth International Conference on the Molecular Biology of Hydrogenase, Albertville, France.
- [13] Weaver, P.F., P.-C. Maness, and S. Markov, 1998, "Anaerobic Dark Conversion of CO into H₂ by Photosynthetic Bacteria," International Conference on Biological Hydrogen Production, Plenum, NY, in press.
- [14] Khaselev, O. and J.A. Turner, 1998, "A Monolithic Photovoltaic-Photoelectrochemical Device for Hydrogen Production via Water Splitting," *Science*, 280, 425.
- [15] Rocheleau, R., 1998, "High Efficiency Photoelectrochemical H₂ Production using Multijunction Amorphous Silicon Photoelectrodes," *Energy & Fuels*, 12 (1), 3-10.

PRODUCTION OF HYDROGEN FROM HEMICELLULOSE-RICH FRACTIONS GENERATED THROUGH STEAM FRACTIONATION OF BIOMASS

S. CZERNIK, R. FRENCH, C. FEIK, AND E. CHORNET*

National Renewable Energy Laboratory
1617 Cole Boulevard, Golden, CO 80401

*Also affiliated with Université de Sherbrooke,
Sherbrooke, Québec, J1K 2R1 Canada

Keywords: biomass fractionation, hemicellulose, steam reforming

INTRODUCTION

Hydrogen is the most environmentally friendly fuel that can be efficiently used for power generation or transportation. At present, however, hydrogen is produced almost entirely from fossil fuels such as natural gas, naphtha, and inexpensive coal. In such a case, the same amount of CO₂ as that formed from combustion of those fuels is released during the hydrogen production stage. Renewable biomass is an attractive alternative to fossil feedstocks because of essentially zero net CO₂ impact. Unfortunately, hydrogen content in biomass is only 6-6.5% compared to almost 25% in natural gas. For this reason, on a cost basis, producing hydrogen by the biomass gasification/water-gas shift process cannot compete with the well-developed technology for steam reforming of natural gas. However, an integrated process, in which biomass is partly used to produce more valuable materials or chemicals with only residual fractions utilised for generation of hydrogen, can be an economically viable option.

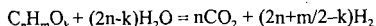
Biomass is comprised of three main constitutive bio-polymers: cellulose, hemicellulose, and lignin. When separated they can be further converted into commercial products of significantly higher value (especially cellulose) than that of the original biomass. Steam-aqueous fractionation is one of the technologies being developed for this application. The concept presented in this paper is an integration of steam-aqueous fractionation of biomass, with catalytic steam reforming of the lower-value hemicellulose-rich liquid by-product to produce hydrogen.

EXPERIMENTAL

Fractionation of poplar wood was performed in a continuous unit described elsewhere [1] employing steam treatment of poplar at a severity of $\text{Log } R_0 = 3.8$. Severity combines the effect of temperature and duration of the process using reaction ordinate defined as $\text{Log } R_0 = \text{Log } t + (T-100)/14.75$. This treatment led to solubilization, after washing, of 30% of the biomass into a hemicellulose-rich aqueous solution. The aqueous solution contained 32.1% of solutes having the elemental composition $\text{CH}_{1.36}\text{O}_{0.67}$. These solutes were mostly oligomeric pentosan and a small amount of dissolved lignin. The aqueous solution was then steam reformed using a bench-scale fluidized bed reactor shown in Figure 1. The two-inch-diameter Inconel reactor supplied with a porous metal distribution plate was placed inside a three-zone electric furnace. The reactor contained 150-200g of commercial nickel-based catalyst from United Catalysts ground to the particle size of 300-500 μ . The catalyst was fluidized using superheated steam, which is also a reactant in the reforming process. Steam was generated in a boiler and superheated to 750C before entering the reactor at a flow rate of 2-4 g/min. Liquids were fed at a rate of 4-5 g/min using a diaphragm pump. A specially designed injection nozzle supplied with a cooling jacket was used to spray liquids into the catalyst bed. The temperature in the injector was controlled by a coolant flow and maintained below the feed boiling point to prevent evaporation of volatiles and deposition of nonvolatile components. The product collection line included a cyclone that captured fine catalyst particles and any char generated in the reactor and two heat exchangers to condense excess steam. The condensate was collected in a vessel whose weight was continuously monitored. The outlet gas flow rate was measured by a mass flow meter and by a dry test meter. The gas composition was analyzed every 5 minutes by a MTI gas chromatograph. The analysis provided concentrations of hydrogen, carbon monoxide, carbon dioxide, methane, ethylene, and nitrogen in the outlet gas stream as a function of time of the test. The temperatures in the system as well as the flows were recorded and controlled by the G2/OPTO data acquisition and control system. The measurements allowed to determine total and elemental balances as well as to calculate the yield of hydrogen generated from the biomass-derived liquid feed.

RESULTS AND DISCUSSION

The overall steam reforming reaction of any oxygenated organic compound can be presented as follows:



Thus the maximum (stoichiometric) yield of hydrogen is $2+m/2n-k/n$ moles per mole of carbon in feed. Prior to the experiments of steam reforming complex biomass-derived liquids such as hemicellulose-rich solution obtained by biomass fractionation we performed tests using simpler model compounds (methanol, acetic acid, hydroxyacetaldehyde, syringol, and others). These tests were carried out using different commercial and research nickel-based catalysts designed for reforming natural gas and naphta. Results obtained employing a fixed-bed reactor configuration showed that within the temperature range 650-800°C and using commercial catalysts model compounds were converted to hydrogen with a yield greater than 85% of that possible for stoichiometric conversion [2-4]. However, the oligomeric compounds are more difficult to reform because of their tendency to decompose thermally in the reactor leading to char formation. The attempts of reforming hemicellulose-rich solutions in the fixed-bed reactor were not very successful [5]. After a short time (30 min), thermal decomposition led to the formation of carbonaceous deposits on and above the catalyst bed that resulted in an excessive pressure build-up in the system and made the deepest layers of the catalyst bed inaccessible to contact with the feed. Therefore, we decided to use a fluidized bed reactor for processing thermally unstable liquids because it exposes the whole amount of the catalyst to the contact with catalyst.

Steam reforming of the hemicellulose-rich liquid was carried out at the catalyst fluid bed temperature of 800°C with the feed rate of 4 g/min and steam flow of 2.4 g/min. The produced gas composition is shown in Figure 2. At the beginning of the run the hydrogen concentration was 65% but decreased to 60% after three hours on stream. This suggests that catalyst deactivated during the experiment. Hydrogen yield was 67.3% of that which could be obtained by stoichiometric conversion. Mass balances indicated that 73% of carbon from hemicellulose was converted to CO₂ and CO. The remaining 27% could thus form char entrained from the system and coke deposits on the catalyst surface, which would explain the loss of its activity. The activity of the catalyst used for reforming was easily restored by steam or carbon dioxide gasification of the deposits. The catalyst was reused in next experiments showing the same efficiency. The regeneration also resulted in producing additional amounts of hydrogen from the conversion of C (in coke) to CO + H₂ (in gas). At present, our efforts focus on finding optimum process conditions (temperature, steam to carbon ratio) to maximise hydrogen production and minimise coke formation.

CONCLUSIONS

Biomass can be a resource for hydrogen production providing that higher value fractions will be used for other applications. Hemicellulose-rich fraction from aqueous/steam fractionation of poplar wood was processed by catalytic steam reforming to generate hydrogen. So far tests have led to hydrogen yields of 67.3% of stoichiometric values. Fluidized bed is a better configuration than than fixed-bed reactor for reforming biomass-derived liquid streams that tend to decompose thermally producing undesired carbonaceous residues. Catalysts used for steam reforming can be efficiently regenerated by steam or carbon dioxide gasification. The reforming process needs to be optimised to determine conditions that allow for maximum (near stoichiometric) yields of hydrogen and minimum coke formation.

ACKNOWLEDGMENTS

The authors are thankful to the U.S. Department of Energy Hydrogen Program, managed by Mr. Neil Rossmessel and Ms. Catherine Grégoire-Padró, for financial support of this work.

REFERENCES

1. Heitz, M.; Capeck-Ménard, E.; Koeberle, P.G.; Gagné, J.; Chornet, E.; Overend, R.P.; Taylor, J.D.; and Yu, E.; *Bioresource Technology*, **1991**, 35, 23-32.
2. Wang, D.; Montané, D.; Chornet, E., *J. Appl. Catal. A* **1996**, 143, 245-270.
3. Wang, D.; Czernik, S.; Montané, D.; Mann, M.; Chornet, E., *Ind. Eng. Chem. Res.* **1997**, 36, 1507-1518.
4. Wang, D.; Czernik, S., and Chornet, E., *Energy&Fuels* **1998**, 12, 19-24.
5. Markevich, M.; Montané, D.; Wang, D.; Czernik, S., and Chornet, E., *Biomass for Energy and Industry, Proceedings of the International Conference, Würzburg, Germany, 8-11 June 1998*. Kopetz, H; Weber, T.; Palz, W.; Chartier, P; Ferrero, G.L., Eds., pp. 1648-1651.

Figure 1. Schematic of the 2" fluidized bed reactor system

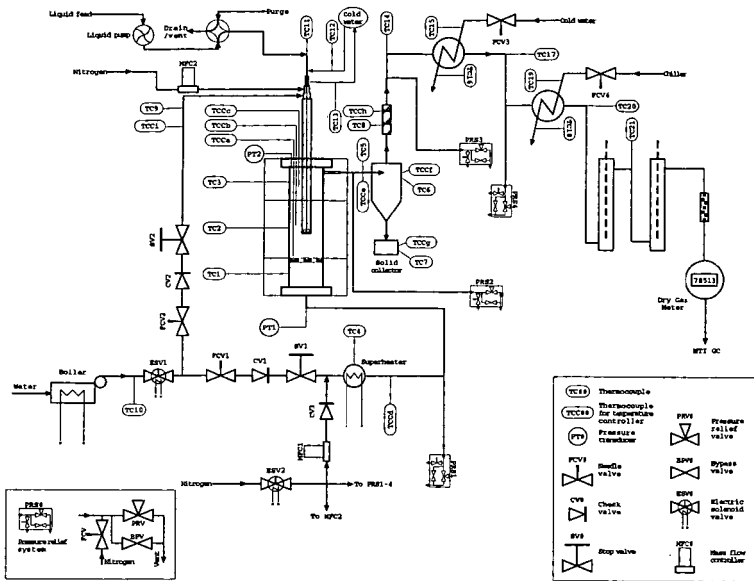
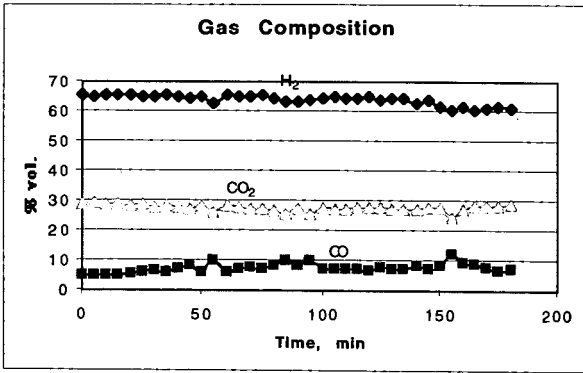


Figure 2. Gas composition from steam reforming of hemicellulose-rich fraction



RENEWABLE FUELS FROM THE GASIFICATION OF FOOD AND AGRICULTURAL WASTES

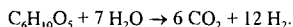
Xiaodong Xu and Michael Jerry Antal, Jr.

Hawaii Natural Energy Institute

University of Hawaii at Manoa, Honolulu, HI 96822

INTRODUCTION

Renewable fuels can be produced from biomass feedstocks such as food and agricultural wastes at a competitive price. One method of achieving this goal is the steam reforming of biomass (Antal, 1975):



In this idealized, stoichiometric equation, cellulose (represented as $C_6H_{10}O_5$) reacts with water to produce hydrogen and carbon dioxide, mimicking the commercial manufacture of hydrogen from methane by catalytic steam reforming chemistry. More realistically, a practical technology must be able to convert the cellulose, hemicellulose, lignin, and extractive components of the biomass feedstock to a gas rich in hydrogen and carbon dioxide, including some methane and carbon monoxide. Unfortunately, biomass does not react directly with steam to produce the desired products. Instead, significant amounts of tar and char are formed, and the gas contains higher hydrocarbons in addition to the desired light gases (Antal, 1978, 1983, 1985). The recent work of Corella and his colleagues (Herguido et al., 1992) nicely illustrated this situation. In a fluid bed operating at atmospheric pressure Corella's group observed yields of char from the steam gasification of wood sawdust in the range of 20 to 10 wt %, and yields of tar decreasing to 4 wt % as the temperature of the bed increased from 650 to 775 °C. But at the highest temperature, only 80% of the carbon in the feedstock is converted to gas. By employing a secondary, fluidized bed of calcined dolomite operating at 800 to 875 °C, Corella and his co-workers (Delgado et al., 1997) were able to convert almost all of the tar to gas. Nevertheless, the char byproduct was not converted and represents an effective loss of gas.

The objective of this work is to define conditions which enable the steam reforming of biomass feedstocks such as food and agricultural wastes to produce renewable fuels.

EXPERIMENTAL

The gasification reactor (see Figure 1) is fabricated from Hastelloy C276 tubing with 9.53 mm OD x 6.22 mm ID x 1.016 m length (Xu et al., 1996; Matsumura et al., 1997). The feedstock is quickly heated by an annulus heater (located along the reactor's centerline) and an entrance heater outside the reactor to temperatures above 650 °C. The annulus heater (3.18 mm OD x 15.2 cm heated length) delivers all its heat directly to the feed. The entrance heater is made from a split stainless steel tube that is held in good thermal contact with the reactor, and an electrical heater coiled around the outer surface of the stainless steel tube. Downstream of the entrance heater, the reactor's temperature is maintained in an isothermal condition by a furnace. The chief purpose of the furnace is to prevent heat loss. Most of the heat required to lift the feedstock flow to reaction temperature is provided by the entrance heater and the annulus heater. Carbon catalyst is usually packed in about 60% of the heated zone of the reactor, as well as to the downstream cold section of the reactor. The reactor's temperature profile is monitored by 12 fixed, type K thermocouples held in good thermal contact with the reactor along its outer wall. The feedstock reaches to a peak temperature at the end of the heat up/cracking zone. Pressure in the reactor is measured by an Omega PX302 pressure transducer. A Grove Mity-Mite model 91 back-pressure regulator reduces the pressure of the cold, two-phase, product effluent from 28 to 0.1 MPa. After leaving the back-pressure regulator, the reaction products pass through a gas-liquid separator. The liquid product is collected over a measured time period to calculate the liquid outlet flow rate. The gas flow rate is measured using a wet test meter.

The feedstock is usually made of about 10 wt% biomass with about 4 wt% corn starch. The biomass is ground with a Wiley mill (Thomas Scientific) to 40 mesh before mixed with corn starch to form a paste. The feeder consists of a cylinder, a movable piston, and two end-caps (High Pressure Equipment). The cylinder is first filled with the paste feedstock, then the piston is placed on top of the feed, and the two end-caps are installed. Both the feeder and the reactor are pressurized separately to 28 MPa at the beginning of a run. During the time that the system is being brought up to temperature, water is pumped into the reactor by a Waters 510 HPLC pump. When the main body of the reactor reaches the desired temperature (usually about 650 °C), the feeder is connected to the reactor. Thereafter, water flow to the reactor is terminated, and water flow to the feeder is initiated, displacing the paste feedstock into the reactor. Because the thermophysical properties of the paste are considerably different than those of water, and possibly also because of exothermic pyrolysis reactions associated with the decomposition of the paste, the temperature of the feed rises very rapidly in the entrance region of the reactor. To

avoid excessively high temperatures, usually it is necessary to reduce the heat input to the feed from the annulus heater and the entrance heater.

Gas samples are taken by gas-tight syringes from the gas sample outlet of the separator. Analysis of the gas is conducted using a Hewlett-Packard model 5890 gas chromatograph equipped with flame ionization and thermal conductivity detectors. A 80/100 mesh carbosphere molecular sieve packed column is used, operating at 35 °C for 4.2 min, followed by a 15 °C/min ramp to 227 °C, another ramp of 70 °C/min to 350 °C, and a 5 min hold at 350 °C. The carrier gas is a mixture of 8% hydrogen in helium (AIRCO). A standard gas mixture obtained from AIRCO is used for day-to-day calibration. The COD in the liquid effluent is determined by a HACH COD analyzer.

RESULTS AND DISCUSSION

The poplar wood sawdust paste was made by mixing sawdust into a starch gel. Large quantities of wood sawdust are available at \$30 per dry ton, and the quoted price of corn starch in bulk is \$0.12 per pound. Using these values, the price of a 10 wt% sawdust with 4 wt% starch paste is \$0.045 per pound. For comparison, the price of low sulfur coal is about \$0.025 per pound. Sawdust paste gasification results from two runs are displayed in Table 1. Complete gasification was achieved in both cases. The product gas was composed of mainly hydrogen, carbon dioxide, methane, and a trace of carbon monoxide. The gas product distribution was effectively identical between these two runs.

Table 2 displays results from the gasification of three feedstocks, sugar cane bagasse with corn starch, banagrass with corn starch, and onion with corn starch. In all three cases, the gas products consisted of about 28% hydrogen, 44% carbon dioxide, 24% methane, and 2% carbon monoxide, however, the runs with banagrass and onion were prone to plugging. As a result, the gas yield, and the carbon efficiency were significantly reduced due to carbon deposits on the reactor wall.

As mentioned earlier, carbon catalyst was usually packed in about 60% of the heated zone of the reactor. The reaction temperature reached to its peak value at the end of the heat up /cracking zone. Figure 2 shows the effect of peak temperature on the gasification of 10.6 wt% poplar wood sawdust with 4.0 wt% corn starch while keeping the catalyst bed temperature at 710°C. As the reactor peak temperature increased the hydrogen yield increased while the methane yield decreased, indicating high peak temperatures favored the methane steam reforming reaction.

To gain insight into the role of the reactor's wall as a catalyst for the steam reforming reaction, we wrapped the annulus heater with a nickel wire. We estimated that the surface area of the wire was about 30% of the surface area of the hot region of the reactor. As seen in Table 3, the results indicate that nickel has no special effect on the reaction chemistry. Molybdenum is another important component of Hastelloy, the alloy that the reactor is made of. To test its effect on the reaction chemistry, we mixed molybdenum powder with sawdust paste and delivered it to the reactor. The metal powder catalyzed char forming reactions which significantly reduced the gas yield, the carbon efficiency, and the global mass balance. Evidently, molybdenum is not a catalyst for the gasification reactions.

The liquid water effluent from the reactor usually has a neutral pH value, no color, and is odorless. Table 4 lists the COD (Chemical Oxygen Demand) measurements of the liquid effluent from the reactor. The mineral concentration of tap water was measured by drying tap water in an oven at 105°C. It is clear that there was only a trace of organics in the liquid effluent.

CONCLUSIONS

1. Onion, sugar cane bagasse, banagrass, poplar sawdust, and other food and agricultural wastes can be mixed into a corn starch gel (5 wt% or less) to form a thick paste. This paste is easily delivered to a supercritical flow reactor by a feeder.
2. Food and agricultural wastes can be steam reformed over a carbon catalyst to a gas composed of hydrogen, carbon dioxide, methane, and a trace of carbon monoxide. The liquid water effluent from the reactor has a low COD value, neutral pH, no color, and is odorless.
3. Coconut shell activated carbon catalyst is effective for the conversion of organic feedstocks, however, nickel and molybdenum have no catalytic effect on the gasification reactions.
4. High peak temperatures favor the methane steam reforming reaction.

ACKNOWLEDGEMENT

This work is Supported by NREL/DOE under cooperative agreement DE-FG36-94AL85804, and the Coral Industries Endowment of the University of Hawaii at Manoa. We thank Neil Rosmeissl (DOE), Dr. Ralph Overend (NREL), Dr. Patrick Takahashi and Dr. Richard Rocheleau (UH) for their interest in this work. The authors also thank Sonia Campbell (UH) and Dr. Heije Westberg (Chalmers University of Technology, Sweden) for their assistance with the experiments and discussion.

REFERENCES

- Antal, M.J. In *Hydrogen Energy, Part A*; Veziroglu, T.N., Ed.; Plenum: New York, 1975.
- Antal, M.J. In *Energy from Biomass and Wastes*; Klass, D.L., Ed.; I.G.T.: Chicago, 1978.
- Antal, M.J. "Effects of Reactor Severity on the Gas-Phase Pyrolysis of Cellulose- and Kraft Lignin-Derived Volatile Matter". *Ind. Eng. Chem. Prod. Res. Dev.* Vol. 22, 366-375, 1983.
- Antal, M.J. In *Fundamentals of Thermochemical Biomass Conversion*; Overend, R.P., Milne, T.A., Mudge, L.K., Ed.; Elsevier: London, 1985.
- Delgado, J.; Aznar, M.P.; Corella, J. "Biomass Gasification with Steam in Fluidized Bed: Effectiveness of CaO, MgO, and CaO-MgO for Hot Raw Gas Cleaning". *Ind. Eng. Chem. Res.* Vol. 36, 1535-1543, 1997.
- Herguido, J.; Corella, J.; Gonzalez-Saiz, J. "Steam Gasification of Lignocellulosic Residues in a Fluidized Bed at a Small Pilot Scale. Effect of the Type of Feedstock". *Ind. Eng. Chem. Res.* Vol. 31, 1274-1282, 1992.
- Matsumura Y.; Xu, X.; Antal, M.J. "Gasification Characteristics of an Activated Carbon in Supercritical Water". *Carbon*, Vol. 35, 819-824, 1997.
- Xu, X.; Matsumura Y.; Stenberg, J.; Antal, M.J. "Carbon Catalyzed Gasification of Organic Feedstocks in Supercritical Water". *Ind. Eng. Chem. Res.* Vol. 35, 2522-2530, 1996.

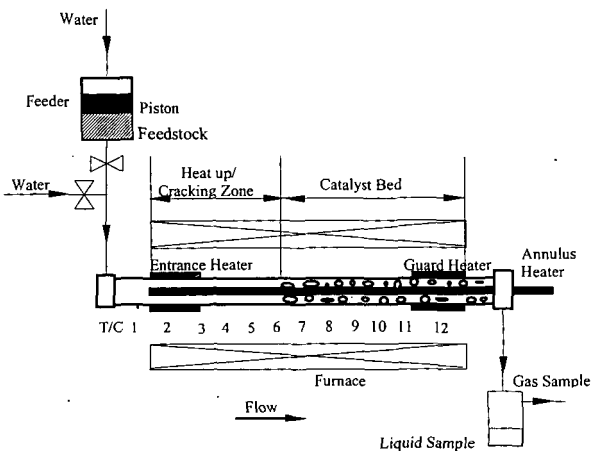


Figure 1. Gasification Reactor.

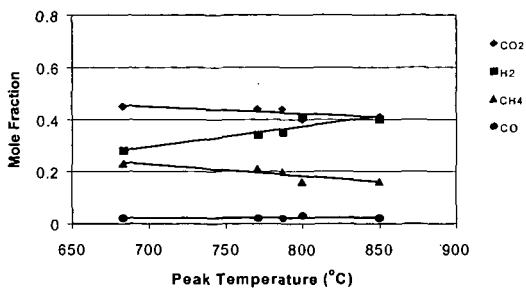


Figure 2. Effect of Peak Temperature on the Gasification of 10.6 wt% Poplar Wood Sawdust with 4.0 wt% Corn Starch (Catalyst Bed Temperature: 710°C).

Table 1. Gasification of Poplar Wood Sawdust /Corn Starch with Coconut Shell Activated Carbon Catalyst in Supercritical Water at 28 MPa.

Experiment Date	12/17/97	4/21/98
Feedstocks (dry basis)	Sawdust 9.47 wt% + Corn Starch 3.55 wt%	Sawdust 10.64 wt% + Corn Starch 3.88 wt%
Reactor Peak Temp / Catalyst Bed Temp	750°C/ 700°C	739°C/ 710°C
Flow Rate (g/min)	2.0	
Time on Stream (hr)	1.37	1.95
Product	Mole Fraction	
H ₂	0.27	0.26
CO	0.02	0.02
CO ₂	0.46	0.46
CH ₄	0.24	0.23
Total Gas Yield (L gas /g solid in feed)	1.36	1.15
(g gas /g solid in feed)	1.34	1.21
C Efficiency	0.98	0.96
Global Mass Balance	0.95	1.00

Table 2. Gasification of Food and Agricultural Wastes with Coconut Shell Activated Carbon Catalyst in Supercritical Water at 28 MPa.

Experiment Date	5/6/98	6/3/98	6/24/98
Feedstock (dry basis)	Sugar cane bagasse 10.70 wt% + Corn starch 4.28 wt%	Banagrass 11.70 wt% + Corn starch 4.60 wt%	Onion 11.10 wt% + Corn starch 4.20 wt%
Flow Rate (g/min)	2.0		
Reactor Peak Temp / Catalyst Bed Temp	749°C/ 716°C	751°C/ 717°C	750°C/ 716°C
Time on Stream (hr)	1.23	0.73	0.96
Product	Mole Fraction		
H ₂	0.28	0.30	0.28
CO	0.02	0.02	0.02
CO ₂	0.44	0.44	0.44
CH ₄	0.23	0.24	0.25
Total Gas Yield (L gas /g solid in feed)	1.16	1.02	1.06
(g gas /g solid in feed)	1.22	1.02	1.02
C Efficiency	0.97	0.72	0.80
Global Mass Balance	1.02	0.93	0.92

Table 3. Effect of Metal Catalyst on the Gasification of Poplar Wood Sawdust / Corn Starch in a Reactor with a Packed Coconut Shell Activated Carbon Bed in Supercritical Water at 28 MPa.

Experiment Date	2/12/98	2/19/98	12/17/97
Feedstocks (dry basis)	Sawdust 10.04 wt% + Corn Starch 3.65 wt%	Sawdust 10.5 wt% + Corn Starch 3.8 wt%	Sawdust 9.47 wt% + Corn Starch 3.55 wt%
Metal Catalyst	Ni Wire (wrapped around annulus heater)	Mo Powder (mixed in the Feedstock)	None
Reactor Peak Temp / Catalyst Bed Temp	740°C/ 715°C	730°C/ 680°C	750°C/ 700°C
Flow Rate (g/min)	2.0		
Time on Stream (hr)	1.53	0.60	1.37
Product	Mole Fraction		
H ₂	0.31	0.29	0.27
CO	0.02	0.02	0.02
CO ₂	0.42	0.46	0.46
CH ₄	0.24	0.21	0.24
Total Gas Yield (L gas/g solid in feed)	1.16	0.90	1.36
(g gas/g solid in feed)	1.22	0.90	1.34
C Efficiency	0.91	0.66	0.98
Global Mass Balance	0.97	0.89	0.95

Table 4. COD Measurements of the Liquid Effluent from the Reactor.

Experiment Date	Feedstock	COD in Liquid Effluent
4/21/98	Poplar Sawdust /Corn Starch	56 mg/L
6/24/98	Onion /Corn Starch	64 mg/L
8/10/98	Tap Water	Mineral Concentration 250 mg/L

PYROLYSIS OF BIOMASS MODEL COMPOUNDS USING FLASH VACUUM PYROLYSIS: MECHANISMS OF POLYCYCLIC AROMATIC HYDROCARBONS FORMATION

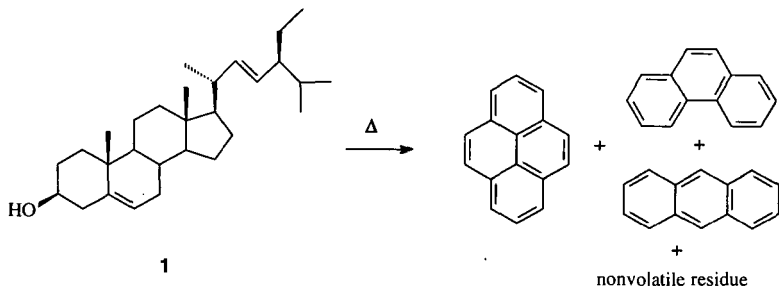
Jeffrey R. Ammann, Phillip F. Britt, and A. C. Buchanan, III, Chemical and Analytical Sciences Division, Oak Ridge National Laboratory, P. O. Box 2008, Oak Ridge TN 37831-6197

KEYWORDS: Pyrolysis mechanisms, biomass model compounds, polycyclic aromatic hydrocarbons

INTRODUCTION

There is a sharp contrast between the level of interest in the formation of polycyclic aromatic hydrocarbons (PAHs) and the level of understanding of their formation pathways. PAHs are classically formed from the incomplete combustion of carbon resources such as coal, petroleum, and biomass.¹ PAHs have also been found in emissions from incineration of plastic solid waste (polyethylene, polystyrene, polypropylene, and PVC),² emissions from home heating systems,³ and in sites adjacent to high volume vehicle areas.⁴ The formation of PAHs is of great interest in the thermal processing of carbonaceous materials, but there have been few detailed mechanistic studies on their formation pathways, and many of the mechanistic details, such as reaction intermediates and rate controlling step, are still largely unknown.

We are interested in the formation of PAHs in the thermal processing of coal and biomass into liquid products. Biomass model compounds such as plant sterols are known to yield PAHs under pyrolytic conditions. Badger et al. showed that atmospheric pyrolysis of stigmasterol (1)



at 700 °C yielded a complex mixture of hydrocarbons including pyrene, phenanthrene, and anthracene.⁵ Although the authors speculated on possible mechanisms of PAH formation, there was no direct evidence for the proposed intermediates and reaction pathways. The pyrolysis of cholesterol has also been investigated in sealed tubes under conditions to simulate geochemical transformations (140 °C, 16 h).^{6a,b} The degradation products included cholestane, cholestene isomers, and unidentified aromatic compounds; however, these studies were done on sediment support which may have induced acidic catalysis. Although there have been many studies on the formation of PAHs via thermal degradation of natural products, the reaction mechanisms and intermediates remain unclear.

The objective of this study is to gain fundamental insight into the reaction pathways that lead to PAHs in biomass model compounds. Flash vacuum pyrolysis (FVP) and atmospheric flow pyrolysis will be used as mechanistic probes for the identification of reaction intermediates and reaction pathways in the formation of PAHs. This investigation will focus on the pyrolytic degradation of plant sterols such as β -sitosterol (2a) and stigmasterol (1).

EXPERIMENTAL

Benzene (EM) was freshly distilled from lithium aluminum hydride prior to use. Tetrahydrofuran (J.T. Baker, HPLC grade) was freshly distilled from potassium/benzophenone ketyl prior to use. β -Sitosterol (Acros, mixture of 79.6% β -sitosterol, 12.5% campersterol, and 7.6% stigmasterol by GC) was used without further purification. Gas chromatography was performed using a Hewlett-Packard 5890 Series II gas chromatograph equipped with a J&W Scientific 30 m \times 0.25 mm id, 0.25 μ m film thickness DB-1 column and a flame ionization detector. Mass spectra were obtained at 70 eV on a Hewlett-Packard 5972 GC-MS equipped with a capillary column identical with that used for GC analysis. Relative molar responses were measured against *n*-tetradecane which was used as an internal standard.

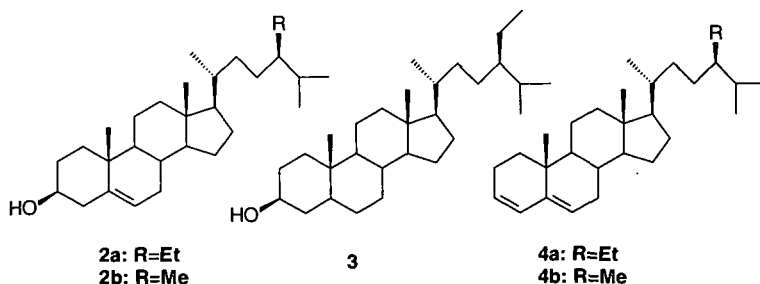
FVP Conditions: In a typical run, the substrate (typically 200 mg) was weighed into a pyrex sample chamber. The sample was warmed via an aluminum shroud wrapped with heat tape surrounding the sample chamber. The temperature of the shroud was monitored via a thermocouple. The sample chamber was attached to a 26 in. quartz tube (25 mm O.D.) via a 40/35 ground glass joint. The tube was packed with quartz chips (18 in.) to increase the residence time in the furnace. The other end of the quartz tube contained a right angle elbow with an O-ring joint (size 226) coupled to a Trahanovsky-style cold trap. The elbow was wrapped with heat tape and heated to ~65 °C to prevent deposition of the pyrolysate upon exiting the oven. The pyrolysis tube was heated by a horizontally mounted Carbolite tube furnace (model TZF 12/38/400) operating at a temperature range of 400 - 700 °C (± 2 °C). The high vacuum end of the trap was equipped with an O-ring joint (size 226) that coupled to a vacuum connector. The sample chamber, quartz tube and trap were connected in series to an Edwards diffusion pump (model EO50/60) with a Welch DuoSeal mechanical backing pump (model 1405). High vacuum pressures ($>10^{-3}$ Torr) were detected with a Hastings vacuum gauge; low vacuum pressures ($<10^{-3}$ Torr) were detected with a Varian 571 Bayard-Alpert type hot filament ionization gauge head with a Varian Multi-Gauge display. FVP runs were typically performed at a baseline pressure range of $2.0\text{-}7.0 \times 10^{-5}$ Torr.

Preparation of *p*-Toluenesulfonic acid (3%)/Silica gel Dehydrating Reagent⁷: A solution of *p*-toluenesulfonic acid monohydrate (2.96 g, 15.6 mmol) in acetone (20 mL) was added in one portion with rapid stirring to silica gel (99.96 g, Baker Analyzed, 60-200 mesh) in a 500 mL triple-neck round bottom flask equipped with an overhead mechanical stirrer. The mixture was stirred for 1 h at RT in an argon atmosphere. A vacuum adapter was attached to the flask and the volatiles were removed *in vacuo* (1.5 Torr) at 45-55°C with stirring. The TsOH/silica gel reagent was stored in a tightly stoppered round bottom flask prior to use.

Dehydration of β -Sitosterol: A solution of β -sitosterol (0.83 g, 2.0 mmol) in dry benzene (170 mL) was added to 12.01 g TsOH/silica gel (3%) in a 500 mL round bottom flask equipped with a reflux condenser. The mixture was refluxed for 2 h in an argon atmosphere. The flask was allowed to cool to RT followed by addition of petroleum ether (100 mL, low boil). The contents of the flask were filtered through a 2 in. pad of silica gel and eluted with 1:1 benzene/petroleum ether (*v/v*). Solvent was removed from the filtrate *in vacuo* and the residue was flash chromatographed twice on silica gel using 100% hexane as the eluent. The yield of dehydration product **4a** was 0.33 g (0.84 mmol; 42% yield; 85% purity by GC); GCMS: *m/z* 396, (M^+ , 100%).

RESULTS AND DISCUSSION

The β -sitosterol was a mixture composed of three major compounds discernible by GC: β -sitosterol (**2a**), stigmastanol (**3**), and campesterol (**2b**) with effective (GC) molar ratios of 10.5, 1.7, and 1.0, respectively. We will focus on the pyrolysis pathways of **2a** since the pyrolysis of the methyl derivative **2b** should be very similar. The FVP of **2a** was investigated from



400 - 700 °C to determine the primary pyrolysis product in the degradation of sterols. The principal product observed by GC from the FVP of **2a** and **2b** is stigmasta-3,5-diene **4a** and **4b** respectively. Chemical confirmation was established through comparison of the GC retention times and MS data of the pyrolysate with an authentic sample of **4a** prepared by dehydration of **2a**. No other products (peaks) of any significance were observed by GC or GC-MS analysis. Figure 1 shows a plot of the percent conversion of **2a** and percent formation of dehydration product **4a** versus pyrolysis temperature. At lower FVP temperatures (< 500 °C), the data show a trend that correlates the disappearance of **2a** with the appearance of **4a**. At higher

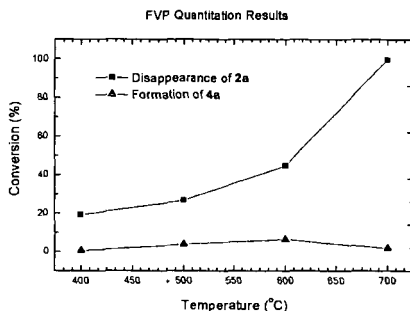


Figure 1. Conversion of **2a** and formation of **4a** as a function of temperature.

pyrolysis temperatures, a nonlinear increase in the disappearance of **2a** occur with concomitant decrease in the formation **4a**. This is an indication that at higher temperatures, either the dehydration products **4a** are undergoing secondary pyrolysis or a mechanism other than dehydration is operating. We are currently investigating the pyrolysis of dehydration product **4a** to determine if it forms PAHs. Preliminary results show that **4a** readily decomposes at 500 °C (36.2 % conversion) but few products are observed by GC analysis.

There is a significant discrepancy between the yield of **4a** (1-6 %) and the recovery of **2a** (see Figure 1). This discrepancy in mass balance may be due to fragmentation of the steroidal skeleton to form gaseous hydrocarbons. At high temperatures and low pressures, β -scission is faster than bimolecular hydrogen abstraction. Hydrocarbon radicals tend to break down all the way to a methyl radical or hydrogen atom and several molecules of ethylene (i.e. the Rice-Kossiakoff mechanism). We are investigating the formation of light gases from the FVP of **2a** by GC-MS and pyrolysis-GC-MS. We are also investigating the possibility that **2a** is undergoing a bimolecular condensation to form an ether which might not be volatile and would escape GC detection. We are currently screening the reaction mixtures by HPLC with refractive index detection.

Preliminary results have also been obtained on the atmospheric pyrolysis of **2a** at 500 °C. The major product by GC analysis is **4a**, i.e. dehydration. A significant number of products are formed in low yields. We are currently screening the reaction mixture by reverse-phase HPLC with diode array detection and GC-MS for PAHs.

ACKNOWLEDGMENT

This research was sponsored by Philip Morris USA and the Division of Chemical Sciences, Office of Basic Energy Sciences, U.S. Department of Energy under contract DE-AC05-96OR22464 with Oak Ridge National Laboratory, managed by Lockheed Martin Energy Research Corporation.

REFERENCES

- (1) Jacob, J. *Pure & Appl. Chem.* **1996**, *68*, 301.
- (2) Durlak, S.K.; Biswas, P.; Shi, J.; Bernard, M.J. *Environ. Sci. Technol.* **1998**, *32*, 2301.
- (3) Launhardt, T.; Strehler, A.; Dumler-Grادل, R.; Thoma, H.; Vierle, O. *Chemosphere* **1998**, *37*, 2013.
- (4) Muller, J.F.; Hawker, D.W.; Connell, D.W. *Chemosphere* **1998**, *37*, 1369.
- (5) Badger, G.M.; Donnelly, J.K.; Spotswood, T.M. *Aust. J. Chem.* **1965**, *18*, 1249.
- (6) (a) Sieskind, O.; Joly, G.; Albrecht, P. *Geochimica et Cosmochimica Acta* **1979**, *43*, 1675. (b) A similar experiment with a series of sterols that included β -sitosterol has been published, however, no data on the thermolysis products was given. Shanchun, J.; O'Leary, T.; Volkman, J.K.; Huizhi, Z.; Rongfen, J.; Suhua, Y.; Yan, W.; Zuofeng, L.; Zuoqing, S.; Ronghua, J. *Org. Geochem.* **1994**, *21*, 415.
- (7) D'Onofrio, F.; Scettri, A. *Synthesis* **1985**, 1159.

FORMATION OF AROMATIC HYDROCARBONS FROM PYROLYSIS OF CARBOHYDRATES

Mohammad Hajaligol, Bruce Waymack, and Diane Kellogg
Philip Morris USA Research Center, P. O. Box 26583, Richmond, VA. 23261

KEYWORDS: Pyrolysis, Carbohydrates, Cellulose, Glucose, Pectin, Aromatic Hydrocarbons

INTRODUCTION

Formation of aromatic hydrocarbons is one of the major areas of interest in pyrolysis and combustion processes (1-5). The secondary cracking of initial pyrolysis products in the gas phase is considered to be the major pathway producing aliphatic and aromatic hydrocarbons under conditions approaching flaming combustion. A second, but less studied route for aromatics formation is evolution of aromatics from the solid char as it is formed and degassed during the pyrolysis process. While this second route may not be important in flaming combustion, it may be of significant importance in the smoldering combustion of solids. Under these conditions, the char generated during the primary pyrolysis is the fuel for sustained combustion (6-7). Furthermore, the products generated during primary pyrolysis have little probability of experiencing a higher temperature than the temperature at which they were formed.

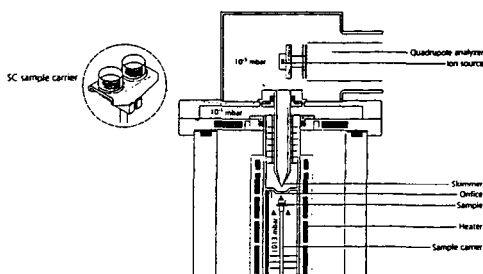
The ongoing research at Philip Morris USA is directed toward studying the significance of the latter route in the production of aromatic hydrocarbons. Numerous literature reports on the secondary pyrolysis of biomass primary products (8-14) exist, but there has been little emphasis on the formation of aromatic hydrocarbons (2, 5, 11). This is likely due to the lower probability of forming aromatic structures from pyrolysis of heavily oxygenated species. Furthermore, to the Authors best knowledge, there is little literature reporting this second pathway during pyrolysis. The most notable exception is the work of Shafizadeh and his co-workers (15, 16) which focused on the aromatic structure formed in the char during pyrolysis, but not on the evolution of gaseous chemical species from the char during the charring process.

In this study, the second route for formation of aliphatic and aromatic hydrocarbons is examined using small sample sizes (1-20 mg) of starting material; and in order to eliminate the possibility of including gas-phase secondary cracking of the primary pyrolysis products, pre-charred samples of starting materials are separately prepared and pyrolyzed under identical conditions to the starting materials. The major plant carbohydrates cellulose, glucose, and pectin, are used as the starting materials. The starting materials were pyrolyzed at constant heating rates from 5 - 60 °C/min up to a temperature of 1000 C in a TG/DSC/MS. Complementary data was also collected on the same materials by pyrolyzing them in a CDS Pyroprobe followed by analysis of products in a GC/MS. Under our experimental conditions, aliphatic and aromatic hydrocarbons evolve over the temperature range of 350 °C - 600 °C, with hydrogen continuing to evolve above 600 °C. We observed one evolution temperature for small aliphatic compounds; and a second evolution temperature for the larger aliphatic and aromatic compounds. Some kinetic parameters for hydrocarbon formation are deduced and discussed.

EXPERIMENTAL PROCEDURES

The main experimental setup for this study is a Netzsch TG/DSC/MS. A schematic of the reaction zone and sampling system is shown in Figure 1.

Figure 1.
Schematic of TG/DSC/MS



The carrier gas flows upward and around the sample pan and leaves the reaction zone quickly to evacuate the volatile products evolved from the reaction zone, thereby reducing the probability of secondary reaction of these volatile products. The sample probe for the MS is located about 5 mm above the sample, in order to minimize the time lag between reaction time and sampling time. About 10 mg of pure material (or about 20 mg of previously charred material) is heated in flowing helium (150 cc/min) at constant heating rates of 5-60 °C/min. From this experimental data, we obtained temperature dependent weight loss profiles, rate of weight loss, heat of reaction, and the evolution profiles of volatile products as determined by key masses monitored by the MS.

The second experimental setup used in this study is a CDS Pyroprobe pyrolysis device interfaced to a Varian Saturn GC/MS for analysis of volatile products. For these experiments, samples of about 1 mg of pure or previously charred materials are pyrolyzed in helium and the volatile products are swept into the GC/MS for analysis. The pyroprobe samples are heated to the set temperature at about 100 °C/sec and held there for 20 sec. The set temperature for the pure pectin and glucose are 300 °C and for the cellulose is 360 °C. The pyrolysis temperature for all the chars samples was 900 °C. The PP/GC/MS data was used to aid identification and relative quantification of the TG/MS results.

Starting materials are reagent grade d-glucose (Acros, less than 0.004% ash); practical grade citrus pectin (Acros, less than 1% ash, and 70 % esterification); and two forms of cellulose. The first cellulose sample is Whatman #41 filter paper (less than 0.007% ash), and the second is a griegre (raw) cotton duck fabric from Wellington-Sears (duck #4, average 5000 ppm K). The latter cellulose sample is used to study the effects of inorganic species which are known to affect cellulose decomposition reactions and char yield. Pre-charred samples of the above materials are prepared in a tube furnace in flowing helium (200 ml/min) heating at 20 °C/min up to 300 °C for glucose and pectin, and 360 °C for cellulose. To ensure the primary decomposition of the materials is complete, samples are held for 10 minutes at the final temperatures.

RESULTS AND DISCUSSION

Primary Decomposition

First, we characterize the primary decomposition of the pure materials and then discuss the evolution of hydrocarbons from the chars. Glucose is the basic building block of cellulose, and it undergoes major decomposition in the temperature range of 200-400 °C with peaks at 230 and 270 °C. The DSC data shows that glucose melts at about 150 °C and undergoes some endothermic processes up to 300 °C, and then it goes through a mildly exothermic process. The major products of glucose pyrolysis detectable by MS are H₂O, CO₂, CO as well as furans and furfural derivatives. Glucose produces about 35% char at 300 °C and about 15% char at 1000 °C. Aliphatic and aromatic hydrocarbons are evolved from glucose starting about 350 °C where the primary decomposition of the material is largely complete and continues until about 600 °C. Hydrogen continues to evolve at higher temperatures.

Pectin undergoes a major decomposition in the temperature range of about 200 - 300 °C which continues through about 400 °C. Pectin undergoes melting at about 150 °C with a second major endothermic process around 250 °C followed by an exothermic process during the major weight loss around 300 °C. Pectin produces about 40% and 25% char at about 300 °C and 1000 °C respectively. The primary pyrolysis products of pectin are similar to glucose with the exception of increased amounts of methanol and large esters. Pectin, like glucose, begins to produce hydrocarbons above 350 °C and continues to produce H₂ after the hydrocarbons production ceases around 600 °C.

The presence of impurities is known to affect the decomposition pathways during cellulose pyrolysis. We used both "pure" and "impure" cellulose samples. The pure Whatman paper decomposes in one sharp endothermic process starting at about 320 °C and peaking at 365 °C. This cellulose sample produces about 10 % char at 400 °C and about 5 % char at 1000 °C. The cotton duck material was a raw cotton cellulose with about 5000 ppm K as well as other naturally occurring inorganic species. The cotton duck peak decomposition was at about 355 °C. The most notable differences between the two cellulose samples is that the cotton decomposition is less endothermic, approximately -100 J/g compared to approximately -470 J/g for the pure cellulose. The amount of char produced by the cotton duck is about 25 % at 400 °C and about 16 % at 1000°C, comparing to 10% and 4% at the same temperature for the pure cellulose. The major products detectable by MS for cellulose decomposition are H₂O, CO₂, and CO, as well as some aldehydes, furans, pyrones and other oxygen-containing products (levoglucosan). Another notable difference in the MS profiles of the pure cellulose and cotton fabric is a much higher ratio of mass 31 to mass 60 for the cotton, indicating much less levoglucosan (predominately mass 60) relative to mass 31 (probably mostly hydroxyacetaldehyde). This is consistent with previous literature (ref.) reports.

Hydrocarbon Formation

Now, we focus our attention on the formation of hydrocarbons from pyrolysis of the above carbohydrates. Pyrolysis of previously charred samples eliminates the probability of including any secondary reactions of the primary products, as well as focusing on the temperature ranges where hydrocarbons evolve from these materials under the pyrolysis conditions in this study. Figure 2 shows the temperature dependence for masses 2, 15, 27 and 78, representing primarily H_2 , CH_4 , C_2 hydrocarbons, and benzene from pectin char. Our data indicate similar temperature dependence for masses 78 and 92, primarily benzene and toluene, for untreated glucose and pectin, and their respective chars. We have used masses 78, 92, 106, 116, 118, 128, 166, and 178 to follow evolution profiles of aromatics from the carbohydrates. Figure 3 is an example showing masses 78, 92, 128 and 178 representing primarily benzene, toluene, naphthalene and anthracene/phenanthrene from cotton duck char. These data show that all the hydrocarbons from these chars evolve over a similar temperature range with a few exceptions, such as the evolution of CH_4 and benzene (second peak) at above 500 °C and H_2 at temperatures above 600°C. The presence of these chemical species from the char materials is confirmed by the Pyroprobe/GC/MS data showing that these compounds generally account for most of or are the major compound contributing to the above ascribed masses. However there are other compounds that contribute to different extents to the specific masses monitored during pyrolysis. Other benzoid compounds (such as benzenediols and coumaranone) contribute to mass 78. There were significant oxygenated compounds (pyrones) contributing to mass 128 for cellulose. We are continuing to investigate all the products contributing to masses used to monitor aromatic hydrocarbons.

These experimental results indicate that substituted benzene, larger aromatic and aliphatic hydrocarbons evolve first, and as they are depleted, continued evolution of CH_4 and benzene occurs, and as these are depleted evolution of H_2 continues. At this point, a highly carbonaceous char has been produced. This is consistent with Shafizadeh's work (15) where he studied the aliphatic and aromatic concentration of char as a function of temperature. Shafizadeh did not measure the evolved gases in his study, but his data on the solid concentration and our data on the evolved gases over the temperature range studied matches well. From comparing mass 78 profiles from the different carbohydrate chars, the relative distribution of benzene in the two peaks differs among the carbohydrates. Glucose and pure cellulose char are very similar, the pectin and cotton chars produce more benzene above 500°C. The pectin, glucose and pure cellulose all produced comparable amounts of benzene, the cotton produced more benzene which may be an effect of the high inorganic content. A table of relative amounts of some aromatics (using pyroprobe/GC/MS experiments) from the chars are presented in Table 1.

Table 1. Relative abundance of different masses from pyrolysis of carbohydrates

	78	92	106	116	118	128	166	178
Pectin	91,372	143,892	123,503	19,587	50,444	63,436	7,915	12,878
Cotton	1,343,907	209,604	221,938	48,996	34,142	141,962	40,346	44,653
Cellulose	56,868	107,414	138,885	46,716	59,409	113,237	21,751	33,598
Glucose	42,551	91,351	129,130	24,116	55,828	56,181	14,393	17,795

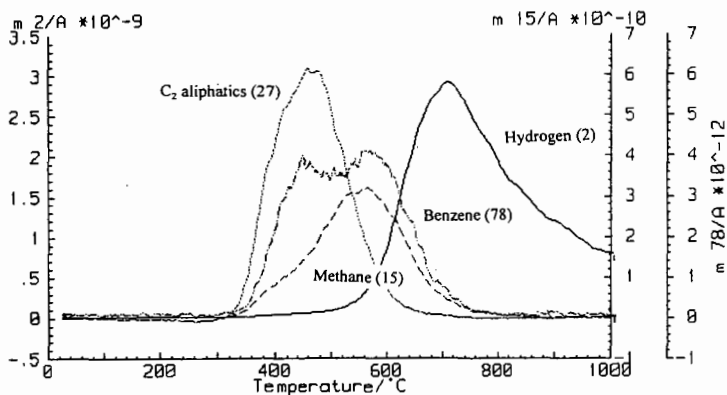
By performing TG experiments at three different heating rates; 5, 20, and 60°C/min we can deduce some comparative activation energies for the formation of hydrocarbons by plotting the heating rate vs. inverse of formation peak temperatures. These results are shown in Figure 4 for cotton duck char. This graphical representation demonstrates the temperature separation or coincidence of the classes of species, and a comparison of activation energies from their slopes. The activation energies fall into three groups - Hydrogen and methane (about 150 kJ/mol), benzene (about 240 kJ/mol), and all other species (about 200kJ/mol).

CONCLUSIONS

This study clearly indicates that there is a second pathway for production of aliphatic and aromatic hydrocarbons during pyrolysis of carbohydrates. The temperature range where this pathway becomes significant correlates with the temperature range where the char structure develops first an aliphatic and then a more aromatic structure. This study shows that inorganic species could significantly change the yields of hydrocarbons.

Figure 2

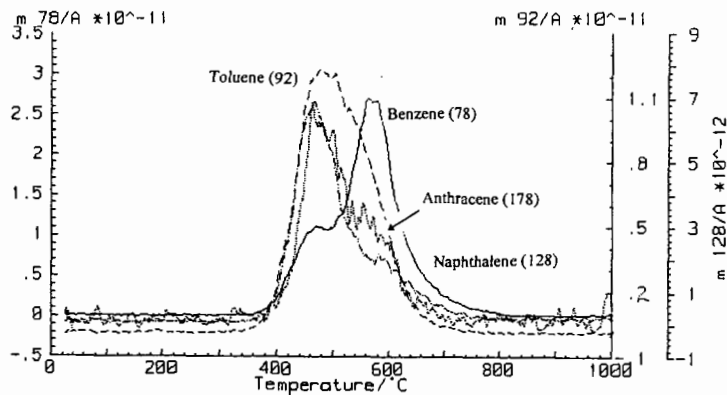
Product Yield of 320°C Char Pectin Pyrolysis



IDENTITY No.	320apech4dscn20	SAMPLE	ac320tfchrpectn 20.77
DATE	18 Nov 1998	ATMOSPHERE	Helium /150.25 ccm
LABORATORY	badlab	REMARK	MID16s5.0e-6orf
OPERATOR	bewdsk		
NETZSCH	409/429-403		

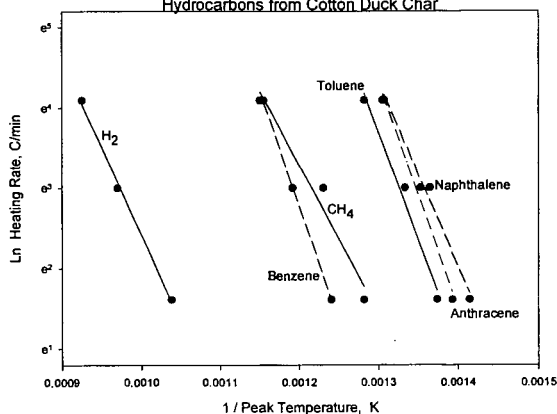
Figure 3

Product Yield of 360°C Char Cotton Duck Pyrolysis



IDENTITY No.	360dckch5dscn20	SAMPLE	duck4 370-60020 17.01
DATE	19 Nov 1998	ATMOSPHERE	Helium /150.25 ccm
LABORATORY	badlab	REMARK	MID16s5.0e-6orf
OPERATOR	bewdsk		
NETZSCH	409/429-403		

Figure 4
Activation Energies for the Formation of
Hydrocarbons from Cotton Duck Char



ACKNOWLEDGEMENTS

The Authors wish to thank Philip Morris Management for their encouragement and financial support for this research.

REFERENCES

1. Beer, J. M., Twenty Second Symposium On Combustion, The Combustion Institute, 1988, 1.
2. Handa, T.; Yamauchi, T.; and Ikeda, H., Fire Science Tech., 1987, Vol. 4 No. 2, 111.
3. Ledesma, E. B.; Nelson, P. F.; and Mackie, J. C., Twenty Seventh Symposium on Combustion, The Combustion Institute, 1998.
4. Wang, R.; and Cadman, P., Combustion & Flame, 1998, 112, 359.
5. Brage, C.; Yu, Q.; and Sjostrom, K., Fuel, 1996, Vol. 75 No. 2, 213.
6. Ohlemiller, T. J., Prog. Energy Combust. Sci., 1985, Vol. 11, 277.
7. Summerfield, M.; Ohlemiller, T. J.; and Sandusky, H. W., Combust & Flame, 1978, 33, 263.
8. Scott, D. S.; Piskorz, J.; Bergougnou, M. A.; Graham, R.; and Overend, R. P., Ind. Eng. Chem. Res., 1988, 27, 8.
9. Boroson, M. L.; Howard, J. B.; Longwell, J. P.; and Peters, W. A., AIChE J., 1989 Vol. 35, No. 1, 120.
10. Antal, M. J., Jr., in Fundamental Thermochemical Biomass Conversion, Eds., R. P. Overend, T. A. Milne, and L. K. Mudge, Elsevier Applied Science Publishers, New York, 1984, 511.
11. Radlein, A. G.; Mason, S. L.; Piskorz, J.; and Scott, D. S., Energy & Fuels, 1991, 5, 760.
12. Boroson, M. L.; Howard, J. B.; Longwell, J. P.; and Peters, W. A., Energy & Fuels, 1989, 3, 735.
13. Donnot, A.; Magne, P.; and Deglise, X., J. Analytical & Applied Pyrolysis, 1991, 22, 47.
14. Evans, R. J.; and Milne, T. A., Energy & Fuels, 1987, 1, 123.
15. Shafizadeh, F.; and Sekiguchi, Y., Combustion & Flame, 1984, 55, 171.
16. Sekiguchi, Y.; and Shafizadeh, F., J. Applied Polymer Science, 1984, 29, 1267.

FORMATION OF AROMATIC HYDROCARBONS DUE TO PARTIAL OXIDATION REACTIONS IN BIOMASS GASIFICATION

Robert J. Evans, Carolyn C. Elam, Michael Looker, and Mark Nimlos
National Renewable Energy Laboratory
1617 Cole Blvd.
Golden CO 80401

Keywords: Biomass, Pyrolysis, Oxidation

ABSTRACT

Biomass gasification is primarily a gas phase process due to its high reactivity, with 90% direct (primary) conversion to volatile material under high heat transfer conditions. Subsequent, vapor-phase (secondary) pyrolysis and oxidation reactions lead to the formation of gaseous products, such as hydrogen and carbon monoxide, and condensable materials, such as polynuclear aromatic hydrocarbons. This paper reports the results of studies of vapor-phase thermal and oxidative pathways for major biomass constituents under typical gasification conditions. Carbohydrate-derived primary products, including anhydrosugars, low-molecular-weight aldehydes and furan and pyran derivatives are converted into a different distribution of products in the presence of low levels of oxygen. Enhanced conversions of alcohols to aldehydes are observed. Major oxidation products include formaldehyde, ketene, acrolein and furan. Lignin-derived volatiles are methoxyphenols, which undergo a greater cracking rate to aromatics and phenolics in the presence of oxygen.

INTRODUCTION

Biomass gasification is a complex combination of pyrolysis and oxidation reactions in the condensed and vapor phases. Evans and Milne [1,2] identified reaction regimes and characterized the gaseous constituents present and the nature of the major solid- and vapor-phase reactions. The product distribution in each regime is a function of process variables, such as oxygen level, steam-to-biomass ratio, pressure, and the time and temperature history of the solid and gaseous materials. Under typical gasification conditions, oxygen levels are restricted to less than 30% of that required for complete combustion (including the oxygen in the wood), and CO and H₂ are the major products. This paper describes the organic products that typically are formed and presents the changes in product composition as a function of reaction severity. The goal of this work is to develop an understanding of the chemical and physical processes of biopolymer pyrolysis and oxidation leading to aromatic hydrocarbon formation.

Evans and Milne [1-3] used molecular beam mass spectrometry (MBMS) to suggest that a systematic approach to classifying pyrolysis products as primary, secondary, and tertiary products can be used to compare products from the various reactors that are used for pyrolysis and gasification. Four major product classes were identified as a result of gas-phase thermal cracking reactions:

1. Primary products characterized by cellulose-derived products, such as levoglucosan, hydroxyacetaldehyde, and furfurals; analogous hemicellulose-derived products, and lignin-derived methoxyphenols;
2. Secondary products characterized by phenolics and olefins;
3. Alkyl tertiary products that include methyl derivatives of aromatics, such as methyl acenaphthylene, methyl naphthalene, toluene, and indene;
4. Condensed tertiary products that show the polynuclear series without substituents: benzene, naphthalene, acenaphthylene, anthracene/phenanthrene, and pyrene.

In this paper we report the study of carbohydrates and lignin studied at three temperatures under pyrolysis and partial oxidation conditions. The three temperatures and gas phase residence times were selected to correspond to primary, secondary and tertiary regimes.

EXPERIMENTAL

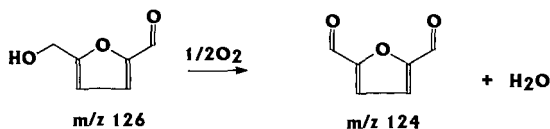
Small scale, batch pyrolysis experiments are conducted in tubular reactors by introducing a sample of biomaterial into flowing gas that is preheated to the temperature of interest. The composition of the flowing gas is typically helium for pyrolysis and He/oxygen mixtures for oxidative studies. Oxygen can be introduced after the sample to focus on gas-phase oxidation. For primary pyrolysis, the products of the initial pyrolysis step are sampled as rapidly as possible with a residence time of less than 50 ms. In the work reported here, primary conditions are at a temperature of 500 °C and a residence time of 50 ms. Gas-phase reaction time is added to achieve secondary and tertiary conditions. To enhance mixing and to achieve isothermal conditions, a tubular reactor packed with quartz chips was used to give a residence time of 250 ms. Secondary and tertiary reactions were performed at 650 °C and 750 °C, respectively. For oxidation studies, the oxygen was included in the gas before preheating for primary conditions,

but was added after the sample for secondary and tertiary studies. A level of 5% by volume was used for partial oxidation.

The analysis of the products was performed in real time with the NREL molecular beam mass spectrometry technique (MBMS) [1-3]. Illustrative data are shown in Figs. 1-2. These data are processed by averaging the spectra that are acquired over the pulse from the batch experiments. Collision induced dissociation (CID) experiments were conducted in the same way and the first quadrupole mass filter of the MBMS was tuned to only pass the ion of interest. A second quadrupole is used as a collision cell by introducing argon gas. Collisions between the energetic ions and the argon result in fragments that are introduced into a third quadrupole mass filter for analysis of the dissociation products.

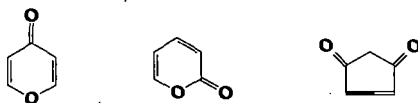
RESULTS AND DISCUSSION

All materials were screened at three temperatures for both pyrolysis and oxidation. The carbohydrates studied were cellulose, glucose, sucrose, levoglucosan and pectin. The results for sucrose are shown in fig. 1. Pyrolysis causes the cracking to low molecular weight products. The oxidation results show the formation of ions at m/z 124, 96, 68, 56, 42 and 30. This series is common to all the carbohydrates studied under these conditions. The m/z 124 is derived from m/z 126 and is probably formed by the oxidation (dehydrogenation) of the alcohol function of 5-hydroxymethyl furfural to form a di-aldehyde.



Analysis of m/z 124 by CID shows major peaks at m/z 39, indicating retention of the furan ring, and m/z 123, showing lose of one hydrogen, which is characteristic of aldehydes. This same reaction occurs to a lesser extend in pyrolysis reactions. An interesting question is the extent that the reaction under pyrolysis conditions is the result of hydrogen abstraction from other pyrolysis products.

The predominance of m/z 96 at 650 °C and 5% O₂ is significant since CID analysis show that this is not due entirely to furfural. In addition to m/z 95 and 39, which are the main daughters from furfural, the carbohydrates under these conditions show additional peaks at m/z 97, 41 and 69. The m/z 97 is an M+1 peak, which shows that ion-molecule reactions must be occurring in the collision cell, possibly between the aldehyde hydrogen in furfural and the other compounds at m/z 96. Three additional possibilities are shown below with the same empirical formula, C₅H₄O₂, as furfural. There are probably multiple sources of the m/z 96 products under these conditions, since a variety of starting materials give rise to a strong m/z 96 signal. This includes levoglucosan and Avicel (which pyrolyzes to give high yields of levoglucosan) and the simple sugars and 5-HMF.



4H-Pyran-4-one 2H-Pyran-2-one 4-Cyclopentene-1,2-dione

An analogous dehydrogenation reaction as described above for 5-HMF occurs with hydroxyacetaldehyde (HAA) with conversion to glyoxal. Hence, the m/z 60 intensity is reduced in the oxidation product slate at 650 °C and m/z 58 is enhanced. Other products of interest under the oxidation regime are furan (m/z 68), acrolein (m/z 56), ketene (m/z 42), and formaldehyde (m/z 30). M/z 56 is most likely to be acrolein and the CID results are supportive of this showing the loss of hydrogen in the daughter ion spectrum. The formation of butenes contributing to the signal at m/z 56 is not significant, since no hydrocarbon fragments were present in the m/z 40-44 range as would be expected for butenes. The formation of acrolein, ketene and formaldehyde are important observations since these species will be highly reactive and may lead to aromatics. Their formation may be difficult to follow by other analysis techniques since they may react during sample collection and handling.

The peaks at m/z 18, 28, and 44 are due to water, CO, and CO₂ with some possible contribution at m/z 28 and 44 from other products. The CID intensities for major daughter ions of m/z 44 for carbohydrates and model compounds are shown in Table 1. Under pyrolysis conditions, the daughter ions at m/z 15, 43 and 45 are evidence for acetaldehyde. Under oxidation conditions however, the CID evidence is that all of m/z 44 is due to CO₂.

CID of m/z 126 for the carbohydrates and model compounds studies is shown with intensities for major peaks in table 2. The base peak for pectin, sucrose and glucose is m/z 41 which is the same as for 5-HMF indicating that this is the major product at m/z 126. All three have higher intensities at m/z 126 than 5-HMF, which indicate that there is a contribution from other compounds. Trihydroxybenzenes (THB) have been identified as pyrolysis products of carbohydrates. The three isomers of THB all show base peaks at m/z 126 in their CID spectra. They also show significant intensities at m/z 43 as does the 1,3,5-THB isomer. The pectin CID is different than glucose and sucrose with intensities at m/z , 52 and 80 which corresponds to peaks for the 1,2,3- and 1,2,4- isomers of THB. The lack of m/z 108 in the pectin spectrum indicates that the 1,2,4- isomer is the predominant of the two for pectin

Phenolic compounds were studied, including lignin, coniferyl alcohol, vanillin, catechol, phenol and guaiacol. The results for lignin are shown in fig. 2. Oxidation accelerates the cracking of the phenolics compared to pyrolysis, with much higher amounts of benzene, toluene and xylene under oxidative tertiary conditions.

CONCLUSIONS

Paths to aromatic hydrocarbons have been shown for the major compound types studied with varying influences of temperature and the effect of oxygen. For carbohydrates, the effect of oxygen increases the rate of secondary cracking and primary pyrolysis products undergo highly specific oxidation reactions including 5-HMF to the di-aldehyde, HAA to glyoxal and a predominance of acrolein, formaldehyde, and furan. Within the kinetic regime studied, lignin and related phenolic model compounds had the highest rate of aromatic hydrocarbon formation and oxygen accelerated the rate of formation.

REFERENCES

1. Evans, R. J. and T. A. Milne (1987) *Energy and Fuels*, 1, p. 123-137.
2. Evans, R. J. and T. A. Milne (1987) *Energy and Fuels*, 1, p. 311-.
3. Evans, R. J. and T. A. Milne (1997) in *Developments in Thermochemical Biomass Conversion* (eds. A.V. Bridgwater and D.G. B. Boocock) Blackie A&P, London, pp. 803-816.

Table 1. CID daughter Ion Intensities for M/Z 44 for pyrolysis and oxidation at 650 C.

M/Z	Levog.		HAA		Avicel		pectin		sucrose		Glucose		CO2		HAc	
	Py	Ox	Py	Ox	Py	Ox	Py	Ox	Py	Ox	Py	Ox	Py	Ox	Py	Ox
15	7	1	8	0	8	1	3	1	12	1	9	1	0	0		18
27	5	0	0	0	5	0	1	0	3	0	3	0	0	0	0	0
28	3	4	4	4	3	4	3	4	3	3	3	5	7	2		5
29	4	0	1	0	4	0	1	1	3	1	3	0	0	0		1
42	5	1	4	1	5	1	2	1	7	1	5	1	1	1		8
43	45	10	47	8	46	9	23	10	66	13	56	11	9	5		100
44	100	100	100	100	100	100	100	100	100	100	100	100	100	100		69
45	15	2	6	1	17	1	6	2	13	2	14	1	2	2		80

Table 2. CID daughter Ion Intensities for M/Z 126 for pyrolysis at 650 C.

	Pectin	sucrose	glucose	135-THB	123-THB	124-HB	5-HMF
39	21	13	13	3	0	2	29
41	100	100	100	6	1	3	100
43	31	38	37	29	0	3	1
52	20	7	7	15	77	84	1
69	55	67	65	23	0	3	63
80	13	4	2	7	41	37	0
85	0	0	1	28	0	0	0
97	54	72	67	2	1	5	66
108	1	1	0	0	15	3	0
125	14	13	13	4	5	8	10
126	83	68	74	100	100	100	44
127	9	8	14	7	9	9	7

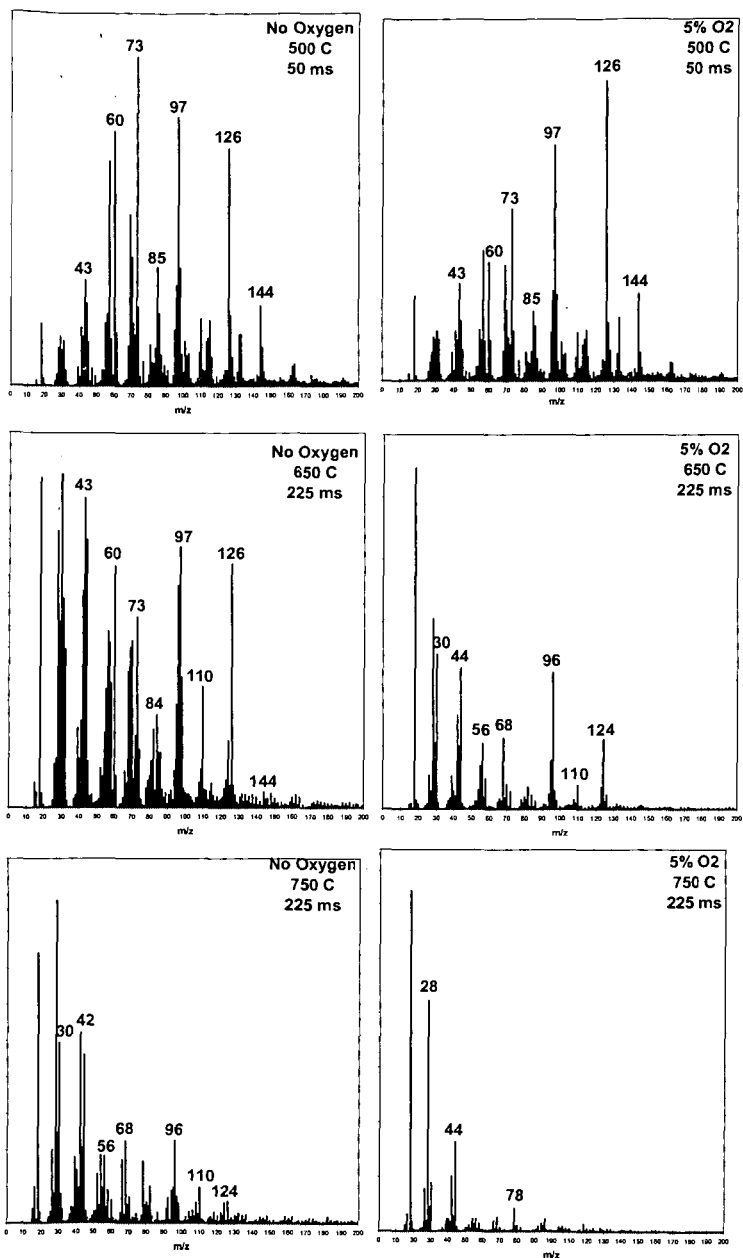


Fig. 1. Mass Spectra of Products for the pyrolysis (left) and oxidation (right) of sucrose at 550 °C (top), 650 °C (middle) and 750 °C (bottom). The 550 °C spectra are with a residence time of 50 ms. The 650 °C and 750 °C are for 225 ms residence time. The oxidation experiments were performed by injecting oxygen after the sample holder. The Oxygen level was 5% by volume.

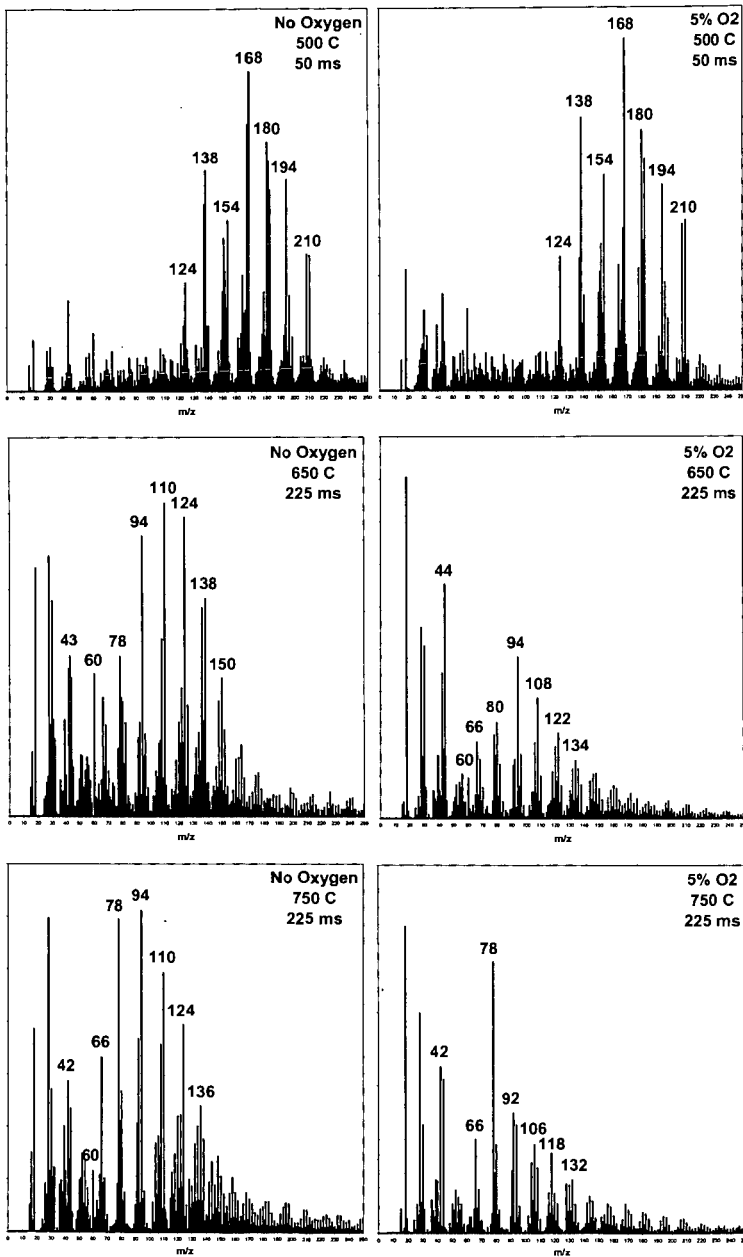


Fig. 2. Mass Spectra of Products for the pyrolysis (left) and oxidation (right) of ball milled lignin at 550 °C (top), 650 °C (middle) and 750 °C (bottom). Same conditions as Figure 1.

TAR CRACKING STUDIED WITH A PULSED MICROREACTOR

Mark R. Nimlos, Diedre Belle-Oudry, Robert J. Evans, David C. Dayton
National Renewable Energy Laboratory
Golden, Colorado
Sreela Nandi, G. Barney Ellison
University of Colorado
Boulder, Colorado

ABSTRACT

We have developed a new technique for investigating reactions that are important during pyrolysis and combustion. Molecules of interest are pulsed through a small tubular furnace and the products analyzed using photoionization Time-of-Flight Mass Spectrometry (TOFMS) and matrix isolation Fourier-Transform Infrared (FTIR) spectroscopy. The short residence times (10–100 μ s) and high temperatures (up to 1800K) of these reactors make them ideal for measuring the initial products during thermal reactions since important reaction intermediates can be identified and quantified. We have used these reactors to study the pyrolysis of compounds of relevance to the pyrolysis and combustion of biomass. We have trapped and measured reactive intermediates as well as stable products. The combination of these two analytical techniques provides a powerful and unique method for understanding the thermal chemistry of biopolymers.

INTRODUCTION

Thermal treatment of biomass remains appealing as a source of energy, fuels and chemicals, but a thorough understanding of the chemical processes involved in pyrolysis and combustion remains elusive. The complicated chemical composition of lignocellulosic materials make development of complete elementary reaction mechanisms unrealistic for thermal processes, but an understanding of some of the most important reactions would be very valuable for understanding currently used biomass technologies and for developing new ones. Many of reactions associated with pyrolysis and combustion of biomass have been inferred from indirect experimental evidence. We have started an investigation to directly measure some of these reactions. Our initial studies focus on the formation and cracking of "tar" compounds and we will use new experimental and analytical techniques that will help unravel this chemistry. We will present experimental results which demonstrate these new capabilities.

EXPERIMENTAL

We use tubular reactors that are similar to the supersonic nozzles developed by Chen *et al.* [1] and used by others [2,3] for the preparation of radicals in molecular beams. Our version of the "Chen Nozzle" is shown in Figure 1 and it consists of a small tube (1mm i.d.) of silicon carbide that is resistively heated up to 1800 K. Gas mixtures are pulsed through the heated tube and expanded into a vacuum chamber for analysis. The supersonic cooling and low number densities in this expansion instantly quench and cool reactive intermediates, which are then analyzed using TOFMS or matrix isolation FTIR spectroscopy. The very high temperatures and short residence times (10–100 μ s) in the heated tubes allows one to trap and isolate primary intermediates from thermal reactions, while reducing secondary reactions.

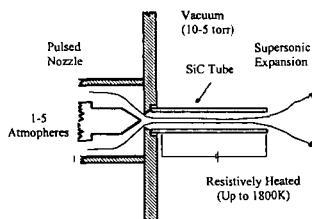


Figure 1. Schematic drawing of pulsed microreactor used in these experiments

TIME-OF-FLIGHT MASS SPECTROMETRY

We have used a newly built TOF mass spectrometer to investigate the pyrolytic reactions of a number of molecules. The expansion from the Chen Nozzle was skimmed and formed into a molecular beam, which was crossed by a vacuum ultraviolet (VUV) light beam. VUV (118 nm, 10.5 eV) photons were formed by tripling the third harmonic of a Nd/YAG laser in a xenon cell. The energy of these photons is sufficient to ionize most organic molecules and radicals while

reducing ion fragmentation relative to electron impact ionization. As an example, consider Figure 2. This figure shows the TOF mass spectrum of the products from the pyrolysis of furan in our Chen Nozzle (top) compared to the mass spectra obtained from a molecular beam mass spectrometer (MBMS). As can be seen, fragmentation is lower for the TOFMS even when the MBMS is run at an electron impact energy of 18 eV. TOFMS is also very sensitive (detection limits down to 10 ppb) and capable of high resolution. Figure 3 compares the mass resolution of peaks from the pyrolysis furan using TOF and quadrupole MBMS. TOF peak widths are about 0.06 AMU, while peak widths are about 0.7 AMU for quadrupole. The high resolution, low fragmentation and high sensitivity make TOFMS ideal for identifying pyrolysis products.

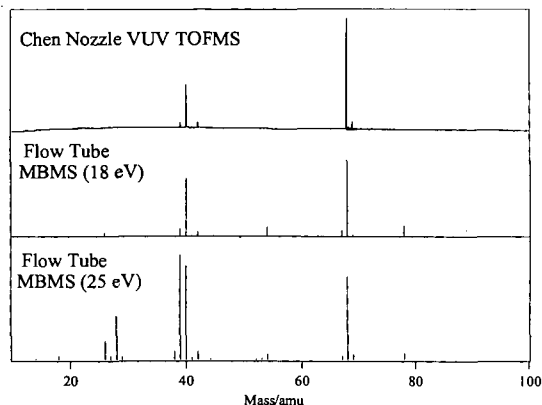


Figure 2 Mass spectra of the pyrolysis products of furan. The top spectrum shows the products from pyrolysis in a Chen Nozzle while the bottom two spectra show products from a heated flow tube reactor (1 cm i.d., ~1 sec. residence time, 750 °C).

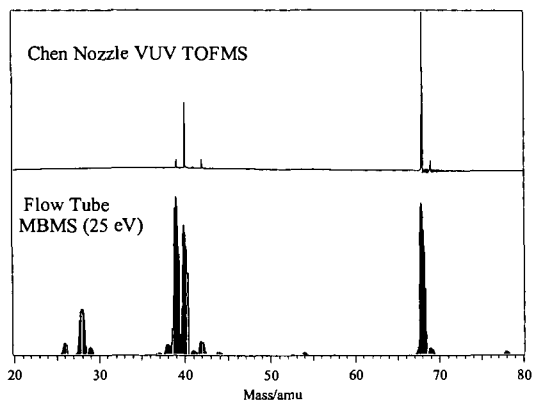


Figure 3 Mass spectra of the pyrolysis products of furan showing the superior mass resolution of the TOFMS (top) relative to the quadrupole MBMS (bottom).

We measured the pyrolysis TOF mass spectra of a number of different compounds using the Chen Nozzle. As an initial test of the Chen Nozzle, we pyrolyzed ethyl acetate and used the TOFMS to identify the well known products, ethylene and acetic acid[4]. We have also measured the products obtained from the pyrolysis of allyl bromide and allyl iodide. Our preliminary TOF mass spectra of allyl bromide and its pyrolysis products are shown in Figure 4. The middle spectrum in this figure shows that the pyrolysis of allyl bromide in the Chen Nozzle produces primarily allyl radical. This demonstrates that we can use this reactor to measure primary pyrolysis products such as radicals. When we conduct pyrolysis experiments using a

conventional flow tube reactor (1 cm diameter quartz tube heated to 500–800 °C, 100–1000 ms residence times) we only detect stable products that result from the reaction of ally radical. The spectrum at the top of Figure 4 shows the products produced when allyl bromide is heated above 1500 K (the exact temperatures could not be measured) in the Chen Nozzle. The products identified in this spectrum are similar to what is seen in conventional flow tubes. This demonstrates that the Chen Nozzle can also be used to study the thermal decomposition of reactive intermediates and bimolecular reactions.

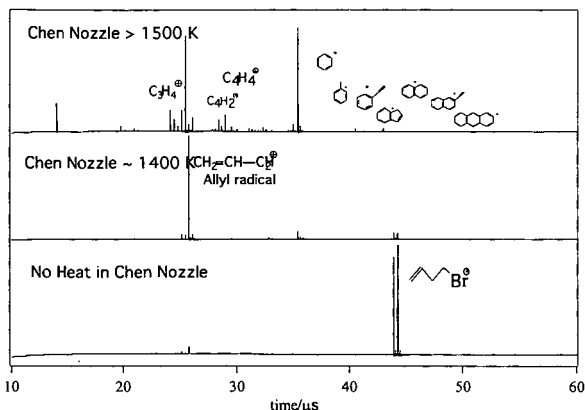


Figure 4 The products from the pyrolysis of allyl bromide in a Chen Nozzle

MATRIX ISOLATION ANALYSIS

While mass spectrometry is a powerful technique for identifying products from thermal reactions, it suffers from its inability to distinguish isomers and from its difficulty with quantitative analysis. Thus, we have developed experimental hardware that allows us to trap the pyrolysis products from a Chen Nozzle in an argon matrix. The compound of interest is diluted in argon and passed through our Chen Nozzle and the products are deposited on a cold (12K) CsI window. Identification of the pyrolysis products is then carried out using FTIR spectroscopy.

Figures 5 show some results for the pyrolysis of allyl iodide. The products from allyl iodide should be the same as those from allyl bromide, but the iodide requires a lower pyrolysis temperature. The matrix isolation spectrum shown in Figure 5 is obtained by subtracting our any residual allyl iodide and clearly shows the formation of allyl radical, allene, ethylene and acetylene. These peak assignments are made based upon the literature assignments of matrix isolation spectra [5-8]. The matrix results are consistent with the TOFMS results and demonstrate that matrix isolation spectroscopy is ideal for unambiguous product identification

THE PYROLYSIS OF FURAN

Furan was initially chosen as a model compound because it is known to be an important intermediate in the pyrolysis and combustion of biopolymers [9]. Figure 6 shows the TOF mass spectra resulting from the pyrolysis of furan in our Chen Nozzle. Our TOFMS measurements agree qualitatively with those reported in the literature [10,11]. As with allyl bromide, higher temperature allows the measurement of products from secondary, bimolecular reactions.

Matrix isolation FTIR spectroscopy was used to identify the molecular structure of the compounds products identified by TOFMS. The preliminary results from this experiment are shown in Figure 7. The bottom spectrum shows portions of the furan spectrum when the Chen Nozzle is unheated, while the top shows the spectrum when the nozzle is heated to approximately 1400 K. As can be seen, the matrix isolation technique can differentiate between methyl acetylene, allene and cyclopropene, all of which have the same mass and so are indistinguishable with TOFMS. Thus, both the allyl bromide and the furan example demonstrate the complementary and consistent nature and matrix isolation FTIR and TOFMS.

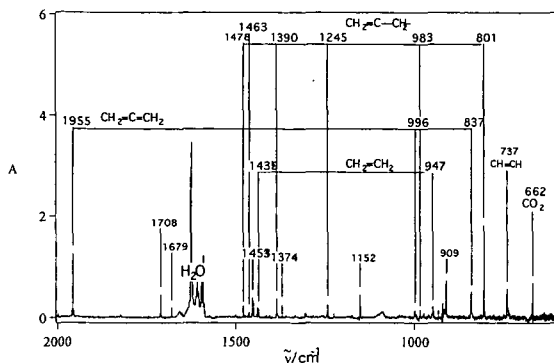


Figure 5 Matrix isolation FTIR spectrum of the products obtained from the pyrolysis of allyl iodide in a Chen Nozzle. Allyl radical ($\text{CH}_2=\text{CH}-\text{CH}_2^\bullet$), allene ($\text{CH}_2=\text{C}=\text{CH}_2$), ethylene ($\text{CH}_2=\text{CH}_2$), and acetylene ($\text{CH}\equiv\text{CH}$) are identified in the spectrum

Pyrolysis of Furan: Time-of-Flight Mass Spectra

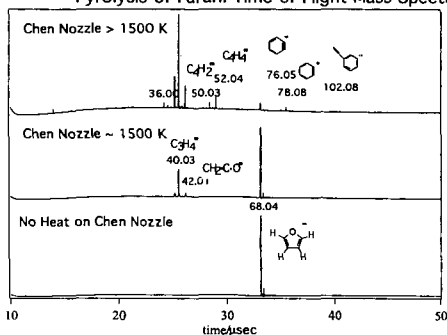
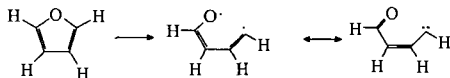


Figure 6 TOF mass spectra of the products of pyrolysis of furan in a Chen Nozzle (top and middle) compared to the TOF mass spectrum of furan (bottom).

Earlier studies of the pyrolysis of furan are consistent with our results in that allene, methyl acetylene, acetylene and ketene are reported as primary pyrolysis products. Our possible observation of cyclopropene is unique but consistent with proposed mechanisms. In the mechanisms proposed in the literature [11], the first step in the destruction of furan is the breaking of the C-O bond in the ring:



It is unclear how much energy would be required to break this bond. Typically, ether C-O bonds are weak (82 kcal/mol) [12], but aromatic stabilization energy will be sacrificed, though some stabilization energy will be regained in the resulting diradical. An alternative mechanism involving the attack of furan by hydrogen atoms is shown in Scheme I. Hydrogen atom is reformed in each branch of the mechanism, making the reaction catalytic. This could account for the low observed Arrhenius activation energy (78 kcal/mol) [6,7]. Hydrogen atom could be formed by the rupture of the C-H bond. The bond dissociation energy for this bond has not been measured though our *ab initio* calculations give a value of 118 kcal/mol.

Matrix Isolation FTIR

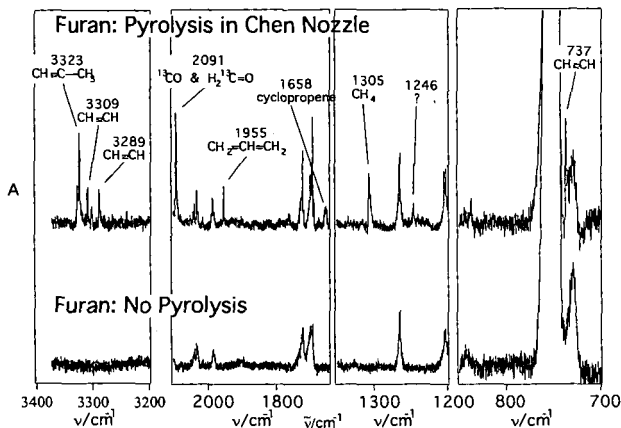
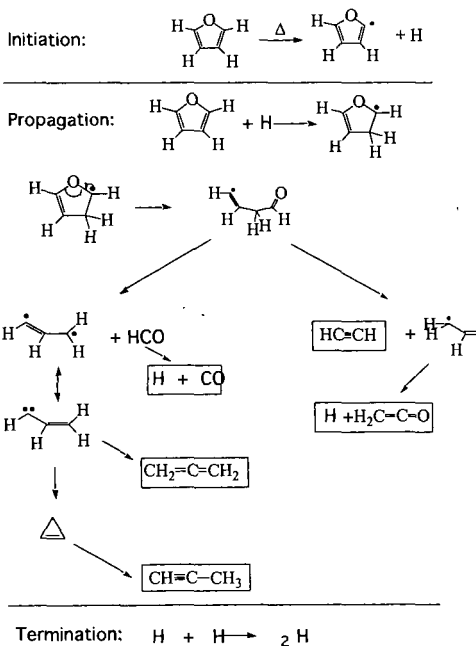


Figure 7 Matrix isolation FTIR spectrum of the pyrolysis products of furan (top) compared to the spectrum of furan alone.

Scheme I: Mechanism for Furan Decomposition



CONCLUSIONS

The combination of high temperature Chen Nozzles with TOFMS and matrix isolation FTIR spectroscopy is a powerful tool for understanding the thermal chemistry occurring during the combustion and pyrolysis of biopolymers. It allows the unambiguous identification of reaction intermediates as well as stable products.

ACKNOWLEDGEMENT

We would like to acknowledge the support of Phillip Morris Corp. for this work and would like to thank Mohammad Hajaligol for stimulating discussion.

REFERENCES

1. Chen, P. in *Unimolecular and Bimolecular Reaction Dynamics*, Ng, C.Y.; Baer, T.; Powis, I., Eds., John Wiley, 1994, p371.
2. Rihrs, H. W.; Wickham-jones, C. T.; Ellison, G. B.; Berry, D.; Argrow, B. M. *Rev. Sci. Instrum.* **1995**, *66*, 2430.
3. Yao, J.; Bernstein, E. R. *J. Chem. Phys.* **1997**, *107*, 3352.
4. Norfolk, S. B.; Taylor, R. *J. Chem. Soc. Perkin II* **1976**, 280.
5. Jacox, M. E. "Vibrational and Electronic Energy Levels of Polyatomic Transient Molecules," *J. Phys. Chem. Ref. Data* Monograph 3. **1994**.
6. Getty, J. D.; Burmeister, M.J.; Westre, S. G.; Kelly, P. D. *J. Am. Chem. Soc.*, **1991**, *113*, 801.
7. Ball, D. W.; Pong, R. G. S.; Kafafi, Z. H. *J. Am. Chem. Soc.*, **1993**, *115*, 2864
8. Shimanouchi, T. *Tables of Molecular Vibrational Frequencies Consolidated Volume I*, **1972**, NSRDS-NBS 39.
9. Evans, R. J.; Milne, T. A. *Energy and Fuels*, **1987**, *1*, 123.
10. Lifshitz, A; Bidani, M.; Bidani, S. *J. Phys. Chem.* **1986**, 5373.
11. Organ, P. P.; Mackie, J. C. *J. Chem. Soc. Faraday Trans.* **1991**, *87*, 815.
12. Benson, S. W. "Thermochemical Kinetics", **1976**, Wiley.

CONVERSION OF LIGNIN. 2. PRODUCTION OF HIGH-OCTANE FUEL ADDITIVES

Joseph Shabtai,* Włodzimierz Zmierczak,* Esteban Chornet,** and David K. Johnson**

*Department of Chemical and Fuels Engineering, University of Utah
Salt Lake City, UT 84112

**National Renewable Energy Laboratory, Golden, CO 80401

Keywords: lignin conversion, high-octane fuel additives

ABSTRACT

Lignin conversion procedures have been developed, allowing for preferential production of specific high-octane fuel additives of two distinct types, i.e., (1) C₇-C₁₀ alkylbenzenes; and (2) aryl methyl ethers, where aryl mostly = phenyl, 2-methylphenyl, 4-methylphenyl, and dimethylphenyl. Process (1) comprises base-catalyzed depolymerization (BCD) and simultaneous partial (~ 50%) deoxygenation of lignin, followed by exhaustive hydrodeoxygenation and attendant mild hydrocracking of the BCD product to yield C₇-C₁₀ alkylbenzenes as main products. Process (2) involves mild BCD with preservation of the lignin oxygen, followed by selective C-C hydrocracking, preferentially yielding a mixture of alkylated phenols, which upon acid-catalyzed etherification with methanol are converted into corresponding aryl methyl ethers (see above) possessing blending octane numbers in the range of 142-166.

INTRODUCTION

It was previously reported that lignin is susceptible to high-yield depolymerization/upgrading leading to reformulated gasoline compositions as final products.¹ Two different processes were developed, i.e., (1) a two-stage process comprising base-catalyzed depolymerization (BCD) of the lignin feed in supercritical methanol as reaction medium, followed by deoxygenative hydroprocessing (HPR) to yield a reformulated hydrocarbon gasoline, consisting of a mixture of C₅-C₁₁ mostly multibranched paraffins, C₆-C₁₁ mono-, di-, tri-, and polyalkylated naphthenes, and C₇-C₁₁ alkylbenzenes,² and (2) another two-stage process comprising mild BCD, followed by non-deoxygenative hydrotreatment/mild hydrocracking (HT), to yield a reformulated, partially oxygenated gasoline, consisting of a mixture of (substituted) phenyl methyl ethers and cycloalkyl methyl ethers, C₇-C₁₀ alkylbenzenes, C₅-C₁₀ mostly multibranched paraffins, and polyalkylated cycloalkanes.³

Alternative procedures based on lignin as feed have been now developed, specifically oriented toward production of valuable, high-octane fuel additives of two types, i.e., (a) C₇-C₁₀ alkylbenzenes; and (b) aromatic ethers, *viz.*, aryl methyl ethers, where aryl mostly = phenyl, methylphenyl, or dimethylphenyl.

C₇-C₁₀ alkylbenzenes, in permissible concentrations of about 25 wt%, are considered as essential components of current gasolines. Therefore, it was an objective of the present work to demonstrate that lignin could provide an abundant renewable source of such compounds as gasoline additives. Aryl methyl ethers, due to their extraordinarily high octane numbers, could likewise be of considerable potential value as lignin-derived fuel additives.

EXPERIMENTAL

Materials. Three different lignin samples were used in the study, i.e. (1) a Kraft Indulin AT sample, pretreated by washing with aqueous KOH and water; (2) an organosolve sample, supplied by REPAP Technologies, Inc.; and (3) a sample obtained as by-product in the NREL ethanol process.⁴ Relatively small differences in chemical reactivity were observed for these samples.

Catalysts. The preferred base catalyst-solvent systems used in BCD runs were methanolic solutions of NaOH with concentrations in the range of 5.0 to 7.5 wt%.

Two hydrodeoxygenation catalysts possessing high C-O hydrogenolysis selectivity and low ring hydrogenation activity,⁵ i.e., CoMo/Al₂O₃ and RuMo/Al₂O₃, were employed. The preparation of these catalysts is described elsewhere.⁵ Mild hydrocracking catalysts used for conversion of residual oligomeric components in the production of C₇-C₁₀ alkylbenzenes (see next section) included CoMo/SiO₂-Al₂O₃ and solid superacids. The preparation of the latter type of catalysts, e.g., sulfated oxides, was described in detail elsewhere.^{6,7}

Selective mild hydrocracking catalysts, *viz.*, catalysts causing selective C-C hydrogenolysis in oligomeric components of BCD products with preservation of O-containing groups (see next section) included various solid superacids, in particular Pt/SO₄²⁻/ZrO₂, Pt/WO₄²⁻/ZrO₂, and Pt/SO₄²⁻/TiO₂.³

Etherification catalysts used included previously described superacids,^{6,7} and some recently reported sulfated oxide systems, e.g., $\text{SO}_4^{2-}/\text{MnO}_2/\text{Al}_2\text{O}_3$, $\text{SO}_4^{2-}/\text{MoO}_3/\text{Al}_2\text{O}_3$ and $\text{SO}_4^{2-}/\text{WO}_3/\text{Al}_2\text{O}_3$.⁸ **Reactors.** Both 300 cc autoclaves and 50 cc Microclaves (Autoclave Engineers) were used in the BCD runs. Most of the hydroprocessing runs were performed in 50 cc Microclaves.

Experimental Procedures.

Base-catalyzed depolymerization (BCD). The BCD procedure is illustrated by the following example of a typical run. A 15.0 g sample of pretreated Kraft Indulin AT lignin (elemental composition, wt%: C, 66.30; H, 6.03; N, 0.10; S, 1.23; O, 26.34) was introduced in a 300 cc autoclave and 120 g of a 7.5 wt% NaOH solution in methanol was added to it (methanol/lignin wt ratio = 7.4:1). The autoclave was purged with nitrogen and the mixture was brought with constant stirring (100 rpm) to 290°C, left to react at this temperature for 10 min with faster stirring (500 rpm), and then quickly cooled down to room temperature. The product was removed from the autoclave, 100 cc of water was added, and the mixture was acidified to a pH of ~ 2.0, using an aqueous 2N HCl solution. The mixture was kept overnight and the accumulated organic liquid/semi-solid phase was separated from the water-methanol layer, washed with some water, dried under a stream of nitrogen, and subjected to Soxhlet extraction with ether. The extract was dried with anhydrous MgSO_4 , filtered, and then freed from the ether on a Rotavapor to obtain the final BCD product. The water-methanol layer was worked up (including methanol removal and subsequent liquid-liquid extraction) to obtain a small portion of organic material which was added to the main BCD product. The total conversion of the lignin feed was 94.6 wt% as determined by the weight of unreacted solid residue. The distribution of the total product (wt%, calculated on converted lignin) was as follows: liquid/semi-solid depolymerized compounds, 98.4; gaseous products (mainly C_1 - C_4 gases and CO_2), 1.6. GC/MS analysis of the liquid/semi-solid BCD product showed that it is mainly composed of mono-, di-, and trialkylsubstituted phenols and methoxyphenols, accompanied by smaller amounts of C_7 - C_{11} alkylbenzenes and branched paraffins (alkyl = mostly methyl and some ethyl or isopropyl substituents). The product also contained some amounts of oligomeric components, which are convertible to monomers by additional treatment (see below). The elemental composition of the BCD product was as follows (wt%): C, 78.46; H, 8.54; N, 0.08; S, 0.05; and O, 12.87. This composition showed that, under the experimental conditions used in this run, the BCD reaction proceeded with a decrease of ~ 50 wt% in oxygen content and with essentially complete sulfur elimination.

Hydroprocessing (HPR) Procedure. For conversion to C_7 - C_{10} alkylbenzenes, the BCD product was subjected to two sequential hydroprocessing steps in autoclave reactors, i.e., exhaustive hydrodeoxygenation (HDO), followed by mild hydrocracking (HCR). These two steps can be performed as a single operation in a flow reactor system in series. The two-step HPR procedure is illustrated by the following typical run. 10.0 g of BCD product and 2.0 g of a $3\text{Co}8\text{Mo}/\text{Al}_2\text{O}_3$ catalyst were introduced into a 50 cc Microclave reactor and the latter was sequentially purged with nitrogen and hydrogen and then pressurized with hydrogen. The reactor was heated to 360°C with stirring (100 rpm) and then kept at this temperature under a H_2 pressure of ~ 1800 psig for 2 h with increased stirring (500 rpm). At the end of the run the reactor was quickly cooled down to room temperature and the hydrodeoxygenated oil product was separated from the catalyst and water (formed during the HDO reaction) by centrifugation. To eliminate any small amounts of residual oligomeric compounds, 15.0 g of HDO product (accumulated from two HDO runs) was subjected to mild hydrocracking in a 50 cc Microclave as follows: 3.0 g of a $3\text{Co}8\text{Mo}/\text{Al}_2\text{O}_3$ catalyst was added to the feed, the reactor was purged and pressurized with hydrogen, heated up to 375°C, and the feed allowed to react at this temperature with constant stirring for 10 min under a H_2 pressure of 2400 psig. The final HPR product was analyzed by GC/MS and found to predominantly consist of C_7 - C_{10} alkylbenzenes (see Results and Discussion).

Selective Hydrocracking (HT) Procedure. BCD products obtained at lower temperatures (250-270°C) contain significant amounts of incompletely depolymerized, oligomeric components. To complete the depolymerization of such components, with attendant preservation of O-containing functional groups, the BCD products were subjected to supplemental mild hydrocracking as illustrated in the following typical example. 10.0 g of a BCD product obtained under mild conditions (265°C; MeOH: lignin ratio = 5:1; 10.0 wt% of added water) and 2.0 g of $\text{Pt}/\text{SO}_4^{2-}/\text{ZrO}_2$ catalyst were mixed and subjected to reaction in a Microclave at 350°C and an H_2 pressure of 1500 psig, for 2 h. A portion of the dark liquid product accumulated from several identical runs (35.8 g) was vacuum distilled and the monomeric distillate fraction, b.p. up to 105°C/0.1 torr (82.2 wt% of the total starting liquid) was analyzed by GC/MS and found to consist predominantly of alkylated phenols and methoxyphenols (see Results and Discussion).

Etherification Procedure. The procedure used for converting the phenolic products into corresponding aryl methyl ethers is illustrated by the following example. A 5.0 g sample of the above vacuum distillate, 15.0 g of methanol, 2.0 g of $\text{SO}_4^{2-}/\text{ZrO}_2$ catalyst, and 1.0 g of a water-absorbing agent were subjected to reaction in a Microclave under the following conditions: temperature, 275°C, autogeneous reaction pressure, ~ 1200 psig, time, 2 h. The yield of etheric products, as determined by GC analysis, was 89.4 wt%.

RESULTS AND DISCUSSION

Figure 1 outlines the scheme of the two-stage (BCD-HPR) procedure for preferential conversion of lignin to C₇-C₁₀ alkylbenzenes. Stage I of the procedure comprises BCD treatment of the wet lignin feed (permissible water/lignin weight ratios in the approximate range of 0.1 to 1.5) using an alcoholic solution of NaOH or KOH in methanol or ethanol as depolymerizing agent. The BCD temperature range is between 260-290°C and preferably around 270°C. At this temperature the methanol or ethanol medium is under supercritical condition, which is an essential requirement for effective hydrolysis of the etheric linkages in the lignin structural network. The preferred range for methanol/lignin or ethanol/lignin weight ratios in the feed solution is from 2:1 to 5:1. In this range of weight ratios, and by proper reduction in reaction time, the total number of alkyl substituents in the depolymerized product components can be regulated not to exceed 1 to 3 substituents per depolymerized molecule. These 1 to 3 substituents (mostly methyl groups in the presence of methanol as reaction medium) include some residual alkyl groups originally present in the monomeric lignin units, but, mainly, methyl groups inserted in these units during the BCD reaction. Under selected processing conditions, the BCD reaction is characterized by a very high lignin conversion rate which is reflected in a high-yield (>95 wt%) performance, both in autoclave and flow reactors. The preferred reaction time is between 5 to 10 min in autoclave reactors, and between 1 to 5 min in a continuous flow reactor. At such short reaction times, and particularly for low methanol/lignin ratios, the extent of ring alkylation in the depolymerized products can be easily controlled to the desirable level. As indicated in Figure 1, the depolymerized lignin product obtained by BCD treatment consists of a mixture of alkylated phenols and alkoxyphenols, accompanied by smaller amounts of hydrocarbons. Description of a typical BCD run is provided in the Experimental section.

In Stage II of the procedure (Figure 1) the depolymerized lignin product is subjected to hydroprocessing (HPR) predominantly yielding C₇-C₁₀ alkylbenzenes accompanied by smaller amounts of C₇-C₁₀ branched paraffins and C₆-C₁₀ alkylated naphthenes. HPR comprises two sequential steps, i.e., exhaustive hydrodeoxygenation (HDO) with a catalyst possessing low ring hydrogenation activity, e.g., CoMo/Al₂O₃ or RuMo/Al₂O₃,³ followed by mild hydrocracking (HCR) with a CoMo/SiO₂-Al₂O₃, or preferably with a solid superacid catalyst. The supplemental HCR step results in the effective conversion of some residual oligomeric (mainly dimeric) hydrodeoxygenated products into alkylbenzenes. Work is continuing on the combination of the HDO and HCR steps into a single hydroprocessing operation. The final HPR product consists predominantly of C₇-C₁₀ alkylbenzenes, accompanied by smaller amounts of C₇-C₁₀ branched paraffins and C₆-C₁₀ alkylated naphthenes.

Figure 2 provides the scheme of the two-stage (BCD-ETR) procedure for preferential conversion of lignin to aromatic ethers. Stage I of the procedure comprises mild BCD at 250-265°C, using low MeOH/lignin ratios, e.g., 3:1 to 5:1, and short reaction time, e.g., 5 to 10 min. Under such conditions, the BCD product retains most (>90 wt%) of the original oxygen content of the lignin feed, which is important for the high-yield production of the final etheric products. On the other hand, the BCD product under the above mild conditions contains significant concentrations (about 25-40 wt%) of incompletely depolymerized components. This necessitates a supplemental depolymerizing treatment of the BCD product, i.e., selective C-C hydrocracking with preservation of the O-containing groups, viz., with minimal concurrent C-O hydrocracking. Such a selective treatment is achieved by the use of platinized solid superacids, i.e., Pt/SO₄²⁻/ZrO₂ or Pt/WO₄²⁻/ZrO₂, at 350-365°C under moderate H₂ pressure, e.g., ~1500 psig. Under such conditions, there is essentially no loss of oxygen and the content of oligomeric components in the phenolic product is reduced to <10 wt%. In Stage II of the procedure the distilled monomeric phenols are subjected to etherification with methanol, at 225-275°C, in the presence of a solid superacid catalyst, e.g., SO₄²⁻/ZrO₂, WO₄²⁻/ZrO₂, SO₄²⁻/MnO₂/Al₂O₃ or SO₄²⁻/WO₄/Al₂O₃. In order to displace the equilibrium between phenols and aryl methyl ethers in the direction of the desired etheric products, water-absorbing agents, including zeolites and specially designed pillared clays, are currently being added to the reacting mixture.

Figure 3 provides an example of GC/MS analysis of a vacuum distilled BCD-HT product from Kraft (Indulin AT) lignin. The BCD conditions used in this early run were: temperature, 270°C; MeOH/lignin wt ratio, 7.5; reaction time, 30 min. The BCD product obtained was used as feed for the subsequent HT step which was performed under the following conditions: temperature, 350°C; catalyst, Pt/SO₄²⁻/ZrO₂; feed/catalyst wt ratio, 5:1, H₂ pressure, 1500 psig; reaction time, 2 h. Under these conditions the final BCD-HT product of this early run contained about 73.5 wt% of C₁-C₃ alkylated phenols and methoxyphenols, where C₁-C₃ indicates the total number of carbons in alkyl substituents, viz., 1, 2 or 3 alkyl (predominantly methyl) groups per molecule. In recent optimization of the BCD-HT procedure, the BCD step was performed at 265°C, using a lower MeOH/lignin ratio, e.g., 5:1, and a shorter reaction time, i.e., 5 min. Further, the HT step was performed at a higher H₂ pressure, i.e., 1800 psig. Under these modified conditions a highly desirable BCD-HT product, containing 79.1 wt% of C₁-C₂ alkylated phenols and 2-methoxyphenols (where C₁-C₂ indicates mostly methyl and dimethyl substitution), was obtained. The product contained 12.9 wt% of hydrocarbons and only ~8 wt% of higher phenols. Etherification of the vacuum distilled product with methanol (see Experimental) produced a mixture of the corresponding aryl methyl ethers, which are characterized

by blending octane numbers in the approximate range of 142-166.

Figure 4 provides an example of GC/MS analysis of a BCD-HPR product from NREL lignin as feed, i.e., a lignin sample obtained as by-product in the NREL ethanol process.⁴ The selectivity for production of C₇-C₁₀ alkylbenzenes in this early run is only moderate due to the use of an extended reaction time (1 h) and a high MeOH/lignin wt ratio (7.5:1) in the BCD step, and the use of an extended reaction time (2 h) in the HT step. In order to increase the selectivity of the BCD/HT procedure, the extent of ring alkylation and, in particular, the extent of undesirable ring hydrogenation of the C₇-C₁₀ alkylbenzene products to corresponding alkylated cyclohexanes and cyclopentanes is subjected to sharp decrease in current work by using shorter reaction times and lower MeOH/lignin ratios in the BCD step, and a combination of shorter reaction times and catalysts of lower ring hydrogenation activity, e.g., RuMo/SiO₂-Al₂O₃ or a solid superacid, in the HT step. Under such modified conditions the BCD-HT product predominantly consists of C₇-C₉ alkylbenzenes (approximately 80-85 wt%) accompanied by desirable C₆-C₁₀ multibranching paraffins, 12-19 wt%, and < 4 wt% of alkylated naphthenes.

ACKNOWLEDGMENT

The authors wish to thank the U.S. Department of Energy, Biofuels Systems Division, for financial support through Sandia Corp.(AU-8776).

REFERENCES

1. Shabtai, J., Zmierczak, W., and Chornet, E., *Proc. 3rd Biomass Confer. of the Americas, Montreal, Elsevier, 1997*, Vol. 2, pp 1037-1040.
2. Shabtai, J., Zmierczak, W., and Chornet, E., *U.S. Patent Appl.* No. 09/136,336 (1998).
3. Shabtai, J., Zmierczak, W., and Chornet, E., *U.S. Provisional Patent Appl.* No. 60/097,701 (1998).
4. Hinman, N.D., Schell, D.J., Riley, C.J., Bergeron, P.W., and Walter, P.J., *Appl. Biochem. Biotechnol.*, **1992**, 34/35, 639-649.
5. Shabtai, J., Nag, N.K., and Massoth, F.E., *J. Catal.*, **1987**, 104, 413-423.
6. Zmierczak, W., Xiao, X., and Shabtai, J., *Energy Fuels*, **1994**, 8, 113-116.
7. Shabtai, J., Xiao, X., and Zmierczak, W., *Energy Fuels*, **1997**, 11, 76-87.
8. Mossman, A.B., *U.S. Patent 4,611,084* (1986); *U.S. Patent 4,675,455* (1987).

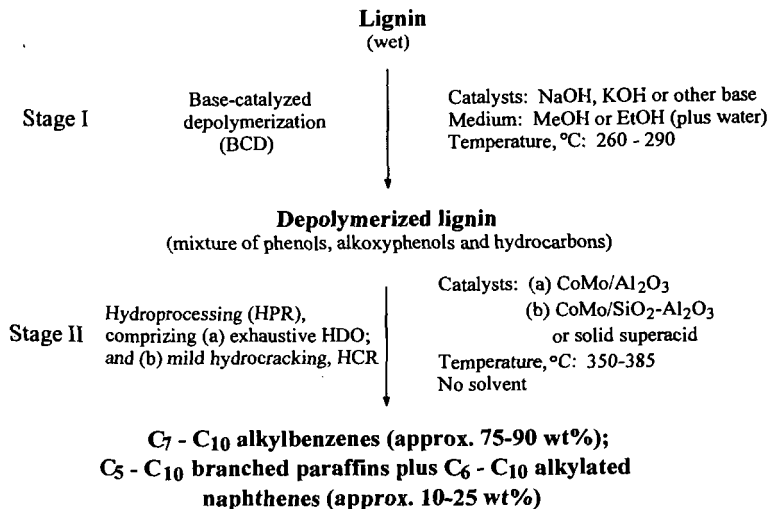


Figure 1. Scheme of two-stage (BCD-HPR) procedure for preferential conversion of lignin to C₇ - C₁₀ alkylbenzenes as fuel additives

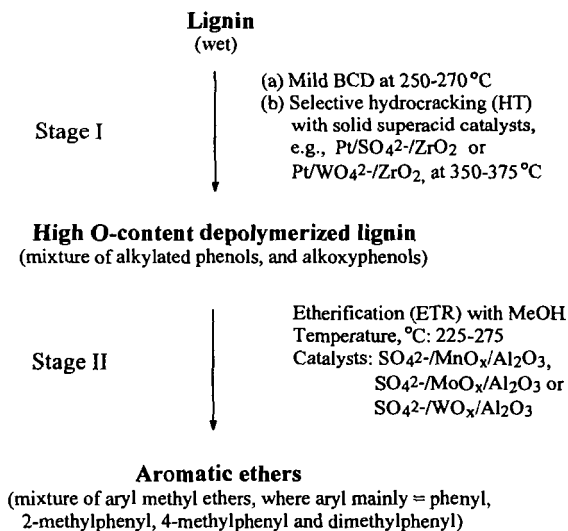


Figure 2. Scheme of two-stage (BCD-ETR) procedure for preferential conversion of lignin to aromatic ethers as fuel additives

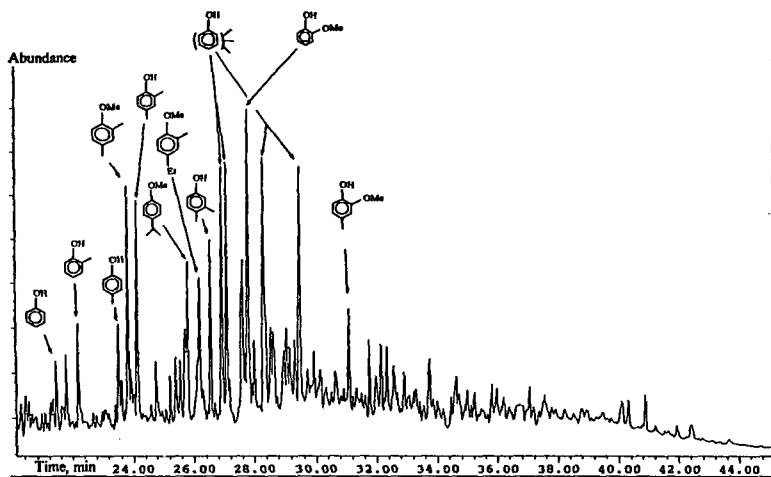


Figure 3. Example of GC/MS analysis of vacuum distilled BCD-HT product from Kraft lignin

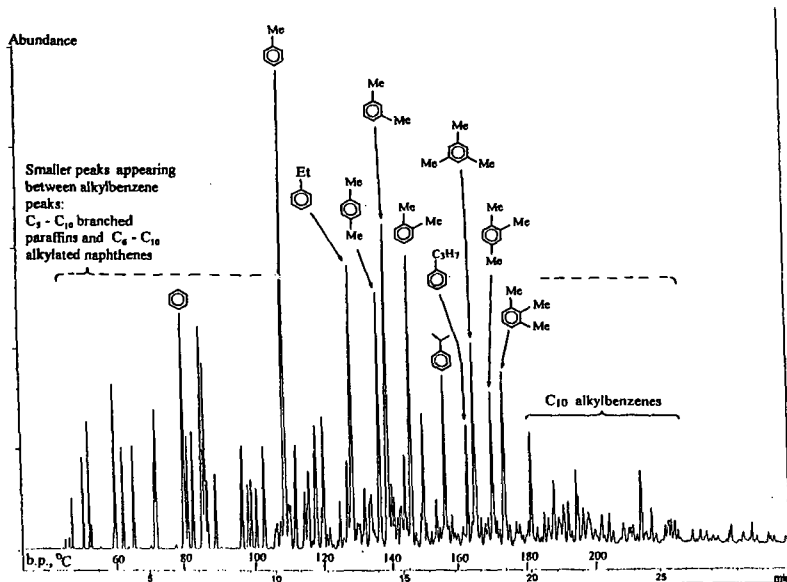


Figure 4. GC/MS analysis of BCD-HPR product from NREL lignin (lignin obtained as by product in the NREL ethanol process)

BATCH MICROREACTOR STUDIES OF BASE CATALYZED LIGNIN DEPOLYMERIZATION IN ALCOHOL SOLVENTS

James E. Miller, Lindsey Evans, Alicia Littlewolf, Matthew Lopez
Sandia National Laboratories
Albuquerque, NM 87185

Keywords: lignin, depolymerization, base catalysis

The depolymerization of organosolv-derived lignins by bases in methanol or ethanol solvent was studied in rapidly heated batch microreactors. The conversion of lignin to ether solubles by KOH in methanol or ethanol was rapid at 290 °C, reaching the maximum value within 10-15 minutes. An excess of base relative to lignin monomer units was required for maximum conversion. Strong bases (KOH, NaOH, CsOH) convert more of the lignin to ether soluble material than do weaker bases (LiOH, Ca(OH)₂, and Na₂CO₃). Ethanol and methanol are converted to acetic and formic acid respectively under the reaction conditions with an activation energy of approximately 50 kcal/mol. This results in a loss of solvent, but more importantly neutralizes the base catalyst, halting forward progress of the reaction.

INTRODUCTION

Drawing on previous experiences with coal liquefaction,¹ Shabtai and coworkers have recently developed a two-stage process for conversion of lignin to reformulated gasoline compositions.² The first stage of this process involves low-temperature (250-290 °C) base-catalyzed depolymerization (BCD) using supercritical methanol or ethanol as a reaction medium, whereas the second stage involves hydroprocessing of the depolymerized lignin intermediate. Using batch microautoclave reactors we have studied the lignin depolymerization reaction and here we report results for the time dependence of lignin depolymerization and the effect of base type and concentration. In previous model compound studies we observed the conversion of ethanol to acetic acid under reaction conditions.³ As this reaction has the potential to neutralize the base catalyst, we have also conducted controlled studies of the conversion of methanol and ethanol to formic and acetic acid under the lignin depolymerization conditions.

EXPERIMENTAL

The Alcell lignin samples used in this study were obtained from Repap Technologies Inc. (Valley Forge, PA) by the National Renewable Energy Laboratory and supplied to Sandia National Laboratories where they were used in the as-received condition. Alcell lignin is derived from mixed hardwoods by an ethanol organosolv pulping method.

Baseline Depolymerization Studies:

The reaction studies were conducted in microreactors consisting of capped 3/8" Swagelok bulkhead unions (internal volume approximately 14 cm³). In each baseline run, 0.434 g of as-received Alcell lignin was weighed into the reactor, and then 4.4 ml of a 10% (w/w) solution of KOH in research grade methanol or ethanol was added. The reactor was then securely sealed and heated in a fluidized sand bath to 290 °C. The fluid in the reactor equilibrates at the bath temperature in 90 seconds. After the desired reaction time had elapsed (0-60 minutes), the reactors were removed from the bath and rapidly quenched in water. One to three duplicates were performed for each reaction time. As a control, blank runs with no heating were also carried out.

After the reactors were cooled, the liquid and solid products of the reaction were rinsed from the vessel with deionized water and acidified to a pH of 2 with concentrated HCl. The recovered products were then covered and refrigerated overnight to allow the precipitate to grow and settle. The solid products were then recovered with a preweighed Whatman 541 filter. The solids were rinsed/extracted with deionized water followed by diethyl ether until the filtrate ran clear. The filter paper and remaining solids were allowed to air dry, and were then transferred to a 45 °C vacuum oven. After drying overnight, the filter papers and remaining solids were removed from the oven, allowed to air equilibrate for at least one hour and weighed. The results are expressed as the mass of unconverted lignin as a percentage of the original mass. The amount of converted material that was ether soluble, but not water soluble, was obtained by difference by following a similar procedure in experiments that eliminated the ether extraction step.

Effect of Base Type and Concentration: To evaluate the effect of base type and concentration, the reaction conditions were standardized at 290 °C, 60 minute reaction time, and ethanol solvent. Similar ion equivalents of the bases were added to the reactors to evaluate and compare

the bases individually and in combination. NaOH was added to the reactor as an ethanolic solution. CsOH, LiOH, Ca(OH)₂, and Na₂CO₃ were weighed into the reactors as solids.

Neutralization of Base by Organic Acids: To evaluate the rate of conversion of alcohols to acids, 3 mL aliquots of a solution consisting of 10% (w/w) base in alcohol solvent were transferred to microreactors fashioned from capped ¼" Swagelok unions (internal volume approximately 8 cm³). As before, the sealed reactors were heated in a fluidized sand bath to the desired reaction temperature (260-290 °C), and after the desired reaction time had elapsed, the reactors were removed from the bath and quenched in water. The contents of the reactor were then quantitatively sampled, diluted with deionized water and titrated with HCl to determine the free hydroxide content. In cases where solid precipitates formed in the reactor, the entire contents were dissolved in DI water and titrated. Titrations were performed with a Mettler DL70ES autotitrator.

RESULTS AND DISCUSSION

Lignin Depolymerization:

Figure 1 illustrates the solubility results from the baseline lignin depolymerization studies. The maximum conversion to water and ether solubles occurs during the first 15 minutes of the reaction. Conducting the reactions in ethanol rather than methanol resulted in a smaller amount of insoluble products. This is in contrast to results reported for coal, where the methanol/KOH combination resulted in a greater conversion to THF solubles than did ethanol/KOH.¹ The ethanol-derived products appeared to have an oily character, causing problems in determining the water insoluble fraction. In this case it was impossible to be certain when a sample was fully dry due to the apparent presence of volatile organics. This uncertainty may account for the increase in water insolubles for this material occurring after 10 minutes. The conversion data compares well to the results of Shabtai and coworkers. Our data for Alcell lignin in 10% KOH/methanol shows average yields of insolubles ranging from 14 to 17% at reaction times of 15 to 60 minutes. The data of Shabtai and coworkers collected for experiments conducted in a 300 ml autoclave over reaction times of 15 to 90 minutes shows average yields of insolubles ranging from 6.5 to 9.0% of the original mass.^{2,4}

Figure 2 illustrates the effect of different bases on lignin conversion. Note that the bases are compared at comparable concentrations rather than weight loadings. Clearly the stronger bases, NaOH, KOH, and CsOH are required to achieve significant depolymerization. Figure 3 illustrates the effect of base concentration on the lignin conversion for the three bases that exhibited significant conversion. Included on the figure is a line separating regions where the base concentration is either in stoichiometric excess or stoichiometric deficit. In other words, the line represents the amount of base where there is one equivalent of hydroxide ion for each lignin monomer. The calculation assumes an average molecular weight of 180 g/mol for a lignin monomer.⁵ The figure plainly shows that a stoichiometric excess of base is required for maximum lignin conversion.

In previous model compound studies of the lignin depolymerization reaction, we have detected the formation of acetic acid from ethanol.³ This suggests that the reason excess base is required is that the base catalyst is neutralized during the reaction by conversion of the solvent to organic acids. Figure 4 illustrates that this reaction proceeds relatively rapidly for KOH and ethanol at 290 °C. Almost all the base is neutralized within the first 15 minutes of reaction. This, of course, would effectively end any base-catalyzed lignin conversion. Note that in Figure 1, lignin conversion has reaches its maximum at about 15 minutes reaction time. Assuming first order kinetics, reaction rate constants and Arrhenius parameters can be calculated for the reactions. The lines in Figure 4 are the first order fit to the data. Figure 5 is the resulting Arrhenius plot for the data in Figure 4 and for similar reactions carried out with methanol and NaOH. The lines in the Arrhenius plot are nearly parallel suggesting that a similar reaction pathway is followed for all the cases and giving an average activation energy of 50 kcal/mol. As can be seen in Figure 4, this relatively large activation energy results in a significant temperature effect on the reaction rate. The combination of NaOH and methanol is the best case, giving the lowest conversion to acids. Thus by lowering the reaction temperature to 250 °C and by using NaOH and methanol rather than KOH and ethanol, the first order reaction rate constant for acid production (base neutralization) is lowered by a factor of more than 750. Additional work is required to determine the effects of these parameters on the lignin depolymerization reaction rate for comparison.

ACKNOWLEDGEMENTS

This work was supported by the United States Department of Energy under Contract DE-AC04-94AL850000. Sandia is a multiprogram laboratory operated by Sandia Corporation, a Lockheed Martin Company, for the United States Department of Energy.

REFERENCES

- ¹ Shabtai, J. S., Saito, I. U.S. Patent 4,728,418, 1988.
- ² Shabtai, J., Zmierzak, W., Chornet, E. In: Proc. 3rd Biomass Confer. of the Americas, Montreal; Elsevier, 1997, Vol. 2, p. 1037.
- ³ Miller, J. E., Evans, L., Littlewolf, A., Trudell, D. E. submitted to Fuel.
- ⁴ J. Shabtai, University of Utah, personal communication, February 1997.
- ⁵ D. Johnson, National Renewable Energy Laboratory, unpublished analysis of Alcell lignin.

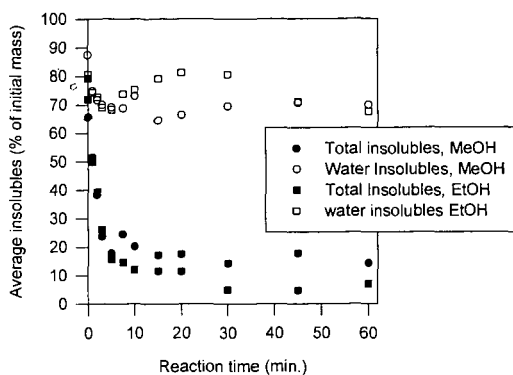


Figure 1. Conversion of Alcell lignin to water and ether solubles by KOH in methanol and ethanol.

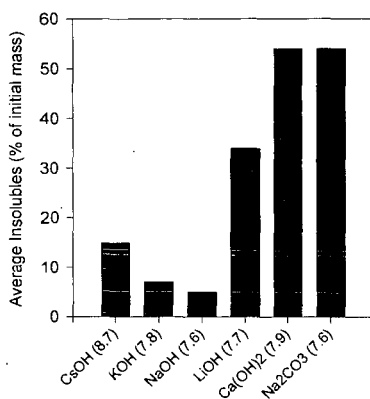


Figure 2. Conversion of Alcell lignin by different bases in ethanol solvent at 290 °C. Numbers in parentheses represent the milliequivalents of base in the reactor.

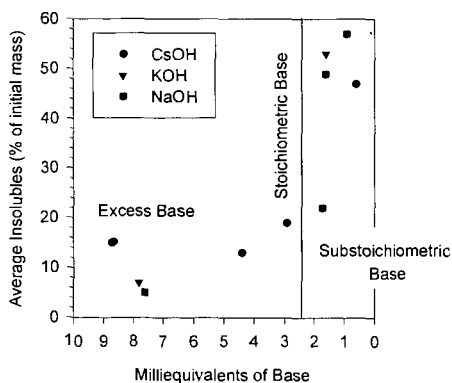


Figure 3. Effect of base concentration on conversion of Alcell lignin in ethanol at 290 °C.

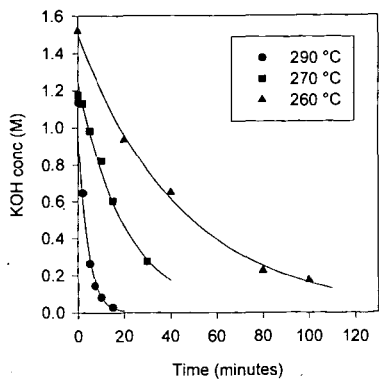


Figure 4. Rate of ethanol conversion to acetic acid in the presence of KOH as measured by the neutralization of KOH.

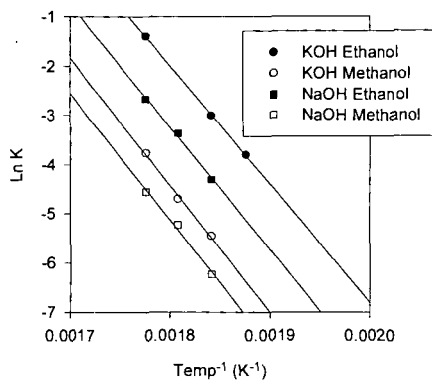


Figure 5. Arrhenius plots for the conversion of ethanol and methanol to organic acids by NaOH and KOH.

BIOMASS CHAR AND LIGNIN: POTENTIAL APPLICATION

N.N. Bakhshi*, A.K. Dalai*, R.W. Thring¹

*Department of Chemical Engineering, University of Saskatchewan, 110 Science Place, Saskatoon, SK S7N 5C9, ¹Chemical Engineering Department, University of New Brunswick, P.O. Box 4400, Fredericton, NB E3B 5A3

Keywords: Biomass Char, High Btu Gas, Hydrogen

INTRODUCTION

It is well known that biomass can be converted to a liquid product (usually called bio-oil or biofuel) using fast pyrolysis. This technology has now reached commercial stage. For example, two commercial plants using this technology (ENSYN Technologies Inc. of Ottawa, ON, Canada) are being operated by Red Arrow Products, Co., Inc. in Wisconsin (~ 50 tonnes/day). Also, a pilot demonstration unit (3 tonnes/day) is being operated in Galicia, Spain, using a bubbling fluidized bed (i.e. using the technology developed at the University of Waterloo, Canada). In these processes, the product slate consists of approximately 70 wt% liquid, 15 wt% char and 15 wt% gas. Thus, a certain amount of char is produced which needs to be disposed of (either by burning or some other method).

Furthermore, laboratory studies on upgrading this bio-oil using a zeolite (such as HZSM-5) have shown that in addition to hydrocarbon content in the liquid product, an additional amount of char (~ 10 – 20 wt%) also is produced. This char is in addition to the coke formed on the catalyst.

Also, lignin is a byproduct of little or no commercial value in the pulp and paper industry. In the dominant pulping process, namely kraft pulping, it is used primarily as a low grade fuel in the recovery boiler. It would be highly desirable to produce value-added products from lignin. Not only that, but its mere removal from the kraft process would allow many pulp mills, which are recovery boiler capacity limited to increase their pulp production.

Furthermore, an alternative pulping process (using an organic solvent vs. the more common kraft process) typically employs an organic solvent (or a solvent-aqueous mixture) with an acid catalyst for delignification at prescribed temperature and time sequences. An "organosolv process", the Alcell® process has been used by Repap Enterprises Corporation Inc. on an industrial demonstration scale in Miramichi, NB, Canada. We have attempted to convert the lignin produced from this process (Alcell® lignin) using acetone as solvent and treating it with HZSM-5 catalyst.

Thus, the thrust of this paper is to attempt to convert these materials – chars and lignins that are essentially waste materials – to useful and value-added products using steam gasification and catalytic upgrading techniques.

EXPERIMENTAL

(a) Steam Gasification of Chars and Lignins

Two chars were gasified with steam. Char A was obtained during the bio-oil production from biomass and was supplied by ENSYN Technologies Inc. of Ottawa, Canada. Char B was obtained during the catalytic upgrading of bio-oil using HZSM-5 catalyst (These runs were carried out in our laboratory).

Both the chars (A and B) were characterized thoroughly. The physical characteristics determined were: density, ash content, elemental analysis (CHN analysis), methylene blue number, Iodine number and BET surface areas (using ASAP Micromeritics 2000 equipment). The results are shown in Table 1.

Lignin (Kraft-1) was obtained from mostly spruce wood at Irving Pulp and Paper Company, New Brunswick, Canada. It was found to have a number average molecular weight of 1750 g/mol³.

The lignin used for converting to hydrocarbons (using acetone as the solvent) was the Alcell^(R) lignin. It was supplied by Alcell Technologies Inc. (Miramichi, New Brunswick, Canada) where it was isolated from a hardwood mixture in a demonstration facility. This lignin, available as a free-flowing powder of 20-40 µm median particle size, is hydrophobic, has a weight-average molar mass of <2000 g/mol, an ash content of <1 wt %, a C and H content of 66 and 6 wt %, respectively. Other typical characteristics of Alcell^(R) lignin have been presented elsewhere^{1,2}.

(i) Experimental Procedure for Steam Gasification of Chars and Kraft Lignin

Steam gasification was carried out at atmospheric pressure in a continuous down-flow fixed-bed microreactor operated at 600, 700 & 800°C. The reactor was 500 mm long, 11 mm i.d. 1-2 g of lignin/char was held on a plug of quartz wool, which was placed on a supporting mesh inside the microreactor. The top of the lignin/char sample was covered by another quartz wool plug of ~40 mm length. Each steam gasification run required the feeding of steam into the reactor at the prescribed feed rate.

A typical run was carried out as follows: the reactor was filled with a sample of accurately weighed lignin/char (1-2 g) mixed with quartz chips (mass ratio 1:8). The system was tested for leaks prior to the steam gasification run. Heating was started and when the reactor attained a temperature of ~110° C, water was fed into the reactor at the desired flow rate using a micrometering syringe pump (Eldex model A-60-S). The reactor had a long preheating section. Thus, there was sufficient time for the water introduced into the reactor to vaporize and to produce steam (at the gasification temperature used) before contacting the lignin/char. It took approximately 25-30 min to reach the desired operating temperature. The run was continued for another 30 min until no more gas was produced from the reactor. The product leaving the reactor was condensed and separated into liquid (mainly unreacted water) and gaseous fractions. The liquid product fraction was collected in a glass trap, which was cooled with flowing tap water. The gases were collected over saturated brine.

After each run, the spent lignin/char was removed from the reactor and weighed. The difference in combustible content of lignin/char before and after the run was taken as an estimate of the lignin or char converted.

(ii) Experimental Procedures for Catalytic Conversion of Alcell® Lignin Using HZSM-5 Catalyst

In this study, HZSM-5 zeolite catalyst was used for upgrading lignin (dissolved in acetone). This work was based on our earlier work which showed that biomass-derived oil (liquid product obtained from fast pyrolysis of biomass) and plant oils (such as canola) can be converted to value-added products such as aromatic hydrocarbons and cyclic aliphatic hydrocarbons over HZSM-5 zeolite catalyst.

The experiments were conducted at atmospheric pressure using a continuous down-flow fixed bed micro-reactor operated over a temperature range of 500 – 650 °C and WHSV range of 2.5 – 7.5 h⁻¹ (for the lignin and acetone solution). The reactor was a 400 mm long, 11.5 mm ID (made of 316 SS) placed coaxially in a furnace. The catalyst particle size range was 500 – 1410 µm. The catalyst was held by a plug of quartz glass wool which was placed on a supporting mesh inside the micro-reactor.

Additional details on the catalyst preparation and characterization are given elsewhere⁴.

The Alcell® lignin was found to be completely soluble in acetone. The liquid feed for the present study was prepared as a solution of this lignin in acetone in the weight ratio of 1 to 2 (lignin to acetone); other experimental details and product analysis details are given elsewhere⁴.

RESULTS AND DISCUSSION

(a) Steam Gasification of Chars and Lignin

Steam gasification of chars was carried out at three temperatures (600, 700 and 800 °C) and four steam feed rates (5, 10, 15 and 20 g of steam per h per g of char). It was found that the best char conversions were obtained at a temperature of 800 °C and steam feed rate of 10 g/h per g of char.

Table 2 shows the char and lignin conversion, total gas produced and product gas composition at the optimum conditions of steam feed rate at 10 g/h per g char and a temperature of 800 °C.

The results show that catalytic char (char B) is more reactive, i.e. has a higher conversion than commercial char (char A). Also, its heating value is higher 788 Btu/SCF vs 566 Btu/SCF (for char A). The product gas, has a high concentration of methane for char B (46.2 wt% vs. 41.1 mol %).

On the other hand, char A (commercial char) produces a higher volume of gas (124 L/100 g char) than char B which produced only 97L of gas / 100 g char. Furthermore, the product gas was rich in hydrogen (33.6 mol % for char A vs. 11.6 mol % for char B).

Kraft-1 lignin was the most reactive of all the three materials (94 wt%) and also, resulted in the highest amount of product gas (180 L/100 g lignin). It also produced the highest amount of hydrogen (36.9 mol %) amongst the three materials studied. However, the product gas heating value was the lowest (550 Btu/SCF) of the three.

(b) Catalytic Conversion of Alcell® Lignin Over HZSM-Catalyst

As has been stated earlier, Alcell® lignin was solubilized completely in acetone in the weight ratio 2:1 of acetone to lignin. This solution was used as the feed for lignin conversion.

The experimental conditions and mass balance are shown in Table 3. The lignin conversion to gaseous and liquid products greatly depends on the operating conditions and ranged from 50-85 wt%. The maximum conversion was 85 wt% and was obtained at 600 °C and a WHSV of 2.5 h⁻¹. Also, with increasing reaction temperature, increasing amounts of gas are produced with decreasing yields of liquid and solid residue (carbonaceous deposits left on the catalyst). The dramatic rise in total gas yield from 500 °C to 650 °C for a WHSV of 5 h⁻¹ is indicative of the extensive cleavage of the major bonds in lignin (-C-O-C- and -C-C-) via demethoxylation, demethylation, deoxygenation and pyrolytic reactions with increasing temperature. The maximum amount of liquid product (43 wt%) was obtained at 550 °C and a WHSV of 5 h⁻¹. It is interesting to note that the yield of liquid produced does not decrease as much as the solid residue (coke and char), which is reduced by almost 50% when the temperature was increased from 550 °C to 600 °C. However, the liquid product decreased dramatically to 11 wt% when the temperature was increased to 650 °C at a WHSV of 5 h⁻¹ due to more gas formation.

The char was the solid carbonaceous material which formed primarily above the catalyst bed. The formation of this material was exclusively the result of the thermal sensitivity of the lignin used, since cracking of the acetone solvent alone at these conditions only produced a gas. It is well known that char and coke formation is a major problem in any cracking process. Char and coke formation in the cracking of organic materials such as lignin is probably due to the condensation or polymerization reactions dominating over the cracking reactions.

In each experimental run, a mass balance over the entire process was found to be 95% or better.

ACKNOWLEDGEMENTS

Financial assistance from Natural Sciences and Engineering Research Council of Canada (NSERC) is greatly appreciated.

Table 1: Various Characteristics of Chars and Lignins

Char/ Lignin	Density g/mL	Ash Content wt %	Elemental Analysis				Methylene Blue No. mg/g	Iodine Number mg/g	BET surface area m ² /g
			C	H	O	N			
Char A	0.20	4.2	79.6	2.4	18	0	1.5	4.7	0.25
Char B	0.10	0.25	75.5	4.8	19.7	0	10	45	51
Kraft 1 Lignin	0.35	4.1	66.08	4.9	34.3	0	0.5	1.1	0.75

Table 2: Products Obtained and Conversions for the Steam Gasification of Chars and Lignin

Basis: 100 g of char or lignin

	Char B	Char A	Kraft-1 Lignin
Conversion, wt%	84.2	65.2	94.0
Total gas produced, L	97	124	180
Total gas produced, SCF	3.43	4.38	6.36
Gas Heating Value, Btu/SCF	788	566	550
Gas Composition, mol%			
Component			
H ₂	11.6	33.6	36.9
CO	14.4	11.4	17.1
CO ₂	14.9	13.4	9.5
CH ₄	46.2	41.1	35.5
C ₂	8.0	0.3	0.9
C ₃	3.4	0.2	0.1
C ₄ ⁺	1.5	0	0
Total	100.0	100.0	100.0

Table 3: Overall Material Balances and Liquid Product Composition from the Conversion of Alcell® Lignin Over HZSM-5

Temp., °C	500	550	600			650
WHSV, h ⁻¹	5	5	2.5	5	7.5	5
Yield of Products*, wt%						
Gas	11	19	51	54	58	68
Liquid	39	43	34	30	22	11
Char+Coke	50	33	15	16	20	21
Conversion	50	67	85	84	80	79
Composition, wt% of Liquid Product						
Alcohols	-	-	-	-	0.3	-
Ketones	-	-	-	-	0.2	-
Benzene	8.6	9.4	9.3	13.6	14.5	14.4
Toluene	33.1	36.7	31.0	42.4	41.9	43.7
Xylenes	31.5	33.0	25.0	22.7	24.8	21.0
Ethyl Benzene	3.0	2.1	2.2	1.9	1.5	1.3
Propyl Benzene	4.2	2.5	3.7	1.3	1.5	1.0
C ₉ + Aromatics	9.0	5.1	6.4	6.0	3.1	3.0
Total Aromatics	89.4	88.8	74.6	87.9	87.8	84.4
Total Aliphatic Hydrocarbon	-	-	-	0.5	0.6	0.5
Unidentified	10.6	11.2	25.4	11.3	11.3	15.1
Total	100	100	100	100	100	100

*wt% of lignin in the feed

REFERENCES

1. Lora, J.H., A.W. Creamer, L.C.E. Wu and G.C. Goyal, "Chemicals Generated During Alcohol Pulping: Characteristics and Applications", 6th International Symposium on Wood and Pulping Chemistry, Conference Proceedings, 431-438 (1991).
2. Pye, E.K. and J.H. Lora, "The Alcell Process. A Proven Alternative to Kraft Pulping", TAPPI, (73)3, 113-118 (1991).
3. Thring, R.W. and S.L. Griffin, "The Heterogeneity of Two Canadian Kraft Lignins", Can. J. Chem. 73, 629 (1995).
4. Thring, R.W., S.P.R. Katikaneni and N.N. Bakhshi, "The Production of Gasoline Range Hydrocarbons from Alcell® Lignin using HZSM-5 Catalyst, Fuel Processing Technology. (1998) submitted.

FLASH VACUUM PYROLYSIS OF LIGNIN MODEL COMPOUNDS: REACTION PATHWAYS OF AROMATIC METHOXY GROUPS

Phillip F. Britt, A. C. Buchanan, III, and Dan R. Martineau
Chemical and Analytical Sciences Division, Oak Ridge National Laboratory
P. O. Box 2008, MS-6197, Oak Ridge, TN 37831-6197

Keywords: Pyrolysis mechanisms, lignin, model compounds

ABSTRACT

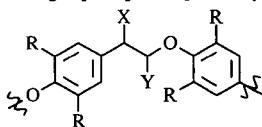
Currently, there is interest in utilizing lignin, a major constituent of biomass, as a renewable source of chemicals and fuels. High yields of liquid products can be obtained from the flash or fast pyrolysis of biomass, but the reaction pathways that lead to product formation are not understood. To provide insight into the primary reaction pathways under process relevant conditions, we are investigating the flash vacuum pyrolysis (FVP) of lignin model compounds at 500 °C. This presentation will focus on the FVP of β -ether linkages containing aromatic methoxy groups and the reaction pathways of methoxy-substituted phenoxy radicals.

INTRODUCTION

The thermochemical conversion of lignin, the second-most abundant naturally occurring biopolymer and a by-product of the pulping process, into higher value products is of interest as a consequence of its availability and its potential to produce higher value products [1]. However, in spite of the extensive research to expand the use of lignin, the efforts have been only moderately successful [2]. To enhance the economic production of liquid products from lignin, it is necessary to understand those factors that maximize product yields and promote product selectivity. Currently, the most promising process to maximize the yields of liquid products from biomass and lignin is flash or fast pyrolysis in which the substrate is heated to moderate temperatures, typically 500 °C, for contact times typically less than two seconds [3]. However, the fundamental chemical reactions that lead to the complex array of products remain poorly understood, and there is little insight into how to control product selectivity [4]. This is a consequence of the chemical and structural diversity of the lignin, the complexity of the product mixture, and the thermal instability of the primary products [1-4]. To overcome some of these complexities, we are investigating pyrolysis of compounds which model key structural features found in lignin to gain mechanistic insight into the reaction pathways and products [5].

To investigate the pyrolysis reactions at short contact times, lignin model compounds will be investigated by flash vacuum pyrolysis (FVP). In FVP experiments, the substrate is sublimed through a pyrolysis tube (at 500 °C for this study) under vacuum ($<10^{-3}$ mm Hg) and the products are quenched at low temperatures, typically 77 K. The contact time is typically <0.1 s and there are low steady-state concentrations of the reactants and products in the hot zone so that only very fast bimolecular reactions (such as radical-radical coupling reactions) can occur. Thus, the primary reaction pathways and reactive intermediates can be identified with a minimum of interference from bimolecular reactions. In future studies, the pyrolysis will be investigated at higher pressures (0.1 mm Hg to 1 atmosphere) under a flow of inert gas to determine the more complex secondary reaction pathways.

Lignin is a complex, heterogeneous, three-dimensional polymer formed from the enzyme-initiated, dehydrogenative, free-radical polymerization of three *p*-hydroxycinnamyl alcohol precursors that differ by the number of methoxy groups on the aromatic ring [1a, 6]. As opposed to other biopolymers such as cellulose, lignin has many different types of linkages between monomer units. The dominant interunit linkage in lignin is the arylglycerol- β -aryl ether linkage, commonly referred to as the β -O-4 linkage which accounts for approximately 48-60 % of the total interunit linkages [1a, 6], exemplified by the structure below. If this structure is



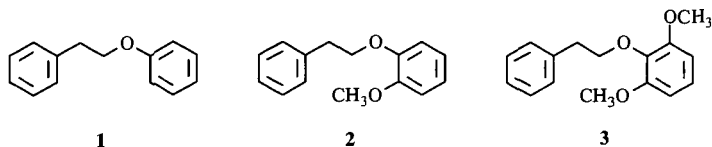
R = H or OCH₃

X = OH, OAr or =O

Y = CH₂OH or CH₂OR

stripped for all its substituents, the skeletal remnant would be phenethyl phenyl ether ($\text{PhCH}_2\text{CH}_2\text{OPh}$), the simplest model of the β -O-4 linkage, and the starting point for this mechanistic investigation.

In this investigation, the FVP of phenethyl phenyl ether (1), phenethyl *o*-methoxyphenyl ether (2), and phenethyl 2,6-dimethoxyphenyl ether (3) was studied at 500 °C under low pressures ($<10^{-3}$ mmHg) to determine the impact of methoxy substituents on the reaction pathways of the β -O-4 linkage of lignin. The methoxy-substituents accelerate the decomposition of the β -O-4 linkage and produce a complex array of products by a variety of reaction channels. Surprisingly, *o*-cresol was the major product in the FVP of 3. The reaction pathways for the decomposition of 1-3 and the formation of products are discussed below.



EXPERIMENTAL

Analyses were performed on a Hewlett-Packard 5890 Series II gas chromatograph equipped with a J&W 30 m x 0.25 mm i.d. (0.25 μm film thickness) DB-1 methylsilicone capillary column, a flame ionization detector, and a Hewlett-Packard 7673 autosampler. Detector response factors were determined for authentic samples relative to cumene, diphenyl ether, and 3,5-dimethylphenol or 3,4-dimethylphenol as internal standards or were based on carbon number. Mass spectra were obtained at 70 eV on a Hewlett-Packard 5972 GC/MS equipped with a capillary column identical to that used for GC analysis.

The syntheses of phenethyl phenyl ether (1) and $\text{PhCD}_2\text{CH}_2\text{OPh}$ (1- d_2) have been previously described [5b]. Phenethyl *o*-methoxyphenyl ether (2) and phenethyl 2,6-dimethoxyphenyl ether (3) were prepared by coupling 2-phenylethyl tosylate with guaiacol or 2,6-dimethoxyphenol in DMF with K_2CO_3 [5]. All compounds were purified by vacuum fractional distillation: 2, 99.8 % purity by GC: bp 109–110 °C (0.05 mmHg); MS m/z (relative intensity) 228 (32), 124 (16), 109 (11), 105 (100), 103 (12), 91 (9), 79 (18), 77 (32); 3, 99.5% purity by GC: bp 138–139 °C (0.025 mmHg); MS m/z (relative intensity) 258 (36), 154 (43), 139 (10), 105 (100), 103 (10), 95 (11), 91 (5), 79 (15), 77 (18).

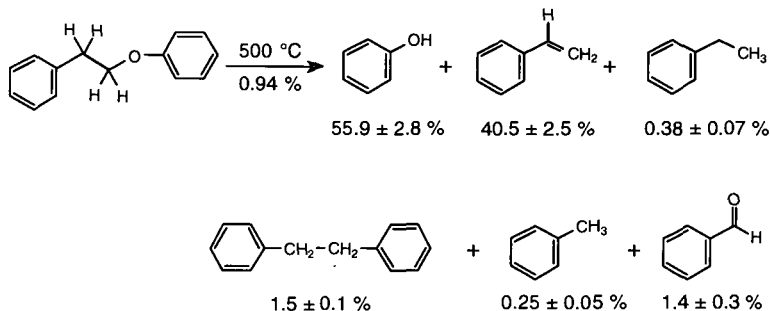
The FVP apparatus was based on the design reported by Trahanovsky and has been previously described [5a, 7]. All pyrolyses were run at $<10^{-3}$ mmHg and at 500 ± 1 °C. Sample throughput was typically 50–100 mg h^{-1} . Under these conditions, contact time is estimated at 2 ms and the steady state concentration of materials in the hot zone is 10^{-9} – 10^{-10} mol L^{-1} [8]. To check the long term reproducibility of the pyrolysis reactor to ensure that the relative reactivity of the substituted phenethyl phenyl ethers could be compared over time, the FVP of 2 was run after every 4–5 pyrolyses as a control sample. Similar pyrolysis results (± 10 %) have been obtained for 2 over a six-month period.

RESULTS AND DISCUSSION

FVP of 1. The major products from the FVP of 1 at 500 °C are shown below (average mol % from three runs). As a consequence of the low % conversions (0.94 ± 0.16 %), the reproducibility and the mass balances (95 ± 3 %) were not as good as that found at higher conversions. In addition to the products shown below, a small amount (typically, ≤ 1 % of the starting material) of rearranged 1, *o*-(2-phenylethyl)phenol and *p*-(2-phenylethyl)phenol, was also found. At higher temperatures (550 and 600 °C), the conversion of 1 increased to form the products shown above, but the yield of the rearranged products did not increase. It seems unlikely that the phenoxy and phenethyl radicals underwent recombination since no cross-coupling products, phenoxyphenol or 1,4-diphenylbutane, were observed [7b]. Therefore, the rearranged products were attributed to a small amount of acid catalysis from the quartz chips.

The major products from the FVP of 1 can be formed by cleavage of the C–O bond, i.e. the weakest bond in the molecule ($D^{\circ}_{\text{C-O}}$ and $D^{\circ}_{\text{C-C}}$ estimated as 63 and 72 kcal mol^{-1} , respectively) [5a]. Homolytic cleavage of the C–O bond forms $\text{PhO}\cdot$ which can pick up a hydrogen atom from the walls of the reactor to form PhOH [9] and $\text{PhCH}_2\text{CH}_2\cdot$ which can lose a hydrogen atom by β -scission to form $\text{PhCH}=\text{CH}_2$. In the decomposition of an analogous alkyl phenyl ether, *n*-butyl phenyl ether, it was proposed that products were formed by C–O homolysis ($\log k$ (s^{-1}) = 16.0 -

65.5 kcal mol⁻¹/ 2.303RT) and by 1,2-elimination through a four centered transition state (log k (s⁻¹) = 13.6 - 57.4 kcal mol⁻¹/ 2.303RT) [10]. At 500 °C, the ratio of homolysis to 1,2-

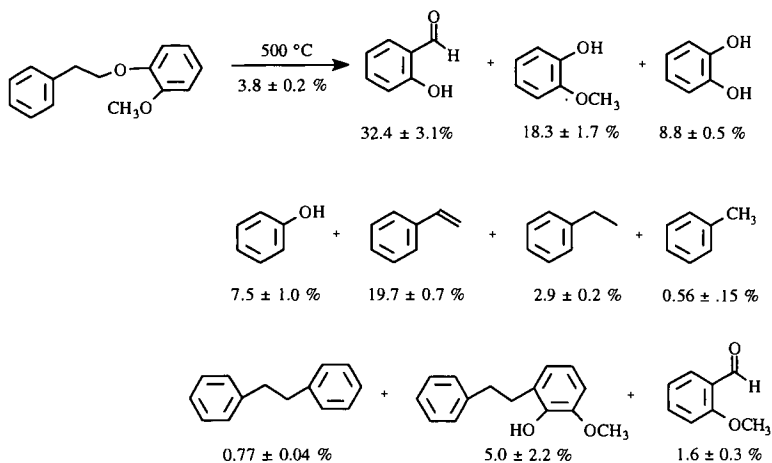


elimination is calculated to be 1.3:1. In the pyrolysis of **1**, 1,2-elimination would also produce styrene and phenol so that it is very difficult to deconvolute the homolysis and 1,2-elimination pathways in the decomposition of **1** since both routes lead to the same products. However, if **1** is substituted with deuterium in the benzylic position (PhCD₂CH₂OPh, **1-d₂**), the rate of 1,2-elimination would be slower, as a consequence of the deuterium isotope effect in breaking the C-D bond in the transition state, while the homolytic cleavage should not be influenced by the substitution. At 500 °C, a maximum rate difference ($k_{\text{H}}/k_{\text{D}}$) in the absence of tunneling) of 2.1 is predicted for the 1,2-elimination of **1**. In the pyrolytic 1,2-elimination of hydrogen halide from ethyl chloride, ethyl bromide, and their deuterated analogues, the measured isotope effect was ($k_{\text{H}}/k_{\text{D}}$) 2.0 - 2.2 at 500 °C [11]. Comparison of the % conversion from three FVP runs of **1-d₂** and **1** under similar conditions found that **1-d₂** reacted approximately 20 % slower than **1** indicating that the 1,2-elimination contributes to the decomposition of **1** at low pressures [12]. At higher pressures, radicals produced from C-O homolysis can start chain reactions and the contribution of 1,2-elimination will be small.

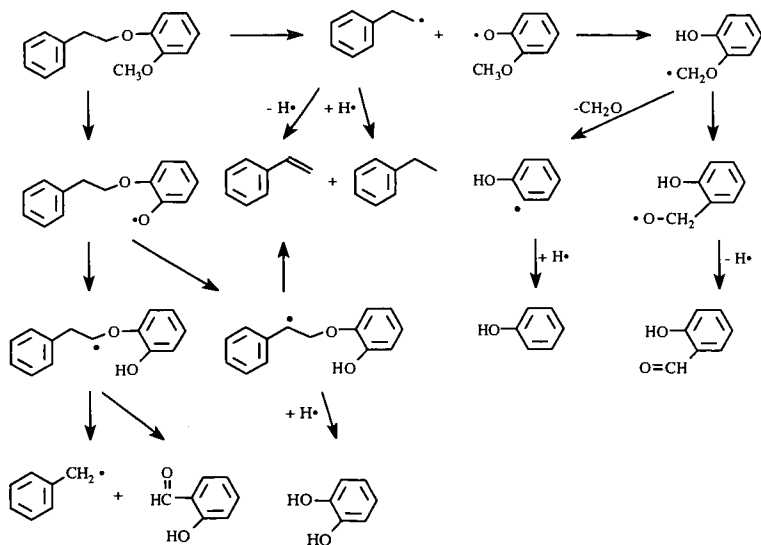
A small amount of toluene, bibenzyl, and benzaldehyde are formed from C-C homolysis. Under the low-pressure reaction conditions, a majority of the benzyl radicals couple to form bibenzyl. The phenoxy radical (PhOCH₂•) produces benzaldehyde by a 1,2-phenyl shift, to form the benzyloxy radical (PhCH₂O•), followed by loss of a hydrogen atom. The Arrhenius parameters for the formation of benzaldehyde from the phenoxy radical (PhOCH₂•) have been reported as log k (s⁻¹) = 12.5 - 21 kcal mol⁻¹/ 2.303RT [13]. β-Scission of the benzyloxy radical to form the phenyl radical and formaldehyde (log k (s⁻¹) = 14.0 - 24.5 kcal mol⁻¹/ 2.303RT) is approximately 100-times slower than loss of a hydrogen atom (log k (s⁻¹) = 13.9 - 17.2 kcal mol⁻¹/ 2.303RT) [14]. Thus, benzene is not predicted to be a primary pyrolysis product.

FVP of 2. The major products from FVP of **2** are shown below (average mol % from six runs). The conversion and mass balance for the FVP of **2** was 3.8 ± 0.2 % and 98.2 ± 4.6 %, respectively. Only a small amount (5.0 ± 2.2 mol %) of rearranged starting material (2-(2-phenylethyl)-6-methoxyphenol) was observed indicating that the surface mediated, acid-catalyzed reactions are of minor importance.

The decomposition of **2** is ca. four times faster than that for **1**. On the basis of the FVP results of **1**, the major products should arise from C-O homolysis and 1,2-elimination. The *o*-methoxy group is expected to accelerate the homolysis of the β-ether linkage since *o*- and *p*-methoxy groups have been shown to lower the bond dissociation energy of anisole by 4 kcal mol⁻¹ [15]. This would correspond to a rate enhancement of 13.5 at 500 °C. Homolysis of the O-CH₃ bond of the methoxy group is expected to be approximately four times slower than that for O-CH₂CH₂Ph basis on the average Arrhenius parameters for the homolysis of anisole (PhOCH₃) and phenetole (PhOCH₂CH₃) [16]. The rate of 1,2-elimination is predicted to be less sensitive to the methoxy substituent on the basis of the similar Arrhenius parameters obtained in the 1,2-elimination of *iso*-butylene from phenyl *tert*-butyl ether (log k (s⁻¹) = 14.3 ± 0.2 - 50.4 ± 0.7 kcal mol⁻¹/ 2.303RT) and *p*-methoxyphenyl *tert*-butyl ether (log k (s⁻¹) = 14.5 ± 0.3 - 50.2 ± 0.9 kcal mol⁻¹/ 2.303RT) [17]. Therefore, in addition to C-O homolysis, 1,2-elimination must have a significant contribution to the overall rate of decomposition of **2**, since the full rate enhancement predicted for the methoxy substituent was not realized.



The reaction pathways for the formation of the major products from the FVP of **2** are shown below. 1,2-Elimination from **2** produces styrene and guaiacol (not shown). Homolysis of C–O bond in **2** produces the *o*-methoxyphenoxy radical and the phenethyl radical, which will form styrene by β -scission of a hydrogen atom. The *o*-methoxyphenoxy radical can abstract hydrogen internally through a six-centered transition state to form the *o*-hydroxyphenoxyethyl radical. No guaiacol should be formed since internal hydrogen abstraction is fast compared to bimolecular wall associated hydrogen abstraction reactions [9]. Mulder has also shown that in the atmospheric pressure pyrolysis of dimethoxybenzene, hydrogen abstraction by *o*-methoxyphenoxy radical from a ten-fold excess of *p*-fluorotoluene is slower than internal

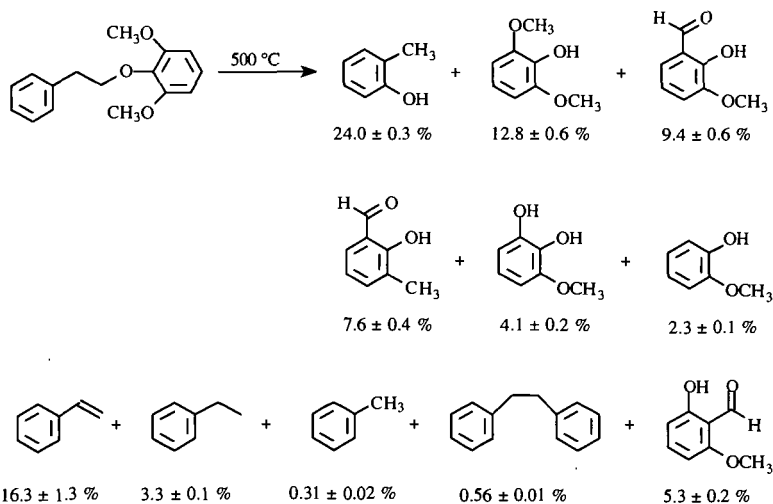


hydrogen abstraction [18]. The *o*-hydroxyphenoxyethyl radical can undergo a 1,2-phenyl shift, similar to that discussed above for the phenoxyethyl radical, to form the *o*-hydroxybenzyloxy radical which can lose a hydrogen atom to form *o*-hydroxybenzaldehyde. The loss of formaldehyde from the *o*-hydroxybenzyloxy radical is not expected to contribute to the formation of phenol on the basis of the rate constant for the β -scission of benzyloxy radical

reported above [14]. Phenol and formaldehyde can be produced from the β -scission of the *o*-hydroxyphenoxymethyl radical followed by hydrogen abstraction. Mulder has estimated the rate constant for this reaction to be $\log k (s^{-1}) = 14 - 28.4 \text{ kcal mol}^{-1} / 2.303RT$ from the ratio of hydroxybenzaldehyde and phenol produced in the pyrolysis of dimethoxybenzene. At 500 °C, the ratio is 3.9:1 [18]. In the FVP of **2**, the experimentally measured ratio of hydroxybenzaldehyde to phenol is 4.3:1, which is in good agreement with Mulder's data. The possibility that phenol arises from the pyrolysis of *o*-hydroxybenzaldehyde was ruled out since *o*-hydroxybenzaldehyde was stable under the reaction conditions.

Catechol could be formed by the pyrolysis of guaiacol since the *o*-hydroxy substituent lowers the bond dissociation energy of anisole by 7 kcal mol⁻¹ [15]. The FVP of guaiacol at 500 °C produced catechol as the major product. The average conversion from two runs was 4.5 ± 0.8 % and the mass balance was 98.2 ± 0.5 %. In the FVP of **2**, the ratio of guaiacol to catechol is 2.1. Therefore, pyrolysis of guaiacol is a only minor pathway for the formation of catechol. Catechol could also be formed from the cleavage of the methyl group from the *o*-methoxyphenoxy radical to form *o*-benzoquinone which could pick up hydrogen from the reactor walls to form catechol. However, Mulder did not observe catechol or *o*-benzoquinone in the pyrolysis of 1,2-dimethoxybenzene or 2,3-dihydro-1,4-benzodioxin [18]. Moreover, the cleavage of the methyl group must compete with intramolecular hydrogen transfer. Although reliable thermochemical kinetic estimates are not available for the partitioning between the two reaction channels, it is predicted that intramolecular hydrogen abstraction will be favored [19]. Another possible pathway for the formation of catechol is by C-O homolysis of the methoxy group to produce the methyl radical and PhCH₂CH₂OC₆H₄O•. Cleavage of the O-CH₃ bond is estimated to be ca. four times slower than cleavage of the phenethyl group [16]. Intramolecular hydrogen abstraction could occur at the β - or α -carbons (i.e. a 1,5 or 1,6-hydrogen transfer). Theoretical calculations on the isomerization of alkyl radicals predict that the 1,5-hydrogen shift will be responsible for over 70% of the isomerization, but 1,6-hydrogen shifts could contribute 10-25 % [20]. The ring strain for both 1,5- and 1,6-hydrogen transfer reactions were estimated to be less than 2 kcal mol⁻¹. Bimolecular hydrogen abstraction by the phenoxy radical is favored at the benzylic α -carbon over the β -carbon by a 3:1 ratio [5b]. Therefore, a 1,6-hydrogen transfer reaction may be competitive with the 1,5-hydrogen transfer. Intramolecular hydrogen abstraction from the α -carbon forms an intermediate that can cleave to produce styrene and *o*-hydroxyphenoxy radical, which can pick up hydrogen to form catechol. Intramolecular hydrogen abstraction from the β -carbon produces a radical which can undergo a 1,2-phenyl shift and cleavage to produce *o*-hydroxybenzaldehyde and the benzyl radical. Additional reaction pathways contributing to the formation of catechol are still under investigation.

FVP of 3. The major products from the FVP of **3** are shown below (average mol % from 3 pyrolyses). The conversion and mass balance for these runs are 9.9 ± 0.6 % and 99.7 ± 0.9 %, respectively. The second methoxy group accelerates the decomposition of the β -O-4 linkage (by



a factor of 2.6 compared to 2), but not to the same extent as the first methoxy group. Surprisingly, the major product in the FVP of 3 is *o*-cresol. On the basis of the pyrolysis of 2, the major product was predicted to be 2-hydroxy-3-methoxybenzaldehyde which was formed in only 9.4 % yield. The reaction pathways of the 2,6-dimethoxyphenoxy radical leading to the formation of *o*-cresol are currently under investigation.

ACKNOWLEDGMENTS

Research sponsored by the Division of Chemical Sciences, Office of Basic Energy Sciences, U.S. Department of Energy, under contract DE-AC05-96OR22464 with Oak Ridge National Laboratory, managed by Lockheed Martin Energy Research Corp.

REFERENCES

1. (a) Bridgwater, A. V. (Ed.), *Thermochemical Processing of Biomass*, Butterworths, London, 1984. (b) Soltes, E. J. and Milne, T. A. (Eds.), *Pyrolysis Oils from Biomass-Producing, Analyzing, and Upgrading*, ACS Symposium Series No 376, American Chemical Society, Washington, DC 1988. (c) Goldstein, I. S. (Ed.), *Organic Chemical from Biomass*, CRC Press, Boca Raton, FL 1981, Chapters 5 and 8.
2. Glasser, W. G.; Sarkanen, S. (Eds.), *Lignin Properties and Materials*, ACS Symposium Series No. 397, American Chemical Society, Washington, DC, 1989.
3. (a) Elliott, D. C.; Beckman, D.; Bridgwater, A. V.; Diebold, J. P.; Gevert, S. B.; Solantausta, Y. *Energy Fuels* **1991**, *5*, 399. (b) Bridgwater, A. V.; Cottam, M-L. *Energy Fuels* **1992**, *6*, 113.
4. a) Antal, Jr., M. J. in Boer, K. W. and Duffie, J. A. (Eds.), *Advances in Solar Energy*, Vol 2, ASES Publication, New Toyk, 1985, p.175 and references therein. (b) Evans, R. J.; Milne, T. A.; Soltys, M. N. *J. Anal. Appl. Pyrolysis* **1986**, *9*, 207. (c) van der Hage, E. R. E.; Mulder, M. M.; Boon, J. J. *J. Anal. Appl. Pyrolysis* **1993**, *25*, 149.
5. (a) Cooney, M. J.; Britt, P. F.; Buchanan, III, A. C. *Prepr. Pap.- Am. Chem. Soc., Div. Fuel Chem.* **1997**, *42(1)*, 89. (b) Britt, P. F.; Buchanan, III, A. C.; Malcolm, E. A. *J. Org. Chem.* **1995**, *60*, 6523. (c) Britt, P. F.; Buchanan, III, A. C.; Thomas, K. B.; Lee, S.-K. *J. Anal. Appl. Pyrolysis* **1995**, *33*, 1.
6. Glasser, W. G.; Glasser, H. R.; Morohoshi, N. *Macromolecules* **1981**, *14*, 253. (b) Nimz, H. *Angew. Chem. Int. Ed. Engl.* **1974**, *13*, 313.
7. (a) Trahanovsky, W. S.; Ong, C. C.; Pataky, J. G.; Weilt, F. L.; Mullen, P. W.; Clardy, J. C.; Hansen, R. S. *J. Org. Chem.* **1971**, *36*, 3575. (b) Trahanovsky, W. S.; Ong, C. C.; Lawson, J. A. *J. Am. Chem. Soc.* **1968**, *90*, 2839.
8. (a) Brown, R. F. C. *Pyrolytic Methods in Organic Chemistry*, Academic Press, New York, 1980. (b) Seybold, G. *Angew. Chem. Int. Ed. Engl.* **1977**, *16*, 365. (c) Schaden, G. *J. Anal. Appl. Pyrolysis* **1985**, *8*, 135. (d) Wiersum, U. E. *Rec. Trav. Chim. Pays-Bas* **1982**, *101*, 317 and 365. (e) Hedaya, E. *Acc. Chem. Res.* **1969**, *2*, 367. (f) Golden, D. M.; Spokes, G. N.; Benson, S. W. *Angew. Chem. Int. Ed. Engl.* **1973**, *12*, 534.
9. In the very low-pressure pyrolysis of diphenyl ether, molecular products (phenol and benzene) were observed by mass spectrometry rather than the radical species. It was proposed that wall associated hydrogen transfer reactions quenched the radical intermediates before arriving at the analyzer. Van Scheppingen, W.; Dorrestijn, E.; Arends, I.; Mulder, P.; Korth, H.-G. *J. Phys. Chem. A* **1997**, *101*, 5404.
10. Walker, J. A.; Tsang, W. *J. Phys. Chem.* **1990**, *94*, 3324.
11. Maccoll, A. *Chem. Rev.* **1969**, *69*, 33.
12. A 25 % reduction in conversion is predicted for a 1:1 ratio of homolysis to 1,2-elimination. The standard deviations of the % conversions are 10-20 %.
13. Mulcahy, M. F. R.; Tucker, B. G.; Williams, D. J.; Wilmshurst, J. R. *Aust. J. Chem.* **1967**, *20*, 1155.
14. Brezinsky, K.; Litzinger, T. A.; Glassman, I. *Int. J. Chem. Kinet.* **1984**, *16*, 1053.
15. Suryan, M. M.; Kafafi, S. A.; Stein, S. E. *J. Am. Chem. Soc.* **1989**, *111*, 1423.
16. Mallard, W. G.; Westly, F.; Herron, J. T.; Hampson, R. F.; Frizzell, D. H. *NIST Chemical Kinetics Database: Version 5* National Institute of Standards and Technology, Gaithersburg, MD, 1993.
17. a) Martin, G.; Martinez, H.; Ascanio, J. *Int. J. Chem. Kinet.* **1989**, *21*, 193. (b) Martin, G.; Martinez, H.; Ascanio, J. *Int. J. Chem. Kinet.* **1990**, *22*, 1136.
18. Schráa, G.-J.; Arends, I. W. C. E.; Mulder, P. *J. Chem. Soc. Perkin Trans. 2* **1994**, 189.

19. The activation energy for the hydrogen abstraction is estimated to be ca. 20 kcal mol⁻¹ based on Arrhenius parameters for hydrogen abstraction reactions in reference 5b and ΔH_{rxn} of ca. 9 kcal mol⁻¹. The A-factor for the intramolecular hydrogen abstraction reaction should be larger than that observed in solution (typically $10^{8.5 \pm 0.5} \text{ M}^{-1} \text{ s}^{-1}$). For example, the A-factor for 1,5-hydrogen shifts in alkyl radicals is $10^{9.2} \text{ s}^{-1}$ (Dobe, S.; Berces, T.; Reti, F.; Marta, F. *Int. J. Chem. Kinet.* **1987**, *19*, 895). The A-factor for the intramolecular hydrogen abstraction from 2-methylbenzoyloxy radical to form 2-carboxybenzyl radical has been reported to be $10^{10.5} \text{ s}^{-1}$ (Wang, J.; Tsuchiya, M.; Sakuragi, H.; Tokumaru, K. *Tetrahedron Lett.* **1994**, *35*, 6321). The cleavage of the methyl group from the methoxyphenoxy radical is estimated to have an activation energy over 40 kcal mol⁻¹ ($\Delta H_{\text{rxn}} = 35 \text{ kcal mol}^{-1}$) and the A-factor will be on the order of $10^{14-15} \text{ s}^{-1}$. Using these crude estimates, intramolecular hydrogen abstraction is predicted to be ten-times more favored than cleavage at 500 °C.
20. Viskolcz, B.; Lendvay, G.; Seres, L. *J. Phys. Chem. A* **1997**, *101*, 7119.

RESTRICTED MASS TRANSPORT EFFECTS ON THE PYROLYSIS PATHWAYS FOR LIGNIN MODEL COMPOUNDS. ARYL ETHER LINKAGES

A. C. Buchanan, III and Phillip F. Britt

Chemical & Analytical Sciences Division
Oak Ridge National Laboratory
1 Bethel Valley Road
P.O. Box 2008, MS-6197
Oak Ridge, Tennessee 37831-6197

Keywords: Lignin, model compounds, pyrolysis, restricted diffusion, aryl ethers

ABSTRACT

Aryl ethers are important linking units in the structure of lignins and low rank coals that are thermally labile at 375°C. Mass transport limitations experienced in these cross-linked macromolecular solids can lead to alterations in thermochemical processing kinetics and product yields. The molecular level details of these alterations on reaction pathways are revealed through studies of model compounds that are constrained to an inert silica surface through covalent attachments. The thermolysis mechanisms for the silica-immobilized (\approx) β -aryl ether model compounds, \approx PhCH₂CH₂OPh, \approx PhOCH₂CH₂Ph, \approx PhCH₂CH₂OPh-*o*-OCH₃, and the α -aryl ether model, \approx PhOCH₂Ph, have been investigated at 275-375°C. Free-radical rearrangement pathways involving O, C-phenyl shifts are found to be significant for these aryl ethers under diffusional constraints leading to new, unpredicted pyrolysis products. The selectivity for these rearrangement pathways depends strongly on the structure of neighboring molecules, as determined from studies of two-component surfaces containing spacer molecules.

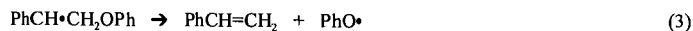
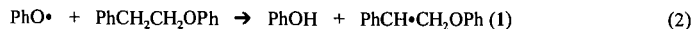
INTRODUCTION

Lignin is a complex, heterogeneous, three-dimensional biopolymer formed from the enzyme-initiated, dehydrogenative, free-radical co-polymerization of *trans-p*-coumaryl alcohol, *trans*-coniferyl alcohol, and *trans*-sinapyl alcohol.⁽¹⁾ Although there are several different types of linkages between monomer units, aryl ether linkages are dominant. In particular, β -aryl ether linkages, as typified by the simplest model compound, phenethyl phenyl ether (C₆H₅CH₂CH₂OC₆H₅ or PPE), can account for up to half of the total number of linkages. In addition, α -aryl ether linkages, as typified by the simplest model compound, benzyl phenyl ether (C₆H₅CH₂OC₆H₅ or BPE), can account for another 6-8 % of the linkages. The β -aryl ether linkages are typically less reactive thermochemically, since the C-O bond in PPE (ca. 63 kcal mol⁻¹) is about 11 kcal mol⁻¹ stronger than in BPE (ca. 52 kcal mol⁻¹).⁽²⁾ However, pyrolysis products and rates can not be easily predicted based solely on bond strength arguments.

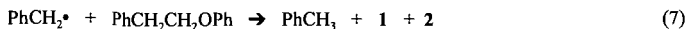
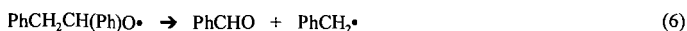
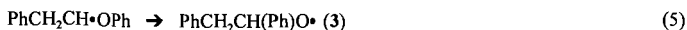
For example, in our earlier study of the pyrolysis of PPE in the liquid and vapor phases at 330-425°C,⁽²⁾ four major products were found (Eq. 1), and an activation energy of only 46 kcal mol⁻¹ was measured. We showed that the expected phenol and styrene products were formed



by a free radical chain process (propagation steps shown in Eqs. 2-3) following initial C-O homolysis. Even more striking was the discovery of a second previously unreported reaction



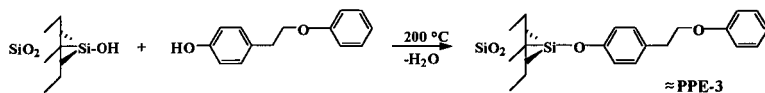
pathway that produced toluene and benzaldehyde in significant yields. This path (Eqs. 4-7), which accounted for typically 25 % of the pyrolysis products, involved the key rearrangement step 5, a 1,2-phenyl shift from oxygen to carbon (neophyl-like rearrangement) in radical intermediate, **2**, followed by β -scission of the rearranged radical, **3** (Eq. 6). The selectivity for these two competing pathways, which cycle through the α -carbon radical (**1**) and the β -carbon radical (**2**) was found to be 3.1 ± 0.1 independent of extent of reaction or initial PPE concentration.



We have been exploring in detail the effects of restricted mass transport on pyrolysis reaction mechanisms for a variety of fossil and biomass model compounds.⁽³⁾ Mass transport limitations are known to impact the global kinetics and product yields and distribution in the thermochemical processing of fossil and renewable organic energy resources.⁽⁴⁾ In our studies, restricted mass transport has been simulated through covalent attachment of the model compounds to a silica surface by means of a thermally robust Si-O-C_{aryl} linkage. This research has uncovered numerous examples where product selectivities and reaction rates are significantly altered compared with corresponding fluid phase models. In particular, retrogressive rearrangement and cyclization pathways can be promoted under restricted mass transport conditions. We have now examined several silica-immobilized (\approx) model compounds containing the β -aryl ether linkage, $\approx\text{PhCH}_2\text{CH}_2\text{OPh}$ ($\approx\text{PPE-3}$), $\approx\text{PhOCH}_2\text{CH}_2\text{Ph}$ ($\approx\text{PPE-1}$), $\approx\text{PhCH}_2\text{CH}_2\text{OPh-}o\text{-OCH}_3$ ($\approx\text{PPE-3-}o\text{-OMe}$) to see the effect of diffusional constraints on the selectivity for the new reaction path involving rearrangement step 5. Furthermore, we have examined the pyrolysis of a model of the α -aryl ether linkage, $\approx\text{PhOCH}_2\text{Ph}$ ($\approx\text{BPE}$), and discovered that an analogous 1,2-phenyl shift occurs leading to new products not reported in fluid phases. The influence of the structure of neighboring molecules on the selectivity for these rearrangement pathways has been examined through the use of two component surfaces containing spacer molecules of varying structure.

EXPERIMENTAL

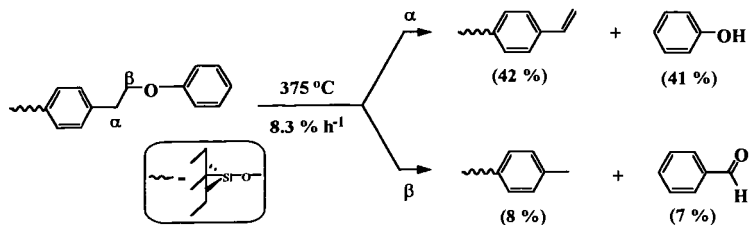
Preparation of the silica-immobilized model compounds involved condensation of phenolic precursors with the surface silanol groups on a fumed silica as shown below for the case of $\approx\text{PPE-3}$. The syntheses of the precursor phenols, *p*-HOPhCH₂CH₂OPh,⁽⁵⁾ *p*-HOPhOCH₂CH₂Ph,⁽⁵⁾ *p*-HOPhCH₂CH₂OPh-*o*-OCH₃,⁽⁵⁾ and *m*-HOPhOCH₂Ph⁽⁶⁾ have been previously reported. The general methods for attachment of the phenols to the silica surface (200 m² g⁻¹; 12 nm primary particle size) have also been described.⁽⁴⁻⁶⁾ Two component surfaces containing an ether model compound and a spacer compound such as biphenyl ($\approx\text{BP}$), naphthalene ($\approx\text{NAP}$), diphenylmethane ($\approx\text{DPM}$), or tetralin ($\approx\text{TET}$) were prepared analogously by co-attachment of the appropriate phenols in a single step.



Thermolyses were conducted in sealed, evacuated (2×10^{-6} torr) T-shaped Pyrex tubes in a temperature controlled ($\pm 1^\circ\text{C}$) furnace.⁽⁴⁻⁶⁾ Volatile products were collected as they were produced in a liquid nitrogen cold trap, and subsequently analyzed by GC and GC-MS with the use of internal calibration standards. Surface-attached products were similarly analyzed after digestion of the silica in aqueous base, neutralization, extraction of the products into an organic solvent, and silylation of the resulting phenols to the corresponding trimethylsilyl ethers.

RESULTS AND DISCUSSION

Phenethyl Phenyl Ether Models. Pyrolysis of $\approx\text{PPE-3}$ (0.56 mmol g⁻¹) at 375°C generates a set of products comparable to that found for PPE in the liquid and gas phases as shown below. Both reaction pathways, cycling through radicals at the α - and β -carbons, are found to be operative under restricted mass transport conditions. The measured α/β path selectivity value is 5, which is slightly higher than for fluid-phase PPE as a consequence of the *p*-silyloxy linkage to the surface that stabilizes the α -radical. This was confirmed by pyrolysis studies of *p*-(CH₃)₃SiOPhCH₂CH₂OPh (as a model for $\approx\text{PPE-3}$) in the gas phase at 375°C, which



gave a comparable α/β selectivity value of 4.4 ± 0.5 . Furthermore, pyrolysis of the isomeric \approx PPE-1 (\approx PhOCH₂CH₂Ph; 0.50 mmol g⁻¹), where the silyloxy substituent is remote from the α - and β -carbons, results in a selectivity value of 3.1 ± 0.3 consistent with the removal of the substituent effect.

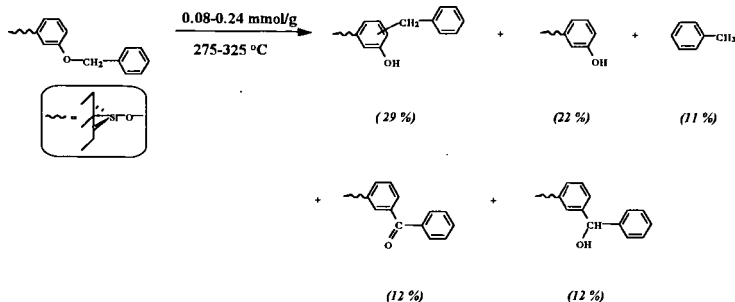
Pyrolysis of \approx PhCH₂CH₂OPh-*o*-OCH₃ (\approx PPE-3-*o*-OMe; 0.55 mmol g⁻¹) was also investigated since this model compound contains the guaiacyl unit that is prominent in lignins from gymnosperms. A comparable product slate to that shown above for \approx PPE-3 is obtained with an α/β path selectivity of ca. 6. It is clear from the pyrolysis of these three model compounds that the new rearrangement/ β -scission path observed for fluid phase PPE is also important under conditions of restricted diffusion.

An examination of the pyrolysis of \approx PPE-3 in the presence of aromatic spacer molecules reveals that the α/β path selectivity is sensitive to the presence and structure of neighboring aromatic molecules on the surface. This effect was not observed for the pyrolysis of PPE in fluid

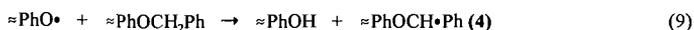
Surface:	\approx PPE-3 / \approx <i>p</i> -BP	\approx PPE-3 / \approx <i>m</i> -BP	\approx PPE-3 / \approx NAP
Coverage: (mmol/g)	0.050 / 0.54	0.066 / 0.51	0.072 / 0.45
α/β Selectivity:	20 ± 4	10 ± 2	20 ± 2

phases⁽²⁾ where the path selectivity was independent of the presence of added biphenyl up to the maximum dilution investigated (90% biphenyl). Since the relative rates of hydrogen abstraction from the α - and β -carbons should not be significantly impacted by the aromatic spacers, our current hypothesis is that the proximate aromatic spacers must be sterically hindering the 1,2-phenyl shift from oxygen to carbon. As illustrated from comparison of the *p*-BP and *m*-BP cases, the degree to which this pathway is hindered will also depend on the orientation and packing efficiency for the molecules on the surface. The effects of spacer structure on the pyrolysis path selectivity for \approx PPE-3 will continue to be investigated.

Benzyl Phenyl Ether Model. Pyrolysis of \approx BPE generated a more complex product mixture than observed for BPE in fluid phases.⁽⁶⁾ Although numerous products have been identified, the major products shown below typically account for > 85 mol % of the pyrolysis

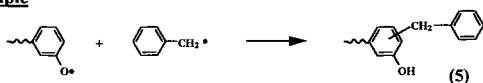


products. As in the case of fluid-phase BPE, the initial event is homolysis of the weak O-C bond as shown in Eq. 8. Arrhenius treatment of 10 pyrolyses (0.24 mmol g⁻¹) at 275-325 °C gave log $k/s^{-1} = (15.4 \pm 0.6) - (51.0 \pm 1.6)/2.303RT$. These Arrhenius parameters are in reasonable agreement with the values obtained for pyrolysis of BPE in fluid phases.⁶⁾ Hydrogen abstraction by the incipient radicals generated the toluene and surface-bound phenol products (Eqs. 9-10).

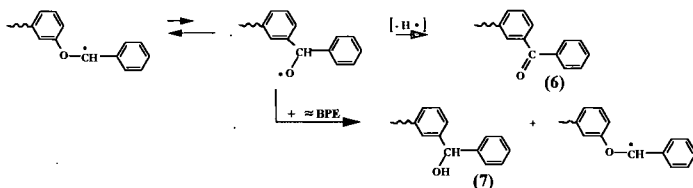


Surprisingly, two additional decomposition routes were found for \approx BPE that involved molecular rearrangements that establish a more refractory diphenylmethane-type linkage, as shown below. The first pathway involves recoupling of the radicals formed in step 8 at the ring carbons of the phenoxy radical to form isomers of silica-immobilized benzylphenol (5). This pathway, which accounts for typically 29-37 mol % of the products over a wide range of surface coverages and temperatures is clearly promoted by restricted diffusion compared with fluid phases, where the corresponding products typically account for only 10-15 mol % of the pyrolysis

Recouple



Phenyl Shift



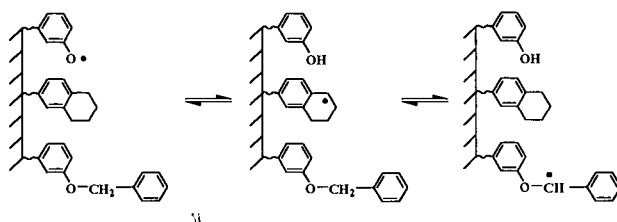
products. The second rearrangement path, not reported in fluid-phase studies of BPE, forms the surface-bound benzophenone (6) and benzhydrol (7) products. As in the case of the PPE models, a 1,2-phenyl shift from oxygen to carbon occurs to generate an oxy-radical intermediate. In contrast to PPE models, this radical does not possess a competitive β -scission pathway and undergoes hydrogen transfer reactions to generate the ketone and alcohol products.

As shown in Table 1, these rearrangement pathways for \approx BPE typically account for ca. 50 mol % of the pyrolysis products. However, the path selectivity is found to be very dependent on both surface coverage and the structure of neighboring spacer molecules (tetralin or naphthalene) on the surface. As the surface coverage decreases, the rates of hydrogen transfer steps on the surface decrease as molecules become increasingly separated on the silica surface.

Table 1. Selectivity for Rearrangement Pathways in \approx BPE Pyrolysis			
surface composition	coverage (mmol g ⁻¹)	product yield, 5 + 6 + 7, (mol %)	path selectivity, (recouple/phenyl shift), 5 / (6 + 7)
\approx BPE	0.24	51.9 \pm 1.3	1.00
	0.18	50.2 \pm 1.8	1.34
	0.094	50.2 \pm 1.5	1.78
	0.084	47.3 \pm 1.6	2.04
\approx BPE/ \approx TET	0.068/0.17	54.3 \pm 3.0	1.21
\approx BPE/ \approx NAP	0.067/0.14	40.7 \pm 2.4	2.94

This reduces the rate of formation of radical 4, as well as subsequent hydrogen transfer steps, and results in an increased selectivity for the simple recoupling path. This premise is further supported by the effect of spacer structure on the rearrangement path selectivity. The aromatic spacer,

naphthalene (\approx NAP), serves as a barrier that further retards hydrogen transfer steps and enhances the selectivity for recoupling. On the other hand, the hydroaromatic spacer, tetralin (\approx TET), is able to participate in a well-established hydrogen transfer, radical relay process (shown below),^(4a,c) which alleviates some of the diffusional constraints in producing radical 4 by reducing the separation between molecules and hydrogen-abstracting radicals on the surface. This results in a path selectivity comparable to that of \approx BPE at high surface coverages.



CONCLUSIONS

Pyrolysis studies of lignin model compounds under restricted mass transport conditions have revealed the significance of new product forming reaction pathways involving 1,2-phenyl shift rearrangements in radical intermediates of the type, \approx PhCH₂CH•OPh and \approx PhCH•OPh. Related rearrangement pathways have been found to be promoted in the pyrolysis of the coal model compounds, silica-immobilized bibenzyl^(4b,c) and benzyl phenyl sulfide,⁽⁶⁾ involving \approx PhCH₂CH•Ph and \approx PhSCH•Ph intermediates, respectively. These rearrangement paths are often promoted by diffusional constraints compared with fluid phases, but can be significantly impacted by the proximity and structure of neighboring molecules.

ACKNOWLEDGMENTS

This research was sponsored by the Division of Chemical Sciences, Office of Basic Energy Sciences, U.S. Department of Energy, under contract No. DE-AC05-96OR22464 with Oak Ridge National Laboratory, managed by Lockheed Martin Energy Research, Corp.

REFERENCES

- (a) Alder, E. *J. Wood Sci. Technol.* **1977**, *11*, 169. (b) Nimz, H. *Angew. Chem. Int. Ed. Engl.* **1974**, *13*, 313.
- Britt, P. F.; Buchanan, III, A. C.; Malcolm, E. A. *J. Org. Chem.* **1995**, *60*, 6523.
- (a) Buchanan, III, A. C.; Britt, P. F.; Thomas, K. B.; Biggs, C. A. *J. Am. Chem. Soc.* **1996**, *118*, 2182. (b) Buchanan, III, A. C.; Dunstan, T. D. J.; Douglas, E. C.; Poutsma, M. L. *J. Am. Chem. Soc.* **1986**, *108*, 7703. (c) Buchanan, III, A. C.; Biggs, C. A. *J. Org. Chem.* **1989**, *54*, 517. (d) Britt, P. F.; Buchanan, III, A. C. *J. Org. Chem.* **1991**, *56*, 6132. (e) Buchanan, III, A. C.; Britt, P. F.; Thomas, K. B. *Energy & Fuels* **1998**, *12*, 649. (f) Britt, P. F.; Buchanan, III, A. C.; Malcolm, E. A.; Biggs, C. A. *J. Anal. Appl. Pyrolysis* **1993**, *25*, 407. (g) Buchanan, III, A. C.; Britt, P. F.; Biggs, C. A. *Energy Fuels* **1990**, *4*, 415.
- (a) Gavalas, G. R. *Coal Pyrolysis*; Elsevier: Amsterdam, 1982. (b) Solomon, P. R.; Fletcher, T. H.; Pugmire, R. J. *Fuel* **1993**, *72*, 587. (c) Suuberg, E. M. in *Chemistry of Coal Conversion*; Schlosberg, R. H., Ed.; Plenum Press: New York, 1985; Chapter 4. (d) Wanzl, W. *Biomass and Bioenergy* **1994**, *7*, 131. (e) Blasi, C. D. *Biomass and Bioenergy* **1994**, *7*, 87. (f) Serio, M. A.; Charpenay, S.; Basilakis, R.; Solomon, P. R. *Biomass and Bioenergy* **1994**, *7*, 107.
- Britt, P. F.; Buchanan, III, A. C.; Thomas, K. B.; Lee, S.-K. *J. Anal. Appl. Pyrolysis* **1995**, *33*, 1.
- (a) Buchanan, III, A. C.; Britt, P. F.; Skeen, J. T.; Struss, J. A.; Elam, C. L. *J. Org. Chem.*, **1999**, in press. (b) Buchanan, III, A. C.; Britt, P. F.; Skeen, J. T. *Prepr. Pap.-Am. Chem. Soc., Div. Fuel Chem.* **1997**, *42*, 15.
- Hatcher, P. G. *Org. Geochem.* **1990**, *16*, 1959.
- Ismail, K.; Mitchell, S. C.; Brown, S. D.; Snape, C. E.; Buchanan, III, A. C.; Britt, P. F.; Franco, D. V.; Maes, I. I.; Yperman, J. *Energy & Fuels* **1995**, *9*, 707.

POTENTIAL BENEFITS OF CO-LOCATING BIOMASS-BASED ETHANOL PRODUCTION AT COAL-FIRED POWER PLANTS

James L. Easterly
DynCorp I&ET
300 North Lee Street
Alexandria, VA 22314

Keywords: Ethanol co-production, coal-fired power plants, biomass hydrolysis

ABSTRACT

Co-locating biomass-based ethanol production facilities adjacent to coal-fired power plants could provide attractive economic and environmental benefits for these power plants, including reduced fuel costs, as well as reduced NO_x and greenhouse gases (GHG) emissions. Hydrolysis technology for producing ethanol from renewable, low-cost cellulosic biomass (such as wood chips, grass clippings or waste paper) is now in the initial phase of commercial development. The lignin byproduct from the ethanol plant is an energy-dense renewable fuel that can be cofired in a coal boiler, and the coal plant could provide process steam for the ethanol plant. Significant NO_x emissions reductions (20% to 30%) may be possible if the lignin is cofired as a water slurry mixed with coal fines (providing a beneficial means for their disposal). Emerging plans for NO_x emissions trading and renewable portfolio standards could enhance the value of this approach.

INTRODUCTION

In the U.S., about 1.3 billion gallons of ethanol are currently consumed as fuel in the automotive sector.¹ Most of this fuel is used as a 10 percent blend with gasoline, either to boost the octane of gasoline or to provide added oxygen content to gasoline. (Increasing the oxygen content of gasoline helps reduce emissions of carbon monoxide from automobiles in communities that are out of compliance with air quality standards.) The U.S. Congress has recently extended the federal excise tax exemption for ethanol fuel to the year 2007.

Virtually all of the ethanol currently used in the U.S. is made from starch-based crops (primarily corn) using conventional fermentation technologies. Advanced fermentation technologies have been developed that allow the use of a wide variety of abundant, low-cost, renewable biomass materials for conversion to ethanol. This biomass material, known as lignocellulosic biomass, includes organic matter such as wood chips, saw dust, waste paper, crop residues, grass clippings, and a variety of fast growing woody and herbaceous energy crops. Energy crops are expected to yield 5 to 10 dry tons per acre per year. There are over 30 million acres of set-aside farm land that could be used to grow perennial energy crops (the roots of these crops remain in the soil from year to year, even with crop harvests, providing continued protection from soil erosion). At a yield of 80 gallons of ethanol per dry ton of biomass, this set-aside land could provide 12 billion to 24 billion gallons of ethanol per year.

Advanced fermentation technologies use acids and/or enzymes to break down (i.e., hydrolyze) lignocellulosic biomass into material that can be fermented to ethanol. Technologies that use acid for the process, known as acid hydrolysis technologies, are being commercially developed today. Ethanol production technologies that use enzymes, known as enzymatic hydrolysis technologies, are also well along in the development cycle. The primary commercialization hurdle for enzymatic technology has been the need to reduce enzyme production costs. Three commercial acid-hydrolysis ethanol plants are currently being developed, two in California and one in New York; a fourth facility is being developed in Louisiana that may use either enzymatic or acid hydrolysis.²

Acid-hydrolysis technologies include weak acid and concentrated acid processes. Concentrated acid hydrolysis technology is somewhat further advanced than weak acid hydrolysis. However, one potential advantage of weak acid systems is that they could be converted to enzymatic hydrolysis plants once the cost of enzymes have been reduced. Enzymatic hydrolysis systems will typically have a weak acid pretreatment phase and are expected to provide improved efficiencies/yields in converting biomass to ethanol.

BENEFITS OF CO-PRODUCTION

Cellulosic biomass, such as wood, typically contains about 25 percent lignin. While the lignin cannot be fermented to ethanol, it is an energy-dense material. The lignin by-product from the ethanol production process can be used as a boiler fuel to produce steam to meet the process heat and electricity needs of the ethanol plant. For a stand-alone hydrolysis-based ethanol production facility, approximately one-third of the capital cost would be for an on-site power plant, including a lignin-

fueled boiler and a turbine generator system.³ Co-locating an ethanol plant next to an existing coal-fired power plant offers the potential for significant cost savings by avoiding the need for a new on-site power plant. Lignin could be sent to the existing power plant for fuel. In return, the power plant could provide process steam and electricity needed for the ethanol production process, with some excess electricity available for export to the grid. Figure 1 provides an overall flow diagram for the co-production approach. The co-production approach is similar to direct cofiring of biomass in coal-fired boilers. The difference is that a preprocessing step is added where the fermentable portion of the biomass is used to make ethanol as a co-product, while the remaining non-fermentable biomass is cofired as a fuel in a coal-fired power plant boiler.

Co-locating ethanol production at existing coal-fired power plants could potentially accelerate commercialization and deployment of hydrolysis-based ethanol technology, while providing economic and environmental benefits to coal-fired power plants. From the perspective of the ethanol plant, the co-location approach offers a number of benefits, including: a supply of process steam, a market for the lignin by-product, reduced capital costs, reduced siting and permitting difficulties, shared management and overhead costs, shared operating and maintenance costs, as well as existing industrial infrastructure. From the perspective of the coal-fired power plant, potential benefits include: increased energy efficiency with cogeneration, potentially lower fuel costs (if lignin is provided to the coal plant at a cost below that for coal), reduced emissions of greenhouse gases, potential reductions in NO_x emissions, and additional revenue from steam/electricity sales to the ethanol plant.

Greenhouse Gas Benefits

The co-production of ethanol at existing coal-fired power plants could offer a cost-effective option for electric utilities to reduce net emissions of greenhouse gases in three ways: 1) Reducing coal use by cofiring renewable biomass fuel in the form of lignin; 2) Increasing the thermal efficiency of coal use (via cogeneration, with lower grade process steam used by the ethanol facility); and 3) By producing liquid renewable fuel that offsets petroleum fuel use for transportation.

The thermal efficiency gains from combined heat and power production and the resulting greenhouse gas benefits for the co-location approach will be dependent on the configuration of specific coal-fired power plants. As a transportation fuel, corn-based ethanol results in about 20% less GHG emissions than gasoline, and cellulose-based ethanol (used in the form of E85, a blend of 85% ethanol and 15% gasoline) results in 80% less GHG emissions than gasoline, based on conservative estimates from the U.S. Department of Energy and Argonne National Laboratory.^{4,5}

ISSUES REGARDING LIGNIN UTILIZATION

What are the characteristics of the lignin that is produced as a by-product from the ethanol process, and how will these characteristics effect the way that it is delivered and utilized as a fuel at a coal-fired power plant? Lignin is in the "stillage" from the ethanol plant and must be dewatered. There are a number of ways that dewatering can be done. To a certain extent, the drying approach selected can be tailored to the needs of the boiler/power plant where it is to be used as fuel. One possibility for the drying process is to use a centrifuge, followed by a rotary vacuum filter.⁶ This would produce a lignin cake with about 55 percent solids, which could then be used as a boiler fuel. It is possible that low-grade waste heat could be available for further drying of the lignin. Another potential approach is to deliver lignin in the form of a slurry to the coal boiler. If lignin can be delivered in a suitable slurry, this approach offers potential advantages in transporting lignin to an adjacent power plant and in feeding the lignin into the coal boiler for combustion. There has been some promising work done in the U.S. to evaluate coal/water slurries for fueling power plants.⁷

Dry lignin from hardwood has a heating value of about 10,600 Btu/lb and dry lignin from softwood has a heating value of about 11,300 Btu/lb. Dry woody biomass has a heating value of approximately 8,700 Btu/lb and dry herbaceous biomass is about 7,500 Btu/lb.⁸ Bituminous coal has roughly 13,000 Btu/lb. The cost of coal for power plants is typically in the range of \$1 to \$1.20/MMBtu (million Btu) and the cost of coal will generally determine the value of the lignin as an alternate fuel source for the power plant (on a \$/MMBtu basis).

Potential NO_x Impacts/Benefits of Lignin Cofiring

Lignin/water slurries could provide reduced NO_x emissions at existing coal-fired power plants. Tests by the GPU electric utility in Pennsylvania and by Pennsylvania State University found that cofiring a coal-water slurry in an existing coal-fired power plant significantly reduced NO_x emissions.⁹ The NO_x reduction begins occurring when the slurry input is at a 10% level (energy basis) and reaches full benefit levels when cofired at a 20% level. A 20% slurry will likely reduce NO_x emissions by 20%. It is quite possible that lignin/water slurries will provide a similar effect.

Electric utilities are under increasing pressure to reduce NO_x emissions. For example, On Sept. 24, 1998, the U.S. Environmental Protection Agency (EPA) directed 23 Midwestern and Northeastern states to reduce NO_x emissions by 28% by the year 2003. This EPA directive includes the

implementation of a NO_x trading system that is technology neutral.¹⁰ NO_x trades are expected to be valued between \$1500/ton to \$2700/ton of avoided NO_x emissions. Testing is needed to verify the ability of lignin/water slurries to reduce NO_x emissions. If a NO_x benefit is demonstrated with this approach, utilities may view a lignin/water slurry as a premium fuel for cofiring in coal-fired power plants. As a premium fuel, lignin could have a higher value, thus improving the economics of ethanol production with the co-location approach. For coal plants with low NO_x burners, a 20% NO_x reduction for lignin/water slurries could provide a credit per gallon of ethanol produced ranging from 2.4 cents/gallon to 4.0 cents/gallon (corresponding to the \$1500/ton to \$2700/ton trade values for avoided NO_x emissions). For coal plants without low NO_x burners, a 20% NO_x reduction for lignin/water slurries could provide a credit per gallon of ethanol produced ranging from 3.5 cents/gallon to 6.3 cents/gallon (corresponding to the \$1500/ton to \$2700/ton trade values for avoided NO_x emissions). Thus NO_x credits for cellulose-derived ethanol (with co-location at a coal-fired power plant) could be valued somewhere between 2.3 and 6.3 cents/gallon. Assuming that the NO_x credit has a value of 3 cents/gallon, from the perspective of the coal plant a 50 million gallon per year ethanol facility could provide \$1.5 million in NO_x credits for an adjacent coal-fired power plant. Another option (and potential side benefit) would be for coal-fired power plants to blend their coal fine residues with the lignin/water slurry, adding fuel value to the slurry, while solving problems with the management and disposal of coal fines.

ETHANOL FACILITY SCALE

It is useful to have a sense of the likely scale anticipated for a cellulose-based ethanol facility, and how this scale would compare to coal-fired power plants. Assuming a yield of 80 gallons of ethanol per dry ton of biomass, a 25 million gallon per year ethanol plant would use an amount of biomass similar to a 43 megawatt stand-alone biomass power plant. This scale is in the range of typical larger biomass power plants that have been developed in the U.S. (assuming the biomass power plant operates at a 25% conversion efficiency -- a reasonable state-of-the-art facility using a boiler for biomass conversion). With wood as the feedstock for ethanol production, the lignin residues from a 25 million gallon per year ethanol facility would provide enough fuel to generate 19 megawatts of electricity when cofired in a coal-fired power plant, assuming the coal plant operates at a 35% conversion efficiency. (Note that this is another advantage of cofiring; larger coal plants typically have higher conversion efficiencies than smaller stand-alone biomass power plants achieve.) At 19 megawatts, the fuel input from lignin would be 10% of a 190 megawatt coal plant -- 10% is a typical range anticipated for viable biomass/coal cofiring approaches.

COGENERATION ISSUES

Assuming separate ownership of the ethanol facility and power plant, how much can the ethanol facility afford to pay for the steam provided by the power plant? Conversely, how much would the power plant need to be paid for steam delivered to the ethanol plant for process heat? The quality of the steam would be a significant factor. High pressure/temperature steam would have a high value for the power plant operation since it could be used to make electricity. Lower grade steam (at lower pressures and temperatures) would be less valuable to the power plant. Most of the steam needed for hydrolysis-based ethanol facilities is lower grade steam. One possible approach would be to establish a streamlined trading agreement between the ethanol producer and the coal-based power plant. The lignin could essentially be traded to the power plant in exchange for the process steam and electricity needed for the ethanol process, with no monetary payments made between the ethanol plant and power plant. However, it may be difficult to reach such an agreement, given the different values for fuel and energy which would "cross the fence" between the two operations. However, this idea has enough merit to warrant further consideration.

THE "VISION 21 ENERGYPLEX" CONCEPT

The DOE Office of Fossil Energy has a major new "Vision 21 EnergyPlex" initiative underway.¹¹ The goal of this initiative is to integrate advanced concepts for high-efficiency power generation and pollution control into a new class of fuel-flexible facilities. These facilities would be capable of co-producing electric power, process heat and high value fuels (such as ethanol) and chemicals. The goal is to achieve "environmentally friendly" facilities that produce virtually no emissions/pollutants. The energyplex concept envisions modular generation facilities that will mix traditional and next-generation technologies (including the use of waste stream "opportunity fuels" such as biomass). The future core technologies anticipated with this concept include coal gasifiers coupled to fuel cells. Coal conversion with greater than 50 percent efficiencies and very low emissions are envisioned. Some form of permanent carbon dioxide storage is being explored with the concept, such as carbon dioxide injection/storage in unmineable coal seams. The Vision 21 concept has been endorsed by the President's Committee of Advisors on Science and Technology (PCAST). The co-production of ethanol from cellulosic biomass at existing coal-fired power plants is consistent with, and complementary to, the Vision 21 concept -- where multiple feedstocks would be processed

at a site for the production of multiple products, with increased overall feedstock conversion efficiencies, and reduced greenhouse gas emissions.

COFIRING STATUS AND ISSUES

There are five utilities currently cofiring biomass in existing coal-fired power plants.¹² There have also been many trial test runs of biomass cofiring at utilities across the U.S. that provide a basis of experience upon which to draw. With assistance from the Federal Energy Technology Center (FETC), the Electric Power Research Institute (EPRI) and the DOE Biomass Power Program are collaborating in efforts to foster increased cofiring by the electric power industry.

With respect to cofiring opportunities, one of the biggest concerns for operators of coal-fired power plants would be procuring biomass fuel. One advantage of the ethanol co-location approach would be the option of having the ethanol facility operator deal with biomass supply contracting (in the same way that biomass-based independent power producers currently operate). In this case, the ethanol facility could offer long-term contracts to the power plant for lignin fuel delivery, dramatically simplifying the fuel procurement process for biomass cofiring.

Marketing Issues Regarding Coal Ash from Biomass Cofiring

Some concerns have been raised regarding the marketing of ash from coal-based power plants when biomass material is cofired with coal. ASTM Standard C-618 narrowly defines acceptable coal ash for cement applications as ash that is exclusively derived from burning coal. Efforts are underway to modify this standard to make it similar to one used in Canada. There, the acceptability of coal ash for cement applications is based on the chemical and physical characteristics of the ash, rather than the fuel/feedstocks that are used for combustion.

MONETIZATION OF GREENHOUSE GAS BENEFITS

If an economic value can be established for reduced greenhouse gas emissions, this will significantly enhance the attractiveness of ethanol co-production at coal-fired power plants. A number of early pilot efforts are underway to establish markets for tradable emissions credits associated with reduced GHG emissions. The success of the sulfur dioxide allowance trading program in the U.S. is considered a potentially attractive model for a trading program that establishes allowances for greenhouse gas emissions reductions.¹³ The most significant progress to date in building a framework that could evolve toward this type of a trading program is in voluntary international greenhouse gas emissions trading. The International Utility Efficiency Partnerships (IUEP) is one of the organizations involved in international greenhouse gas (GHG) reduction efforts. The Edison Electric Institute sponsors IUEP. A key activity of IUEP is to facilitate United States International Joint Implementation (JI) projects for greenhouse-gas credits. Under this structure, electric utilities receive offsets for domestic carbon dioxide emissions by sponsoring projects in developing countries that result in carbon sequestration or reductions in GHG emissions. Efforts are currently underway to set up an "International Offsets Facility" that will operate as a bank for GHG offsets. Initially it was anticipated that GHG credits would be valued in the range of \$1.50 per ton, but their value has already gone as high as \$3 to \$4 per ton of carbon equivalent offset. Procedures are being established for registering, transferring and processing "clean development mechanisms" (CDMs) in order to certify carbon trading offsets (CTOs).¹⁴

Renewable portfolio standards are being implemented by a number of states and are also being considered at the federal level. These standards require that a minimum portion of future electric generating capacity in a state be derived from renewable energy sources. Biomass cofiring offers the most attractive option to utilities for meeting these standards, since it is the lowest-cost renewable option.¹² Thus renewable portfolio standards could be another means of recognizing the GHG benefits of biomass cofiring and ethanol co-production. Implementation of these standards at the state or federal level may open significant opportunities for cofiring (and ethanol co-production) projects in the near- to mid-term.

SUMMARY

From the point of view of a hydrolysis-based ethanol facility, it appears likely that co-locating near a coal-fired power plant would be beneficial. The main uncertainty is the extent to which co-locating will be beneficial for coal-fired power plants. Key questions that need to be answered to determine the attractiveness of ethanol co-locating to coal-fired power plants (and electric utilities) include the following:

- What will be the price of the lignin?
- Will lignin cause boiler tube fouling?
- Will lignin cofiring impact coal ash marketing for cement applications?
- What are the characteristics of the lignin when it is delivered to the coal boiler (e.g., slurry, powder, moisture content, etc.)?

- What quality steam would an ethanol facility need and how much would the ethanol facility be willing to pay for the steam delivered from a coal-fired power plant?
- What would be the revenue for electricity sales to the ethanol plant?
- What are the regulatory or market drivers for reducing greenhouse gas emissions?

For electric utilities, the attractiveness of the ethanol co-location approach would be significantly enhanced if they could receive financial credit for the reduced GHG emissions provided by this approach. While monetization of avoided GHG emissions or, conversely, savings from avoided carbon taxes, are not currently available for U.S. domestic projects, renewable portfolio standards could play an analogous role. These standards are being implemented by a number of states in recognition of the environmental benefits offered by renewables and could play a significant role in fostering cofiring, including the co-production of ethanol at coal-fired power plants.

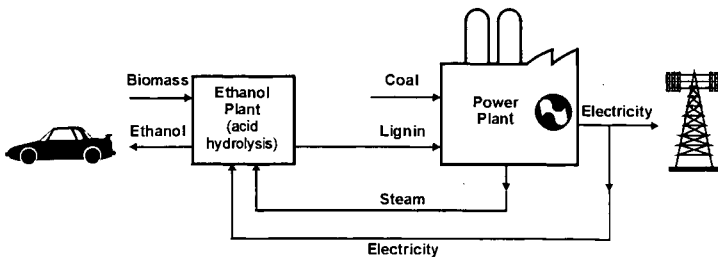
REFERENCES

1. U.S. Department of Energy, Energy Information Administration, *EIA-819 Monthly Oxygenate Telephone Report.*, August 1998, Washington, DC
2. Santos-Leon, G., Ethanol Program Manager, DOE Office of Fuels Development, meeting in Washington, DC, June 22, 1998.
3. Yancey, M., and Sheehan, M. editors, *Northeastern California Ethanol Manufacturing Feasibility Study*, National Renewable Energy Laboratory, November 1997.
4. Wang, M., Saricks, C., Santini, D., Argonne National Laboratory, Center for Transportation Research, *Fuel-Cycle Energy and Greenhouse Gas Emissions Effects of Ethanol*, ethanol meeting at the U.S. Department of Energy, September 29, 1998.
5. Nguyen, T., Office of Fuels Development, U.S. Department of Energy, September 1998, *personal communication.*
6. Stone & Webster, Weyerhaeuser, Amoco, Carolina Power and Light, *New Bern Biomass to Energy Project; Phase I Feasibility Study*, National Renewable Energy Laboratory and Electric Power Research Institute, June 1995.
7. Morrison, J., Miller, B., Scaroni, A., (Pennsylvania State University), *Coal-Water Slurry Fuel Production: Its Evolution and Current Status in the United States*, 14th International Pittsburgh Coal Conference, China, September 23-27, 1997.
8. Domalski, E., Jobe, T., Jr., Milne, T., *Thermodynamic Data for Biomass Materials and Waste Components*, American Society of Mechanical Engineers, 1988.
9. Battista, J., GPU Generation, Inc., September 1998, *personal communication.*
10. National Journal's Greenwire, *SMOG: EPA Unveils Final NO_x Rules for Eastern States*, September 25, 1998.
11. U.S. Department of Energy, "The Vision 21 EnergyPlex Concept", internet site: www.fe.doc.gov/coal_power/fs_vision21.html, June 15, 1998.
12. Hughes, E., Electric Power Research Institute, meeting in Washington, DC, June 22, 1998
13. Sandor, R., "Getting Started with a Pilot: the Rationale for a Limited-Scale Voluntary International Greenhouse Gas Emissions Trading Program," White House Conference on Climate Change, Oct. 6, 1997.
14. Parker, C., Materials Development Corporation, meeting in Washington, DC, June 22, 1998

ACKNOWLEDGEMENTS

This paper summarizes issues evaluated by the author under a project sponsored by the U.S. Department of Energy's Office of Fuels Development.

Figure 1. Integrated production of ethanol at a coal-fired power plant.



THE DIRECT LIQUEFACTION CO-PROCESSING OF COAL, OIL, PLASTICS, MSW, AND BIOMASS

Alfred G. Comolli, Partha Ganguli, Robert H. Stalzer, Theo L.K. Lee, and Peizheng Zhou
Hydrocarbon Technologies, Inc. (HTI)
1501 New York Avenue
Lawrenceville, New Jersey 08648

Key Words

1. Co-processing
2. Liquefaction
3. Direct

ABSTRACT

Hydrocarbon Technologies, Inc. (HTI) and the United States Department of Energy (DOE) have been working on the application of the Direct Liquefaction Process to the conversion of various low-cost, carbon-based feedstocks. In the United States, direct liquefaction has been directed to utilize waste and biomass in combination with coal and oil in order to lower CO₂ emissions and to be cost-competitive. Through collaboration with DOE, HTI has become our country's leading R&D and commercial developer of Direct Liquefaction. Under a current DOE contract, HTI has developed waste plastics/coal co-processing technology to produce fuels that can be produced at a cost comparable to crude oil. Further development would reuse/recycle plastics and waste organics, turn them into valuable feedstocks, remove sulfur and nitrogen, and lower CO₂ emissions, while utilizing domestic feedstocks.

Conversion and yield data will be presented for various feedstock combinations and concepts presented for further studies. The economics of coal and waste co-processing will be forecast based on stand-alone and refinery-integrated facilities.

INTRODUCTION

Direct Liquefaction involves the addition of hydrogen to unsaturated hydrocarbons, followed by rearrangement, cracking of bulky molecules, and removal of heteroatoms to produce lighter and cleaner transportation fuels (gasoline, diesel, and jet) and specialty chemicals and carbon-based products. In the process, the sulfur and nitrogen are removed by reduction and conversion to sulfur and ammonia.

With Direct Liquefaction, fuels are produced in a process similar to the hydrocracking of heavy oils in today's refineries. Hydrogen is added to the carbon chain, heteroatoms are removed, and the larger molecules are cracked and rehydrated to clean fuel molecules at energy efficiencies over 75 percent. In Indirect Liquefaction, fuels and chemicals are constructed from single carbon structures (syngas) produced by gasification into higher molecular weight fuels by Fischer-Tropsch Chemistry and additional processing at overall energy efficiencies approaching 50 percent. Thus, Direct Liquefaction is a more efficient process with lower emissions.

The Direct Liquefaction process for coal and coal/oil/plastics feedstocks has been under development for over 30 years under the auspices of the United States Department of Energy and its predecessors as constituted today. It is an extremely versatile, highly efficient process that can convert nearly all low-cost carbon-based feedstocks into fuels and chemicals. According to the "vision" of the DOE, by the year 2015, large fractions of municipal, agricultural, and industrial wastes will become valuable energy resources. These currently wasted resources can be recovered and recycled in economical and environmentally sound ways through development of co-processing technologies using our abundant fossil fuel resources.

Recently, the technology has been directed to utilize waste plastics and other waste hydrocarbons in combination with coal and heavy oils in order to address waste disposal issues, lower CO₂ contribution emissions, and be more cost-competitive. Through collaboration with DOE and Industry, HTI has developed waste plastics/coal/oil co-processing technology that can produce fuels at a projected cost comparable to crude oil at \$16/barrel. This development would reuse/recycle plastics, turn them into valuable feedstocks, lower emissions, and utilize domestic feedstocks and waste materials to supplement imported oil.

Hydrocarbon Technologies is continuing to direct its R&D activities towards the development of a Renewable Energy Clean Fuels Complex of the future utilizing the energy efficient Direct Liquefaction Process for the production of clean transportation fuels, chemicals, and carbon

products. The HTI CoPro Plus™ process entails co-liquefaction of organic feedstocks with coal and/or oil in a two-stage reactor system using a dispersed catalyst and in-line hydrotreating.

Process Equipment Description

The coal/oil slurry is premixed off-line and charged to a feed tank on a periodic basis. The slurry feed is pumped through both reactors with or without interstage separation. Interstage separation, if used, removes the light oils and the gases from the first reactor so that the second reactor is more efficiently used to upgrade only the remaining heavy material. The effluent from the second reactor is separated in a hot separator. The overhead from the hot separator is sent to a cold separator and separated into a vent gas stream and a separator overhead stream (SOH). The vent gases are metered, sampled, and sent to flare, and the SOH is collected. The second stage hot separator overhead stream can also be sent directly to an in-line hydrotreater for further upgrading and heteroatom removal. For co-processing and heavy oil upgrading, the bottoms material from the hot separator is separated off-line in a batch vacuum distillation into a vacuum still overhead stream (VSOH) and a vacuum still bottoms stream (VSB). These streams are then analyzed. Part of the VSOH is used as a process oil in the buffer pumps for the first and second stage reactors. For coal liquefaction, the bottoms material from the hot separator is separated off-line in a pressure filter into a pressure filter liquid (PFL) and a pressure filter solid (PFS). These streams are then analyzed. Part of the PFL is used as a process oil in the buffer pumps for the first and second stage reactors, and part of the PFL is used as slurry oil for the coal and fed back to the reactors. Figure 1 shows a schematic of the process.

EXPERIMENTAL RESULTS

Throughout the co-liquefaction programs at HTI, various feedstocks have been examined for conversion to either fuels or chemicals utilizing both sub-bituminous and bituminous coal and heavy California (Hondo) oils. Each of the continuous bench scale test runs described herein used a proprietary dispersed iron catalyst called GelCat™.

Tables 1 and 2 present the comparison of runs using Black Thunder sub-bituminous coal, waste curbside plastics, and heavy Hondo resids co-processed in various combinations at several space velocities.

Table 3 shows further comparisons of liquefaction performance with coal and automotive shredder residue, with curbside plastics and plastics-derived pyrolysis oils.

HTI has accumulated extensive data on the direct liquefaction and hydrocracking of lignin, having tested this concept for various clients since the 1970s. Test results indicate that good conversion to phenol and cresol can be obtained using iron-based catalysts. The product oils from a Kraft lignin are a mixture of phenols and cresols as shown in Table 4. This wood waste is also a good source of fuels and chemicals when co-processed with coal and heavy-oil.

The world's vast resources of coal and heavy-oil can be utilized by processing to liquid fuels. The catalytic coal liquefaction process is technically well developed but not economical yet. An innovative process for addition of inexpensive hydrocarbons from MSW into the coal/waste liquefaction and heavy-oil/waste liquefaction processes should make these processes highly economic and, at the same time, alleviate the costly MSW disposal problem and help reduce carbon emissions through the use of renewables. A simplification of a process now under development at HTI is shown in Figure 2.

RESULTS AND CONCLUSIONS

Table 1 shows the operating parameters for the oil, plastics, coal combinations tested. As can be seen, feed conversions vary from 96 to 99.9 wt% maf. The addition of waste plastics shows an increase in residuum conversion and distillate yield. Waste curbside plastics as seen improve performance and also decrease hydrogen consumption due to the higher hydrogen content of the plastics versus the oil and coal feedstocks. Additionally, the addition of plastics controls the manufacture of undesirable light C₁-C₃ gas yields. Thus, the addition of plastics redirects hydrogen to the production of valuable liquids rather than gases.

As seen from Table 2, the overhead products are of excellent quality with high API to 50 and H/C atomic ratios close to 2.0 and nitrogen and sulfur contents below 15 ppm sulfur and 1 ppm nitrogen.

Table 3 represents a comparison of the performance of five run conditions, from the co-processing of auto shredder residue and pyrolysis oil. Co-processing of Black Thunder coal,

Hondo oil, and Auto Shredder Residue (ASR) resulted in 83.6 W% resid conversion and 66.8 W% distillate yield. A dramatic drop in both resid conversion and distillate yield was observed when Hondo oil was removed from the mixture of coal and ASR (PB-04-4). It seemed that vehicle solvent is essential in converting ASR and coal. In Run PB-04-5, 25 W% of plastics was added to the coal and ASR mixture. It is interesting to note that distillate yield was increased from 56.6 to 61.4 W%, while 524°C+ resid conversion was increased proportionally, from 72.4 to 77.2 W%. Also, it is observed that addition of plastics has a significant impact on hydrogen production, but also reduces hydrogen consumption by about 2 W%. Economic analysis showed that by adding plastics to coal/ASR feedstock, the equivalent crude oil price dropped by \$6/barrel.

It was concluded that auto-fluff, containing primarily polyurethanes and high impact polystyrene as its principal polymeric constituents, was not as effective as the Municipal Solid Waste (MSW) plastics in improving the coal hydroconversion process performance, i.e., auto-fluff was not found to either increase the light distillate yields or decrease the light gas make and chemical hydrogen consumption in coal liquefaction, in the manner done by MSW plastics.

Pyrolysis oil derived from curbside plastics was co-processed with Hondo and Coal as seen in Table 3 with similar results as for the Coal/ASR (PB-04-4) with a slight decrease in hydrogen consumption. Run PB-06-4, a mixture of Hondo oil, pyrolysis oil, and coal, was operated at higher space velocity. Thus, resid conversion decreased; however, this was compensated for by a decrease in light gas yield and hydrogen consumption. The projected equivalent crude oil price for this was \$19.6/barrel.

The result and increase in the heating value of the clean solid fuel produced from MSW and the demonstrated conversion of lignin via hydrocracking justify examination of these feedstocks combined with coal, oil, and other waste feedstocks.

ECONOMICS

The examination and projection of plant costs associated with refinery companion plants (integrated) indicate that the co-liquefaction of waste with coal or oil provide a viable, secure alternative to the imported oil.

A techno-economic analysis for a site-specific waste/coal Direct Liquefaction plant at 10,000 bbls/day integrated into an existing refinery with random waste delivered to the plant shows an average required selling price at zero acquisition cost with a 15 percent ROI of \$16/barrel. With a portion of the tipping fees included, the price could be less than \$14/barrel and is cost-effective today. The current average US tipping fee is \$28/ton for land filling and \$54/ton for incineration. See Figure 3, which illustrates the change in product cost with tipping fee.

SUMMARY

Based on the encouraging results from these studies and the need to conserve materials and reduce emissions, continuing studies are warranted using readily available waste materials in combination with coal or heavy resids. The work can lead to the production of low-cost, clean transportation fuels and chemicals while protecting the environment.

FIGURE 1
HTI'S PILOT PLANT UNIT

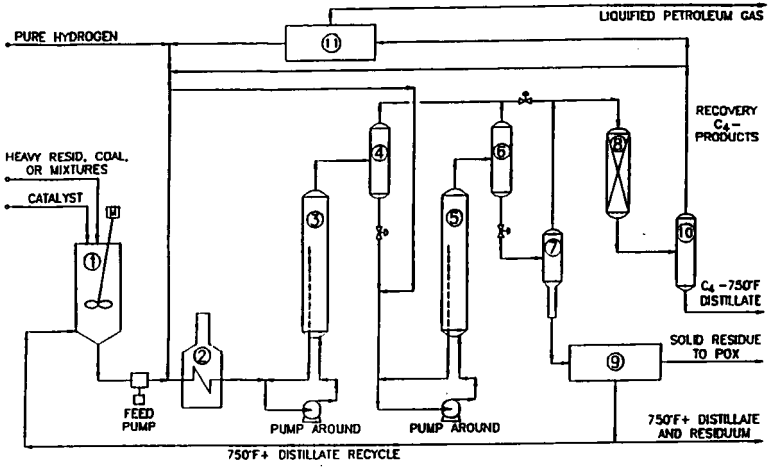
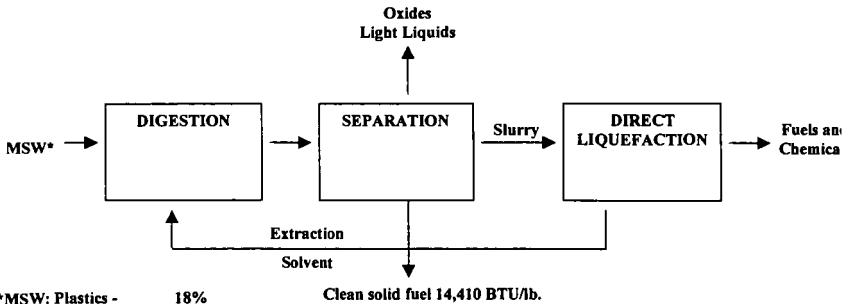


FIGURE 2
PROCESSING OF MUNICIPAL SOLID WASTE TO FUELS



*MSW: Plastics - 18%
Paper - 52%
Wood Waste - 27%
Other 3%

FIGURE 3
PROJECTED ECONOMICS OF CO-LIQUEFACTION
INTEGRATED WITH AN OIL REFINERY

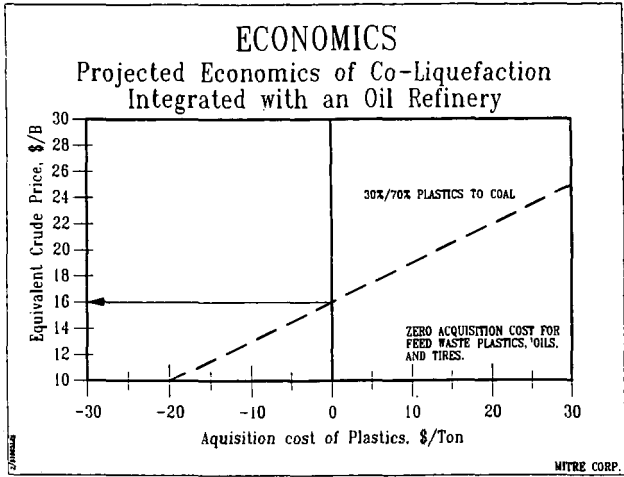


TABLE 1
PERFORMANCE COMPARISON - YIELDS

	OIL	COAL/OIL	COAL/OIL/ PLASTICS	OIL/ PLASTICS
Feed Composition, W%				
Coal, Black Thunder	0	50	33.3	0
Plastic, Curbside	0	0	33.3	50
Oil, Hondo Resid	100	50	33.3	50
Space Velocity, Kg/hr/m ³ rxn stage	1060	870	980	1250
Reactor temperature, °C				
First Stage	441	442	449	451
Second Stage	451	450	459	460
Process Performance, W% maf feed				
Feed Conversion	99.9	96.1	96.7	99.7
C ₄ -524°C Distillate Yield	76.0	69.7	73.9	76.2
524°C+ Conversion	83.3	82.7	83.7	84.0
Hydrogen Consumption	1.72	4.21	3.17	1.35
C ₁ -C ₃ Gas Yield	5.00	7.37	5.31	4.31

TABLE 2
PERFORMANCE COMPARISON - QUALITY

	OIL	COAL/OIL	COAL/OIL/ PLASTICS	OIL/ PLASTICS
Feed Composition, W%				
Coal	0	50	33.3	0
Plastic	0	0	33.3	50
Oil	100	50	33.3	50
SOH Distillate, ASTM D86, W%				
IBP-177°C	39.6	42.1	52.4	53.4
177-343°C	51.1	50.9	40.7	41.7
343°C+	8.3	7.0	6.9	4.9
SOH Quality				
Gravity, °API	49.0	46.1	46.3	51.0
H/C Ratio	1.99	1.96	1.90	1.97
Nitrogen, ppm	32.2	15.5	17.9	5.4
Sulfur, ppm	96.9	52.7	46.2	17.5
% Aromaticity	7.25	17.82	23.49	14.89

TABLE 3
PERFORMANCE OF COAL/WASTE CO-PROCESSING USING GELCAT™

Run ID	PB-04-03	PB-04-4	PB-04-5	PB-06-3	PB-06-4
Feed Comp. W%	Coal/Oil/ASR	Coal/ASR	Coal/ASR/PLS	Coal/Pyr. Oil	Coal/Oil/Pyr
Coal (Black Thunder)	50	75	50	67	45
Hondo Oil	30				28
Plastics			25		
ASR	20	25	25		
343°C+ Pyr. Oil				33	27
Catalyst					
FE GelCat™	1000	1000	1000	1000	1000
Mo	50	50	50	0	0
Space Velocity (kg/h/m ³)	602	632	621	655	1356
Performance (W% maf feed)					
Conversion	94.1	90.5	91.3	91	86
C ₄ -524°C Yield	66.8	56.6	61.4	57	54
524°C+ Conv.	83.6	72.4	77.2	73	66
C ₁ -C ₃ Gas Yield	8.6	6.9	7.8	8.8	3.5
H ₂ Consumption	5.7	6.0	4.0	5.4	2.2

TABLE 4
300-465°F OIL COMPOSITION FROM KRAFT LIGNIN

	RUN 184-4	RUN 184-5
Phenol	6.5	7.8
o-Cresol	3.6	6.0
m-p-cresols	21.6	24.9
2,4 xyleneol	7.0	8.8
p-ethyl phenol	33.2	28.8
o-n-propyl phenol	8.0	9.1
p-n-propyl phenol	20.1	14.6
	100.0	100.0

PET COPROCESSING WITH YALLOURN BROWN COAL UNDER HYDROLIQUEFACTION CONDITIONS

G. D. Bongers, T. V. Verheyen, D. J. Allardice, and Toshiaki Okui*

HRL Technology Pty Ltd, Melbourne, Australia.

*New Energy and Industrial Technology Development Organisation, CCT Centre, Tokyo, Japan.

KEYWORDS: Hydroliquefaction, PET, brown coal, coprocessing.

INTRODUCTION

Polymer feedstocks such as polyethylene terephthalate (PET) are all prepared from non-renewable fossil fuels such as natural gas and petroleum sources, and as such need to be responsibly managed to increase the life of these resources. Post consumer plastics represent an increasing problem in terms of their disposing with many Governments tightening controls on their dumping as waste and encouraging recycling via legislation. Coprocessing of waste polymer within a brown coal liquefaction plant offers an alternative disposal option for these wastes, a supplementary source of hydrogen and the potential to increase the hydrocarbon content the liquid products [1-5].

The objectives of this study were to evaluate the efficacy of PET coprocessing in regard to the first stage hydroliquefaction of Yallourn Eastfield brown coal. The investigation of the molecular coal-PET interactions was an integral component to evaluate the coprocessing mechanisms.

EXPERIMENTAL

Pyrolysis Gas chromatography mass spectrometry (PY GC/MS) analysis was conducted using chromatography conditions previously reported [6].

Liquefaction experiments were conducted under similar conditions to those used by others [7], except that the autoclaves agitated in the horizontal direction.

RESULTS AND DISCUSSION

PY GC/MS ANALYSIS OF POLYMER FEEDSTOCK

PY GC/MS of the virgin PET was conducted to characterise its thermal breakdown products in the absence of any interferences from coal, solvent or catalyst. The pyrograms obtained for the sequential 340,450 and 720°C flash pyrolysis of the polymer is presented in Figure 1. Thermal cleavage produces the expected benzene, benzoic and dibenzoic acid products. Dimer and trimer sections of the original polymer dominate the PET pyrogram at 720°C.

PET melts but does not significantly decompose at 340°C or even 450°C under flash pyrolysis conditions as seen by a lack of peaks in Figure 1a & b. Pyrolysis is important from the coprocessing viewpoint as it implies that unless liquefaction conditions have some promoting effect, pyrolytic cleavage would occur only slowly at typical hydrogenation reaction temperatures (eg. 430°C). Competing effects of pressure, catalyst, solvent and reaction time during liquefaction make it difficult to predict its reactivity. However, it should be noted that PET is not going to simply fall apart during the reactor warm-up phase.

COPROCESSING WITH DIFFERENT PET LOADINGS

The yield data in Figure 2 suggests that PET addition is synergistic at very low levels and has a negative effect at higher loadings. Asphaltene yield appears unaffected by coprocessing and suggests negligible interaction between the coal and polymer at this level. PY GC/MS provides further information on the degree of interaction between coal and PET.

The pyrograms for the asphaltenes produced from both 100% coal and coal coprocessed with 1% PET under catalysed conditions (refer to Figure 3) reveal negligible differences in the type and distribution of the compounds released. Coprocessing with 10% PET

results in the asphaltenes incorporating additional toluene and C2 benzene's. Very few aromatic acids are present in the asphaltenes with benzoic acid undetected and only a trace of its methyl derivatives, in contrast to neat PET.

At a 50% PET loading, the pyrogram of the coprocessed asphaltene product contains proportionately more toluene and xylenes but is again devoid of acidic PET fragments. 100% PET when subjected to catalysed hydroliquefaction produces asphaltenes that are dominated by benzoic and methyl benzoic acids. The concentration of these acids is negligible in the asphaltenes produced under coprocessing conditions. Even the 50% PET coprocessing pyrogram includes negligible acids suggesting Yallourn coal promotes their decarboxylation to aromatic hydrocarbons, thus a better quality oil. Toluene and C2 benzenes are the dominant products in the 50% PET coprocessing pyrogram.

The pyrograms from the corresponding residue or insoluble hydroliquefaction products reveal the expected increase in PET derived compounds with higher polymer coprocessing ratios. However, these pyrograms of coprocessed residues do reveal some more interesting features:

- a reduction in the coal derived alkene/alkane ratio compared with 100% coal,
- different distribution and types of PET breakdown products in the asphaltenes,
- a lack of poly aromatic ketone species found in the 100% PET experiment.

The first observation lends support to synergism at low PET levels whilst the second is in accord with the differing origin of the two fractions. Solubility constraints imposed by THF would explain the structural differences between asphaltenes and residues. The absence of any larger PET derived fragments in the coprocessing residues suggests the coal either promotes their destruction or they may be incorporated into its macromolecular structure.

The PET present in the residue has been modified by the hydroliquefaction conditions with a loss of the more complex benzoic acid derivatives present in the virgin polymer decomposition products (Figure 1). This means that the PET is not unreactive with its thermal cleavage products simply incorporated into the residue, instead it is being converted into an insoluble product which has less carboxyl groups and is more intractable. The coal-derived phenols are still discernable in the 50% coprocessing level pyrogram but the pyrogram is dominated by a number of partially hydrogenated PET derived compounds along with benzoic acid.

The fact that some carboxyl groups survive the hydroliquefaction treatment indicates that these conditions are not as extreme as first thought. The compounds identified by PY GC/MS suggest PET may have the ability to become partially incorporated into the brown coal's structure. Some PET decomposition products may become chemically bound to the macromolecular structure of the insoluble coal products. Hydroliquefaction of neat PET results in a residue that produces relatively little toluene on flash pyrolysis in contrast to the coprocessing experiments. The opposite is true for benzoic acid suggesting that the coal may be incorporating the benzoic acid hydroliquefaction products within its insoluble product to be released as toluene on flash pyrolysis.

EFFECT OF TEMPERATURE ON PET COPROCESSING

Reducing the reaction temperature by 60°C to 370°C produced the expected reduction in conversion for Yallourn Eastfield coal. However, the effect when 10% PET was coprocessed was more marked with a decline of more than 10% in both conversion and asphaltene yield. These results suggest that the polymer is not only failing to contribute towards the coal conversion process at 370°C but is actually hindering it. This behavior is consistent with the polymer not dissolving and decomposing sufficiently at the lower temperature as shown in the pyroprobe work (refer to Figure 1). Pyroprobe experiments reveal that the PET is molten at this temperature under ambient pressure but shows little sign of decomposition. The polymer may swell reducing the supply of solvent and hydrogen available to react with the coal.

The asphaltene pyrograms in Figure 4 reveal that the long chain aliphatic hydrocarbons in the 370°C pyrogram are three times the size of those in the 430°C derived sample. This confirms that at the lower liquefaction temperatures these long chain aliphatic hydrocarbons are not formed or released from the coal into the oil fraction. The input from PET degradation products in terms of higher benzene and C2 benzenes becomes

more obvious with increasing temperature, however, these peaks are still proportionately larger in the 370°C pyrogram than they are for 100% coal.

The pyrograms from the residues reveal additional insights into the effect of lower reaction temperature on coprocessing at the molecular level. The pyrograms of the residues contrast those from the asphaltenes by their significant differences in the types and yields of peaks. The 370°C pyrogram has more coal related long chain aliphatics in accord with less severe processing leading to their retention in the residue.

Tetralin is released from this residue but not from the 430°C suggesting it may have been locked away from THF by incorporation within the PET. The residue produced under these milder conditions releases less benzoic acid and PET fragments than the 430°C. This suggests that the two PET derivatives present in the different residues are undergoing different pyrolytic fragmentation. It is not simply a case of better preservation of PET from the 370°C run as its products are not the same as those are for 100% PET as viewed in Figure 1. The PET derivative prepared at 370°C may contain sufficient solvent to undergo a separate copyrolysis leading to a different product distribution.

CONCLUSIONS

Coprocessing brown coal with PET has minimal impact on first stage hydroliquefaction at low PET loadings. Therefore hydroliquefaction is a possible beneficial disposal alternative for PET on an industrial scale.

The lower amounts of aromatic acids and higher alkyl benzenes produced on the flash pyrolysis of coprocessed products compared to 100% coal or polymer is evidence at the molecular level for the formation of coal/polymer compounds.

Solvent is absorbed into PET at low liquefaction reaction temperatures (370°C). At normal liquefaction temperatures (eg. 430°C) the polymer melts but does not readily decompose.

PET requires severe reaction conditions to completely decompose as evidenced by the residual benzoic acid released from the catalysed 430°C residue.

REFERENCES

- [1] Anderson L.L., Tuntawiroon and Ding W.B., (1995). *Coal Science*, pp1515-1518.
- [2] Rothenberger K.S., Cugini A.V., Cocco M.V., Anderson R.R. and Veloski G.A (1995). *ACS preprints*, Vol 40, No. 1, pp38-43.
- [4] Davidson R.M., (1997). *Coprocessing Waste with Coal*, IEA Coal Research 1997, pp21-27 and references therein.
- [3] Taghiei M.M., Huggins F.E. and Huffman P. (1993). *ACS preprints*, Vol38. No. 3, pp810-815.
- [5] Rothenberger K.S., Cugini A.V., Thompson R.L. and Ciocco V. (1997). *Energy & Fuels*, Vol 11, pp849-855.
- [6] Jackson, W.R., Bongers, G.D., Redlich, P.J., Favas, G. and Fei, Y. (1996). *International Journal of Coal Geology*. Vol 32, pp229-240
- [7] Hulston, C.K.J., Redlich, P.J., Jackson, W.R., Larkins, F.P. and Marshall, M. (1996). *Fuel* 75 Vol 1, pp43-45

ACKNOWLEDGEMENTS

Funding of this research project by New Energy and Industrial Technology Development Organisation (NEDO) via Nippon Brown Coal Liquefaction Co Ltd (NBCL), Japan, is gratefully acknowledged.

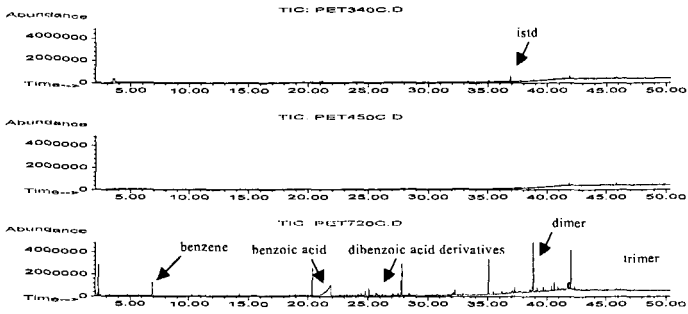


Figure 1. Pyrograms for PET revealing the minor loss of volatiles at the lower flash pyrolysis temperatures

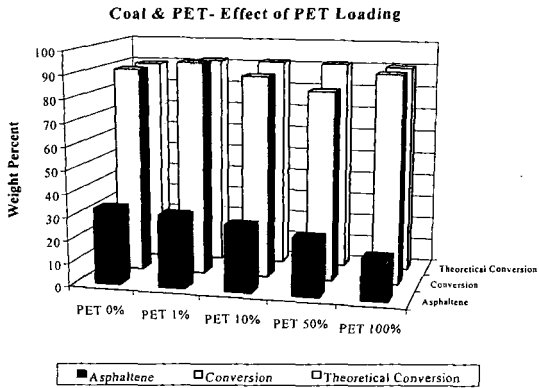


Figure2 Yield data covering the effect of coprocessing Yallourn Eastfield coal with PET at different polymer loadings.

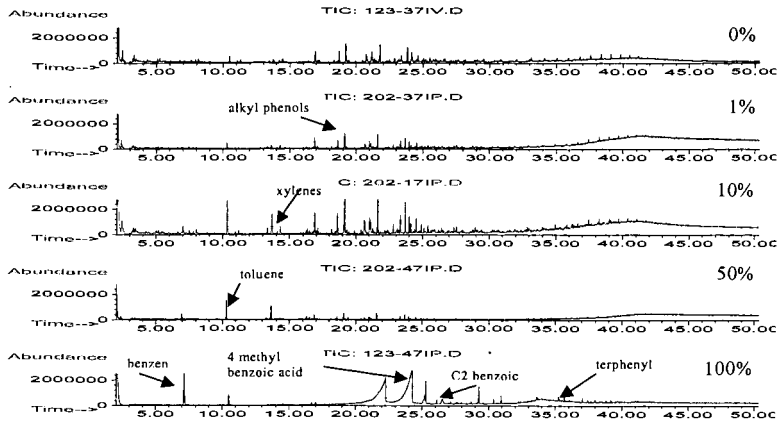


Figure 3 PY GC/MS pyrograms for asphaltenes from a PET profile: 0, 1, 10, 50 and 100% PET loading for catalysed coprocessing with Yallourn Eastfield coal.

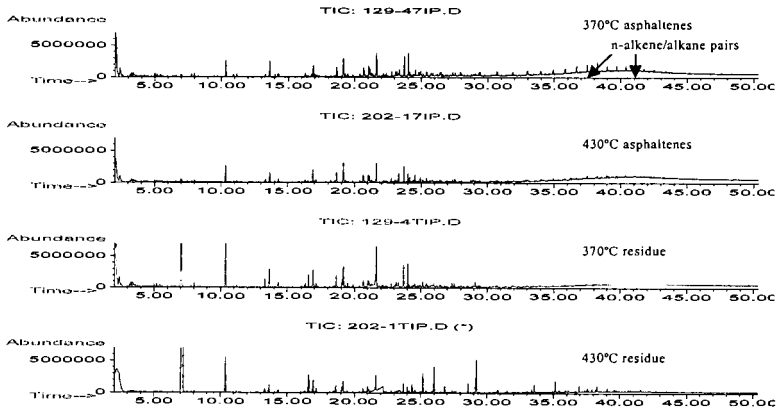


Figure 4 PYGC/MS chromatograms comparing the effect of 370°C vs 430°C liquefaction temperature on the asphaltenes and residues

CO-LIQUEFACTION OF COAL AND HIGH-DENSITY POLYETHYLENE

Dady B. Dadyburjor, Humair Z. Shaikh and John W. Zondlo

Department of Chemical Engineering, West Virginia University, P.O. Box 6102,
Morgantown WV 26506-6102

KEYWORDS: Polyethylene, Co-liquefaction of wastes, coal.

INTRODUCTION

High-density Polyethylene (HDPE) is a versatile polymer used as the material for containers, bottles, caps and films. Most HDPE is discarded after a single use and generally finds its way to a landfill. It has been estimated that waste plastics, including HDPE, comprise about 11% by weight but 21% by volume of landfills in the US. The properties that make HDPE a problem in the landfill are those that make HDPE a useful packaging agent, viz., its chemical stability and biological inertness. HDPE can be thermally degraded, of course, but a relatively high temperature is required. Further, the products of thermal degradation are not monomers but fragments of various molecular weights. Accordingly, using the HDPE as a co-liquefaction agent with coal could be promising.

Earlier work in this laboratory (1) has enumerated the properties/requirements of an ideal waste material as a co-liquefaction agent. It should be available in large supply; it should be manufactured cheaply, but should be expensive to dispose off, in a landfill or otherwise; and it should have one or more favorable properties -- a catalytic function, or hydrogen-transfer characteristics, or free-radical formation -- such that co-liquefaction is superior to the separate processes of coal liquefaction and the liquefaction of the waste material. HDPE certainly meets the first two of these criteria. In the present work, we examine its role in the third criterion.

Previous work in our laboratory has used a variety of waste materials as co-liquefaction agents: sawdust (1); agricultural waste (1); poly(vinyl chloride) (2); and automobile tires. This last material has been extensively studied, both from a reaction kinetic standpoint (3) and in terms of process design (4). The use of these co-liquefaction agents were studied both thermally and using a ferric-sulfide-based catalyst. This catalyst has been shown (5) to be remarkably effective for direct coal liquefaction. The superior performance of this catalyst is perhaps due to the intimate contact of pyritic and pyrrhotitic materials formed during the disproportionation of ferric sulfide at temperatures above 10°C. However, for space considerations, in this preprint we consider only the non-catalytic co-liquefaction of HDPE and coal. The effects of temperature, reaction time and the ratio of HDPE to coal on the conversion and product type are shown.

EXPERIMENTAL

Details can be found elsewhere, e.g., (3). In brief, all reactions were carried out in duplicate (at least) in a batch-tubing microreactor. This consists of a short section of heavy pipe of volume 27 ml with screw-on caps at each end (for insertion and removal of solid and liquid reactants and products), and a thin tube welded at the pipe middle and perpendicular to the axis (for addition of vapor-phase reactants and/or inerts, and for removal of vapor-phase products). Typically, 3 g of total feed (coal alone, HDPE alone, or coal plus HDPE) were placed in the reactor, the vapor phase was added, and the reactor was sealed off. Two such reactors were placed in a vertical-agitation unit, and a fluidized sandbath was used to heat the reactor contents rapidly to the final temperature. Most runs were performed between 350°C and 450°C, for reaction times between 15 min and 1 h, at a pressure of 2000 psig (at reaction temperature, i.e., "hot") of hydrogen and/or helium. Ratios of HDPE to coal (*P/C*) ranged from 0 to 1; it was felt that larger values of *P/C* are unrealistic from the standpoint of commercial availability.

After the required time of reaction had elapsed, the sandbath was lowered and the reactors were cooled. The gas phase was captured and analyzed by gas chromatography. Other products were identified and quantified by solubility in tetrahydrofuran (THF) and hexane. Three fractions were measured: f_{TI} , the fraction of entering material insoluble in THF; f_{HI} , the fraction of material soluble in THF but insoluble in hexane; and f_G , the fraction of material present in the gas phase. A fourth parameter, f_{HS} , the fraction of material soluble in both THF and hexane, was obtained by difference:

$$f_{HS} = 1 - f_{TI} - f_{HI} - f_G \quad (1)$$

(For liquefaction runs involving coal only, the conversion, X , is typically given by:

$$X = 1 - f_{TI} \quad (2a)$$

the yield of the asphaltene fraction, A , by:

$$A = f_{HI} \quad (2b)$$

and the oil fraction yield, O , by:

$$O = f_{HS} \quad (2c)$$

However, as discussed below, we do not use this nomenclature here, and especially for runs involving HDPE, either alone or in combination with coal.) For co-liquefaction runs involving both coal and HDPE, overall fractions f_{HS} , f_{TI} , f_{HI} , and f_G were obtained as defined above. However, in order to compare co-liquefaction results using different ratios of HDPE to coal with one another and with liquefaction results using only coal, these fractions were also calculated on a coal-alone basis. The coal-alone fractions were obtained by subtracting off, in a proportional sense, the contribution of the HDPE as determined in the HDPE-only runs. If there are no additional effects when HDPE is added to coal, then co-liquefaction results on a coal-alone basis should be identical to (liquefaction) results for the coal-only experiments. Put differently, when HDPE is added to coal, any additional effects show up as differences, positive or negative, between the co-liquefaction results calculated on a coal-alone basis and the (liquefaction) results of the coal-only runs. This is consistent with the approach used in our previous work (1 - 4).

RESULTS AND DISCUSSION

Particular attention was paid to base-case runs involving coal only and HDPE only. A statistically designed set of experiments using the Box-Behnken three-factor approach was used to obtain the dependence of both these materials on the three parameters of temperature, time, and hydrogen partial pressure, keeping the total pressure constant at 2000 psig by using helium. Ranges of the parameters were 350-450°C, 15-60 min., and 0-2000 psig, respectively. The results were fitted to a second-order polynomial in normalized temperature, normalized time, and normalized hydrogen partial pressure:

$$f = A_0 + A_T T^* + A_t t^* + A_P P^* + A_{TT} T^{*2} + A_{Tt} T^* t^* + A_{TP} T^* P^* + A_{tt} t^{*2} + A_{PP} P^{*2} \quad (3)$$

where the normalized time is given as:

$$t^* = \{t[\text{min}] - 30\} / 30 \quad (4)$$

and the other normalized parameters are similarly defined in terms of their center point values. The complete set of data and the statistical analyses can be found elsewhere (6). The values of the statistically significant parameters for coal and HDPE are shown in Table 1. The values for coal are consistent with those obtained by other workers in our laboratory (2,7,8).

From Table 1, it can be seen that the products of coal-only liquefaction are about equally divided between HI and HS, but most of the material is TI. Further the temperature is the most important parameter for HI, HS and G. Also from Table 1, the major product of HDPE-only liquefaction is HS, with more than half of the material being TI.

At room temperature, almost all the coal is found to be TI, *i.e.*, negligible amounts of coal are soluble in THF or hexane. However, when the experiment was repeated with HDPE, the value of f_{HI} was found to be approximately 0.97, while f_{HS} was found to be approximately 0.005, the remainder being f_{TI} . Since the amount of TI actually increases between room temperature and the temperatures of liquefaction, it is not reasonable to consider the conversion of HDPE to be given by the righthand side of Eqn (2a). Clearly, the temperature converts the THF-soluble, hexane-insoluble material to THF-insoluble material and (THF-soluble) hexane-soluble material.

Figure 1 shows the effect of the ratio of HDPE to coal, P/C , on the products formed. The results are on a coal-alone basis so, as noted earlier, an increase in an f value over the corresponding one for only coal ($P/C = 0$) implies that co-liquefaction results in a net increase in that parameter, even when the effect of the HDPE is taken into account. From Figure 1, f_{TI} and f_G increase steadily with an increase in P/C . The increase in f_G is large relative to the value for only coal,

but about equivalent to that in f_{TI} on an absolute basis. The value of f_{HS} decreases with increasing P/C .

Figure 2 shows the effect of temperature on the co-liquefaction when P/C is kept at its highest value (= 1). At higher temperatures, f_{HS} increases dramatically, while f_G , f_{HI} , and f_{TI} fall.

Finally, Figure 3 shows the effect of time at the highest temperature and largest P/C value. Larger reaction times increase HS and G, and decrease the amount of TI.

CONCLUSIONS

At room temperature, HDPE consists of primarily THF-soluble, hexane-insoluble matter. When heated to around 400°C, the HI material forms HS material and some TI material.

For co-liquefaction of HDPE with coal, high P/C ratios, high temperatures, and large times of reaction appear to be helpful in terms of increasing the relative amount of HS material.

ACKNOWLEDGMENTS

This work was supported by the US Department of Energy Contract No. DE-FC22-90PC90029 under a Cooperative Agreement with the Consortium for Fossil Fuel Liquefaction Science.

REFERENCES

1. Stiller, A.H., Wann, J.-P., Tian, D., Zondlo, J.W. and D.B. Dadyburjor, *Fuel Proc. Technol.* **49**, 167 (1996).
2. Ch., Dhaveji, Zondlo, J.W. and Dadyburjor, D.B., *Preprints - ACS Div. Fuel Chem.* **42**, 1077 (1997).
3. Sharma, R.K., Zondlo, J.W. and Dadyburjor, D.B., *Energy and Fuels* **12**, 589 (1998).
4. Sharma, R.K., Tian, D., Zondlo, J.W. and Dadyburjor, D.B., *Energy and Fuels*, in press (1998).
5. Stohl, F.V., Diegert, K.V., and Goodnow, D.C., *Proceedings, Coal Liquefaction and Gas Conversion Contractors Rev. Conf.*, U.S. Department of Energy, Pittsburgh Energy Technology Center, Pittsburgh, PA, 679 (1995).
6. Shaikh, H.Z., *Effect of Process Parameters upon Coal Liquefaction and Coal / High-Density Polyethylene Co-liquefaction*, MSChE Thesis, West Virginia University, Morgantown WV (1998).
7. Bennett, B., *Effect of Reaction Parameters upon Coal and Tire Liquefaction and Coal / Tire Co-liquefaction using Two Bituminous Coals*, MSChE Thesis, West Virginia University, Morgantown WV (1995).
8. Hu, F., *Coal / Tire Co-liquefaction Using Pyrrhotite / Pyrite Catalysts*, MSChE Thesis, West Virginia University, Morgantown WV (1995).

Table 1. Coefficients of Eqn (3) for Liquefaction Using Coal and HDPE Separately

f	A_D	A_T	A_I	A_P	A_{TI}	A_{TP}	A_{IP}	A_{TT}	A_H	A_{PP}
For Coal										
HI	13.48	-3.37	-2.79	2.63	-1.47	--	0.83	-7.22	1.68	1.01
G	3.17	5.29	1.44	0.42	1.30	--	0.62	2.81	--	0.65
HS	13.19	6.07	4.84	1.52	--	--	--	-1.75	-3.79	--
For HDPE										
HI	1.87	0.16	0.49	--	-0.20	--	--	-0.61	-0.89	-0.55
G	3.35	1.85	1.04	0.71	--	--	--	0.70	--	0.50
HS	42.55	28.56	5.13	1.68	--	--	--	4.67	-4.86	--

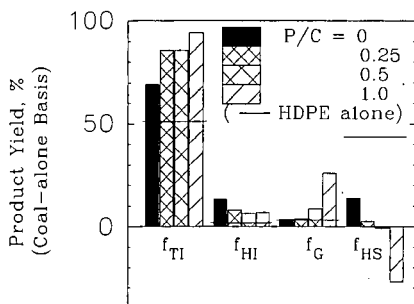


Figure 1. Effect of feed ratio, P/C , on product yields. Reaction conditions: 400°C, 1000 psig H_2 , 30 min.

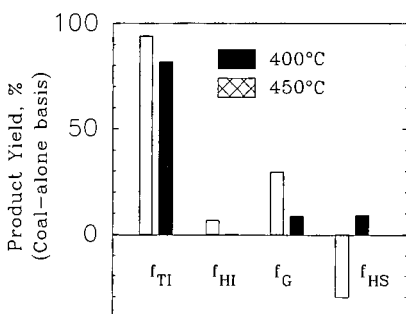


Figure 2. Effect of temperature on product yields. Reaction conditions: 1000 psig H_2 , 30 min, $P/C = 1$.

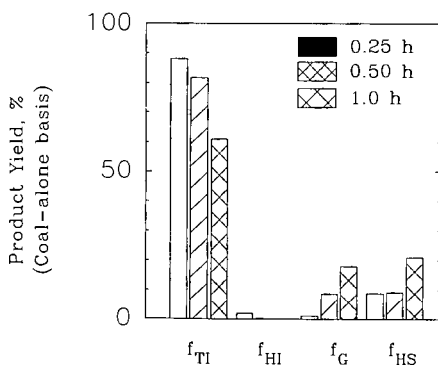


Figure 3. Effect of time on product yields. Reaction conditions: 450°C, 1000 psig H_2 , $P/C = 1$.

ATOM-ECONOMICAL PATHWAYS TO METHANOL FUEL CELL FROM BIOMASS

D. Mahajan and J.E. Wegrzyn
Building 815, Energy Science and Technology Division
Department of Applied Science, Brookhaven National Laboratory
Upton, New York 19173-5000

(Keywords: biomass, fuels, methanol fuel cell)

ABSTRACT

An economical production of alcohol fuels from biomass, a feedstock low in carbon and high in water content, is of interest. At Brookhaven National Laboratory (BNL), a Liquid Phase Low Temperature (LPLT) concept is under development to improve the economics by maximizing the conversion of energy carrier atoms (C,H) into energy liquids (fuel). So far, the LPLT concept has been successfully applied to obtain highly efficient methanol synthesis. This synthesis was achieved with specifically designed soluble catalysts at temperatures $<150^{\circ}\text{C}$. A subsequent study at BNL yielded a water-gas-shift (WGS) catalyst for the production of hydrogen from a feedstock of carbon monoxide and H_2O at temperatures $<120^{\circ}\text{C}$. With these LPLT technologies as a background, this paper extends the discussion of the LPLT concept to include methanol decomposition into 3 moles of H_2 per mole of methanol. The implication of these technologies for the atom-economical pathways to methanol fuel cell from biomass is discussed.

INTRODUCTION

Though still controversial, global warming from increasing trace gases in the atmosphere is now generally accepted [1]. The role of CO_2 , a greenhouse gas resulting from natural phenomenon and burning of fossil fuels, is particularly important. Due to its origin, biomass by definition is considered essentially CO_2 neutral in the growth/usage cycle. It is, thus, of interest to develop efficient processes that utilize biomass feedstock to produce fuels and chemicals. Traditionally, ethanol production via biomass fermentation is widely recognized as an acceptable route. But fuels other than ethanol can be produced from biomass. This paper focusses on methanol and subsequent production of H_2 with specific application to methanol fuel cell. A scheme is presented that can allow production of 3mol H_2 per mol methanol via less intensive energy pathways i.e. via an atom-economical route.

EXPERIMENTAL

Materials

Sodium and potassium formates, metal complexes that served as catalysts, triethyleneglycol dimethyl ether (triglyme), and methanol were purchased from either Aldrich or Alfa. CO , H_2 gases ($>99.9\%$ pure) were obtained from Scott Specialty Gases.

Batch Unit

All runs were conducted in a 0.5L AE Zipperclave constant stirred tank reactor (CSTR) available commercially from Autoclave Engineers (AE) but modified at BNL. The batch unit was fitted with a Dispersamax six-blade impeller and a removable metal ring inserted into the reactor to break up any vortices that may form during stirring. The heating / cooling was attained through a Parr temperature controller. The system had provisions for inlets and outlets for gases and liquids sampling during the run. The unit was rated at 20 MPa at 350°C .

Run Procedure and Analysis

In a typical run related to water-gas-shift (WGS) reaction, sodium or potassium formate, metal complex catalyst and solvent mixture were loaded into the reactor under an inert atmosphere. The reactor was sealed, pressurized and heated at a desired temperature. Once isothermal condition was attained, evolved gases were identified and quantified by gas chromatographs.

RESULTS AND DISCUSSION

Discussed below are novel technologies, under development at BNL, that could be adapted to biomass feedstock. Targeted is production of methanol and H₂ fuels with relevance to methanol fuel cells.

Low Temperature Catalytic Methanol Synthesis



To sustain increasing natural gas usage, remote natural gas and non-conventional resources such as gas hydrates are being developed. The challenge is to retain atom-economy by developing technologies that allow processing and transport of available natural gas with minimum energy input. At BNL, the Liquid Phase Low Temperature (LPLT) concept has been developed to achieve this goal. A successful application of this concept to methanol synthesis utilized a designed alkoxide base-activated nickel catalyst (2). This catalyst system operates in homogeneous liquid phase and allows high syngas gas conversion (>90%) per pass at high reaction rates (without optimization up to 9g-mol MeOH/g-mol cat.h) under thermodynamically allowed low temperature (<150°C) and low pressure (<5 MPa). These features simplify the overall methanol synthesis process in two ways:

- **Natural Gas to Syngas - Step 1.** The low pressure operation combined with inertness of the catalyst to N₂ permits partial oxidation of natural gas with air during syngas manufacture. **This feature eliminates a need and, therefore, the cost of the AIR to O₂ separation plant.**
- **Syngas to Methanol - Step 2.** A high syngas to methanol conversion (>90%) achieved with the designed catalyst **eliminates syngas recycle.**

With a target of 40% cost reduction over the conventional process for methanol synthesis, a second-generation methanol synthesis catalyst is being formulated and evaluated at BNL. A successful development of this atom-economical process would provide an economical edge over well advanced concepts of liquefied natural gas (LNG) and Fischer-Tropsch (F-T) liquids. Though not discussed in detail but relevant to this paper, syngas generated by gasification of biomass (3) could become the feedstock to produce methanol via the BNL low temperature methanol synthesis technology.

Low Temperature Catalytic Methanol Decomposition



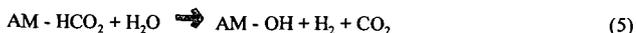
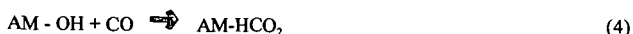
Several catalytic systems have been evaluated for methanol decomposition but high temperatures and side reactions present problems (4). By utilizing the LPLT concept, catalysts are being formulated at BNL that operate at a temperature of <150°C. At low temperatures, selectivity to desired products is enhanced. Though not discussed here, catalytic H₂ production via reaction (2) at low temperature is relevant.

Low Temperature Water-Gas-Shift (WGS) Catalysis

The emphasis of the present paper is on development of water-gas-shift (WGS) catalysts (Equation 3) that effectively operate at low temperatures of <150°C:



Commercially, several heterogeneous metals (5) and homogeneous metal complexes (6) have been employed as catalysts. Under basic conditions, the reaction proceeds through a formate intermediate (Equations 4 and 5):



Thus, the ability of any catalyst to decompose an inorganic formate via reaction 5 is a measure of its effectiveness as a WGS catalyst. Table 1 lists several catalyst formulations that were evaluated to decompose potassium methyl formate. Since an equimolar amount of H_2 is expected per mol of $KHCO_2$, the direct measurement of H_2 production via gas chromatography allows assessment of reaction efficiency. Notable in Table 1 is Run 4 in which 94% decomposition was achieved at $120^\circ C$ in <5 minutes and Run 9 where complete decomposition was achieved at $140^\circ C$ in <2 minutes. The absence of CO (to $<0.01\%$ instrument sensitivity) is also noteworthy. The results show that the equilibrium reaction (3) can be driven essentially to the right with the low temperature catalysts developed at BNL (7).

Methanol Fuel Cell Application

Methanol fuel cells are of commercial importance but several technological hurdles remain to generate pure H_2 feed from methanol feedstock. Methanol reforming with steam generates 3 mol H_2 and 1 mol CO_2 per mol methanol whereas methanol oxidation produces 2 mol H_2 and 1 mol CO_2 but both systems operate at high temperatures. Direct methanol fuel cells are also being evaluated (8). Work, ongoing at BNL, envisions an integrated system that operates at low temperatures. The system consists of two steps: 1) catalyzed methanol decomposition at $T < 150^\circ C$ to produce 1 mol CO and 2 mol H_2 , followed by; 2) fast and complete CO conversion to CO_2 with concomitant production of 1 mol H_2 , via the present invention. Thus the BNL integrated system produces 3 mol H_2 per mol methanol at $T < 150^\circ C$ compared to other schemes for methanol fuel cell system that are under development.

CONCLUSIONS

The emphasis of this paper is to produce fuels and chemicals from biomass. The approach, presented here, involves biomass gasification to yield a dilute and "wet" syngas stream. The LPLT concept, developed at BNL, is applied to yield a low energy input pathway for catalytic conversion of syngas to methanol. A low temperature catalytic decomposition produces 2 mol H_2 and 1 mol CO. The produced CO is effectively converted to CO_2 and equimolar H_2 catalytically via WGS reaction. This scheme produces essentially a pure stream of 3 mol H_2 per mol methanol. If further purification (removal of any residual CO) of H_2 is required, methanol can be catalytically reacted with CO to produce methyl formate. Thus, methanol and H_2 are recognized as potential fuels from biomass. For application to fuel cells, H_2 can be further purified with coproduction of methyl formate, a specialty chemical. The overall emphasis at BNL is to develop technologies that are atom-economical thus retaining maximum energy of the original feedstock molecule in to fuel or chemical product.

ACKNOWLEDGMENTS

Work at Brookhaven National Laboratory is supported by U.S. Department of Energy Contract No. DE-AC02-98CH10886.

REFERENCES

1. National Research Council Report, "Changing Climate," National Academy Press, Washington, DC, 1983. LaMarche, Jr., V.C., Graybill, D.A., Fritts, H.C., and Rose, M.R., *Science* 225, 1019 (1984).
2. Mahajan, D., Sapienza, R.S., Slegeir, W., and O'Hare, T.E., U.S. Patent \$4,935,395 (1991).
3. Wang, Y. and Kinoshita, C.M. in 1991 Solar World Congress Vol. 1, Part II, Arden, M.E., Burley, S.M.A., and Coleman, M. (eds.), Pergamon Press, New York (1991). pp. 799.
4. Weissmel, K., Arps, H.-J., *Industrial Organic Chemistry*, Verlag Chemie, New York, 1978.
5. Satterfield, C.N., "Heterogeneous Catalysis in Practice"; McGraw-Hill, New York, 1980, p. 292.
6. Halpern, J. *Comments In Inorg. Chem.* 1(1), 3 (1981).
7. Mahajan, D. Record of Invention, Brookhaven National Laboratory. November 13, 1998.
8. American Methanol Institute Report, "The Promise of Methanol Fuel Cell Vehicles." 1998 and references therein.

Table 1. Decomposition of Inorganic Formates Catalyzed by Metal Complexes.

0.5LAE Zipperclave batch reactor, Solvent: 5% H₂O / 10% Methanol / 85% Triglyme = 130 mL, KHCO₂ = 50 mmol, T=120°C, P_{Ar} = 1.4 Mpa.

Run #	Catalyst	Final Gas Analysis H ₂ CO mmol		Time min	%KHCO ₂ Decomposition
1	----	1	-	140	2
2	B-2	35	-	80	70
3	NB-3	5	-	120	10
4	RB-4	47	-	<5	94
5	RLB-5	40	-	<30	80
6	CLB-6	2	-	55	4
7	PCL-7	43	-	<10	86
8	FLB-8	3	-	30	6
9	RB-4-T	50	-	<2	100* *(T=140°C)

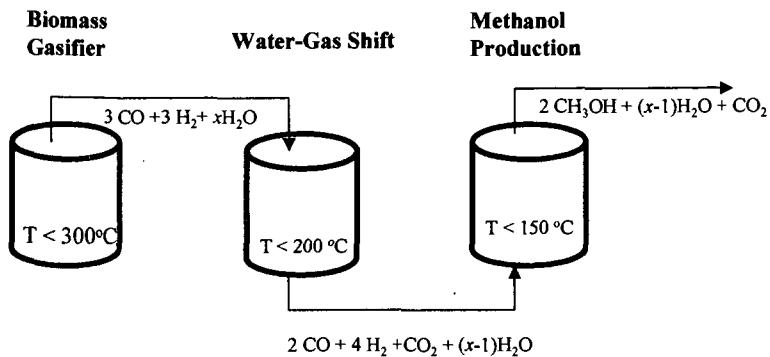


Figure 1. Production of Biomass-Derived Methanol

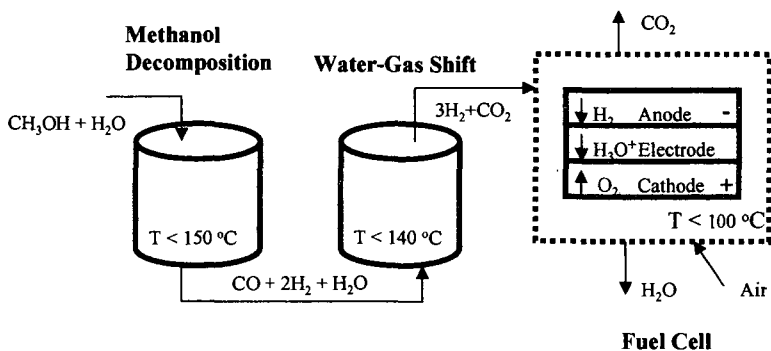


Figure 2. Scheme for High Efficiency Methanol Fuel Cell

SHALLOW PAN CULTIVATION TO ENHANCE THE YIELD OF BACTERIAL CELLULOSE

Hiroshi Tamura, Yukihiko Tsuruta and Seiichi Tokura*

Faculty of Engineering, Kansai University and HRC
3-3-35 Yamate-cho, Suita, Osaka 564-8680, Japan

ABSTRACT

Continuous filamentation of bacterial cellulose (BC) was successfully achieved by applying shallow incubation pan to regulate thickness of the BC gel produced by *Acetobacter xylinum*. Though the better yield of BC was shown by applying aerobic rotary cultivator than that by the static one, the yield of BC filament was enhanced remarkably by applying shallow pan cultivator with continuous wind up roller from the surface of the culture medium. The X-ray diffraction analysis and scanning electron microscopic observation of the BC filament showed that the filament was smooth and the fairly good orientation of BC molecules. The best average tensile strength was obtained for the filament prepared by hot alkaline treatment and subsequent washing with distilled water followed by drying under tension. A carboxymethyl glucose (CM-Glc) residue was found in BC whose ion exchange capacity was enhanced remarkably only for lead ion, when *Acetobacter xylinum* was cultured in SH medium containing CM-Glc, CM-cellulose oligomer or CMC and glucose.

INTRODUCTION

The bacterial cellulose (BC) is well known as one of extracellular poly-saccharides to be produced by *Acetobacter xylinum*¹⁾ in Schramm-Hestrin (SH) medium containing D-glucose (Glc) as a carbon source²⁾. Because BC is a pure cellulose, it has attracted much attention in various manufacturing fields. In our previous studies on the preparation of BC, we developed novel procedures to produce molecular variants of BC. Incorporation of aminosugar residues has been successfully attained by incubation of the bacteria that had been subcultured repeatedly in the medium containing *N*-acetylglicosamine (GlcNAc) and Glc or only GlcNAc as carbon source^{3,4)}. Under rotary but not static conditions, a similar degree of GlcNAc incorporation was also observed when cultivation was carried out with air bubbling in the medium containing Glc and ammonium chloride⁵⁾.

Although much effort has been developed to the preparation and utilization of BC and its analogs, these methods and agents have not yet been incorporated as industrial resources, largely because of the high production costs involved. Given that complicated procedures are required for the preparation of fibers and films from these biosynthesized polysaccharides, a simple method, one that can serve to reduce these high production costs, has been requested.

In this paper, we describe the results of our investigations for such a simplified process, which was prompted by recent success with regard to surface polymerization of nylon capable of giving superpolymer films or filaments directly from the interface of organic and aqueous phases^{6,7)}. We have designed a shallow stainless pans⁸⁻¹¹⁾ to regulate the gel thickness better during the incubation and physical properties of the resultant filaments were examined. An introduction of carboxymethyl glucose (CM-Glc) residue in BC was succeeded when *Acetobacter xylinum* was cultured in SH medium containing carboxymethyl cellulose (CMC) and glucose. The ion exchange capacity of BC containing CM-Glc residue was enhanced remarkably only for lead ion.

EXPERIMENTAL

Culture conditions

A wild type of *Acetobacter xylinum* ATCC 10245 strain was subcultured at 28 °C in Schramm-Hestrin (SH) medium containing Glc as a carbon source, and repeatedly transferred to the new culture medium every 3 days. Shallow pans (100 mm or 200 mm of width, 400 mm of length and 7 mm of depth) were designed to prepare a thin BC gel first and then wind up to roller at the rate of 35 mm/h directly from cultivation medium as shown in Figure 1. The cultivation of *A. xylinum* was proceeded for a couple of days under static condition and then thin gel formed on the surface of medium was picked up to wind up roller continuously for a week. A separator was attached to prepare the strips of 30 mm width for the pan of 200 mm width. The whole apparatus was set in an incubator in which temperature was maintained at 28 °C and filtered air was passed through the incubator. For the incorporation of CM-Glc residue into BC, CMC was mixed into glucose SH medium on the cultivation of BC. The content of the CMC in SH medium was 0.5% (w/v).

Purification of filament

The wound filament was boiled for 3 h in 2% SDS solution, washed with distilled water, and boiled again in the 4% aqueous sodium hydroxide solution for 1.5 h. Three samples of the filaments were prepared by washing of the resulting filament with distilled water (W), with 10 % aqueous ethylene glycol (E), or with both 10 % aqueous ethylene glycol and distilled water (WE). All filaments were subjected to air-drying under tension at less than 60 °C.

Measurements

The stress-strain diagrams of the filaments were obtained using a Shimadzu Auto Graph AGS-500D apparatus at a guide distance of 25 mm. Wide-angle X-ray diffraction patterns were recorded by using a MAC M18XHF X-ray diffractometer. The X-rays were generated at 40 kV and 100 mA using nickel-filtered $\text{CuK}\alpha$ radiation.

RESULTS AND DISCUSSION

To make thinner BC gel suitable for direct and continuous filamentation, we devised a shallow pan for the incubation of *A. xylinum*. In a preliminary incubation under static conditions, we found that thin BC gel was obtained on the surface of the culture medium, and that the gel were strong and elastic enough to pick up and manipulate. One side of the shallow pan was curved gently to permit harvest of the pellicle through a narrow mouth. The yield of the BC was enhanced using shallow pan method (4.1 - 5.6 %) compared with static (1.6 %) and rotatory (2.7 %) methods^{10,11}. The thin BC gel was to be directly passed through a bath containing aqueous SDS solution to reduce the bacterial activity and then the filament would be wound slowly on an attached basket. Produced fibrous gel was stretched under slightly twisted mode. The shallow pan would be also effective in conserving the total amount of culture medium used for the incubation. As the filament was too thick to prepare filament in the case of wider pan (200mm width), a separator was attached to prepare the strips of 30mm width. The separator was so effective to prepare thinner filament. Treatments of the BC fiber was easy because the obtained fibrous BC was collected wound with bobin. In addition, winding by a wide roller has the possibility to prepare the BC film.

A SEM image of BC filament showed that the BC filament with normal water-washing (Filament W) has good alignment cellulose moieties and slightly twisted fiber mode. The cut surface of filament shows the melting of the inner part of filament to form a fiber bundle. The X-ray diffraction pattern suggested that Filament W has a higher orientation of molecules than either Filament E or WE. This finding is consistent with those from SEM observation.

The tensile properties and the stress-strain curves for the filaments obtained by different washing procedures (Filaments W, E, and WE) are summarized in Table 1 and Figure 2, respectively. The stress-strain diagram shows that Filament WE has poor tensile strength. Deniers of ethylene glycol-treated filaments (Filament E) tended to become double compared with the filament prepared by normal water-washing (Filament W), a finding that might reflect the slightly disturbed orientation of molecules in the filaments by the trapping of ethylene glycol in the network. Among these three kinds of filaments, normal water-washing filament (Filament W) had good mechanical strength; the best sample revealed 6.1 g denier¹ for the tensile strength and 106 g denier¹ for Young's module and their average values were 4.4 g denier¹ and 90.4 g denier¹, respectively. They were significantly stronger than the original BC filament and were comparable to cotton (3.0 - 4.9 g denier¹ for the tensile strength and 68 - 93 g denier¹ for Young's module¹²) and the other fibers¹³. The filaments prepared by ethylene glycol treatment (Filaments E and WE) seem less suitable for practical use. The low tensile strength and Young's modulus obtained by aqueous ethylene glycol treatment after cleaning of the filaments may be due to obstruction of molecular orientation followed by incomplete crystallization of cellulose molecules.

The CM-Glc residue was incorporated using the SH medium containing CMC. Around 10% of residual incorporation of CM-Glc was the maximum at 0.5%(w/v) of CMC mixing in the SH medium. Produced CM-BC was applied to investigate the ion exchange properties following to extensive washing with SDS and 4% sodium hydroxide aqueous solutions at boiling temperature, respectively. A significant increase of adsorption for lead ion was observed on the CM-BC as shown in Figure 3 comparing with ion exchange profile of original CMC.

CONCLUSIONS

Continuous filamentation using a shallow pan for the incubation was found to be useful for the regulation of the thickness of the BC gel. The yield of the BC was enhanced remarkably by applying this method compared with static and rotatory methods. The tensile

strength of the filament was found to be significantly stronger than the ordinary cellulose fibers and a good orientation of molecules was shown by both the X-ray diffraction pattern and SEM observation. Around 10% of residual incorporation of CM-Glc was successfully performed using CMC containing SH medium. A significant increase of absorption for lead ion was observed on the CM-BC comparing with ion exchange profile of original CMC.

ACKNOWLEDGEMENTS

This work was performed through a Grani-in-Aid of Scientific Research (Promotion of Life Science-Directive Local Research Project) from the Science and Technology Agency of the Japanese Government.

REFERENCES

- 1) A. J. Brown, *J. Chem. Soc.*, **49**, 432 (1886).
- 2) S. Herstein and M. Schramm, *Biochem. J.*, **58**, 345 (1954).
- 3) R. Ogawa and S. Tokura, *Carbohydr. Polym.*, **19**, 171 (1992).
- 4) R. Ogata, Y. Miura, S. Tokura and T. Koriyama, *Int. J. Biol. Macromol.*, **14**, 343 (1992).
- 5) A. Shirai, M. Takahashi, H. Kaneko, S. -I. Nishimura, M. Ogata, N. Nishi, and S. Tokura, *Int. J. Biol. Macromol.*, **16**, 297 (1994).
- 6) E. E. Magat and R. D. Strachan, *U. S. Patent*, 2,708,617.
- 7) E. L. Wittbecker and P. W. Morgan, *J. Polym. Sci.*, **60**, 289 (1959).
- 8) N. Sakairi, H. Asano, M. Ogawa, N. Nishi and S. Tokura, *Carbohydr. Polym.*, **35**, 233 (1998).
- 9) S. Tokura, H. Asano, N. Sakairi and N. Nishi, *Macromol. Symp.*, **127**, 23 (1998).
- 10) S. Tokura, *Cellulose Commun.*, **5**, 29 (1998).
- 11) H. Asano, T. Kawai, H. Kawahara, N. Sakairi, N. Nishi and S. Tokura, *Kobunshi Ronbunshu*, **55**, 207 (1998).
- 12) Japan Chemical Fibers Association, *Sen-i Handbook*, p294 (1990).
- 13) L. Rebenfeld and W. P. Virgin, *Textile Res. J.*, **27**, 286 (1957).

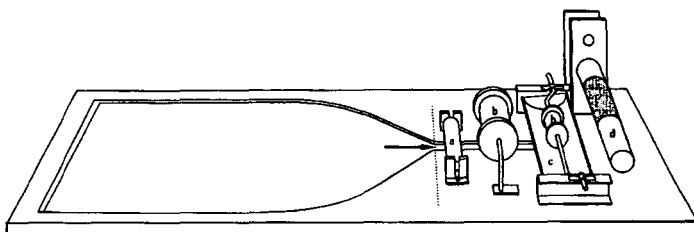


Fig. 1 Outline of culture pan for the direct filamentation of BC. a, sinker; b, roller; c, washing pan; d, wind up roller

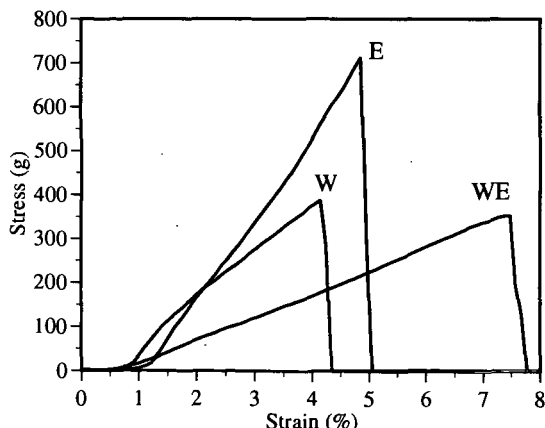


Fig. 2 Stress-strain diagram properties of BC filaments.

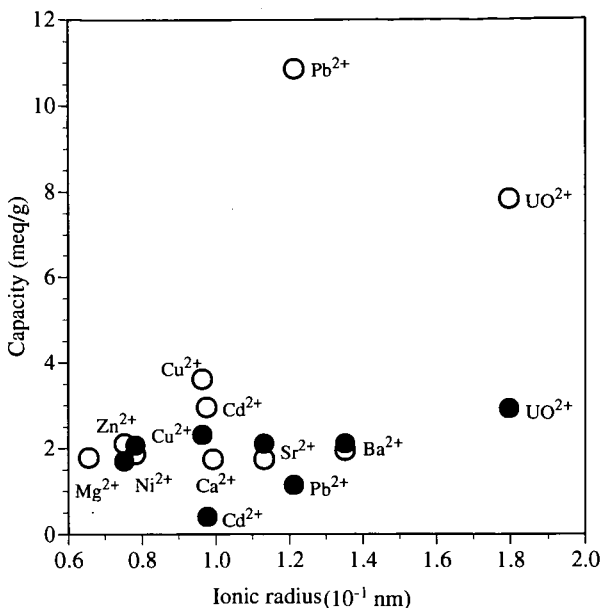


Fig. 3 Metal ion adsorption profile of CM-BC (O) and that of original CMC (●).

Table 1 Tensile Properties of BC Filament

Sample ^a	Elongation (%)	Size (denier)	Tensile stress (g/denier)	Tensile strength (g/denier)	Young's modulus (g/denier)
W1	4.2	108.0	267.4	3.9	93.8
W2	6.0	169.2	223.3	5.6	93.6
W3	4.5	108.0	431.5	3.6	80.5
W4	3.8	108.0	242.4	3.0	78.9
W5	5.8	140.4	386.4	6.1	105.4
E1	5.2	216.0	310.2	3.6	67.9
E2	3.7	216.0	386.4	3.5	93.7
E3	3.8	216.0	284.7	3.1	83.1
WE1	7.7	180.0	293.6	2.1	27.3
WE2	3.7	180.0	249.3	1.9	52.5
WE3	4.2	180.0	341.3	3.1	74.8

a) Obtained filament was rinsed extensively with water (W), with 10% aqueous ethylene glycol (E), or successively with 10% ethylene glycol and water (WE). All filaments were air-dried under tension.

OVERVIEW OF THE REACTIVITY OF ORGANICS IN SUPERHEATED WATER: GEOCHEMICAL AND TECHNOLOGY IMPLICATIONS

Michael Siskin,* and Alan R. Katritzky†

*Exxon Research and Engineering Company, Corporate Research Laboratories,
Clinton Township, Route 22 East, Annandale, NJ 08801

†Center for Heterocyclic Compounds, Department of Chemistry, University of Florida, P.O. Box
117200, Gainesville, FL 32611

Keywords: aquathermolysis, kerogen, cleavage chemistry.

ABSTRACT

The reactivity of organic molecules in hot water is a field of chemistry developing from studies aimed at understanding how organic matter (kerogen) forms in natural environments and then breaks down into energy source materials. In natural systems where kerogens are depolymerized, water is ubiquitous and hot and usually contains salt and minerals. Reactions such as cleavages and hydrolyses in these media are facilitated by changes in the chemical and physical properties of water as temperature increases. These changes make water more compatible with the reactions of organics. We will present a brief geochemical background, discuss chemical and physical properties of water, key features of known kerogen structural models and the aqueous chemistry of cleavage and hydrolysis reactions involved in kerogen depolymerization. Based on the understanding of the roles of water as a solvent, reagent and catalyst, potential applications in areas such as plastics recycling and synthesis of chemicals will be described.

INTRODUCTION

This article describes an emerging area of chemistry: the reactivity of organic compounds in superheated water. We begin with a brief geochemical background and then discuss the implications of the aqueous chemistry to understanding the formation of oil from the solid, insoluble, organic material (kerogen) in resources such as shale and coal. Finally, we point out potential implications to more technological areas such as plastics recycling.

Common organic molecules that were previously considered unreactive in liquid water undergo many chemical reactions when the temperature is increased to 250-350 °C; these reactions were previously expected only in the presence of strong acid or base. For example, ethers and esters, which are unreactive to heat alone, undergo facile cleavage and hydrolysis, respectively, in water at 250-350 °C.¹ Ethers and esters are major cross-links in several oil shale kerogens and are illustrated in a portion of the detailed structural model of a Rundle Ramsay Crossing Type I kerogen in Figure 1. Analogously, polyethylene terephthalate polymers (found in plastic soft drink bottles) can be hydrolyzed quantitatively back to their starting materials in superheated water in less than an hour.² Other polyesters, and also polyamides (like nylon), are equally susceptible to hydrolysis. A major analogy to such polymer degradation reactions in nature is catagenesis: the process by which solid petroleum source rock kerogens, which are cross-linked macromolecular structures, are converted into liquid petroleum. Natural catagenesis takes place at temperatures below 200 °C over millions of years in aqueous environments at pressures of about 600 atmospheres. Because of the relatively low temperatures, it has been hypothesized that some of the chemistry by which petroleum is formed is catalyzed by clay minerals in the formations.³ Recent studies in our laboratories have made it clear that two additional factors can affect and catalyze the kerogen depolymerization chemistry that leads to petroleum formation. One factor is that simple aqueous chemistry generates water-soluble products that are acidic or basic, or have redox properties. The other factor involves the salts present in sea water or aqueous environments.^{4,5}

High temperature water under autogenic pressure provides a significantly more favorable reaction medium for ionic reactions of non-polar organic compounds than does water up to its boiling temperature (Table 1). At 300 °C, water exhibits a density and polarity similar to those of acetone at room temperature.⁶ The dielectric constant of water drops rapidly with temperature, and at 300 °C has fallen from 80 (at 20 °C) to 2⁷ and its solubility parameter decreases from 23.4 to 14.5 cal/cm.⁸ This means that, as the water temperature is increased, the solubility of organic compounds increases much more than expected for the natural effect of temperature. Furthermore, the negative logarithmic ionic product of water at 250 °C is 11, and of deuterium oxide is 12, as compared to 14 and 15, respectively, at 20 °C.⁹ This means that water becomes both a stronger acid and a stronger base as the temperature increases. Therefore, in addition to the natural increase in kinetic rates with temperature, both acid and base catalysis by water are enhanced at higher temperatures.

Table 1. Chemical/Physical Properties of Superheated Water Become More Compatible to Reaction with Organics at High Temperature

T (°C)	Density (g/cm ³)	Dielectric Constant	Solubility Parameter (cal/cm ³) ^{1/2}	-logKw	Vapor Pressure (psi)
25	0.997	78.85	23.4	13.99	23.8
150	0.917	43.89	20.6	11.64	69.0
200	0.863	34.59	19.0	11.30	225.5
250	0.799	26.75	17.0	11.20	576.6
300	0.713	19.66	14.5	11.30	1245.9
350	0.572	12.61	10.3	-----	2397.8

Geochemical Background

Jurg and Eisma¹⁰ reacted samples of behenic acid (*n*-C₂₁H₄₃COOH) with the acidic clay mineral, montmorillonite, in sealed tubes in the presence and absence of water at 200 °C for 89 and 760 h. They found significant hydrocarbon formation only in the presence of the clay catalyst. The ratios of iso- to normal-butane (1:40) and iso- to normal-pentane (1:40) were raised significantly in the presence of water (1:1) in both cases, indicating that the water induces carbocation chemistry. The proportion of saturated hydrocarbons increased with time at the expense of unsaturated hydrocarbons, suggesting alkylation and/or hydrogenation reactions. Among the higher molecular weight hydrocarbons (C₁₄-C₃₄), there was a strong predominance (55-60%) of C₂₁H₄₄, the direct decarboxylation product of behenic acid.

Johns¹¹ studied kinetically the decarboxylation of behenic acid using a series of clays under anhydrous conditions. Arrhenius plots of the data show large decreases in activation energy (from 58.4 to 24.7 kcal/mol) for decarboxylation in the clay-catalyzed reactions compared to the reaction without clay catalysis. The effects of these catalysts were shown dramatically, by calculating the time required for 90% decarboxylation at 60 °C, which ranged from 2.9 x 10²⁰ years for the thermal conversion to only 0.03 year (11 days) when nontronite, an iron-containing clay, was present. Johns points out that the catalytic activity measured in these laboratory studies surpasses that of the natural shale kerogen systems, a finding partially explained by the sharp decrease in clay acidity with increasing water content.

Frenkel and Heller-Kalai¹² demonstrated that the main reaction of the low molecular weight terpene, limonene (VII), in the presence of montmorillonites, is conversion to the aromatic hydrocarbon *p*-cymene (VIII) and to *p*-menthane (IX) and *p*-menthene (X), demonstrating that kerogens could be converted by surface-active materials in sediments to low molecular weight aromatic compounds of the type found in petroleum. A subsequent study by Goldstein¹³ showed that geraniol (VI), a biologically synthesized unsaturated alcohol, undergoes stepwise catalytic conversion in the presence of water, clays, and other sediments at <100 °C initially to form polymeric materials. These polymeric materials were converted into the more thermodynamically stable phenyl, naphthyl, and higher condensed aromatic products. This model system study nicely demonstrates that clay, limestone, and other sediments catalyze a wide variety of reactions in closed, water-containing systems of varying pH (3.9-9.7).

In addition, several other studies have considered the reaction of resource materials (kerogens) in hot water as an alternative to anhydrous pyrolysis at higher temperature. Simulation of petroleum formation required hydrous conditions because water is ubiquitous in sediments. Winters et al.¹⁴ demonstrated that the characteristic low olefin (high saturates) content of natural petroleum oils could be produced by hydrous pyrolysis of Woodford (Devonian), Phosphoria (Permian), and Kimmeridge (Jurassic) source rock shales at 330 °C. Thus, hydrous pyrolysis in a closed system appeared to be a more realistic reaction system than anhydrous pyrolysis in an open system which, by contrast, generates large amounts of olefins. This work is complemented by that of Tannenbaum and Kaplan¹⁵ who carried out a comparative study in which low molecular weight hydrocarbons were generated from Green River oil shale kerogen by both hydrous and anhydrous pyrolysis. At 300 °C, production of initial C₂-C₆ olefins was comparable in both systems, but under aqueous conditions, their concentrations then started to decrease with time (also observed by Jurg and Eisma¹⁰). This high reactivity of the olefins may explain why olefins were not previously observed under hydrous conditions.

The hydrous pyrolysis¹⁶ of a benzene-methanol extracted Messel shale at 330 °C for 3 days in the presence of D₂O gave saturated hydrocarbon products multiply (1-14) substituted by deuterium. Heating the saturated hydrocarbon docosane (C₂₂H₄₆) with a sample of solvent-extracted shale in an excess of D₂O showed only minor deuteration of the re-isolated docosane (80%). This result suggested that simple hydrogen exchange on saturated molecules can be ruled out as a major pathway. However, under similar conditions in the aqueous system, the olefin 1-octadecene was completely reduced to octadecane (60%) with simultaneous significant deuterium incorporation. Hoering applied similar treatment to a kerogen- 2-ethylheptadecanoic

acid mixture and found that the acid decarboxylated to 2-methylheptadecane in 10% yield, while facile deuterium exchange took place at hydrogen atoms adjacent to (α -to) oxygenated functional groups. In other studies, Hoering and Abelson¹⁷ showed that deuterated hydrocarbons are generated from kerogen heated in D₂O at 100 °C and then dried and pyrolyzed in an inert atmosphere. They proposed that olefins, or olefin intermediates generated during pyrolysis, exchanged with the D₂O. Alexander et al.¹⁸ found considerable exchange of isotopic hydrogen between naphthalenes and the acidic clay surfaces, at 23 °C, or in aqueous slurries at 70 °C.

Eglington et al.¹⁹ carried out the hydrous pyrolysis of a Kimmeridge kerogen (Type II) at 280 or 330 °C for 72 h in the presence of clay or carbonate minerals. They found that more organic-soluble pyrolyzate was formed when calcium carbonate was the inorganic phase, which suggests significant base catalyzed cleavage of cross-links.

Graff and Brandes²⁰ found that a steam pretreatment of an Illinois bituminous coal (Type III kerogen) between 320 and 360 °C dramatically improved the yield of liquids upon subsequent conversion or solvent extraction. The steam-modified coal contains twice the hydroxyl groups of the raw coal. This leads to the conclusion that steam reacts with the ether linkages in coal, forming hydroxyl groups, and thereby substantially reducing an important covalent cross-link in the coal structure.²⁰ These conclusions are consistent with model compound studies on ether reactivity in hot water.^{1,20,21}

Aqueous Cleavage/Hydrolysis Reactions

1. Neutral Reactions

Rapid and clean ring cleavage of the cyclic aromatic ether 2,5-dimethylfuran in pure deuterium oxide at 250 °C yielded 2,5-hexanedione quantitatively and irreversibly within 30 min.²² the 2,5-hexanedione product undergoes no ring closure at this temperature in 1 h. These reaction conditions are in contrast to those reported in a mechanistic study of this reaction, in which a 0.1M DCl solution at 70 °C was required to cleave the ring.²³ Dibenzofuran¹ and 2-hydroxydibenzofuran²⁴ proved to be stable to aquathermolysis even at 460 °C.

Acetals and ketals are highly reactive to neutral aquathermolysis, undergoing in nearly all cases 100% hydrolysis within 30 min at 205-250 °C without side or secondary reactions.²² Greater than 90% deprotection of cyclopentanone ethylene ketal and 1,4-cyclohexanedione bis(ethylene ketal) was achieved at 250 °C. Equal reactivities to pure water were determined for benzaldehyde and tolualdehyde diethyl acetals at 186 and 250 °C resulting, during 30 min reaction, in 91-94% and 100% conversion, respectively. Hydrolysis of benzaldehyde diethyl acetal went to completion overnight at room temperature but decreased to 33% in the presence of basic barium oxide at 80 °C over 45 min. At 254 °C, quantitative hydrolysis of this acetal in aqueous KOH at acetal:base molar ratios as low as 1:0.25 (72.5 mM in KOH) was followed by a Cannizzaro disproportionation, as indicated by the formation of benzyl alcohol, benzoic acid, and, via subsequent decarboxylation of the acid, small amounts of benzene. Formation of Cannizzaro products of benzaldehyde in the presence of a much weaker base, pyridine, was reported previously.²⁵ Tsao and Houser suggested the possibility of a Cannizzaro reaction of this aldehyde catalyzed by ammonia in supercritical water, but, product distributions indicate the involvement of radical pathways.²⁶

Diacetone-D-glucose (0.31 M) and 1,6-anhydro- β -D-glucose (0.30M) were converted quantitatively at 205 °C to predominantly D-glucose and traces of another glucose isomer.¹⁶ Under the same conditions in the presence of 1 equivalent of KOH (0.29 M), 1,6-anhydro- β -D-glucose was unreactive and only the exocyclic, 5,6-acetone moiety of diacetone-D-glucose was cleaved. Cellulose is rapidly converted to soluble species with relatively high glucose yield in pure water near its critical temperature.²⁷ In a semi-batch or flow reactor, 100% conversion of cellulose was achieved in 1 h or less (15 sec at 400 °C). Parallel thermal transformations of the glucose product take place to form fructose, 1,6-anhydro D-glucose, erythrose, glycolaldehyde, glyceraldehyde, dehydroxyacetone, pyruvaldehyde, and acids.

2. Other Cleavage Reactions

The thermally stable ester, methyl 1-naphthoate is quantitatively hydrolyzed after 2 h and 5.5 day treatments at 343 and 250 °C, respectively.¹ Naphthoic acid is the major product at 250 °C, but its decarboxylation led predominantly to the formation of naphthalene during a 2 h conversion at 343°C; a reaction catalyzed by the generated carbonic acid. Examinations of methyl benzoate and its 4-chloro, 4-methyl, and 4-methoxy derivatives revealed up to 50% hydrolysis within 30 min at 250°C,²² but no evidence of decarboxylation. Partial cleavage of the *p*-methoxy group is assumed to be caused by the increased acidity of the medium resulting from carboxylic acid formation, since no ether cleavage was observed for α -ethyl-4-methoxybenzyl alcohol, in neutral water under otherwise more extreme conditions (277 °C, 75 min). Aliphatic 1,1-dicarboxylic acids are more reactive and Brill followed the decarboxylation of 1.07 M malonic acid to CO₂ and H₂O and the slower decarboxylation of monosodium malonate to CO₂ and acetate ion at 120-230 °C and 275 bar.²⁸ In a reaction typical of β -keto esters, ethyl

acetoacetate underwent complete conversion to acetone, ethanol, and CO₂ (not analyzed) in 30 min at 250°C.²² Under similar conditions, *tert*-butyl acetate decomposed to a bright red, highly insoluble mixture of unidentified products resulting from polymerization of isobutylene;¹³ but methyl trimethylacetate was unreactive.

Cyclohexyl-*x*-phenyl compounds, characteristic of structures found in Type II Kimmeridge shales, with oxygen, sulfur, and nitrogen links were shown to be relatively unreactive thermally but readily cleaved in water at 250 °C to form methylcyclopentene together with phenol, thiophenol, or aniline, respectively (Eq 5).²¹

Ionic reactions of these types are enhanced in 10% NaCl (acting as a weak acid) and in the presence of an acidic clay, but are depressed by basic calcium carbonate. This evidence supports an acid-catalyzed carbocation mechanism for this system in water at high temperature. Although an acyclic diaryl ether (diphenyl ether) and a cyclic diaryl ether (dibenzofuran) were unreactive under both aqueous and thermal conditions, an activated diaryl ether (4-phenoxyphenol) was cleaved in water to form phenol (Eq 6).¹ Penninger and Kolmschate treated 2-methoxynaphthalene with supercritical water at 390 °C for 1.5 h to give 2-naphthol and methanol as main reaction products.²⁹ Benzyl aryl ethers were also much more susceptible to cleavage under aqueous than thermal conditions at 250 °C. Klein reported that phenethyl phenyl ether formed phenol and styrene as the primary products after 1 h at 400 °C and dibenzyl ether yielded benzyl alcohol, toluene, and benzaldehyde after treatment in water at 374 °C for 1 h.³⁰

The thermally stable diaryl ether 1-phenoxy-naphthalene is cleaved in water at 315 °C after three days to phenol and 1-naphthol (95% conversion) and is thus significantly more reactive than diphenyl ether.³¹ In aqueous sodium formate reduction of the 1-naphthol to naphthalene and dihydronaphthalenes occurs. 9-Phenoxyphenanthrene similarly yields phenol and 9-hydroxyphenanthrene (Eq 8) and is more reactive than its 1-phenoxy isomer.³² Interestingly, the rate of hydrolysis of such diaryl ethers is affected dramatically by additives such as NaCl, LiCl, KBr, and Na₂SO₄.³³ The conversion of 1-phenoxy-naphthalene in water alone at 315 °C after 72 hours was 94.6%; on reaction of this substrate with a 1% aqueous solution of each of the above salts, the conversion was reduced to 7.4%, 4.8%, 3.8%, and 0%, respectively. These results strongly suggest that at high temperatures, alkali metal halides and sodium sulfate behave as salts of strong bases and weak acids and reduce the hydrogen ion activity of the solutions, in agreement with previous indications.³³

Hydrogen Exchange Reactions

When the ring cleavage reaction of 2,5-dimethylfuran was conducted in deuterium oxide,³⁴ extensive deuteration of the methyl and methylene groups in the product, 2,5-hexanedione, was observed; the same result was detected by ¹H and ¹³C NMR when this dione was the initial reagent. Thus, it became evident that this medium was suitable for ¹H/²H exchange.²² These exchange reactions afforded an additional means to study organic transformations in a reaction environment undergoing minimal changes; for example, no products are formed that have significantly different properties or reactivities from those of the initial reagents. Also, no changes occur in reaction mechanisms, volume, vapor pressure, or the dielectric or dissociation constants of deuterium oxide because of the formation of ionic products and potential catalysts or co-solvents.

Deuterium oxide treatment of methyl (300 °C, 93 h), isopropyl, and neopentyl alcohol (200 °C, 30 min and 300 °C, 60 min, respectively) did not induce any exchange of C-H hydrogens; the same negative results were obtained in experiments with ethylene glycol (300 °C, 60 min) and pentaerythritol (250 °C, 60 min).²² Hydrogen exchange was achieved rapidly and nearly quantitatively in the α and α' (where applicable) positions of ketone carbonyl groups. Table 2 lists the extents and sites of deuteration observed in selected ketones. In all cases, the operating enol-keto tautomerism led exclusively to hydrogen exchange; no aldol products were observed.

Table 2. Hydrogen/Deuterium Exchange in Ketones

Compound	% D (position)	Reaction Conditions	
		°C	Min
Pinacolone ^a	100 (α CH ₃)	277	60
Acetone	97 (α , α' CH ₃)	200	60
Cyclopentanone ^b	100 (α , α' CH ₂)	225	30
1,4-cyclohexanedione	100 (α , α' CH ₂)	225	30
Acetophenone	>88 (α CH ₃)	250	60
Deoxybenzoin ^c	99 (α CH ₂)	250	30

a Exchange observed in the rearrangement product of pinacol.

b Exchange observed in the hydrolysis product of the corresponding ethylene ketal.

c PhCH₂COPh.

Nearly quantitative exchange by reaction with only 0.016M sodium deuteroxide solution for 10 min at 400 °C and ~300 bar pressure occurred for molecules having pK_a's up to approximately 43, while longer heating time and more concentrated base solutions allow deuteration of still more weakly acid compounds having pK_a's up to 50.³⁵

Technological Applications

Chemical reactions carried out in hot water have the potential to provide a cleaner, safer environment than reactions in hydrocarbon solvent media. In addition, water acting as a catalyst or reagent could minimize, or possibly eliminate, the need for catalyst synthesis, recycle, regeneration, and disposal. Such application to the recycle of condensation polymers including plastics, synthetic fibers, and polycarbonates is attractive.^{2,36} Another potential application is the use of hot water treatment to upgrade low-value by-products. A demonstrated example occurs in the hydration of propylene with sulfuric acid to form isopropyl alcohol with thermally stable diisopropyl ether as a by-product. Hydrous cleavage of this by-product ether at 315 °C for 30 min readily forms essentially equimolar amounts of the desired product (isopropyl alcohol) and recyclable propylene.³⁷ Di-*sec*-butyl ether, a by-product in the hydration of butylene to *sec*-butyl alcohol in the methyl ethyl ketone (MEK) process, can similarly be converted to the alcohol in hot water³⁷ (Eqs 9 and 10). The aldol condensation by-product of MEK production, a C₈-unsaturated ketone, is quantitatively reversed to MEK by hydration followed by retro-aldol cleavage.³⁸

CONCLUSIONS

This article describes the reactivity of organic molecules in superheated water. Emphasis was placed on the geochemical perspective because, outside of biological processes, where aqueous chemistry predominates and is catalyzed by enzymes, kerogen formation and its subsequent depolymerization into petroleum is the major arena in nature where aqueous chemistry is observed. In this chemistry, water participates as catalyst, reactant, and solvent. While the geochemical aspects serve as a foundation for understanding the aqueous chemistry, the implications for a wide variety of other organic chemical transformations and technological applications are potentially large and just beginning to emerge. The unique ability of water to carry out condensation, cleavage, and hydrolysis reactions and provide an opportunity (not accessible thermally) to effect selective ionic chemistry, is largely due to changes in the chemical and physical properties of water, which become more compatible with the reactions of organics as the temperature is increased. Therefore, its solvent properties at 250-350 °C approach that of polar organic solvents at room temperature. It can act as an acidic or basic catalyst and its reactivity can often be reinforced by autocatalysis from water soluble reaction products generated. Additional positive aspects of the use of aqueous chemistry are its simplicity, low cost, and favorable environmental impact.

REFERENCES

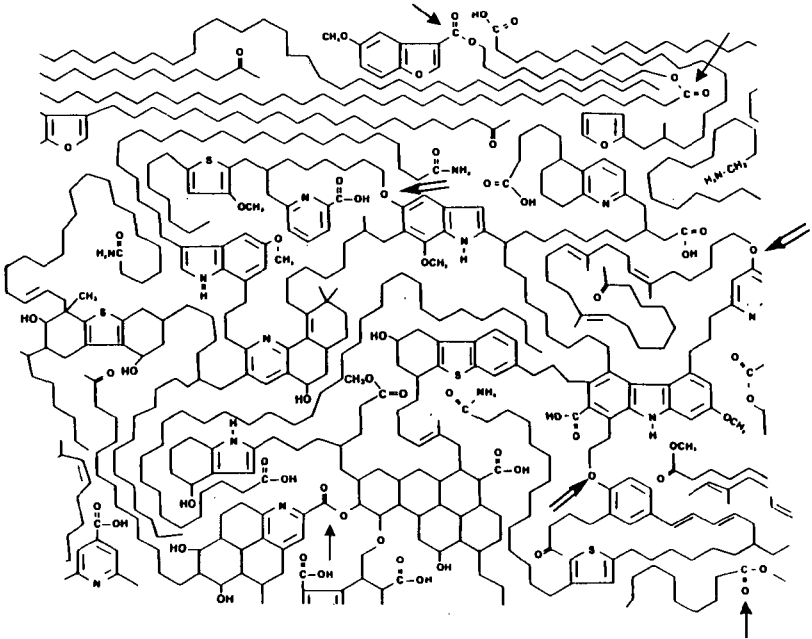
1. Siskin, M.; Brons, G.; Vaughn, S. N.; Katritzky, A. R.; Balasubramanian, M. *Energy Fuels* 1990, 4, 488.
2. Mandoki, J. W. *U.S. Patent* 4 1986, 605, 762.
3. Grim, R. E. *Am. Assoc. Pet. Geol. Bull.* 1974, 31, 1491.
4. Siskin, M.; Brons, G.; Katritzky, A. R.; Balasubramanian, M. *Energy Fuels* 1990, 4, 475.
5. Katritzky, A. R.; Lapucha, A. R.; Murugan, R.; Luxem, F. J.; Siskin, M.; Brons, G. *Energy Fuels* 1990, 4, 493.

REFERENCES (Cont'd.)

6. Pitzer, K. S. *Proc. Natl. Acad. Sci. U.S.A.* **1983**, *80*, 4574.
7. Akerlof, G. C.; Oshry, H. I. *J. Am. Chem. Soc.* **1950**, *72*, 2844. Franck, E. U. *J. Chem. Thermodyn.* **1987**, *19*, 225.
8. Calculated from the specific internal energy of vaporization in Steam Tables by J. H. Keenan, F. G. Hayes, P. G. Hill, J. G. Moore (Wiley Interscience, 1969)
9. Franck, E. U. *J. Chem. Thermodyn.* **1987**, *19*, 225. Akerlof, G. C.; Oshry, H. I. *J. Am. Chem. Soc.* **1950**, *72*, 2844. See also Perrin, D. D. *Ionization Constants of Inorganic Acids and Bases in Aqueous Solutions*, 2nd Ed.; IUPAC Data Series 29; Pergamon, New York, 1982.
10. Jurg, J. W.; Eisma, E. *Science* **1964**, *144*, 1451.
11. Johns, W. D. *Dev. Sedimentol.* **1982**, *35*, 655.
12. Frenkel, M.; Heler-Kalai, L. *Org. Geochem.* **1977**, *1*, 3.
13. Goldstein, T. P. *AAPG Bull.* **1983**, *67*, 152.
14. Winters, J. C.; Williams, J. A.; Lewan, M. D. *Adv. in Org. Geochem.* **1981**, 524.
15. Tannenbaum, E.; Kaplan, I. R. *Nature* **1985**, *317*, 708.
16. Hoering, T. C. *Org. Geochem.* **1984**, *5*, 267.
17. Hoering, T. C.; Abelson, P. H. *Carnegie Inst. Wash. Yearbook* **1963**, *62*, 229 and Hoering, T. C. *Carnegie Inst. Wash. Yearbook* **1968**, *67*, 199.
18. Alexander, R.; Kagi, R. I.; Larcher, A. V. *Geochim. Cosmochim. Acta* **1982**, *46*, 219.
19. Eglington, T. I.; Rowland, S. J.; Curtis, C. D.; Douglas, A. G. *Adv. Org. Geochem.* **1985**, *10*, 1041 and 2589.
20. Brandes, S. D.; Graff, R. A. *Energy Fuels* **1987**, *1*, 84; Brandes, S. D.; Graff, R. A.; Gorbaty, M. L.; Siskin, M. *Energy Fuels* **1989**, *3*, 494.
21. Siskin, M.; Brons, G.; Katritzky, A. R.; Murugan, R. *Energy Fuels* **1990**, *4*, 482.
22. Kuhlmann, B.; Arnett, E. M.; Siskin, M. *J. Org. Chem.* **1994**, *59*, 3098.
23. Kankaanpera, A.; Kleemola, S. *Acta Chem. Scand.* **1969**, *23*, 3607.
24. Siskin, M.; Katritzky, A. R.; Balasubramanian, M. *Fuel* **1995**, *74*, 1509.
25. Katritzky, A. R.; Balasubramanian, M.; Siskin, M. *Energy Fuels* **1990**, *4*, 499.
26. Tsao, C. C.; Houser, T. J. *Prepr. Pap.-Am. Chem. Soc., Div. Fuel Chem.* **1990**, *35*(2), 442.
27. Adschiri, T.; Hirose, R. M.; Arai, K. *J. Chem. Eng. Japan* **1993**, *26*, 676.
28. Maiella, P. G.; Brill, T. B. *J. Phys. Chem.* **1996**, *100*, 14352.
29. Penninger, J. M. L.; Kolmschate, J. M. M. *Supercritical Fluid Science and Technology* eds. Johnston, K. P. and Penninger, J. M. L. *ACS Symp. Series #406*, ACS, Wash. DC **1989**, 245; Penninger, J. M. L. *Fuel* **1988**, *67*, 490.
30. Townsend, S. H.; Abraham, M. A.; Hubbert, G. L.; Klein, M. T.; Paspek, S. C. *Ind. Eng. Chem. Res.* **1988**, *27*, 143.
31. Siskin, M.; Katritzky, A. R.; Balasubramanian, M. *Energy Fuels* **1991**, *5*, 770.
32. Siskin, M.; Katritzky, A. R.; Balasubramanian, M. *Fuel* **1993**, *72*, 1435.
33. Katritzky, A. R.; Balasubramanian, M.; Siskin, M. *J. Chem. Soc., Chem. Commun.* **1992**, 1233.
34. The ion product of D₂O is approximately 1 order of magnitude larger than that of H₂O at equal temperature; e.g. at 250 °C, -log K(H₂O) = 11 and -log K(D₂O) = 12. See: Perrin, D. D. *Ionization Constants of Inorganic Acids and Bases in Aqueous Solutions*, 2nd ed.; IUPAC Data Series 29; Pergamon: New York, 1982.
35. Yao, Y.; Evilia, R. F. *J. Amer. Chem. Soc.* **1994**, *116*, 11229.
36. Kinstle, J. F.; Forshey, L. D.; Valle, R.; Campbell, R. R. *Polym. Prepr. (Am. Chem. Soc., Div. Polym. Chem.)* **1983**, *24* 446. Campbell, G. A.; Meluch, W. C. *Environ. Sci. Technol.* **1976** *10*, 182.
37. Siskin, M.; Brons, G.; Vaughn, S. N.; Saleh, R. Y. *U.S. Patent 5,043,486*, August 27, 1991.
38. Dolfini, J. E.; Glinka, J. *U.S. Patent 4,709,098*, November 24, 1987.

Figure 1

**EXAMPLE OF KEY CLEAVABLE LINKAGES IN RESOURCES ...
... RUNDLE RAMSAY CROSSING OIL SHALE KERGEN**



STRUCTURE-REACTIVITY RELATIONSHIPS FOR ORGANICS IN SUB- AND SUPERCRITICAL AQUEOUS MEDIA: DEVELOPMENT OF A KNOWLEDGE BASE.

Alan R. Katritzky^a, Michael Siskin^b and Daniel A. Nichols^a

^aCenter for Heterocyclic Compounds, Department of Chemistry, University of Florida, P. O. Box 117200, Gainesville, FL 32611

^bExxon Research and Engineering Co., Corporate Research Labs, Rt. 22E, Clinton Twp., Annandale, NJ 08801

Abstract: The products and reactions of diverse classes of organics with superheated water have been analyzed quantitatively by GCMS supplemented by QSPR-derived response factors.

Reaction types to be discussed include: (i) heterolytic carbon-heteroatom bond cleavages and formations catalyzed by water acting as an acid or base, (ii) oxidation-reductions and disproportionations, and (iii) heterolytic carbon-carbon bond formations and cleavages. The results (a) assist the rationalization of aspects of the diagenesis and catagenesis chemistries of kerogens, (b) help in the formulation of superior preparative procedures in which pure water is selected as a solvent, reagent, or catalyst and in special circumstances if it is optimal to add traces of specific reagents, and (c) offer potential solutions for chemical weapons disposal.

Keywords: water, supercritical, organic reactivity

The work carried out at the University of Florida was intended to complement the more applied studies underway at Exxon (see preceding paper) and to help build a knowledge base concerning the reactions undergone by carbon skeletons and typical functional groups found in naturally occurring feedstocks in superheated water. A supplemental objective was to explore the potential of aquathermolysis for chemical weapons disposal. A summary of the work has been published in *Accounts of Chemical Research*¹ and a more detailed overview is in preparation for *Chemical Reviews*.

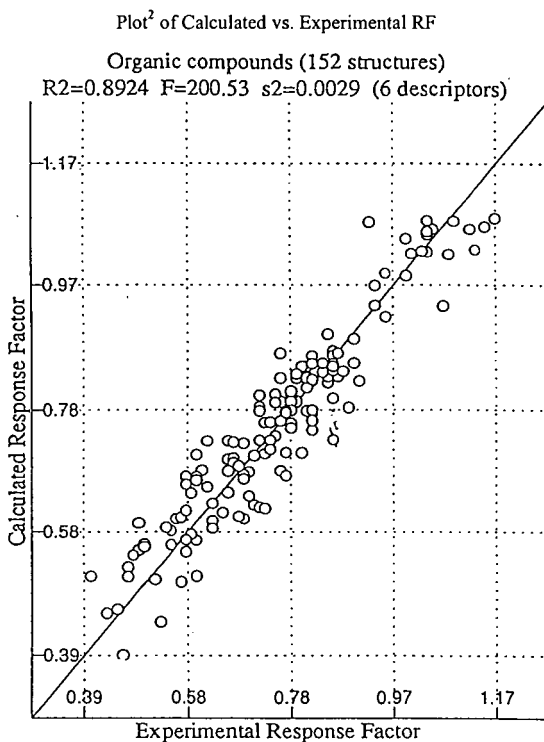
The methodology adopted was to heat known quantities of compounds in water (or water containing definite amounts of such additives as phosphoric acid, sodium hydroxide or formic acid) in small stainless steel bombs. Reactions were analyzed by GC/MS. From the fragmentation pattern and knowledge of the chemistry of the compounds in question at lower temperatures it was usually possible to deduce the structures of the products. This allowed a qualitative analysis. To turn from a qualitative into a quantitative analysis, it was necessary to know the response factors for all the products in the GC flame ionization detector. As it was impractical to measure these, a supplementary investigation was carried out and a quantitative structure property relationship established between chemical structures of a training set of 152 diverse compounds and their flame ionization response factors². It was found possible to correlate response factors with an R^2 value of 0.89 using six theoretical descriptors as shown in the Plot.

Heterolytic carbon-heteroatom bond cleavages and formations were found to be readily catalyzed by water acting as an acid or a base. Oxidation-reductions and disproportionations were also found to be common. Heterolytic carbon-carbon bond formations occurred frequently and sometimes such cleavage reactions were also uncovered.

Thus, benzyl alcohol undergoes a wide variety of condensations to give benzyl benzyl alcohols and polybenzylated benzyl alcohols. Its hydroxy group can also be reduced into a methyl or oxidized into an aldehyde, and further transformations of both of these types of products occur to give a highly complex reaction palette, but one that is completely rationalizable in terms of expected chemical transformations. This research indicated that thermolysis of benzyl alcohol is in effect an aquathermolysis reaction significantly influenced by the water produced during the reaction; however, normal aquathermolysis reaction produces higher quantities of disproportionation products and less dibenzyl ether³.

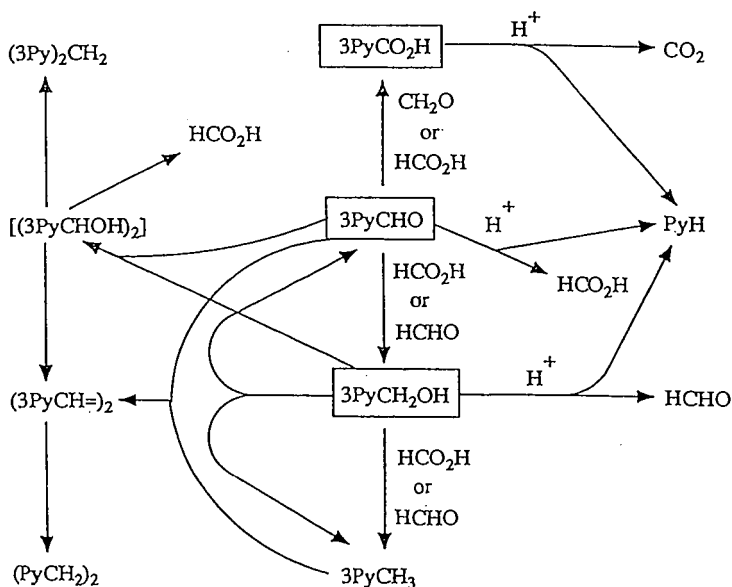
The behavior of hydroxymethyl, aldehyde and carboxyl groups attached to a pyridine ring were studied, and it was found that eventually all these compound types were converted into the parent pyridine together with the corresponding methyl pyridine by disproportionation and substituent cleavage reactions^{4,5}. The overall reaction pathways for pyridines substituted with a carboxyl, aldehyde or hydroxymethyl group in the 3-position⁴ as shown in Scheme 1. The patterns for the corresponding 2-⁶ and 4-⁵ substituted pyridines are still more complex.

In a system simulating water/carbon monoxide, it was found for a series of alkylpyridines that the ring can be cleaved by heating at 350 °C with 50% formic acid ($\text{HCOOH} \rightarrow \text{H}_2\text{O}/\text{CO}$). The products are a series of *N*-substituted piperidines where the *N*-substituent is derived from the fragmentation and C-C bond cleavage at the 3,4 positions of the pyridine ring of a second molecule of the starting pyridine⁷. This process shows considerable similarity to the formation of pyridines from one, two and three carbon building units in commercially well-known catalytic synthetic procedures.



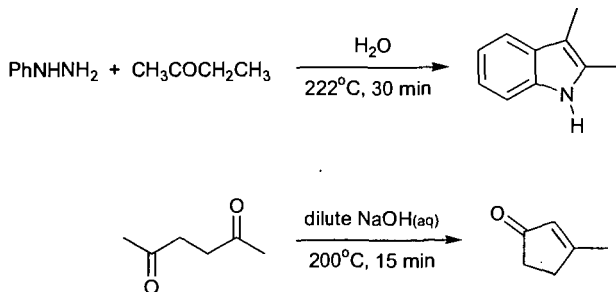
The applications of superheated water as a solvent for superior preparative procedures has been explored particularly by Strauss and his co-workers⁸. As depicted in Scheme 2, such

Scheme 1: Overall Reaction Pathways for 3-Substituted Pyridines⁶



reactions in pure water and in water containing traces of acid or base can have rate enhancements far exceeding those expected for such dilute systems. This is well illustrated by the one step Fisher indole synthesis of 2,3-dimethylindole from phenylhydrazine and butanone in neutral water at 222 °C in 67% yield in 30 minutes⁹. Additionally, although 2,5-hexanedione in neutral water failed to undergo ring closure at 250 °C in 1 hour¹⁰, Strauss found that 3-methylcyclopent-2-enone was formed in 81% yield within 15 minutes at 200 °C from the intramolecular aldol condensation in 0.05% aqueous sodium hydroxide⁸.

Scheme 2: Application of Superheated Water to Preparative Procedures^{8,9}



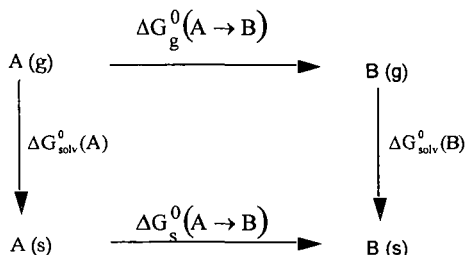
References

- 1 Katritzky, A. R.; Allin, S. M.; Siskin, M. *Acc. Chem. Res.* **1996**, *29*, 399.
- 2 Katritzky, A. R.; Ignatchenko, E. S.; Barcock, R. A.; Lobanov, V. S.; Karelson, M. *Anal. Chem.* **1994**, *66*, 1799.
- 3 Katritzky, A. R.; Balasubramanian, M.; Siskin, M. *Energy Fuels* **1990**, *4*, 499.
- 4 Katritzky, A. R.; Lapucha, A. R.; Murugan, R.; Luxum, F. J.; Siskin, M.; Brons, G. *Energy Fuels* **1990**, *4*, 493.
- 5 Katritzky, A. R.; Lapucha, A. R.; Siskin, M. *Energy Fuels* **1990**, *4*, 510.
- 6 Katritzky, A. R.; Lapucha, A. R.; Siskin, M. *Energy Fuels* **1990**, *4*, 506.
- 7 Siskin, M.; Katritzky, A. R.; Balasubramanian, M.; Ferrughelli, D. T.; Brons, G.; Singhal, G. H. *Tetrahedron Lett.* **1993**, *34*, 4739.
- 8 An, J. Y.; Bagnell, L.; Cablewski, T.; Strauss, C. R.; Trainor, R. W. *J. Org. Chem.* **1997**, *62*, 2505.
- 9 Strauss, C. R.; Trainor, R. W. *Aust. J. Chem.* **1995**, *48*, 1665.
- 10 Kuhlmann, B.; Arnett, E. M.; Siskin, M. *J. Org. Chem.* **1994**, *59*, 3098.

QUANTUM MOLECULAR MODELING OF REACTIONS IN WATER: A DIELECTRIC CONTINUUM APPROACH

Thanh N. Truong
Henry Eyring Center for Theoretical Chemistry
Department of Chemistry, University of Utah
Salt Lake City, UT 84112.

The dielectric continuum solvation approach provides a simple methodology for inclusion of solvent effects directly into the matrix elements of the solute Hamiltonian. This allows that computational procedures for studying reactions in the gas phase such as optimizing transition state structure and determining reaction path, etc. can also be used for reaction in solution. However, direct application of such procedures is not correct. From a thermodynamic cycle, we proposed a rigorous methodology for modeling free energy profiles of reactions in solution within the frame work of the dielectric continuum solvation approach.¹ Let us consider an A \rightarrow B reaction. The standard free energies of reaction in the gas phase and in solution are denoted as ΔG_g^0 and ΔG_s^0 , respectively. Associating with the reactant A and product B are free energies of solvation denoted as ΔG_{solv}^0 . From the thermodynamic cycle given below



the standard free energy of the reaction in solution can be written as

$$\Delta G_s^0 = \Delta G_g^0 + \left\{ \Delta G_{\text{solv}}^0(\text{B}) - \Delta G_{\text{solv}}^0(\text{A}) \right\}, \quad (1)$$

where the gas-phase free energy is given by

$$\Delta G_g^0 = \Delta E - RT \ln \left(\frac{Q^{\text{B}}}{Q^{\text{A}}} \right). \quad (2)$$

Here ΔE is the reaction energy; R is the Boltzmann constant; T is the temperature; Q^{A} and Q^{B} are the total partition functions evaluated with the zero of energy set at the bottom of each respective potential well.

This expression can be generalized for the free energy profile of reaction in solution. In particular, the standard free energy at a point $\mathbf{R}(s)$ along the reaction coordinate s relative to that of the reactant A is expressed as

$$\Delta G_s^0(s) = \Delta G_s^0(\text{A} \rightarrow \mathbf{R}(s)) = V_{\text{MEP}}(s) - RT \ln \left(\frac{Q(\mathbf{R}(s))}{Q^{\text{A}}} \right) + \Delta G_{\text{solv}}^0(\mathbf{R}(s)) - \Delta G_{\text{solv}}^0(\text{A}) \quad (3)$$

where $V_{\text{MEP}}(s)$ is the gas-phase potential energy along the reaction coordinate s with the zero of energy set at the reactant. Eq. (3) indicates that *in order to obtain accurate free energy profile for reaction in solution, one requires to have not only accurate free energy of solvation but also*

accurate gas-phase free energy profile. In calculations of free energies of activation of many reactions in solution, previous studies have focused mostly on the solvation free energy contributions and often overlooked errors in the calculated gas-phase free energy profile.

The central issue here is how to define the reaction coordinate s . Adopting the reaction path Hamiltonian formalism, the reaction coordinate s for reactions in solution is defined as the distance along the minimum free energy path on the free energy surface. However, following the reaction path on the solution-phase free energy surface, as defined in Eq. (3), is almost an impossible task. The major difficulty arises from the necessity to perform normal mode analysis at every point on the gas-phase potential surface in order to calculate vibrational partition functions. To circumvent this problem, an assumption is made that the gas-phase Born-Oppenheimer potential energy surface $E(\mathbf{R})$ has similar topology to the gas-phase free energy surface along the reaction coordinate. In this case, a pseudo-free energy surface $G^*(\mathbf{R})$ in the solute nuclear coordinates \mathbf{R} is related to $E(\mathbf{R})$ by the following expression

$$G^*(\mathbf{R}) = E(\mathbf{R}) + \Delta C_{\text{solv}}(\mathbf{R}). \quad (4)$$

The pseudo-free energy surface defined above allows one to utilize advanced computational methods that have been well developed for following reaction paths in the gas phase. Analogous to the gas phase, the reaction coordinate s in solution is defined as the distance along the minimum free energy path (MFEP) which is the steepest descent path from the transition state toward both the reactant(s) and product(s) on the pseudo-free energy surface $G^*(\mathbf{R})$. To obtain free energy profile of reaction in solution the gas-phase $-RT \ln \left(\frac{Q(s)}{Q^A} \right)$ term is added to the pseudo-free energy profile $\Delta G^*(s)$. In summary, the procedure for calculating free energy profiles of reaction in solution involves three steps: 1) select the appropriate level of theory and basis set that can give accurate gas-phase free energy surface; 2) Determine the transition state and calculate the minimum free energy path on the pseudo-free energy surface defined above; 3) Add contributions from the gas-phase solute internal degrees of freedom along this MFEP. These contributions were mistakenly omitted in previous dielectric continuum calculations of free energies of activation including our own first study of solvent effects on reaction profile of the $\text{S}_{\text{N}}2 \text{ Cl}^- + \text{CH}_3\text{Cl}$ reaction.²

We will discuss advantages and disadvantages of the above methodology in details through applications to several important organic reactions.^{1,3,4}

References

- (1) Truong, T. N.; Truong, T.-T. T.; Stefanovich, E. V. *J. Chem. Phys.* **1997**, *107*, 1881.
- (2) Truong, T. N.; Stefanovich, E. V. *J. Phys. Chem.* **1995**, *99*, 14700.
- (3) Truong, T. N. *J. Phys. Chem. B* **1998**, in press.
- (4) Truong, T. N. *Int. Rev. Phys. Chem.* **1998**, in press.

TRANSITIONS IN THE SOLVATION STRUCTURE ABOUT IONS IN SUPERCRITICAL WATER AND THEIR EFFECTS ON REACTIVITY

John L. Fulton, Markus M. Hoffmann, John G. Darab
Pacific Northwest National Laboratory,
P.O. Box 999 MS P8-19
Richland, WA, 99352.

ABSTRACT

We have determined the molecular structure about ions in water under hydrothermal conditions using X-ray absorption fine structure spectroscopy (XAFS). We report a large decrease in the extent of ion hydration in Ni^{2+} , Sr^{2+} , Rb^+ , and Br^- solutions and the formation of contact-ion pairs in aqueous nickel bromide at temperatures exceeding 325°C. The results demonstrate the large changes in the solvation dynamics that occur in the transition from ambient to supercritical conditions. Such fundamental structural information on the speciation in aqueous solutions under hydrothermal conditions is scarce but needed for an understanding of both inorganic and organic reactions in a supercritical-water solvent. Such an understanding will further the development of new hydrothermal technologies such as organic synthesis or waste destruction processes.

INTRODUCTION

It is well known that ionic species start to associate with their respective counter ions in water at high temperatures. For solutions containing ionic species at moderate concentrations, the onset of this phenomena occurs at temperatures above about 325°C where the breakdown of the water hydrogen-bonding network¹ leads to a dielectric constant (low-frequency) that is dramatically lower than for ambient conditions. The low value of the dielectric constant means that the electrostatic interactions between charged species is no longer effectively screened. A detailed description of the ion-pairing phenomena was first made available through theoretical and simulation work^{2,3}. Some experimental evidence^{4,5} of the existence of ion-pairing was also derived from electronic and Raman spectroscopy but yielded little direct structural information. This XAFS technique⁶⁻⁹ gives the short-range structure of the first several solvation shells about the ion. Therefore, for the first time, we can measure the detailed structural transitions that occur under hydrothermal conditions. We have previously reported observation of significant dehydration occurring under supercritical water conditions for mono- and di-valent cations¹⁰⁻¹² (Sr^{2+} and Rb^+) and for a monovalent anion (Br^-).¹³ More recently we have explored NiBr_2 hydration and ion pairing in moderately dilute systems.¹⁴ Seward et al.¹⁵ have also reported XAFS studies of the hydration and ion-pairing of Ag^+ in subcritical water solutions at their vapor pressure. In this paper, we explore a Ni^{2+} system in which the Br^- concentration is greatly increased through the addition of NaBr . This promotes the formation of the more highly coordinated NiBr_6 species.

Although this presentation will deal with association of inorganic ions in supercritical water ($T_c = 375^\circ\text{C}$), the results are important to systems that also contain organic species. The structural transition that occurs for these inorganic species will also have their analogous transition for organic ionic species. Thus, the existence of ion pairs is an important consideration for manipulating reaction pathways and reaction rates in supercritical water. For instance, ion-pair formation may enhance the reactivity of charged organic molecules if it involves the association of two ionic reactant species (oppositely charged) or it involves an ionic reactant species with an ionic catalytic species. The reactivity may be reduced in those instances where an ionic reactant is sequestered by ion-pair formation with a non-reactive ionic species. Similar mechanisms of enhanced or reduced reaction rates would also affect pathways that involve ionic transition-state species. Finally, the regioselectivity may also be influenced for charged or very polar reactants since the reactants can assume a strongly-bound spatial orientation in an ion-pair structure. It is in this light, that we explore the detailed nature of ion pairing under hydrothermal conditions.

EXPERIMENTAL

In XAFS, the x-ray energy is tuned to the region bounding the electron absorption (in this case the K-edge). The ejected photoelectrons are back-scattered by atoms in the nearest solvation shells giving rise to oscillations in the XAFS spectra on the high energy side of the edge. The Fourier transformation of these *k*-space spectra gives a real-space distribution plot that is closely

related to a radial distribution function. XAFS is a short-range technique, that gives structural information out to one or two solvent shells from the central scattering atom. This is the region of critical importance for understanding ion hydration in a water environment. XAFS spectra were acquired at the insertion device beamline (PNC-CAT) at the Advance Photon Source (Argonne National Laboratory) and at beamline X-19A of the National Synchrotron Light Source (NSLS) at the Brookhaven National Laboratory. A schematic of the high-temperature, high-pressure XAFS equipment and of the data transformation methods are depicted in Figure 1. The details of the experimental techniques^{11-13,16,17} are given elsewhere.

The methods for data collection, background correction and data transformation are well-established^{9,18,19}. The analysis of the $\chi(k)$ function was based upon the standard XAFS relationship

$$\chi(k) = \frac{F(k)S_0^2N}{kR^2} e^{-2k^2\sigma^2} e^{-2R/\lambda(k)} \sin(2kR + \delta(k) - \frac{4}{3}k^3C_3) \quad (1)$$

Where $F(k)$, $\delta(k)$, and $\lambda(k)$ are the amplitude, phase and mean-free path factor, respectively, that are derived from the theoretical standard FEFF.²⁰ Detailed description of fitting methods for these parameters can be found elsewhere.¹⁴ The remaining terms in Equation 1 are N , the coordination number of the shell, R , the shell distance, σ^2 , the Debye-Waller factor which represents the mean-square variation in R due to both static and thermal disorder, and finally C_3 , the anharmonicity of the pair-distribution. These terms, which contain the quantitative structural information, were found using the FEFFIT^{21,22} analysis program that employs a non-linear, least-squares fit to the theoretical standards calculated by FEFF.²⁰

DISCUSSION AND CONCLUSIONS

Figure 2 is a radial structure plot for Ni^{2+} . The figure relates the probability of finding a water molecule or a Br^- at some distance from the central Ni^{2+} ion. Under ambient conditions the Ni^{2+} is octahedrally coordinated with 6 water molecules. As the temperature of the solution is increased, the number of water molecules in the first solvation shell decreases and we observe the appearance of a new peak at about 2.1 Å due to the Br^- counterion. In all the systems that have been studied in detail thus far, the decrease in the extent of hydration occurs concurrent with the formation of the contact ion pairs. This may be primarily a size-exclusion effect or may be in part due to the reduction in the local electric field due to the presence of the counterions.

Table 1 relates the change in the extent of hydration upon going from ambient to a supercritical state for a variety of different cations and an anion. Again there are dramatic reductions in the extent of hydration upon reaching supercritical conditions for these ionic species.

Table 2 reports the detailed structural parameters for a NiBr_2 contact ion pair. The results are derived from a global-model fit to two independent XAFS measurements at both the Ni and Br absorption edges. Thus, a very high degree of confidence is obtained for the NiBr_n ion-pair structural parameters. In this system, the concentration of the Br^- was increased to 6 times the Ni^{2+} concentration in order to favor the formation of Ni^{2+} species with a high degree of ion pairing. The results strongly suggest that there is a transition from octahedral Ni^{2+} coordination at room temperature to tetrahedral coordination at elevated temperatures. The average number of Br^- ions in contact with a Ni^{2+} ion is 3.3. Since electrostatically neutral species are strongly favored in this solvent, the likely species may include dimers $(\text{NiBr}_4\text{Ni}(\text{H}_2\text{O})_n)^0$ or species that also include Na^+ association such as $(\text{NiBr}_3\text{Na}(\text{H}_2\text{O})_n)^0$.

In conclusion, a great deal of structural information is available from XAFS about a wide range of supercritical water systems. Information from these studies will aid in the development of structurally-appropriate models of reaction rates and pathways under hydrothermal conditions.

ACKNOWLEDGMENTS

This research was supported by the Director, Office of Energy Research, Office of Basic Energy Sciences, Chemical Sciences Division of the U. S. Department of Energy, under contract DE-AC06-76RLO 1830.

REFERENCES

- Hoffmann, M. M.; Conradi, M. S. *J. Am. Chem. Soc.* **1997**, *119* 3811-3817.
- Chialvo, A. A.; Cummings, P. T.; Cochran, H. D.; Simonson, J. M.; Mesmer, R. E. *J.*

- Chem. Phys.* **1995**, 1039379-9387.
- Oelkers, E. H.; Helgeson, H. C. *Science* **1993**, 261888-891.
 - Susak, N. J.; Crerar, D. A. *Geochim. Cosmochim. Acta* **1985**, 49555-564.
 - Spohn, P. D.; Brill, T. B. *J. Phys. Chem.* **1989**, 936224-6231.
 - Sayers, D. E.; Stern, E. A.; Lytle, F. W. *Phys. Rev. Lett.* **1971**, 271204.
 - Lee, P. A.; Citrin, P. H.; Eisenberger, P.; Kincaid, B. M. *Rev. Modern Physics* **1981**, 53769-806.
 - Lytle, F. W. In *Applications of Synchrotron Radiation*; Winick, H.; Xian, D.; Ye, M.; Huang, T., Eds.; Gordon and Breach: New York, 1989; pp 135-223.
 - Teo, B. K. *EXAFS: Basic Principles and Data Analysis*; Springer-Verlag: New York, 1986.
 - Palmer, B. J.; Pfund, D. M.; Fulton, J. L. *J. Phys. Chem.* **1996**, 10013393-13398.
 - Fulton, J. L.; Pfund, D. M.; Wallen, S. L.; Newville, M.; Stern, E. A.; Ma, Y. *J. Chem. Phys.* **1996**, 1052161-2166.
 - Pfund, D. M.; Darab, J. G.; Fulton, J. L.; Ma, Y. *J. Phys. Chem.* **1994**, 9813102-13107.
 - Wallen, S. L.; Palmer, B. J.; Pfund, D. M.; Fulton, J. L.; Newville, M.; Ma, Y.; Stern, E. A. *J. Phys. Chem. A* **1997**, 1019632-9640.
 - Wallen, S. L.; Palmer, B. J.; Fulton, J. L. *J. Chem. Phys.* **1998**, 1084039-4046.
 - Seward, T. M.; Henderson, C. M. B.; Charnock, J. M.; Dobson, B. R. *Geochim. Cosmochim. Acta* **1996**, 602273-2282.
 - Fulton, J. L.; Pfund, D. M.; Ma, Y. *Rev. Sci. Instrum.* **1996**, 67(CD-ROM Issue)1-5.
 - Hoffmann, M. M.; Darab, J. G.; Heald, S. M.; Yonker, C. R.; Fulton, J. L. *Chemical Geology* **1999**, Submitted.
 - Stern, E. A.; Heald, S. In *Handbook of Synchrotron Radiation*; Eastman, D. E.; Farge, Y.; Koch, E. E., Eds.; North Holland: Amsterdam, 1983.
 - X-Ray Absorption: Principles, Applications, Techniques of EXAFS, SEXAFS and XANES*; Koningsberger, D. C.; Prins, R., Eds.; John Wiley & Sons: New York, 1988.
 - Zabinsky, S. I.; Rehr, J. J.; Ankudinov, A.; Albers, R. C.; Eller, M. J. *Phys. Rev. B* **1995**, 522995-3009.
 - Newville, M.; Ravel, R.; Haskel, D.; Rehr, J. J.; Stern, E. A.; Yacoby, Y. *Physica B* **1995**, 208 & 209154-156.
 - Stern, E. A.; Newville, M.; Ravel, B.; Yacoby, Y.; Haskel, D. *Physica B* **1995**, 208 & 209117-120.

FIGURES AND TABLES

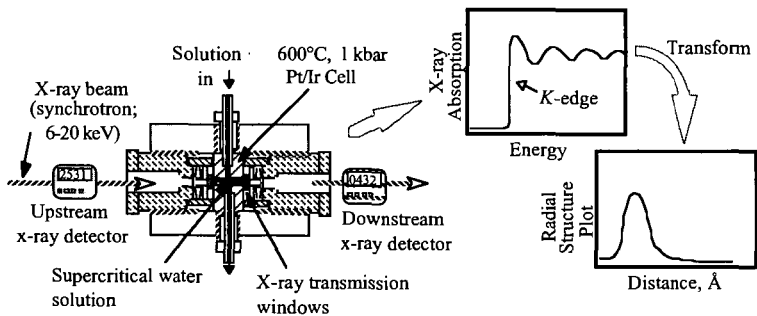


Figure 1. Schematic of the supercritical water XAFS cell and the data analysis technique.

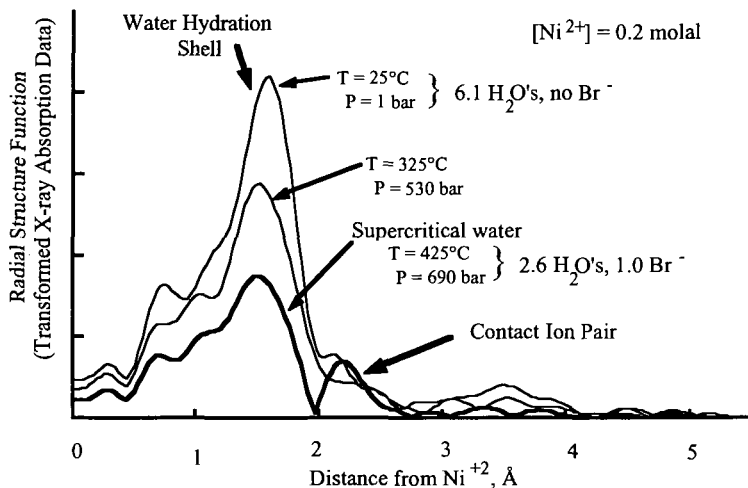


Figure 2. Radial structure around Ni^{2+} ions in supercritical water and the evolution of the Br^- contact ion pair. Distances are not corrected in this figure for the XAFS phase shift but the corrected distances are reported in the following tables.

Table 1. De-hydration of cations/anions in SC Water $[\text{M}^{n+}] = 0.2 \text{ m}$

Ion	Ambient		Supercritical			
	Number of nearest waters	Distance of nearest waters	Temp. °C	Number of nearest waters	Distance of nearest waters	% De-hydration
Rb^{1+}	5.6	2.93 Å	425	3.6	--	36%
Br^{1-}	7.1	3.35 Å	425	2.8	3.39 Å	60%
Sr^{2+}	7.3	2.60 Å	385	3.6	--	51%
Ni^{2+}	6.1	2.06 Å	425	2.6	2.095 Å	57%

Table 2. Hydration and contact-ion pair structure of Ni^{2+} in ambient, subcritical and supercritical water from Ni and Br XAFS measurements. $[\text{NiBr}_2] = 0.2 \text{ molal}$, $[\text{NaBr}] = 0.8 \text{ molal}$.

°C	Density, g/cm^3	Ni^{2+} Hydration / Br^{1-} Hydration ^a			$\text{NiBr}_n^{(2-n)}$ Structure		
		Number $\text{H}_2\text{O}'\text{s}$	Distance $\text{H}_2\text{O}'\text{s}$, Å	σ^2 , $\times 10^{-3} \text{Å}^2$	Number Br^{1-}s	Distance Br^{1-}s , Å	σ^2 , $\times 10^{-3} \text{Å}^2$
25	1.05	5.9/7.1	2.062/3.36	5.9/28	0.0	--	--
325	0.81	^b ---/4.6	^b -----/3.29	^b ---/28	1.1	2.55	11
425	0.65	1.0/4.3	2.091/3.31	3.2/43	3.3	2.405	12

^a Error associated with nearest neighbor numbers is approximately ± 0.3 , error associated with distance is approximately $\pm 0.05 \text{ Å}$, and error associated with σ^2 is ± 0.003

^b The Ni XAFS was not measured for this concentration.

HYDROTHERMAL DECARBOXYLATION OF RCO_2H STUDIED BY REAL-TIME VIBRATIONAL SPECTROSCOPY

T. B. Brill, A. J. Belsky and P. G. Maiella
Department of Chemistry
University of Delaware
Newark, DE 19716

Water at high pressure and high temperature (the hydrothermal environment) is wide spread in the Earth's crust. On the ocean floor the high density of water leads to hot water "black smoker" vents which were first discovered in 1979 on the deep-sea Pacific rift zones.¹ Mineral-laden fluid H_2O flows at temperatures of about 350°C under pressures determined by hydrostatics, e.g. 270 atm at a depth of 2500 meters.^{2,3} At these conditions, H_2O maintains a single fluid phase. A large amount of organic chemical synthesis occurs in the shear layer where the hot vent water interfaces with the cooler sea water.⁴ These unusual conditions thermodynamically drive alterations of relatively simple, but universally important molecules such as H_2 , CO , CO_2 , H_2S , NH_3 , CH_4 and H_2O , to synthesize larger molecules,⁵⁻⁷ such as various carboxylic acids,^{6,8,10} amino acids,⁶ aldehydes¹¹ and metal carboxylate complexes¹². Feeding on the resulting organic compounds, a complex ecosystem ranging from single cell species to large invertebrates develops in the vicinity of these vents¹³⁻¹⁵ and, thus, the synthesis of small organic molecules in the hydrothermal regime is thought to have contributed to the origin of life.^{14,16,17}

Underlying these fascinating and profound issues is a series of basic questions in thermodynamics and kinetics. A large body of measurements and analyses in the references cited above particularly support the notion that thermodynamics is the main driving force for the synthesis of small organic molecules in the hydrothermal environment. On the other hand, it appears that, by comparison, relatively few kinetic considerations have been incorporated into reactions of small organic and inorganic molecules under conditions particular to hydrothermal vents. Instead, most hydrothermal and supercritical water kinetic measurements and analyses have been driven by biomass conversion¹⁸⁻²¹ and waste stream remediation technologies.²²

Hydrothermal vents involve transient phenomena in which temperature gradients exist in the shear layer and where turbulent mixing occurs. As such, kinetic phenomena are likely to be very important factors. The vast majority of kinetic and mechanistic studies of alterations of organic compounds in the hydrothermal medium are based on analysis of products after cooling a tube reactor that was heated in the batch mode or by post-reaction analysis of products from a flow reactor. Comparatively fewer kinetic and mechanism data have been obtained spectroscopically during the reaction, especially in the flow mode.²³⁻³⁴ This method, however, provides an unprecedented level of detail about hydrothermal chemical reactions.

The focus of this talk is on recent work dealing with the kinetics and mechanism of decarboxylation of carboxylic acids in real-time at hydrothermal conditions.^{30,33,34} Such studies augment previous work on kinetics conducted by other experimental methods.^{10,35}

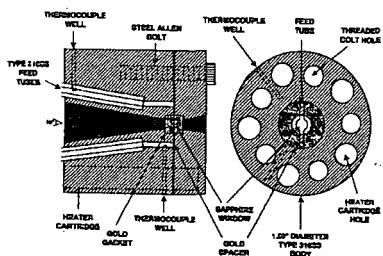


Fig. 1. The flow cell used for real-time IR at hydrothermal conditions.

The experimental methods used in this work are described elsewhere in detail.^{25,27,32} The short-path length IR flow cell is shown in Fig. 1 and is connected to a flow control apparatus that precisely maintains the temperature ($\pm 1^\circ\text{C}$), pressure (± 1 atm) and flow rate (0.01 - 1 ml/min). The resulting residence times in kinetic regime studied are 1-60 sec. These devices enabled a variety of kinetic and mechanistic details to be uncovered that would be opaque in the batch mode where determinations are made at longer times and by post-reaction analyses.

Wall-Assisted Decarboxylation. The clearest evidence that the reactor surface could assist or catalyze the decarboxylation reaction was obtained with formic acid, HCO_2H .³³ Figure 2 shows the rate of formation of CO_2 from a 1.00 M HCO_2H solution as a single phase at 310°C . Two batches of 316 stainless steel (SS) gave somewhat different results but, at least initially, not much different from 90/10 Pt/Ir. Titanium gave a much slower rate of CO_2 formation. These results strongly suggest that the reactor wall can affect the rate of decarboxylation of HCO_2H .

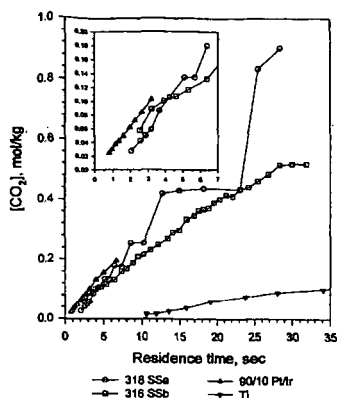


Fig. 2. The concentration of CO_2 from decomposition of 1.00 M HCO_2H at 310°C and 275 atm as a function of residence time in four types of cell materials.

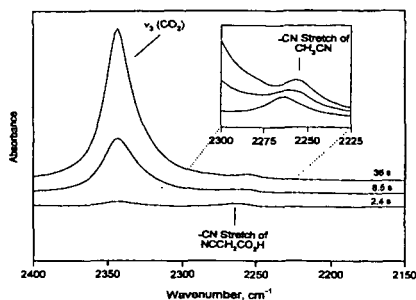


Fig. 3. A time series of IR spectra for 1.00 M $\text{NCCH}_2\text{CO}_2\text{H}$ at 220°C under 275 atm in the 316 SS flowcell. Conversion by reaction (1) is indicated.

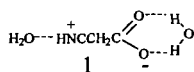
Homogeneous Phase Decarboxylations. The mechanisms of hydrothermal reactions of organic compounds in H_2O solution can be expected to depend on the functional groups attached to the reactive site. This subject has not been investigated previously and was established by the use of the SS and Ti cells in Fig. 1 and with another higher volume cell by Raman spectroscopy.^{30,34} Derivatives of acetic acid were used for this work RCO_2H ($\text{R} = \text{CCl}_3^-$, CF_3^- , CF_3CH_2^- , $\text{HOC}(\text{O})\text{CH}_2^-$, $\text{NH}_2\text{C}(\text{O})\text{CH}_2^-$, NCCH_2^- , and $\text{CH}_3\text{C}(\text{O})^-$). All of these substituents are electron-withdrawing which accelerates the decarboxylation reaction. Relatively small effects were induced by the material of construction (SS or Ti) of the cell. The R group on the other hand exerted a pronounced effect on the rate of decarboxylation, which is described at least initially by reaction 1. Figure 3 illustrates



reaction 1 when $\text{R} = \text{NCCH}_2^-$ in which the reactant -CN stretch, product -CN stretch (CH_3CN), and CO_2 can all be spectrally observed simultaneously. The spectral absorbance can be integrated to obtain the concentrations at all times. Figure 4 is a first-order rate plot for the decarboxylation of $\text{NCCH}_2\text{CO}_2\text{H}$ at 275 atm and the temperatures shown. These data can, of course, be expressed in the Arrhenius form.³⁴ When kinetic constants of this type are determined for all of the substituted acetic acids, the rates or Arrhenius parameters failed to correlate with common linear free energy relations, such as the electronic Hammett or Taft parameters.³⁶ On the other hand, the use of the expanded Taft equation 2 produced useful results. Equation 2 expresses the steric, E_s , and electronic, σ^* , substituent parameters weighted by the adjustable variables ρ and δ in terms of the rate constants, k , normalized to that of acetic acid, k_0 , measured at the same conditions. Figure 5 shows that these categories of compounds separate. The line shown represents the fit for $\rho = 1.5$ and $\delta = -3.6$. The

$$\ln(k/k_0) = \delta E_s + \rho \sigma^* \quad (2)$$

larger absolute value of δ indicates that the steric effect of R is somewhat more important in the rate than the electronic effect. This finding is consistent with structure 1 in which H_2O polarizes the carboxylate group, rather than structure 2 in which H_2O acts as a nucleophile, because the steric bulk of R should impede the reaction in the latter case.



Another category of compounds in Fig. 5 arises when $\text{R} = \text{HOC}(\text{O})\text{CH}_2^-$ and $\text{NH}_2\text{C}(\text{O})\text{CH}_2^-$. These compounds react faster than expected and probably do so as a result of their ability to form the cyclic transition state structure 3. This structure facilitates the unimolecular pathway of decarboxylation. When $\text{R} = \text{CF}_3^-$, Fig. 5 shows the rate of decarboxylation is slower than expected from the substituent effect. The CF_3^- group impedes the process probably because the hyperconjugative interaction shown in structure 4 strengthens the C-C bond.

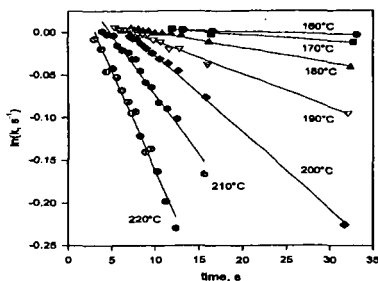


Fig. 4. First-order rate plot of decarboxylation of $\text{NCCH}_2\text{CO}_2\text{H}$ at 275 atm.

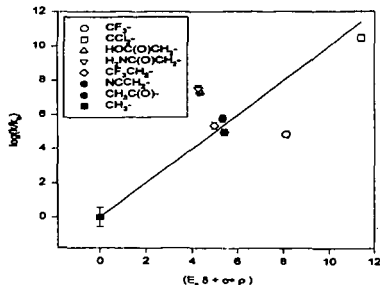
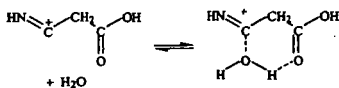
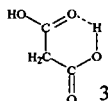


Fig. 5. A Taft plot for decarboxylation of RCO_2H at 200°C and 275 atm.



5

The Effect of pH. Strecker synthesis is believed to provide easy access to α -amino and α -hydroxyl carboxylic acids in the early life forming process.³⁷ In this reaction, NH_3 and HCN react with aldehydes and ketones to form the α -amino and α -hydroxy organonitriles that react with H_2O to form the carboxylic acid. Our study of $\text{NCCH}_2\text{CO}_2\text{H}$ ³⁴ decarboxylation raised a question about the conditions by which H_2O reacts with the $-\text{CN}$ group. To this end, the kinetics of decomposition of $\text{NCCH}_2\text{CO}_2\text{H}$ in 0.3-1.0N HCl was conducted at 150-260°C under 275 atm pressure. The mechanism worked out is shown in Fig. 6. Channel A occurs in the absence of acid as is discussed above. Channels B, C and D are opened by the presence of HCl and channel A does not occur. Hence, the presence of acid makes the $-\text{CN}$ group more reactive than the $-\text{CO}_2\text{H}$ group while the reverse is true in neutral solution. The probable reason is that the $-\text{CN}$ group is protonated by acid which facilitates nucleophilic attack by H_2O as shown in structure 5.

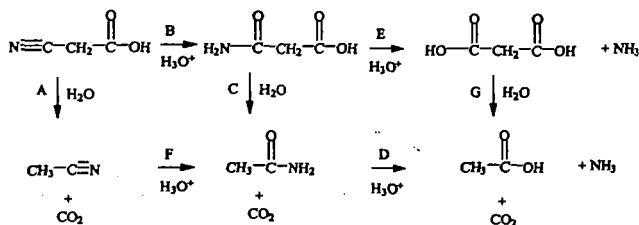


Fig. 6. The pathway of decarboxylation and deamination of $\text{NCCH}_2\text{CO}_2\text{H}$ determined in the hydrothermal regime.

In conclusion, real-time IR and Raman spectroscopy during hydrothermal reactions provides experimentally-based, mechanistic details about hydrothermal reactions under conditions of interest in geothermal vents and in waste steam remediation. Several different types of molecule-dependent decarboxylation mechanisms are uncovered for the seemingly simple reaction 1. In some cases H_2O appears to play a key role whereas in others it does not.

Acknowledgments. We are grateful to the Army Research Office for support of this work on DAAG55-98-1-0253 and to the NSF for support on CHE-9807370.

References

1. RISE Project Group (Spiess, F. N. et al.) *Science*, **207**, 1421 (1980).
2. Rona, P. A.; Bostrom, K.; Laubier, L.; Smith, K. L., Eds. *Hydrothermal Processes at Sea Floor Spreading Centers*, Plenum, NY (1984).
3. Haymon, R. M. and Macdonald, K. C. *Am. Sci.* **73**, 441 (1985).
4. Shock, E. L. *Origins of Life and Evolution of the Biosphere* **22**, 67 (1992).
5. Shock, E. L. *Origins of Life and Evolution of the Biosphere* **20**, 331 (1990).
6. Shock, E. L. *Geochim. Cosmochim. Acta* **54**, 1175 (1990).
7. Shock, E. L. and Helgeson, H. C. *Geochim. Cosmochim. Acta* **54**, 915 (1990).
8. Lundegard, P. D. and Kharaka, Y. K. In *Chemical Modeling of Aqueous Systems II* (ed. D. C. Melchior and R. L. Bassett); *Amer. Chem. Soc. Symp. Series* **416**, 169 (1990).
9. Shock, E. L. *Geochim. Cosmochim. Acta* **57**, 3341 (1993).
10. Pittman, E. D. and Lewan, M. D., Eds. *Organic Acids in Geological Processes*, Springer-Verlag, Berlin, 1994.
11. Schulte, M. D. and Shock, E. L. *Geochim. Cosmochim. Acta* **57**, 3735 (1993).
12. Shock, E. L. and Koretsky, C. M. *Geochim. Cosmochim. Acta* **59**, 1497 (1995).
13. Felbeck, H. and Somero, G. N. *TIBS*, **201** (1982).
14. Brock, T. D. *Science* **23**, 132 (1985).
15. Lutz, R. A.; Shank, T. M.; Fornari, D. J.; Haymon, R. M.; Lilley, M. D.; Von Damm, K. L.; Desbruyeres, D. *Nature* **371**, 663 (1994).
16. Wächtershäuser, G. *Prog. Biophys. Molec. Biol.* **57**, 75 (1992).
17. Huber, C. and Wächtershäuser, G. *Science* **276**, 245 (1997).
18. Katritzky, A. R.; Allin, S. M.; Siskin, M. *Accs. Chem. Res.* **29**, 399 (1996).
19. Mishra, V.; Mahajani, V. V.; Joshi, J. B. *Ind. Eng. Chem. Res.* **34**, 2 (1995).
20. Savage, P. E.; Gopalan, S.; Mizan, T. I.; Martino, C. J.; Brock, E. E. *AIChE J.* **41**, 1723 (1995).
21. Ding, Z. Y.; Frisch, M. A.; Li, L.; Gloyna, E. F. *Ind. Eng. Chem. Res.* **35**, 3257 (1996).
22. Tester, J. W.; Holgate, H. R.; Armellini, F. J.; Webley, P. A.; Killilea, W. R.; Hong, G. T.; Barner, H. E. In *Emerging Technology in Hazardous Waste Management III*; Tedder, D. W., Pohland, F. G., Eds., *ACS Symposium Series 517*; American Chemical Society: Washington, D.C., 1993, pp. 35-75.
23. Masten, D. A.; Foy, B. R.; Harradine, D. M.; Dyer, R. B. *J. Phys. Chem.* **97**, 7557 (1993).
24. Ryan, E. T.; Xiang, T.; Johnston, K. P.; Fox, M. A. *J. Phys. Chem.* **100**, 9395 (1996).
25. Kieke, M. L.; Schoppelrei, J. W.; Brill, T. B. *J. Phys. Chem.* **100**, 7455 (1996).
26. Schoppelrei, J. W.; Kieke, M. L.; Brill, T. B. *J. Phys. Chem.* **100**, 7463 (1996).
27. Schoppelrei, J. W.; Kieke, M. L.; Wang, X.; Klein, M. T.; Brill, T. B. *J. Phys. Chem.* **100**, 14343 (1996).
28. Schoppelrei, J. W. and Brill, T. B. *J. Phys. Chem.* **101A**, 2297 (1997).
29. Schoppelrei, J. W. and Brill, T. B. *J. Phys. Chem.* **101A**, 8593 (1997).
30. Maiella, P. G. and Brill, T. B. *J. Phys. Chem.* **100**, 14352 (1996).
31. Maiella, P. G. and Brill, T. B. *Inorg. Chem.* **37**, 454 (1998).
32. Belsky, A. J. and Brill, T. B. *J. Phys. Chem.*, **102A**, 14509 (1998).
33. Maiella, P. G. and Brill, T. B. *J. Phys. Chem.*, **102A**, 5886 (1998).
34. Belsky, A. J. and Brill, T. B. *J. Phys. Chem.*, submitted.
35. Bell, J. L. S.; Palmer, D. A.; Barnes, H. L.; Drummond, S. E. *Geochim. Cosmochim. Acta* **58**, 4155 (1994).
36. Unger, S. H. and Hansch, C. *Prog. Phys. Org. Chem.* **12**, 91 (1976).
37. Cronin, J. R. and Chang, S. *The Chemistry of Life's Origin*, J. M. Greenberg and V. Pirronella, eds., Kluwer Academic Publ. Dordrecht, The Netherlands, 1993, p. 209.

REACTIVITY OF MONOCYCLIC AROMATIC COMPOUNDS UNDER HYDROTHERMAL CONDITIONS

T. M. McCollom and J. S. Seewald
Woods Hole Oceanographic Institution
MS #4
Woods Hole, MA 02540
e-mail: tmccollom@whoi.edu

INTRODUCTION

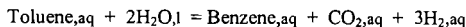
In recent years, there has been an increasing awareness among geochemists that aqueous reactions may play a significant role in the thermal maturation of organic matter in geologic environments (1,2). There are several ways in which water may enhance the reactivity of organic compounds, including serving as a solvent for reactions or participating directly as a reactant in the process. Understanding the role of aqueous reactions in the maturation of organic matter can be substantially improved by examining the reactivity of individual model compounds in laboratory experiments. We will present results from experimental studies on the hydrothermal reactivity of monocyclic aromatic compounds (MAC; benzene, toluene, phenol, cresols, etc.). These compounds are particularly suitable for such studies because MAC have relatively high aqueous solubilities and represent a significant fraction of the organic matter found in geologic environments.

EXPERIMENTAL

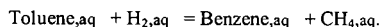
The experiments were conducted in a flexible-cell hydrothermal apparatus (3) using a gold reaction cell with titanium fittings. The reaction cell was equipped with a valve that allowed subsamples to be taken during the course of the experiment, so that the progress of the reactions could be followed over time. Experiments were carried out at either 300° or 330°C and 350 bars. Aqueous solutions of the compound to be studied were either loaded in the cell before heating or injected through the valve after an equilibration period. Assemblages of iron oxide and sulfide minerals were also included within the reaction cell. The intent of including these minerals is two-fold: first, to buffer the oxidation state of the system, and, second, to provide potential catalytic surfaces similar to those typically found in geologic environments. Mineral assemblages used in the experiments included pyrite-pyrrhotite-magnetite (PPM), hematite-magnetite-pyrite (HMP) and hematite-magnetite (HM).

RESULTS AND DISCUSSION

The principal reaction products from heating aqueous solutions of toluene were benzene and CO₂ (Figure 1). Other identified reaction products included phenol, benzoic acid, and cresols. Trace amounts of methane and other hydrocarbons were also observed, but these compounds appeared to derive from small amounts of organic matter in the minerals and not from toluene. Benzene and CO₂ were produced in a one-to-one ratio, suggesting that the formation of benzene from toluene proceeded by an oxidative decarboxylation reaction pathway:



rather than by demethylation:

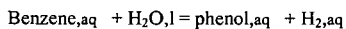


Benzoic acid appears to be an intermediate product of this reaction.

Aqueous solutions of benzoic acid decomposed rapidly during heating to benzene and CO₂ (plus minor phenol and toluene; Figure 2). Production of benzene from benzoic acid was much more rapid than the production from toluene, indicating that the formation of benzoic acid is the rate-limiting step in the reaction pathway from toluene to benzene.

None of the experiments conducted to date have shown any evidence for the decomposition of the aromatic ring from MAC. In all cases, the aromatic moiety from the original compound can be accounted for among the reaction products and remaining reactant. Thus, it appears that the aromatic ring is highly persistent under hydrothermal conditions, and reactions are limited to transformations among MAC with different substituent groups on the aromatic ring.

Comparisons of the relative concentrations of reaction products with predicted equilibrium ratios based on the thermodynamic properties of individual compounds indicates that reactions among several MAC compounds may rapidly approach equilibrium. For instance, equilibrium ratios of benzene to phenol predicted for the reaction



agree closely with the measured ratios in the experiments (Figure 3), suggesting that this reaction equilibrates very rapidly at the experimental temperatures. Consequently, it appears that the relative concentrations of benzene and phenol were controlled by chemical equilibrium between the compounds as the experiments progressed (note that this is strictly a *metastable* equilibrium, since both compounds should decompose almost completely to a mixture of CO₂ and methane as stable thermodynamic equilibrium of the system is approached). The possibility that other pairs of MAC compounds (e.g. toluene/cresols, toluene/benzene) may also reach equilibrium proportions is being investigated in ongoing experiments.

CONCLUSIONS

The experimental results demonstrate that monocyclic aromatic compounds readily undergo reactions in aqueous solutions at elevated temperatures, and indicate that these reactions mostly involve transformations among MAC with different substituent groups. The reactivity of MAC implies that similar reactions may play a large role in controlling the relative proportions of these compounds in geologic environments such as petroleum reservoirs and hydrothermal systems. Furthermore, the results suggest that the relative proportions of benzene and phenol (and perhaps other MAC) may be controlled by metastable equilibrium reactions taking place in the aqueous phase and involving water as a reactant. Since these reactions involve oxidation/reduction, the relative amounts of benzene and phenol in geologic environments should reflect the oxidation state of the system.

REFERENCES

- (1) Lewan, M. D., *Geochim. Cosmochim. Acta*, **61**, 3691-3723 (1997).
- (2) Helgeson, H. C., Knox, A. M., Owens, C. E., and Shock, E. L., *Geochim. Cosmochim. Acta*, **57**, 3295-3339 (1993).
- (3) Seyfried, W. E., Jr., Janecky, D. R., and Berndt, M. E., in *Hydrothermal Experimental Techniques*, Edited by Ulmer, G. C. and Barnes, H. L., John Wiley and Sons, pp. 216-239 (1987).
- (4) Johnson, J.W., Oelkers, E.H., Helgeson, H.C., *Comput. Geosci.* **18**, 899-947 (1992).
- (5) Dale J. D., Shock, E. L., MacLeod G., Aplin A. C. and Larter S.R. *Geochim. Cosmochim. Acta*, **61**, 4017-4024 (1997).
- (6) Shock, E.L., Helgeson, H.C., and Sverjensky, D.A., *Geochim. Cosmochim. Acta*, **53**, 2157-2183 (1989).
- (7) Shock, E.L. and Helgeson, H.C., *Geochim. Cosmochim. Acta*, **54**, 915-945 (1990).

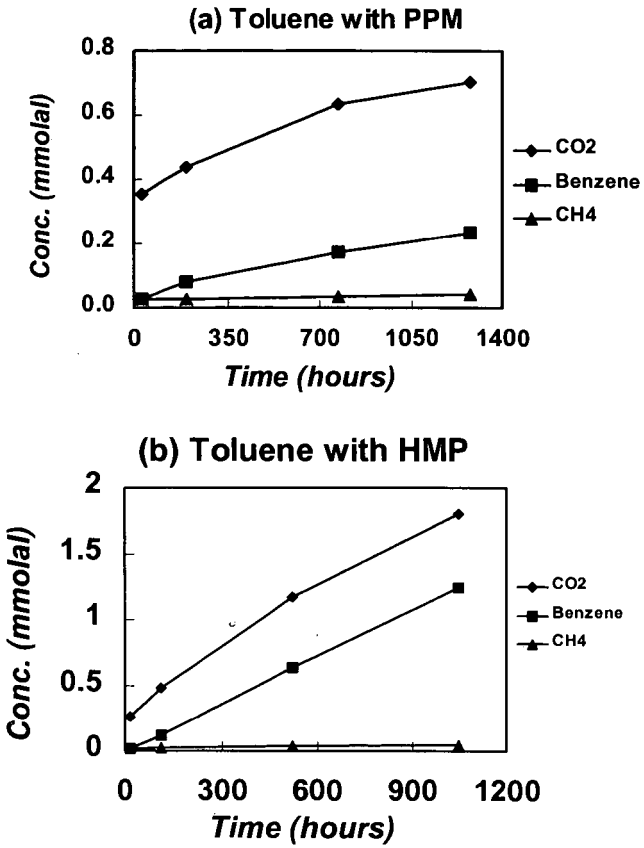


Figure 1. Selected reaction products from heating aqueous solutions of toluene at 330°C in the presence of the mineral assemblages (a) PPM and (b) HMP.

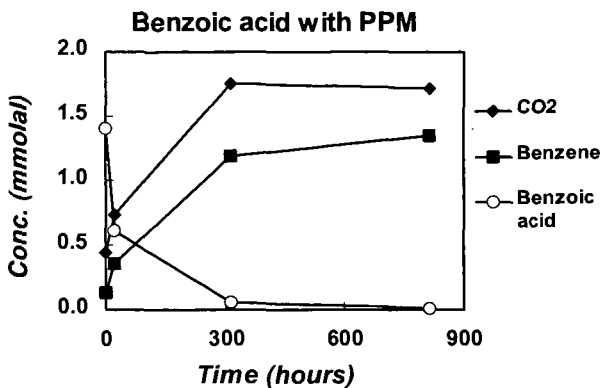


Figure 2. Selected reaction products from heating an aqueous solution of benzoic acid at 330°C in the presence of the mineral assemblage PPM.

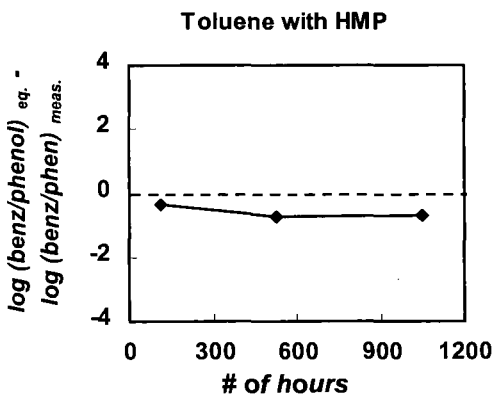


Figure 3. Difference between the predicted equilibrium ratio for benzene to phenol and the measured ratio for reaction products following heating of an aqueous solution of toluene at 330°C in the presence of the mineral assemblage HMP. Note that ratios are given on a log scale. Equilibrium ratios calculated using SUPCRT (4) with thermodynamic data from references 5,6 and 7.

High Pressure Hydrothermal Chemistry of Citric Acid and Related Acids

George D. Cody, Jennifer G. Blank, Jay Brandes, Robert Hazen, and Hatten Yoder, Jr.,

Geophysical Laboratory
Carnegie Institution of Washington
5251 Broad Branch Road, NW
Washington, DC 2001

Abstract High pressure hydrothermal reactions were run using sealed gold tube reactors and an internally heated high pressure apparatus. The reaction conditions varied from 150 to 350° C and from 0.5 to 5.0 Kb. The effects of pressure on a wide range of reactions was clearly evident and in some cases counter intuitive. Although high pressure clearly favored hydration reactions, decarboxylation reactions were greatly accelerated. In the system pyruvic acid - water, the chemistry was dominated by Aldol and Diels-Alder cycloaddition chemistry leading to a broad array of functionalized aromatic molecules which exhibited micellar qualities. The system citric acid - water yielded an interesting reaction network characterized by a number of isomeric equilibria. The effects of pressure operated on displacing the various equilibria towards specific isomers. The effects of pH on the citric acid chemistry also had significant control on metastable equilibria. These results are being integrated into a larger study of the feasibility of biochemistry emerging from the intrinsic organic chemistry associated with hydrothermal vents.

Experimental

All reactions were run in sealed (welded) gold tube reactors. Pressure and temperatures of interest were obtained using an internally heated high pressure apparatus. Following reaction, samples were quenched. Each sample was weighed before and after reaction to ensure sample integrity. Samples tubes were immersed in vials of BF₃/propanol, a known quantity of pentadecane was added as a standard, and heated at 90 °C for 1 hr. to esterify products. The derivitized products were extracted in dichloromethane, dried over NaSO₄, and analyzed with gas chromatography with mass spectrometric detection.

Results and Discussion

In order to better understand the potential for organic synthesis and the feasibility of biochemical reactions under extremes of pressure and temperature characteristic of deep sea hydrothermal vents we have begun to explore the high pressure aqueous chemistry of a number of potentially relevant biochemicals. In particular we have sought to address the question of whether metabolism recapitulate biogenesis, i.e. we are focusing on establishing whether the various metastable equilibria among the principal components of the tricarboxylic acid cycle favor anabolic synthesis at high pressures and temperatures. The results presented below involve high-pressure hydrothermal experiments probing the reactions and stability of pyruvic acid and citric acid, respectively, in CO₂ - H₂ bearing aqueous fluids in the temperature range of 150-350 °C and 0.5 to 5.0 Kbar. At this stage our principal focus is in identifying the effect of pressure on reaction selectivity in systems that exhibit multi-channel reactions. Towards this end, we have focused on two relatively simple systems in order to gain fundamental information on the kinetics of reactions that typify biological processes, albeit under strictly abiotic conditions. The data derived will provide a foundation for subsequent work on the potential for abiotic synthesis of classically bio-organic compounds at extremes of temperature and pressure, conditions that typify deep ocean hydrothermal vents.

In the pyruvic acid system we set out to determine whether pressure would favor the synthesis of oxaloacetic acid through an electrophilic addition of CO₂ at elevated temperatures. Thus far, have not revealed any evidence for the synthesis of oxaloacetic acid. Other interesting reactions, however, are operative within this pressure and

temperature regime. We observe substantial product yields from three reaction channels operating in series and parallel. One of these channels yields appreciable quantities of the five carbon diacid, methyl succinic acid, that forms through a cascade of reactions moving (evidently) through a number of intermediates. There is evidence that this reaction may be concerted (Figure 1). The reaction pathway is superficially similar to the citric acid cycle with the exception of the initial step; i.e. the initial step involves the formation of an Aldol condensation product rather than an electrophilic addition reaction.

A second reaction channel involves the straightforward de-carboxylation of pyruvic acid and is not particularly interesting beyond helping to establish the limits of pyruvic acid stability. On the other hand, the third reaction channel produces a very interesting and complex suite of compounds with amphiphilic qualities (Figure 2). This particular reaction channel operates, in general, through sequential Aldol condensations, Diels-Alder cyclo-additions, decarboxylations, dehydrations, dehydrogenations, and/or hydro-genations. Significant and systematic pressure and temperature induced changes in the distribution of molecules within this suite are observed.

In general, we observe that pyruvic acid is destabilized with increases in temperature and pressure, leading to the formation of the aforementioned products. Clearly evident are pressure effects manifested in the yields of methyl succinic acid and within the amphiphilic suite of compounds.

The system citric acid in CO_2 - H_2 bearing aqueous fluids is equally interesting. As would be expected, the principal reactions involve mono, double, and triple decarboxylations; with and without dehydration, as well as hydrogenation (Figure 3). The product distributions exhibit strong temperature and pressure selectivity (Figure 4). In general the citric system under the range of conditions explored exhibits catabolic chemistry. This is due, principally the apparent irreversibility of acid catalyzed decarboxylations. Surprisingly, pressure enhances the kinetics of these reactions, thus greatly accelerates the catabolic evolution of the system. The citric acid system, does however, serve as a useful and relatively simple system to explore the role of pressure in essentially pure ionic aqueous organic chemistry.

Acknowledgements

Support from NASA is gratefully acknowledged.

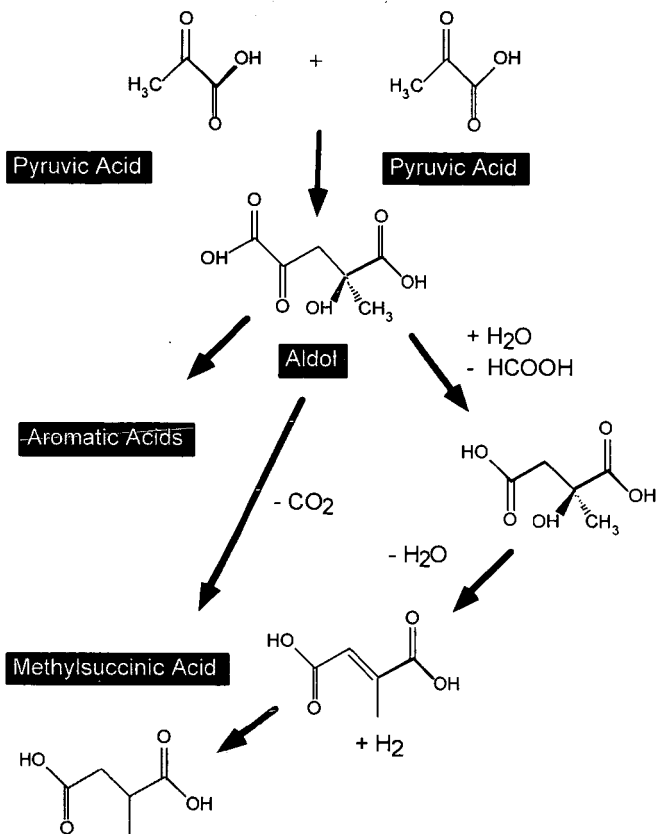


Figure 1: Reaction pathway through which pyruvic acid forms methyl succinic acid. The lack of observation of any of the intermediates suggests a concerted reaction.

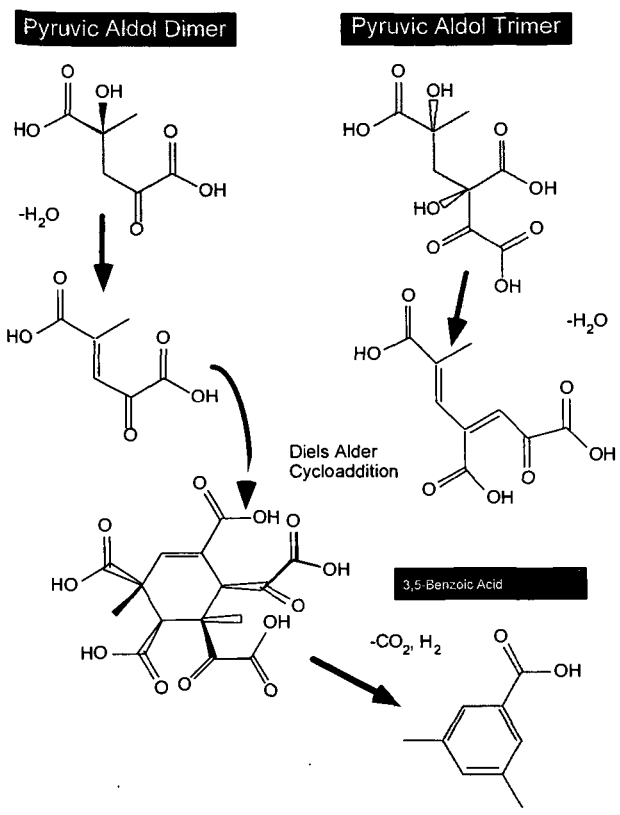


Figure 2: An example of one of many anabolic reactions exploited by pyruvic acid at elevated pressures and temperatures.

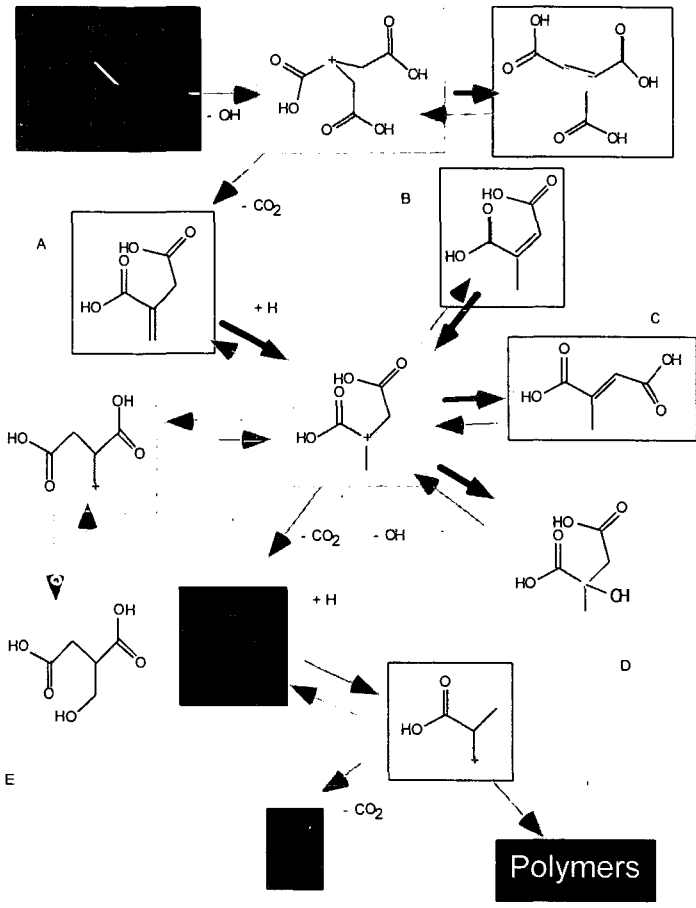


Figure 3: A schematic of the reaction network operational in the system citric acid + water at elevated temperatures and pressures.

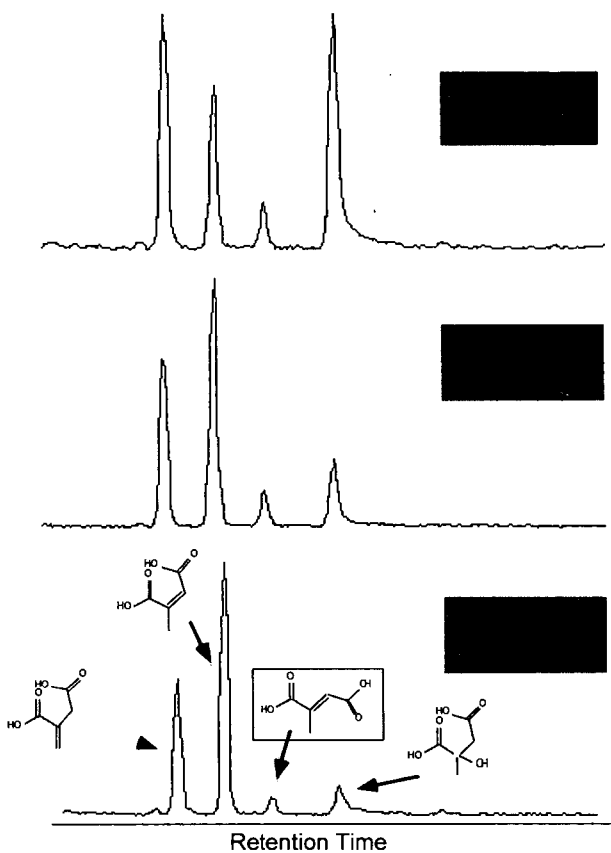


Figure 4: An example of the effect of pressure on displacing the isomeric equilibria within the system citric acid + water. Not surprisingly pressure greatly favors hydrated species.

REACTIONS OF MODEL COMPOUNDS OF PHENOL RESIN IN SUB- AND SUPER-CRITICAL WATER

H. Tagaya, K. Katoh, M. Karasu, J. Kadokawa and K. Chiba
Department of Materials Science and Engineering, Yamagata University
4-3-16 Jonan, Yonezawa, Yamagata, 992-8510 Japan

Key words: Supercritical Water, Chemical Recycling of Polymer, Phenol Resin

INTRODUCTION

The critical temperature and pressure of water at supercritical conditions are 647.2K and 22.1 MPa, respectively. The dielectric constant, ion product, and viscosity of the water at the critical point are 6, 10⁻¹²(Kw:(mol)²), and 0.002, respectively. Under supercritical conditions, water, organic compounds and gases are completely miscible. Furthermore, it is pointed out that the supercritical water is emerging as a medium which could provide the optimum conditions for a variety of chemical reactions among them the destruction of hazardous waste.

In recent years, the amounts of waste plastics increase and it becomes a serious problem because of lack of landfill field. The chemical recycling of waste plastics into their monomers has been gaining greater attention as a means of obtaining valuable products from waste plastics. The plastics are classified into thermoplastic resin and thermosetting resin. In the case of thermoplastic resin such as polyesters and polyamide, chemical recycling process has been reported. However, chemical recycling process for thermosetting resin wastes such as phenol resin waste has not been yet reported. Recently, we have communicated our findings on chemical recycling process for thermosetting resin wastes such as phenol resin waste (1-3). We have been studying on decomposition of polymeric compounds such as cellulose in water at supercritical conditions. In this study to obtain information of the role of water on chemical reaction of phenol resin waste, we have tried the decomposition reaction of model compounds of phenol resin such as p- and o-bis(hydroxyphenyl)methane, and various prepolymers.

EXPERIMENTAL

Decomposition reaction in water was carried out in 10 ml tubing bomb reactor. The reactants such as p- and o-bis(hydroxyphenyl)methanes were commercially available in a purity of 98% or higher and were used without further purification. 0.1g of model compound and 1 - 4 ml of water were introduced in the reactor. The reaction temperatures were 523 to 703K and reaction times were 0.25 to 1h. Reaction products were extracted by ether. The organic phase was concentrated using an evaporator. It was dissolved with organic solvent after adding a standard. The reaction products were identified by GC/MS and quantified by GC with a flame ionization detector (FID). In the case of GC/MS, the oven temperature was held at 333K for 3 min at initial stage. After then the oven temperature increased from 333K to 493K at a rate of 10K/min. The final temperature was maintained for an additional 6 min. In the case of GC the oven initial temperature was 403K and the oven temperature increased 503K at a rate of 10 K/min. The final temperature was maintained for an additional 6 min. Basic compound such as NH₄OH, NaOH, KOH, Na₂CO₃ was added.

RESULTS AND DISCUSSION

Decomposition reaction of model compounds in supercritical water

It is well known that thermal cleavage of methylene bond is not easy. However, we have found that methylene bond was cleaved in the reaction of phenol resin model compound with supercritical water. In the reaction of p-bis(hydroxyphenyl)methane, it was decomposed to their monomers such as phenol, p-cresol, o-cresol and 2,4-dimethylphenol. To obtain information on the reaction mechanism of decomposition reaction in water, p-bis(hydroxyphenyl)methane (compound 1), o-bis(hydroxyphenyl)methane (compound 2), diphenylmethane (compound 3), di-p-tolylmethane (compound 4), dibenzyl (compound 5) were reacted at 573 to 703K for 1h. However, model compounds 3, 4 and 5 were scarcely decomposed even by the reaction at 703K for 1 h. Compounds 1 and 2 easily decomposed in the reaction with supercritical water. It was considered that the presence of hydroxyl groups was essential for the decomposition reaction. We have tried to add phenol in the reaction of compound 3, however, no acceleration of decomposition reaction was observed. It indicates that the reactant

itself should possess hydroxyl groups. Model compound 1 decomposed into monomers such as phenol, p-cresol, o-cresol, and 2,4-dimethylphenol at 703K. Also, we have confirmed the productions of benzaldehyde and p-dihydroxybenzene by the reaction at 573K for 0.25h, although the yields of them were small. They were unstable at high temperature and the presence of them were not confirmed by the reactions at over 623K. The results suggested the direct participation of water as a reactant in the decomposition. Model compound 2 decomposed into their monomers such as phenol, p-cresol, o-cresol and so on. The production of xanthene was also confirmed. Phenol and cresol were main products. Xanthene was undesirable dehydrated product of compound 2. Even in the neat reaction at 703K for 0.25h, the yield of xanthene reached 20.2% although the yield of phenol was only 7.4%. Although conversion of compounds 1 and 2 reached more than 70% at 703K for 1h, the yield of identified products was less than 50%, indicating the presence of unidentified products. We confirmed the presence of trimer of phenol by the GC/MS analysis of water soluble products although we could not quantify. It indicated the presence of condensation reactions.

The effect of hydrogen donor, tetralin on the decomposition reaction

If the decomposition reaction proceeded via radical intermediates, the addition of hydrogen donor should be effective to avoid the condensation reaction. Therefore, hydrogen donor, tetrahydronaphthalene(tetralin), was added to the reaction of compounds 1 and 2 with water. The addition of tetralin for the decomposition reaction of compound 2 was effective. Although the yields of phenol and xanthene were 10.3% and 18.4% at 703K for 0.5h, they became 32.9% and 2.0% by the addition of tetralin. Xanthene was stable in supercritical water.

The addition of tetralin was effective to prevent the production of xanthene. However, the addition of tetralin was not effective for the decomposition reaction of compound 1. Position of hydroxyl groups was important for the decomposition reaction.

The effect of the addition of acid and alkali salt

The addition of hydrogen donor was not effective for the decomposition reaction of compound 1 indicating that radical reaction was not so important. If the ionic decomposition reactions occurred, the addition of acid or alkali salts might be effective to avoid the condensation reaction. The addition of acid was not effective for the reaction of compounds 1 and 2. However, the addition of alkali salts was effective and the yields of reaction products increased on the reactions of compounds 1 and 2. The addition of Na_2CO_3 or NaHCO_3 was more effective than the addition of NH_4OH , NaOH , KOH or K_2CO_3 . In the case of the compound 2, the yields reached more than 60% at 703K for 0.5h and yield of xanthene decreased by the addition of Na_2CO_3 . These results indicated that the reaction proceeded via the ionic processes. It was considered that both ionic radical reactions occurred in the decomposition reaction of compound 2. Even by the addition of small amounts of Na_2CO_3 or NaHCO_3 , a total yield of phenol and cresol reached 50% at 673K for 0.25h when additive/model compound ratio was 0.02. For the yields of phenol in the decomposition reactions, 0.1% was the best among these concentrations.

The effect of the addition of NaCl

To obtain information on the mechanism of the effects of alkali salt addition, neutral salt, NaCl was added. The yield of phenol in the reaction of compound 1 increased from 7.0% to 11.0% at 703K for 0.25h by the addition of NaCl. It is well known that the addition of NaCl increased the density of water at near supercritical region. The increment of the yield was not large. It indicates that the role of Na_2CO_3 was not only to increase water density.

The effect of water density

Decomposition reactions were carried out by varying the injection amounts of water from 1 ml, 2 ml to 4 ml. A yield of products increased for the decomposition reactions of compounds 1 and 2 and yield of xanthene decreased with an increase of injection amounts of water. In the reaction in 4 ml of water, a yield of products also increased by the addition of Na_2CO_3 although the increment of the yield by the addition was small. The large effect of water on the decomposition reaction indicated that the density was important factor for the decomposition of compounds 1 and 2 in these reaction conditions.

Decomposition reaction of prepolymer of phenol resin

Seven prepolymers whose molecular weights were 247-923 were reacted with supercritical water at 703K for 0.5h. Prepolymers were kindly provided by Dainippon Ink & Chemicals Co., Ltd, and their exact compositions were unknown. Main decomposition products from prepolymers A and C were phenol and p-isopropylphenol. It indicated that prepolymers A and C were isopropylphenol resins. Also the main decomposition products from prepolymers F and G were o-cresol, p-cresol and 2,4-dimethylphenol. It indicated that they were cresol resins.

Based on the model compound studies, decomposition reactions of prepolymers were carried out by adding 1wt% Na₂CO₃ for prepolymer. The yields fairly increased in the case of isopropylphenol resins, prepolymers A and C, and yields of phenol reached 48.9% and 58.0%. The total yields of identified products reached more than 90%. Certainly, reactivities of prepolymers were larger than those of compounds 1 and 2.

Conclusions

In this study we have clarified that water is excellent solvent for the decomposition reaction of phenol resin containing methylene bridges. The addition of tetralin was effective for the decomposition reaction of bis(o-hydroxyphenyl)methane. The yields of products increased and yield of xanthene decreased by the addition of tetralin. The addition of alkali salts was effective for the decomposition reactions of bis(p-hydroxyphenyl)methane and bis(o-hydroxyphenyl)methane. The significant increment of the yield was observed by the addition. It was suggested that the density was important factor for the decomposition of phenol resin model compounds such as bis(o-hydroxyphenyl)methane and bis(p-hydroxyphenyl)methane in these reaction conditions. Acceleration mechanism of alkali salts addition for the reaction was not clear, however, effective decomposition of model compounds and prepolymers of phenol resin was attained by the reaction with supercritical water, especially in the conditions adding alkali salt.

REFERENCES

1. H. Tagaya, Y. Suzuki, J. Kadokawa, M. Karasu, K. Chiba, Chem. Lett., 1997, 47.
2. H. Tagaya, Y. Suzuki, T. Asou, J. Kadokawa, K. Chiba, Chem. Lett., 1998, 937.
3. H. Tagaya, K. Katoh, J. Kadokawa, K. Chiba, Polym. Degra. Stab., in press.

EXPERIMENTAL INVESTIGATION OF ORGANIC COMPOUND STABILITY UNDER HYDROTHERMAL CONDITIONS

Mitchell D. Schulte

NASA Ames Research Center
Mail Stop 239-4
Moffett Field, CA 94035

Keywords: hydrothermal, organic compounds, experimental

ABSTRACT

Hydrothermal systems are the most likely locations on the early Earth for the emergence of life due to the abundant chemical energy inherent in the characteristic disequilibrium of these environments. Hydrothermal conditions are theoretically favorable for the formation and stability of organic compounds; we are investigating this hypothesis experimentally. Initial experiments with amino acids at 250°C and 250-350 bars have yielded ammonia, carbon dioxide and carboxylic acids as the main reaction products. While the amino acids decomposed rapidly, the ratios of the products remained constant during the course of the experiments, in agreement with field and experimental observations of other metastable organic states, as well as with calculated organic compound metastability. Further experiments are currently underway and the results will be presented.

INTRODUCTION

Hydrothermal systems are the most likely locations on the early Earth for the emergence of life (1-3). Because of the disequilibrium inherent in such dynamic, mixing environments, abundant chemical energy would have been available for formation of the building blocks of life. In addition, theoretical and experimental studies suggest that organic compounds in these conditions would reach metastable states, due to kinetic barriers to the formation of stable equilibrium products CO₂ and methane (4-7). The speciation of organic carbon in metastable states is highly dependent on the oxidation state, pH, temperature, pressure and bulk composition of the system. The goal of our research is to investigate experimentally the effects of a number external variables on the formation, transformation, and stability of organic compounds at hydrothermal conditions. We have begun work to attempt to control the oxidation state of simulated hydrothermal systems by using buffers composed of mineral powders and gas mixtures. We are also beginning to test the stability of organic compounds under these conditions. The experiments are being performed using a hydrothermal bomb apparatus at the U.S. Geological Survey in Menlo Park, CA (Figure 1) and a supercritical water oxidizer (SCWO; Figure 2) at NASA Ames Research Center in Moffett Field, CA.

EXPERIMENTAL

Initial experiments have been performed using the hydrothermal bomb set-up to test amino acid stability at 250°C and 250-350 bars. In order to attempt to control the oxidation state inside the experimental cells, we added mineral powders to sample cells, along with distilled, deionized water. Two different mineral assemblages were used in two different experiments; pyrite-pyrrhotite-magnetite (PPM) and iron-iron oxide (FeFeO). The cells were then sealed, heated, and pressurized. The bomb assemblies were rocked to ensure continual contact between the solution and fresh mineral surfaces, and the buffers were allowed to equilibrate over a period of weeks. Amino acids were then added to the reaction vessels, and the system was sampled at regular intervals.

The set-up available at NASA Ames Research Center for this work consists of a supercritical water oxidizer, or SCWO, previously used to oxidize waste organic matter to CO₂ and H₂O. Work is currently underway to restore the SCWO to operational status. A schematic diagram of the SCWO is shown in Figure 2.

Because the SCWO is a flow-through apparatus, we can simulate the dynamic mixing environment characteristic of hydrothermal systems. Solutions of differing compositions and temperatures can be combined to investigate the potential for organic compound synthesis or stability. The oxidation state will be controlled using gas mixtures, allowing evaluation of the catalytic effect of minerals which will be added to the reaction vessel.

PRELIMINARY RESULTS

In the experiments conducted using the hydrothermal bombs, the amino acids decomposed rapidly, but yielded ammonia, carbon dioxide and carboxylic acids as the main reaction products. The ratios of the products remained constant during the course of the experiments, in agreement with field and experimental observations of other metastable organic states^{4,6}, as well as with calculated organic compound metastability. Further experiments of this type are currently underway and the results will be presented, along with some preliminary results from our initial SCWO experiments.

ACKNOWLEDGMENTS

I would like to thank Sherwood Chang, James Bischoff, Robert Rosenbauer, Dahlia Chazan, Jennifer Blank and Kathy Cummins for their help with the U.S.G.S. experiments, and Maher Tliemat, Suresh Pisharody, John Fisher and Sherwood Chang for their efforts in setting up the SCWO at NASA Ames. Cindy Lerner and Sandra Pizzarello were instrumental in helping me obtain GC-MS analyses of amino acids. Thanks to George Cody and Mike Lewan for inviting me to contribute to this symposium.

REFERENCES

- (1) Baross, J. A.; Hoffman, S. E. *Orig. Life and Evol. Biosphere*. 1985, 15, 327- 345.
- (2) Corliss, J. B.; Baross, J. A.; Hoffman, S. E. *Oceanologica Acta*. 1981, No. Sp, 59- 69.
- (3) Holm, N. G. *Orig. Life and Evol. Biosphere*. 1992, 22, 5-14.
- (4) Shock, E. L. *Geology*. 1988, 16, 886-890.
- (5) Shock, E. L. *Orig. Life and Evol. Biosphere*. 1992, 22, 67-107.
- (6) Seewald, J. S. *Nature*. 1994, 370, 285-287.
- (7) Shock, E. L.; Schulte, M. D. *J. Geophys. Res.* 1998, in press.

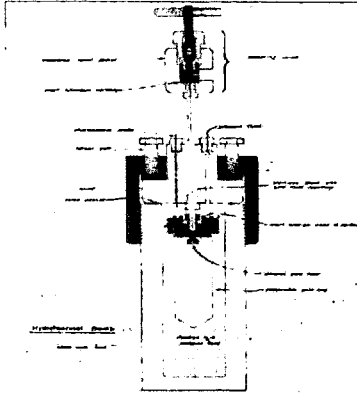


Figure 1. Schematic diagram of the hydrothermal bomb apparatus used for organic compound stability experiments.

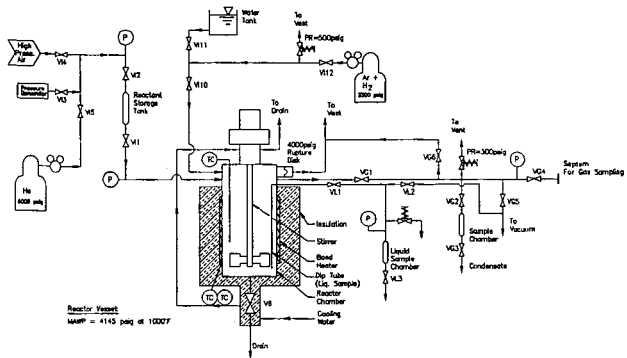


Figure 2. Schematic diagram of the supercritical water oxidizer (SCWO) used for organic compound stability experiments.

THE ROLE OF WATER DURING DECOMPOSITION OF OIL AT ELEVATED TEMPERATURES: CONSTRAINTS FROM REDOX BUFFERED LABORATORY EXPERIMENTS

Jeffrey S. Seewald¹ and Peter J. Saccocia²

¹Woods Hole Oceanographic Institution, MS#4, Woods Hole, MA 02543

²Bridgewater State College, Bridgewater, MA 02325

Keywords: Petroleum Geochemistry, Natural Gas, Hydrous Pyrolysis

INTRODUCTION

Oil and natural gas coexist with water and minerals in sedimentary basins. There is increasing evidence that inorganic chemical processes play a critical role in regulating organic reactions responsible for the generation of oil and its decomposition to form natural gas. In particular, water has been implicated as both a solvent and reactant during organic reactions at elevated temperatures and pressures (1,2,3). Moreover, the redox state of subsurface environments and the presence or absence of catalytically active transition metals may influence the absolute amounts and relative distribution of organic alteration products (2,4,5). Understanding the extent to which such processes affect the stability of petroleum at elevated temperatures is essential to predict the timing and location of natural gas formation.

The present study was undertaken to examine the stability of oil in the presence of water at elevated temperatures and pressures. Hydrous pyrolysis experiments have proven to be an effective tool for examining organic-inorganic interactions during oil and natural gas generation. Experimental apparatus utilized during conventional hydrous pyrolysis, however, results in the coexistence of source rocks, liquid water, floating oil, and volatile species occupying the pressure vessel head space at experimental conditions (6). As a result it is not always possible to distinguish whether secondary reactions involve gaseous, aqueous, or oil phase species. The experiments presented here were designed to minimize such uncertainties and allow a comparison of reactions involving oil dissolved in water with reactions taking place within a separate oil phase. Because organic reactions are influenced by their chemical environment, we used naturally occurring mineral assemblages to regulate key chemical variables such as redox, sulfur fugacity, and pH.

EXPERIMENTAL

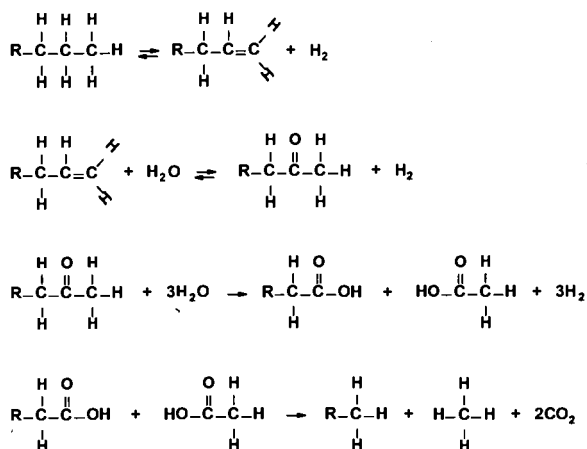
Two experiments examining the decomposition of a medium weight oil from Eugene Island block 330 in the U.S. Gulf Coast were conducted in a flexible-cell hydrothermal apparatus (7) consisting of a flexible gold and titanium reaction cell contained within a stainless steel pressure vessel. This equipment allows external control of pressure at sufficiently high values to preclude the formation of a vapor filled head space during an experiment. A titanium sampling tube connected to the reaction cell allows reaction progress to be monitored as a function of time by periodic extraction of fluid samples. Experiment PPM-AQ was conducted at 350°C and 350 bars and contained 37.2 g an aqueous Na-Mg-Cl solution and 52.9 mg of oil. The relatively small amount of oil in this experiment did not exceed the aqueous solubility of oil at 350°C and 350 bars (8) ensuring all reactions involved aqueous species. In contrast, experiment PPM-OIL was designed to maintain a separate oil phase floating on top of liquid water at experimental conditions. This experiment initially contained 13.3 g of aqueous Na-Mg-Cl solution and 10.7 g of oil. To allow sampling of both the oil and water the flexible-cell hydrothermal apparatus was modified to include two titanium sampling lines at opposite ends of the tubular reaction cell. By orienting the apparatus vertically, the aqueous phase could be sampled through the lower sampling line while the oil was sampled through the upper sampling line. Experiment PPM-OIL was initially conducted at 325°C and 350 bars but after 1130 h of heating the temperature was increased to 350°C.

To regulate redox and sulfur fugacity during the experiments a mineral assemblage containing equal amounts of pyrite, pyrrhotite, and magnetite were added to each experiment. In addition, brucite and amorphous silica were added to PPM-AQ and brucite was added to PPM-OIL to regulate *in situ* pH. Because the densities of the added minerals are greater than water and oil, the minerals resided within the aqueous phase at the bottom of the reaction cell during experiment PPM-OIL. Fluid samples were removed from the experiments at selected times and analyzed for the concentrations of CO₂, H₂, H₂S, inorganic anions and cations, and numerous organic species including C₁-C₆ hydrocarbons, alcohols, aldehydes, ketones, organic acids, and phenols.

RESULTS AND DISCUSSION

Heating of oil in the presence of water and inorganic minerals during both experiments resulted in extensive alteration of the oil and the generation of low molecular weight carbon compounds. In general, generation of dissolved gaseous products proceeded at a faster rate during PPM-AQ relative to PPM-OIL (Fig. 1) and produced dissolved gas containing a substantially higher proportion of CO₂ (Fig. 2). Examination of the dissolved gaseous hydrocarbon fraction reveals a significant enrichment in CH₄ during PPM-AQ relative to PPM-OIL (Fig. 3). Dissolved H₂ concentrations during PPM-AQ were consistent with values predicted for thermodynamic equilibrium between water and the pyrite-pyrrhotite-magnetite mineral assemblage. In contrast, measured H₂ concentrations in the aqueous phase of experiment PPM-OIL were higher than those predicted for equilibrium with a pyrite-pyrrhotite-magnetite mineral assemblage suggesting that the rate of H₂ generating reactions involving carbon compounds in the oil exceeded the rate at which the redox buffer consumed H₂. The higher H₂ concentrations during PPM-OIL in comparison to PPM-AQ indicate redox conditions were considerably more reducing during the PPM-OIL experiment.

Maturation of oil during experiment PPM-AQ also resulted in the continuous generation of substantial amounts of organic acids, ketones, and lesser, but measurable, quantities of alkenes. Production of these compounds is consistent with data from redox buffered experiments examining the stability of individual aqueous hydrocarbons under redox buffered conditions (2,9,10). These experiments have demonstrated the degradation of aqueous *n*-alkanes via a stepwise oxidative processes to produce CO₂ and CH₄. This process can be represented in general as follows:



Reactions in the above scheme that do not involve breaking of C-C bonds are reversible in aqueous solution and may approach a state of redox dependent metastable thermodynamic equilibrium (2,9,10). Under sufficiently reducing conditions the abundance of reaction intermediates decreases, resulting in an overall decrease in the rate of *n*-alkane decomposition. Accordingly, during experiment PPM-OIL, high H₂ produced relatively reducing redox conditions and lower amounts of CO₂ and CH₄ were generated. In the absence of extensive oxidative decomposition during experiment PPM-OIL, it is likely that decomposition of hydrocarbons residing in the oil phase occurred predominantly via thermal cracking to produce a relatively CH₄- and CO₂- poor gas.

The formation of natural gas is conventionally viewed as a two-step process in which kerogen maturation initially produces both oil and gas. Continued heating over geologic time and increasing temperatures associated with progressive burial subsequently results in the decomposition of generated oil to form natural gas. As discussed by Mango *et al.* (5), a purely thermal model for the cracking of *n*-alkanes cannot account for the generation of dry gas at geologically reasonable heating rates. The stepwise oxidation of aqueous *n*-alkanes, however, may represent an alternative mechanism to generate a CH₄-rich gas at relatively low thermal stress. For such a mechanism to be active in natural systems, however, suitable oxidizing agents are required. Likely candidates include sulfate minerals present in evaporites and commonly occurring sedimentary components containing ferric iron, such as pyrite, magnetite, hematite, and a variety of aluminosilicates. In addition to providing a mechanism for the generation of dry-gas at thermal maturities lower than those required for thermal cracking, the absence of a suitable oxidizing agent and/or water could preclude stepwise

oxidation and account for the persistence of oil in a variety of environments at temperatures higher than conventional models predict (11). The results presented here emphasize the fact that time and temperature are not the only variables influencing the stability of petroleum in sedimentary basins.

REFERENCES

- (1) Siskin, M. and Katritzky, A. R., *Science* **254**, 231 (1991).
- (2) Seewald, J. S., *Nature* **370**, 285 (1994).
- (3) Lewan, M. D., *Geochim. Cosmochim. Acta* **61**, 3691 (1997).
- (4) Helgeson, H. C., Knox, A. M., Owens, C. E., and Shock, E. L., *Geochim. Cosmochim. Acta* **57**, 3295 (1993).
- (5) Mango, F. D., Hightower, J. W., and James, A.T., *Nature* **368**, 536 (1994).
- (6) Lewan, M. D., in: *Organic Geochemistry* (eds. M. H. Engel and S. A. Macko.), 419 (1993), Plenum.
- (7) Seyfried, W. E. Jr., Janecky D. R., and Berndt M. E., in: *Experimental Hydrothermal Techniques* (eds. G. C. Ulmer and H. L. Barnes), 216 (1987), John Wiley and Sons.
- (8) Price, L. C., *J. Petrol. Geol.* **4**(2), 195 (1981).
- (9) Seewald, J. S., *Mat. Res. Soc. Symp. Proc.* **432**, 317 (1996).
- (10) Seewald, J. S., unpublished data.
- (11) Price, L. C., *Geochim. Cosmochim. Acta* **57**, 3261 (1993).

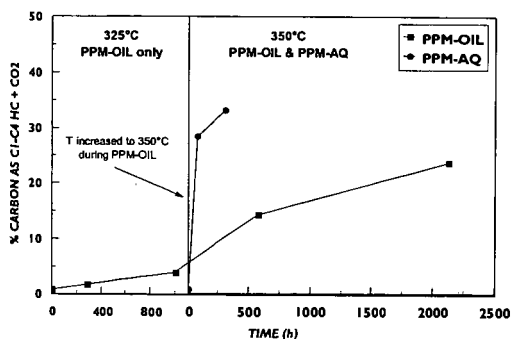


Figure 1. Variations in the percentage of carbon in the total oil as C₁-C₄ hydrocarbons and CO₂ with time during experiments PPM-OIL and PPM-AQ. Note that only experiment PPM-OIL was initially conducted at 325°C.

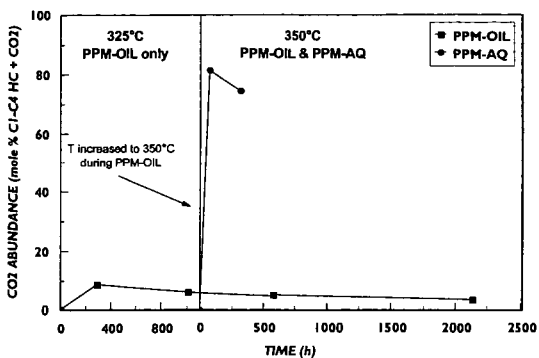


Figure 2. Variations in the relative abundance of CO₂ in the dissolved gas fraction (mole % of C₁-C₄ hydrocarbons and CO₂) as a function of time during experiments PPM-OIL and PPM-AQ. Note that only experiment PPM-OIL was initially conducted at 325°C.

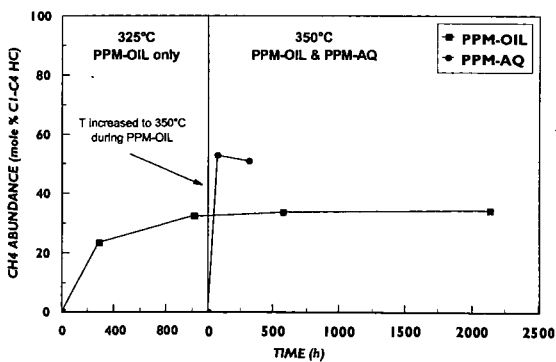


Figure 3. Variations in the relative abundance of CH₄ in the dissolved hydrocarbon gas fraction (mole % of C₁-C₄ hydrocarbons) as a function of time during experiments PPM-OIL and PPM-AQ. Note that only experiment PPM-OIL was initially conducted at 325°C.

RELEASE OF BIOMARKERS FROM SULFUR-RICH KEROGENS DURING HYDROUS PYROLYSIS

Martin P. Koopmans^{1,3}, Jaap S. Sinninghe Damsté¹ and Michael D. Lewan²

¹Netherlands Institute for Sea Research, Department of Marine Biogeochemistry and Toxicology, P.O. Box 59, 1790 AB Den Burg, Netherlands

²U.S. Geological Survey, Box 25046, MS 977, Denver Federal Center, Denver, CO 80225, USA

³Present address: (i) University of Oslo, Department of Geology, P.O. Box 1047 Blindern, 0316 Oslo, Norway, and (ii) Saga Petroleum ASA, P.O. Box 490, 1301 Sandvika, Norway

Keywords: hydrous pyrolysis, generation of biomarkers, S-rich kerogen

INTRODUCTION

Hydrous pyrolysis is an established laboratory technique for the simulation of the natural maturation of kerogen. There has been some debate in the literature whether water plays a purely physical or maybe a chemical role during hydrous pyrolysis (*e.g.* Monthieux *et al.*, 1986; Lewan, 1992). This issue has recently been reviewed by Lewan (1997). Mass balance calculations have shown that CO₂ generated during hydrous pyrolysis derives O from the water added before the experiment (Lewan, 1992). Hydrothermal experiments with ethane and ethene showed that water was a source of H₂ (Seewald, 1994). In addition, experiments with kerogen and heavy water suggested that the deuterated alkanes generated were formed by reaction of alkyl radicals with heavy water-derived D (Hoering, 1984). Thus, the current understanding is that water acts as a source of H to quench thermally generated alkyl radicals, thereby both forming saturated hydrocarbons and inhibiting cross-linking reactions which may lead to the formation of an insoluble pyrobitumen.

The thermal degradation of kerogen has been characterised as a two step process (Lewan, 1992). First, kerogen is partially decomposed to a polar-rich bitumen, which at higher temperatures decomposes to yield free hydrocarbons as thermal stress increases. This sequence was also recognised in a study of a S-rich sample from the Monterey Formation (Baskin and Peters, 1992). However, these observations were based on bulk quantities (*i.e.* kerogen, bitumen, and free hydrocarbons), and a similar sequence based on molecular data using biomarkers has not been clearly established. Here, we describe results of thermal maturation experiments designed to follow the kerogen degradation pathway at a molecular level using a biomarker approach. In addition, we have investigated the role of water by performing experiments in the absence and presence of water.

EXPERIMENTAL

Hydrous and anhydrous pyrolysis experiments (200-360°C; 72 h) were carried out with two sedimentary rocks containing immature sulfur-rich organic matter. Detailed descriptions of the experimental procedures can be found elsewhere (Koopmans *et al.*, 1996, 1998). One sample is a claystone from the Gessoso-solfifera Formation (Upper Miocene, northern Italy), with a TOC content of 2.0 wt.%. Its mineral composition consists of quartz, smectite, illite, chlorite, and dolomite. The other sample is a limestone from the Ghareb Formation (Upper Cretaceous, Jordan), with a TOC content of 19.6 wt.%. Its mineral composition consists almost exclusively of calcite with only minor amounts (<10 wt.%) of quartz and apatite.

RESULTS

The extract of the claystone contains saturated hydrocarbons and organic sulfur compounds (OSC) with mainly normal and isoprenoid alkane skeletons. In addition, the extract comprises a polar fraction which contains molecular aggregates consisting of predominantly isoprenoid and cyclic alkane skeletons linked by S- and O-bonds (Koopmans *et al.*, 1996). The kerogen has been desulfurised and consists mainly of normal, isoprenoid and cyclic alkanes (Schaeffer *et al.*, 1995; Putschew *et al.*, 1998).

Hydrous pyrolysis of the claystone generates large amounts of saturated hydrocarbons and OSC from thermal degradation of the kerogen and the polar fraction (Koopmans *et al.*, 1996). We were able to follow the kerogen thermal degradation pathway at a molecular level by monitoring the speciation of several biomarkers. C₃₇ and C₃₈ alkenones, for example, were present in an S- and O-bound form in the kerogen of the unheated claystone, while their carbon skeletons were absent in the extract. After hydrous pyrolysis at gradually increasing temperatures, these carbon skeletons are first released into the polar fraction, and then as free hydrocarbons, OSC and saturated ketones (Fig. 1; Koopmans *et al.*, 1997).

In order to elucidate the role of water during hydrous pyrolysis, we also conducted experiments in the absence of water (anhydrous pyrolysis). For the claystone, the results are quite dramatic. While hydrous pyrolysis generates large amounts of normal, isoprenoid and cyclic alkanes, anhydrous pyrolysis does not generate these compounds (Fig. 2). For the limestone, normal, isoprenoid and cyclic alkanes are generated in comparable amounts during hydrous and anhydrous pyrolysis, although during anhydrous pyrolysis destruction of alkanes at high temperatures seems to occur at an earlier stage (Fig. 2). In addition, desulfurisation of the polar fraction of the claystone heated at 200°C by anhydrous pyrolysis does not release any biomarkers, in contrast to hydrous pyrolysis. This strongly suggests that anhydrous pyrolysis is not capable of converting S-bound biomarkers in the polar fraction to free biomarkers.

DISCUSSION

Our results suggest that the presence of water and the mineral matrix play an important role in the generation of biomarkers from S-rich kerogens (cf. Fig. 2). Quantitative experimental studies by Huizinga *et al.* (1987a,b) showed that mineral matrix effects on hydrocarbon generation from powdered mixtures of kerogen and minerals were more extreme under anhydrous than hydrous pyrolysis, especially when smectite was the employed mineral. In addition, they found evidence that the combined effect of smectite and a high organic S content leads to increased degradation of bitumen generated from the kerogen. Thus, the combination of smectite and a high organic S content for the claystone in our study may explain the large differences observed between the claystone and the limestone.

The actual mechanism and reactions responsible for smectite inhibiting the generation of biomarkers under anhydrous conditions and not under hydrous conditions remain to be determined. The greater availability of clay mineral interlayers to bitumen under anhydrous pyrolysis may be important, because under anhydrous pyrolysis these interlayers are probably less hydrated than under hydrous pyrolysis. Huizinga *et al.* (1987a) showed that adsorption of the polar constituents of bitumen to smectite was enhanced during anhydrous pyrolysis. For our experiments, this would imply that the polar fraction of the claystone, which contains abundant S-bound biomarkers, would be adsorbed to these clay minerals during anhydrous pyrolysis. Once inside the clay mineral interlayers, the high contact area of mineral surface to organic matter may favor cross-linking reactions that form an insoluble pyrobitumen rather than cracking reactions that form free hydrocarbons. This is supported by our desulfurisation experiments, which showed that S-bound biomarkers in the claystone were destructed during anhydrous at 200°C.

Thus, during anhydrous pyrolysis, the biomarker thermal generation sequence described above, *i.e.* (i) bound moiety in the kerogen, (ii) bound moiety in the polar fraction, (iii) free biomarker, is hindered because no biomarkers are generated from the polar fraction. This explains the differences in the amounts of S-bound biomarkers during hydrous and anhydrous pyrolysis of the claystone, and consequently also the differences in generation of free biomarkers (i) between hydrous and anhydrous pyrolysis of the claystone, and (ii) between anhydrous pyrolysis of the claystone and the limestone.

CONCLUSIONS

Our experiments show that the thermal degradation of kerogen to bitumen to free biomarkers can be monitored on a molecular level. Water is essential in releasing biomarkers from S-rich kerogens, especially when clay minerals are present. The exact chemical role that water plays, however, remains to be determined.

ACKNOWLEDGEMENTS

The Natural Resources Authority of Jordan is gratefully acknowledged for their assistance in helping the authors collect a sample of the Ghareb Formation from the El Lajjun quarry. Analytical assistance was provided by F. Carson, M. Dekker, W.I.C. Rijpstra and Dr W.G. Pool.

REFERENCES

- Baskin, D.K. and Peters, K.E., 1992, Early generation characteristics of a sulfur-rich Monterey kerogen: AAPG Bulletin, v. 76, pp. 1-13.
- Hoering, T.C., 1984, Thermal reactions of kerogen with added water, heavy water and pure organic substances: Organic Geochemistry, v. 5, pp. 267-278.
- Huizinga, B.J., Tannenbaum, E. and Kaplan, I.R., 1987a, The role of minerals in the thermal alteration of organic matter - III. Generation of bitumen in laboratory experiments: Organic Geochemistry, v. 11, pp. 591-604.

- Huizinga, B.J., Tannenbaum, E. and Kaplan, I.R., 1987b, The role of minerals in the thermal alteration of organic matter - IV. Generation of *n*-alkanes, acyclic isoprenoids, and alkenes in laboratory experiments: *Geochimica et Cosmochimica Acta*, v. 51, pp. 1083-1097.
- Koopmans, M.P., de Leeuw, J.W., Lewan, M.D. and Sinninghe Damsté, J.S., 1996, Impact of dia- and catagenesis on sulphur and oxygen sequestration of biomarkers as revealed by artificial maturation of an immature sedimentary rock: *Organic Geochemistry*, v. 25, pp. 391-426.
- Koopmans, M.P., Schaeffer-Reiss, C., de Leeuw, J.W., Lewan, M.D., Maxwell, J.R., Schaeffer, P. and Sinninghe Damsté, J.S., 1997, Sulphur and oxygen sequestration of *n*-C₃₇ and *n*-C₃₈ unsaturated ketones in an immature kerogen and the release of their carbon skeletons during early stages of thermal maturation: *Geochimica et Cosmochimica Acta*, v. 61, pp. 2397-2408.
- Koopmans, M.P., Rijpstra, W.I.C., de Leeuw, J.W., Lewan, M.D. and Sinninghe Damsté, J.S., 1998, Artificial maturation of an immature sulphur- and organic matter-rich limestone from the Ghareb Formation, Jordan: *Organic Geochemistry*, v. 28, pp. 503-521.
- Lewan, M. D., 1992, Water as a source of hydrogen and oxygen in petroleum formation by hydrous pyrolysis: *ACS, Div. Fuel Chemistry Preprints*, v. 37, No. 4, pp. 1643-1649.
- Lewan, M.D., 1997, Experiments on the role of water in petroleum formation: *Geochimica et Cosmochimica Acta*, v. 61, pp. 3691-3723.
- Monthieux, M., Landais, P. and Durand, B., 1986, Comparison between extracts from natural and artificial maturation series of Mahakam delta coals: in Leythaeuser, D. and Rullkötter J., eds., *Advances in Organic Geochemistry 1985*; *Organic Geochemistry*, v. 10, pp. 299-311.
- Putschew, A., Schaeffer-Reiss, C., Schaeffer, P., Koopmans, M.P., de Leeuw, J.W., Lewan, M.D., Sinninghe Damsté, J.S. and Maxwell, J.R., 1998, Abundance and distribution of sulfur- and oxygen-bound components in a sulfur-rich kerogen during simulated maturation by hydrous pyrolysis: *Organic Geochemistry*, in press.
- Schaeffer, P., Harrison, W.N., Keely, B.J. and Maxwell, J.R., 1995, Product distributions from chemical degradation of kerogens from a marl from a Miocene evaporitic sequence (Vena del Gesso, N. Italy): *Organic Geochemistry*, v. 23, pp. 541-554.
- Seewald, J.S., 1994, Evidence for metastable equilibrium between hydrocarbons under hydrothermal conditions: *Nature*, v. 370, pp. 285-287.

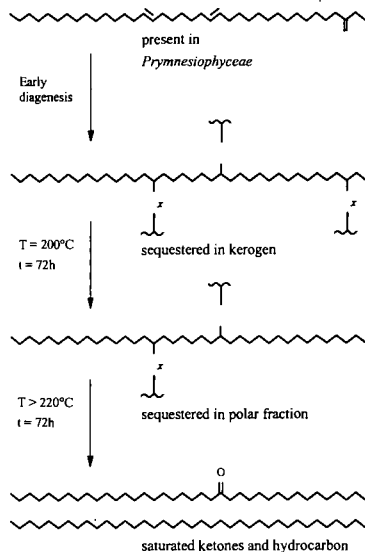


Fig. 1. Biomarker thermal generation sequence for C₃₈ alkenone.

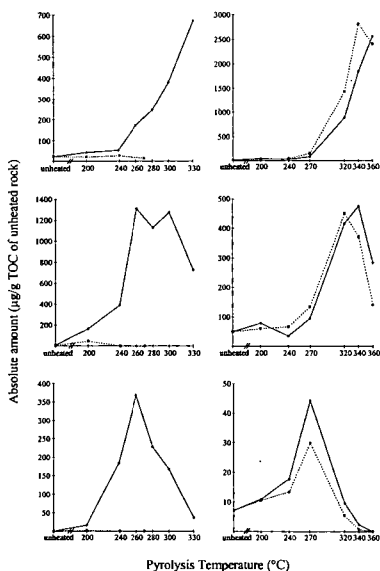


Fig. 2. Generation profiles of (a) octadecane, (b) phytane and (c) (20R)-5 α -24-ethylcholestane for the claystone and (d-f) limestone from hydrous (solid line) and anhydrous pyrolysis (stippled line) for 72 h. Anhydrous pyrolysis of the claystone does not generate biomarkers.

INVESTIGATING THE CONSTITUTION OF MACROMOLECULAR MATERIAL IN METEORITES USING HYDROUS PYROLYSIS

M. A. Sephton, C. T. Pillinger and I. Gilmour

Planetary Sciences Research Institute, Open University, Milton Keynes, MK7 6AA, UK
(m.a.sephton@open.ac.uk)

ABSTRACT

Carbon content analyses of hydrous pyrolysis residues of macromolecular material from the Murchison meteorite reveal that more than 55 % of macromolecular carbon is solubilised by this pyrolysis method. GC-MS analyses indicate that the majority of products are volatile one or two ring aromatic compounds.

Pyrolysis-GC-MS analyses of hydrous and anhydrous pyrolysis residues reveal that the macromolecular material contains a nitrogen-containing moiety. This organic entity is liberated by hydrous pyrolysis. It follows therefore that nitrogen-containing moieties may have been released from the macromolecular material during the aqueous alteration event known to have affected the Murchison meteorite parent body.

INTRODUCTION

Most meteorites are fragments of asteroids propelled into Earth-crossing orbits by relatively recent collisions in the asteroid belt (1). Asteroids, and therefore the meteorites derived from them, have escaped the extensive geological processing experienced on the planets. Due to this quiescent history meteorites contain primitive materials relatively unchanged since their formation of the solar system. The carbonaceous chondrites are especially primitive meteorites and excepting the most volatile elements, have a bulk composition similar to the Sun (2). These meteorites are particularly interesting to the organic cosmochemist as they contain up to several percent carbon which is present as organic matter.

Approximately 25 % of this organic matter is present as solvent-soluble or free molecules while the remaining 75 % is present as a solvent-insoluble macromolecular material (3). The soluble organic matter has been the most intensively studied of the two solubility classes and contains aliphatic hydrocarbons, aromatic hydrocarbons, amides, amines, nitrogen heterocycles, amino acids, carboxylic acids, sulphonic acids, phosphonic acids, alcohols and carbonyl compounds (3).

By comparison, the insoluble macromolecular material has been neglected. Pyrolytic release studies have revealed an empirical formula of $C_{100}H_{48}N_{1.8}O_{12}S_2$ for this organic component in the Murchison meteorite (4). It consists of condensed aromatic cores, connected by aliphatic and ether linkages and with various functional groups attached (5,6). Several techniques have been used to study the macromolecular material including infrared spectroscopy, nuclear magnetic resonance spectroscopy and pyrolysis (5,6).

Pyrolysis thermally dissociates macromolecular material in an inert atmosphere into lower molecular weight moieties. For meteorite research, most analyses of this type have utilised an on-line anhydrous pyrolysis unit directly coupled to a gas chromatograph or mass spectrometer (e.g. 5). Off-line hydrous pyrolysis requires that the heated samples are in contact with liquid water for the duration of the experiment and is used to simulate oil-generation from terrestrial rocks (7). This technique is conventionally performed on several hundred grams of sample (7,8) but has recently been scaled down to accommodate less than two grams of extraterrestrial sample (9).

As hydrous pyrolysis transforms the insoluble macromolecular material into free molecules, an obvious application of this technique is to investigate the relationships between the two organic solubility classes in meteorites. Previous authors have suggested that the free molecules in meteorites cannot be related to the macromolecular material because of the large isotopic differences between these two organic components (10). However isotopic measurements of individual free aromatic hydrocarbons and their structurally identical counterparts, released from the macromolecular material in the Murchison meteorite by hydrous pyrolysis, have revealed that they are related by an extraterrestrial degradative event (11). Whether more polar organic moieties are transferred between solubility classes in the extraterrestrial environment has not previously been established.

Here we report pyrolysis-gas chromatography-mass spectrometry (pyrolysis-GC-MS) and carbon content analyses of meteoritic macromolecular material in the Murchison meteorite both before and after hydrous pyrolysis. This information is used to further understand the yields and nature of the organic moieties liberated by the hydrous pyrolysis procedure. Furthermore, the implications of these analyses to reconstructing the extraterrestrial history of meteoritic organic matter are also considered.

EXPERIMENTAL

Hydrous pyrolysis. Full details of the hydrous pyrolysis method can be found in (9). The insoluble organic material in the Murchison meteorite was isolated by digesting the inorganic matrix with hydrofluoric (HF) and hydrochloric (HCl) acids and by removing any free organic compounds with solvent extraction (11). 136 mg of the HF/HCl residue was placed in a 1ml stainless steel insert and 0.4 ml of high purity water was added. The insert was then purged with nitrogen gas, sealed and placed into a 71 ml stainless steel high pressure reactor

(series 4740, Parr Instrument Co.) which was filled with 20 ml water. The whole arrangement was heated to 320 °C for 72 hours.

Supercritical fluid extraction. Hydrous pyrolysis products were extracted by supercritical fluid extraction (SFE). An initial static extraction with pure CO₂ (99.9995 %, 4000 psi) for 90 mins was followed by a dynamic extraction (4000 psi, 1 ml/min) for 45mins. The extract was collected in diethyl ether cooled to approximately 0 °C. These conditions produced an extract of non-polar compounds dissolved in a few 100 µl of solvent ready for immediate analysis.

Gas chromatography-mass spectrometry. Compound detection and identification was performed by gas chromatography-mass spectrometry (GC-MS) using a Hewlett Packard 5890 gas chromatograph interfaced with a 5971 mass selective detector. Analyses were by on-column injection onto a HP5 capillary column (50 m x 0.2 mm x 0.17 µm). Following a 10 min period at 25 °C the GC oven was programmed from 25 °C to 220 °C at 5 °C min⁻¹ and then from 220 to 300 °C at 10 °C min⁻¹. The final temperature was held for 12 min.

Anhydrous pyrolysis. Samples were prepared for comparisons with the pyrolysis-GC-MS analysis of the hydrous pyrolysis residue. Unheated and hydrously pyrolysed Murchison HF/HCl residue were subjected to off-line anhydrous pyrolysis. Samples were loaded into Pyrex glass tubes followed by the removal of air by purging the tube interior with N₂ gas. These tubes were then sealed and heated at 320 °C for 72 hours.

Pyrolysis-GC-MS. Samples were introduced as dry pellets (typically ca. 1 mg) into a quartz lined pyrojector (S.G.E. Ltd) held at 500 °C. Separation of the flash pyrolysis products was performed using a Hewlett Packard 5890 GC fitted with a Ultra2 capillary column (50 m x 0.2 mm x 0.32 µm). During a run, the GC oven was held at 50 °C for 1 min before a ramp was employed of 10 °C min⁻¹ to 100 °C and 5 °C min⁻¹ to 300 °C where it was held for 14 min. Detection and identification products was performed as for GC-MS.

RESULTS AND DISCUSSION

Fig. 1 shows GC-MS analyses of the hydrous pyrolysate from the Murchison HF/HCl residue. The main pyrolysis products are volatile aromatic and heteroatom-containing aromatic compounds with low molecular weights, suggesting that the majority of aromatic centres within the macromolecular material are small and consist of one or two aromatic rings. Sephton *et al.* (11) calculated a yield of 1.36 % of the high molecular weight starting material based on a solvent extract of the pyrolysate. Table 1 illustrates the carbon contents of the HF/HCl residues before and after the hydrous pyrolysis procedure. The values reveal that the amount of Murchison macromolecular carbon solubilised by hydrous pyrolysis is 55.3 %. Therefore, there is an obvious disagreement between the amount of carbon solubilised by hydrous pyrolysis and the amount of product measured by weighing a solvent extract dried under a stream of N₂. Hence, as indicated by the SFE extract, it appears that the majority of hydrous pyrolysis products from the Murchison macromolecular material are more volatile than the tricyclic PAHs. These volatile products are lost during conventional solvent extraction and evaporation steps, but are retained by SFE.

To investigate the change in the organic constitution of the macromolecular material brought about by the hydrous pyrolysis procedure, unheated Murchison HF/HCl residue and hydrous pyrolysis residue were analysed by pyrolysis-GC-MS (Fig. 2). Analyses of the hydrous pyrolysis residue indicate that some aromatic moieties do remain following the hydrous pyrolysis procedure. Although when compared to the pyrolysis-GC-MS trace for the unheated Murchison HF/HCl residue, it is apparent that much structural diversity has been lost.

To further investigate the nature of the process which liberates organic moieties from the macromolecular material during hydrous pyrolysis, pyrolysis-GC-MS analyses were performed for hydrously pyrolysed residues and samples pyrolysed anhydrously under comparable conditions. One noticeable difference between the two types of pyrolysis is the relative abundance of benzonitrile. This compound is present in small amounts in the unheated Murchison residue, is absent in the hydrously heated sample, but is abundant in the anhydrously heated sample. This suggests that the Murchison macromolecular material contains a substantial amount of organic nitrogen. The host of this organic nitrogen becomes more visible to pyrolysis-GC-MS following off-line anhydrous pyrolysis.

To confirm whether this nitrogen bearing organic component is removed by hydrous pyrolysis or simply hidden by a reaction with water, a hydrous pyrolysis residue was subjected to anhydrous pyrolysis. The residue from this process failed to produce benzonitrile during pyrolysis-GC-MS. Therefore it appears that the Murchison macromolecular material contains a nitrile precursor which is removed from the macromolecular material by hydrous pyrolysis. Nitriles in meteoritic organic matter have attracted some attention in the past due to the possibility that they may be the degradation products of amino acids, although other structures may degrade during pyrolysis to give these compounds. Possible candidates for the nitrile precursor include macromolecularly-bound amides (RCONH₂), imines (R₂CNR) and amino acids (RCH(NH₂)COOH).

Therefore, a nitrogen-containing moiety is transferred from the insoluble macromolecular material to soluble organic molecules by hydrous pyrolysis. These observations suggest that a CM macromolecule may release nitrogen-bearing organic compounds during aqueous alteration. As the Murchison macromolecule has already been subjected to pre-terrestrial aqueous alteration (12), it is reasonable to expect that communication of nitrogen containing organic matter between solubility classes occurred on the Murchison meteorite parent body. This suggestion is consistent with previous work which established that aromatic hydrocarbons have been released from the Murchison macromolecular material during a preterrestrial alteration event (11).

CONCLUSIONS

The majority of hydrous pyrolysis products of meteoritic macromolecular material are volatile, consisting of mono or diaromatic organic molecules. This suggests that meteoritic macromolecular material is comprised of one or two ring aromatic cores connected by aliphatic linkages and heteroatomic groups.

Pyrolysis-GC-MS analyses of pyrolysis residues indicate that a nitrogenous organic moiety is present in the Murchison macromolecular material. This organic unit is released by hydrous pyrolysis. Therefore it appears that some low molecular weight nitrogen-containing organic compounds in the Murchison meteorite may have been released from the macromolecular material during the aqueous alteration event that is known to have affected the Murchison parent body. This is further evidence that aqueous alteration on the meteorite parent body can exert a strong control on macromolecular material structure and can lead to interaction between organic solubility classes.

REFERENCES

- (1) G. W. Wetherill and C. R. Chapman, in *Meteorites and the Early Solar System System* (eds. J. F. Kerridge and M. S. Mathews, M.S.) 35 (Univ. Arizona Press, Tucson, 1988).
- (2) R. T. Dodd, *Meteorites: A Petrological Chemical Synthesis*. (Cambridge University Press, London, 1981).
- (3) J. R. Cronin and S. Chang, in *Chemistry of Life's Origins* (ed J. M. Greenburg) 209 (Kluwer, Dordrecht, 1993).
- (4) E. Zinner, in *Meteorites and the Early Solar System System* (eds. J. F. Kerridge and M. S. Mathews, M.S.) 956 (Univ. Arizona Press, Tucson, 1988).
- (5) R. Hayatsu, S. Matsuoka, R. G. Scott, M. H. Studier and E. Anders, *Geochim. Cosmochim. Acta*, 41, 1325 (1977).
- (6) J. R. Cronin, S. Pizzarello and J. S. Fyre, *Geochim. Cosmochim. Acta*, 51, 229 (1987).
- (7) M. D. Lewan, J. C. Winters and J. H. McDonald, *Science*, 203, 897 (1979).
- (8) M. D. Lewan, in *Organic Geochemistry: Principles and Applications* (eds. M. H. Engel and S. A. Macko) 419 (Plenum Press, New York, 1993).
- (9) M. A. Sephton, C. T. Pillinger and I. Gilmour, *Planet. Space Sci.*, in press.
- (10) R. H. Becker and S. Epstein, *Geochim. Cosmochim. Acta*, 34, 257 (1982).
- (11) M. A. Sephton, C. T. Pillinger and I. Gilmour, *Geochim. Cosmochim. Acta*, 62, 1821 (1998).
- (12) M. Zolensky, and H. Y. McSween, Jr. in *Meteorites and the Early Solar System* (eds. Kerridge J.F. and Mathews M.S.) 114 (Univ. Arizona Press, Tucson, 1988).

Table 1

% carbon of Murchison HF/HCl residue before and after hydrous pyrolysis	
Sample	Carbon (%)
Murchison HF/HCl residue	8.5
Hydrous pyrolysis residue	3.8

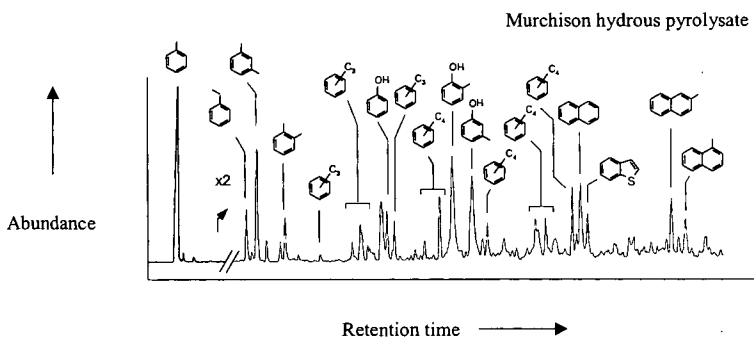


Figure 1. GC-MS analysis of the SFE extract of the hydrously pyrolysed HF/HCl residue from the Murchison meteorite. After Sephton *et al.* (1998).

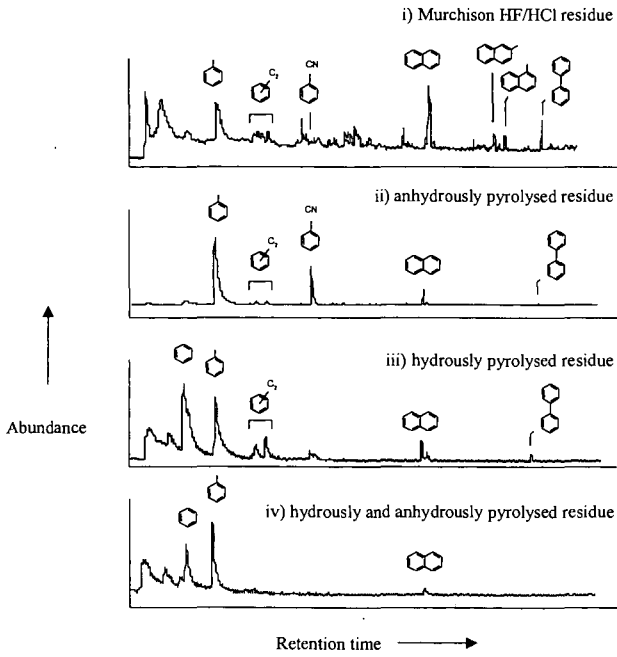


Figure 2. Pyrolysis-GC-MS analyses of i) the unheated Murchison HF/HCl residue, ii) anhydrously pyrolysed residue, iii) hydrously pyrolysed residue, and iv) hydrously and anhydrously pyrolysed residue.

EFFECT OF ACID ADDITION ON THE HYDROTHERMAL DECOMPOSITION OF CHITIN-DERIVED BIOMASS

Kinya Sakanishi¹⁾*, Nobuhide Ikeyama¹⁾, Tsuyoshi Sakaki²⁾, and Masao Shibata²⁾

1) Institute of Advanced Material Study, Kyushu University, Kasuga, Fukuoka 816-8580, JAPAN

TEL 81-92-583-7801 FAX 81-92-583-7797 E-mail: k-saka@asem.kyushu-u.ac.jp

2) Kyushu National Industrial Research Institute, Tosu, Saga 841-0052, JAPAN

ABSTRACT

Hydrothermal decomposition of chitin-derived biomass was carried out using a batch tube reactor or fixed bed flow reactor at 300 - 400 °C for 30 - 120 sec under the pressure of 15 - 30 MPa, in order to clarify the influences of solvation by pressurized water and acid addition on the hydrolysis reactivity. HPLC and TOF-MS analyses of the WS fraction indicated that the decomposition at 300 °C provided oligomer products of 3 to 6 units with a low yield of ca. 5 %. On the other hand, the higher temperature above 350 °C produced the WS fraction with the yield as high as 30 %, however, a large amount of degraded products with UV adsorption was contained in WS, suggesting the ring skeleton of the unit structure as well as the ether linkage between the unit structure should be cleaved under the sub- and supercritical conditions. The addition of acetic acid or formic acid (5 or 10 %) accelerated very much the hydrolysis reaction of chitin to oligomers at the lower temperature of 300 °C, the conversion being increased up to ca. 70 %, although the WS fraction gained its weight by the acid addition. It is pointed out that the control of pH in the acid solution and the dissociation of the aggregate structure in the chitin polymer through the solvation are keys to the enhancement of the hydrothermal decomposition of chitin.

Keywords: Hydrothermal decomposition, acidic hydrolysis, chitin biomass

INTRODUCTION

Chitin, next to cellulose, is one of the major two biomass resources on earth.¹⁻³ Chitin is a natural 1,4-linked polymer which has N-acetyl group at the C-2 position, while the cellulose has hydroxyl group at the same position of the monomer unit. Although chitin and cellulose have the similar skeleton structure, their crystal structure and polymer chain characteristics are completely different depending upon their origins.^{4,5}

Hydrothermal treatments under the sub- or supercritical conditions have been reputed to be efficient for the selective decomposition of biomass.^{6,7} The supercritical water ($T_c= 374$ °C, $P_c= 22$ MPa) accelerates the decomposition of the polymers to produce valuable monomers and clean fuel by shorter reaction times of a few seconds.^{8,9}

In a previous study,¹⁰ it was reported that chitin was much less reactive than cellulose despite their similar unit skeleton structures, probably because their functional groups at C₂ differ (-NHCOCH₃ for chitin; -OH for cellulose), and their structural analyses before and after the hydrothermal treatment indicate that their intra- and intermolecular structures through hydrogen bonds may be the keys to their different hydrothermal reactivities. It was also revealed that the decomposition of chitin under the supercritical water conditions brought about black char materials with increased gas formation, indicating that the ring cleavage of the unit structure should take place above 350 °C, and the supercritical water condition be not favorable probably due to poor solvation of chitin.

In the present study, the effect of acid addition the hydrothermal decomposition reactivity of chitin-derived biomass was examined in order to moderate the reaction conditions for the selective production of chitin oligomers. At the same time, a flow type reactor with the fixed bed of chitin was also designed for the suppression of the secondary decomposition of water soluble fraction.

EXPERIMENTAL

Chitin powder of ca. 100 μ m particle size (deacetylation extent: 38 %) was supplied by courtesy of Japan Health Summit: JHS Co., Ltd. Acetic acid, formic acid of guaranteed grade and bamboo acid solution supplied from Asia Instrument Co.(extract from the carbonized bamboo) were used as additives for the hydrothermal treatment of chitin.

The reactor used for the hydrothermal reactions was a tube reactor (SUS 316, 9.3 mm i.d. X 83 mm length, 6 mL capacity) equipped with a thermocouple, a valve, and a pressure gauge. 0.5 g of chitin and 3.0 g of distilled water were charged into the reactor, and the atmosphere in the reactor was replaced with nitrogen or carbon dioxide gas. Then, the reactor was sealed after nitrogen gas was pressurized to the prescribed initial pressure.

The reactor was heated in two steps using two salt baths which were heated at 250 °C and the prescribed reaction temperature, respectively. The reactor was preheated at 250 °C for 3 min and subsequently heated in the second bath for the prescribed time while shaking at ca. 250 times a minute. The heating rates at the preheating to 250 °C and to the reaction temperature were ca. 100 °C/min and 600 °C/min. After the prescribed soaking time, the reactor was immediately cooled in a water bath to quench the reaction. The reaction conditions were described by both the heating time in the second heater and the final temperature reached during the reaction period. In the case of hot-water flow reactor with a fixed bed, 1 g of chitin was loaded in the cylindrical bed equipped with 5 μ m ceramic filters at both ends, the atmosphere in the reactor system was replaced with N₂ gas, and pressurized to 5 MPa N₂. The preheated water at the prescribed temperature in salt bath was flowed at 10 ml/min, and the extracted fraction(WS) by pressurized hot water was continuously recovered for sampling.

The liquid and solid contents in the reactor were thoroughly washed with water and filtered using No.4 glass filter. The water in the filtrate was distilled off under vacuum, and the water soluble (WS) fraction was recovered. The filter residue was washed with methanol to recover the methanol soluble (MS) and the insoluble (MI) fractions by the removal of methanol and the drying under vacuum. WS, MS, and MI fractions were weighed and each product yield was calculated based on the dry substrate base. The target product of oligomers was fractionated into WS fraction. MS (water insoluble but methanol soluble) fraction include the larger molecular weight products and degraded products such as aromatic and color compounds which are not able to be analyzed by HPLC. MI(insoluble fraction both in water and methanol) is the mixture of the unreacted substrate and char-like residue. Such characteristics were previously reported.^{6,7}

The WS fraction was analyzed by HPLC equipped with two columns(SEC W12 and SEC W13, Yokogawa Co.) and two detectors of UV(254 nm) and RI(refractive index) in series. HPLC was operated at 40 °C with 0.8 mL/min flow of a mixture of water and acetonitrile(70/30 by volume) as an eluting agent. TOF-MS of WS fraction was measured by MALDI(Matrix-assisted laser desorption ionization) method using Voyager of PerSeptive Biosystems.

RESULTS AND DISCUSSION

Decomposition of chitin in hot pressurized water

The conversion and product distributions in the hydrothermal reactions of chitin by a flow reactor are summarized in Table 1. At 350 °C, WS yields were 24.0 and 29.6 % under the reaction pressures of 7.0 and 18 MPa, respectively, being comparable to those obtained by a batch reactor as previously reported.¹⁰ It is marked that the secondary decomposition of WS was effectively suppressed by the flow reactor because WS was continuously extracted by hot water from the fixed bed reactor. A higher temperature of 400 °C at 25 MPa under the supercritical condition increased the WS yield to 35.5 %, while the recovery was lower because of the higher gas yield. In addition, the WI was converted to the black char above 350 °C, indicating that the retrogressive and coking reactions take place under the severer conditions.

Figure 1 shows the HPLC profiles of the WS fraction produced from chitin under the pressurized hydrothermal conditions. A standard sample of chitin oligomer obtained from JHS Co.Ltd. was also measured for comparison in Figure 1 (a), where monomer to pentamer are clearly shown in the chromatogram. The WS produced at 300 °C contained the oligomer products with 3 to 6 units, although the yield was as low as 5 %. The molecular weights of the oligomers were analyzed by MALDI TOF-MS as illustrated in Figure 2, where the corresponding trimer to hexamer were included in the WS. The WS produced at 350 and 400 °C contained a large amount of the degraded products with the adsorption by UV detector, indicating that the ring cleavage reaction of the unit structure should take place under the sub- and supercritical water conditions. The hydrolysis of chitin under the mild conditions is recommended for the selective production of the oligomers.

Effect of acid addition on the hydrothermal decomposition of chitin

Table 2 summarizes the hydrothermal conversion of chitin by a batch reactor with or without acid addition. The conversion to WS at 300 °C increased very much from 11.4 % in water to 22.0 % in bamboo acid solution(pH: ca. 3). A bamboo acid solution contains acids such as formic acid, acetic acid, and higher carbon acids. A higher temperature of 350 °C did not change the WS conversion with the higher gas yield.

5 % acetic acid aqueous solution significantly increased the WS yield to 55.5 % at 300 °C, and its 10 % solution further increased up to 73.7 % at 300 °C. The addition of 10 % formic acid gave a slightly higher WS yield of 76.3 % compared to that with 10 % acetic acid solution at the same temperature, although the some weight gains were observed with the addition of acetic or formic acid, suggesting some contribution of the addition reaction of the acid to the decomposed ether linkage between the unit structures of chitin.

Figure 3 illustrates the effect of pH on the WS conversion at 300 °C. The WS conversion linearly increased with pH, although it was saturated in the pH range between 1 and 2. The higher conversion is suggested to be related to the acidity of aqueous solution under the subcritical conditions. However, HPLC analyses of WS fractions indicated that the higher acidity may accelerate the ring cleavage of the unit structure and the addition reaction of acid.

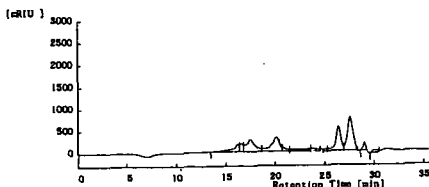
Based on the above results, it is pointed out that the control of pH in the acid solution and the dissociation of the aggregate structure in the chitin polymer through the solvation are keys to the enhancement of the hydrothermal decomposition of chitin.

References

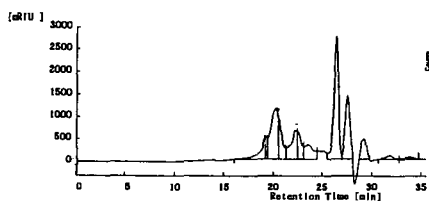
- 1) Muzzarelli, R.A.A., 'Chitin', Pergamon Press, New York (1977).
- 2) Shimahara, K.; Takiguchi, Y.; Ohkouchi, K.; Kitamura, K.; Okada, O. Chitin, Chitosan, and Related Enzymes, Ed.: Zikakis, J.P., Academic Press, Orlando (1984).
- 3) Hoashi, N., Hudson, S.M. Chitin - Healing Power from the Sea. Ed. Morton, R.J. Will Productions, Los Angeles, 1995.
- 4) Atalla, R.H. Conformational Effects in Hydrolysis of Cellulose, Hydrolysis of Cellulose: Mechanisms of Enzymatic and Acid Catalysis, Ed.: Brown, Jr., R.D. and Jurasek, L. Advances in Chemistry Series, Washington, D.C., 1979, vol.181, p. 55.
- 5) Gessler, K.; Krauss, N.; Steiner, T.; Betzel, A. S.; Saenger, W.; J.Am.Chem.Soc., 1995, 117, 11397.
- 6) Sakaki, T.; Shibata, M.; Miki, T.; Hirose, H.; Hayashi, N. Bioresource Technology, 1996, 58, 197.
- 7) Sakaki, T.; Shibata, M.; Miki, T.; Hirose, H. Energy & Fuels, 1996, 10, 684.
- 8) Kabyemela, B.M.; Adschiri, T.; Malaluan, R.M.; Arai, K. Ind. Eng. Chem. Res. 1997, 36, 2025.
- 9) Kabyemela, B.M.; Takigawa, M.; Adschiri, T.; Malaluan, R.M.; Arai, K. Ind. Eng. Chem. Res. 1998, 37, 357.
- 10) Sakanishi, K., Ikeyama, N., Sakaki, T., Shibata, M., Miki, T., Ind.Eng.Chem.Res. in submission.

Table 1 Hydrothermal decomposition of chitin by a fixed bed flow reactor

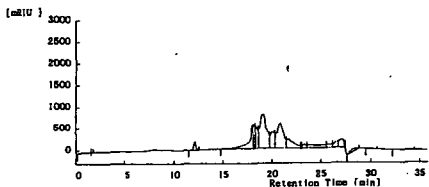
Salt bath temp.(°C)	Reaction press.(MPa)	WS Yield (wt%)	WI yield (wt%)	Recovery (%)
350	7.0	24.0	64.9	89.0
350	18.0	29.6	63.3	92.9
400	25.0	35.5	44.7	80.2



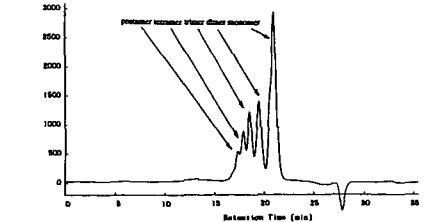
(d)



(c)



(b)



(a)

Fig. 1 HPLC profiles of the WS fractions produced under variable conditions

(a) standard chitin oligomers (b) 300 °C in water (c) 350 °C in water (d) 300 °C in 5%CH₃COOH aq.

Table 2 Effect of acid addition on the hydrothermal decomposition of chitin by a batch tube reactor¹⁾

Additives (-)	Salt bath temp.(°C)	Reaction temp.(°C)	Yields (wt%)			
			WS	MS	MI	Gas
water	300	285	11.4	1.2	75.6	11.8
bamboo acid 100%	300	279	22.0	0.0	75.8	2.2
bamboo acid 100%	350	323	21.1	1.0	73.1	4.8
acetic acid 5 %	300	287	55.5	3.6	52.9	-
acetic acid 10 %	300	286	73.7	1.8	39.7	-
formic acid 10 %	300	288	76.3	0.4	29.2	-

1) reaction time 60 sec after the preheating at 250 °C for 3 min
chitin 0.5 g + solvent 3.0 g for water and bamboo acid,
chitin 0.4 g + solvent 2.4 g for acetic acid and formic acid solutions

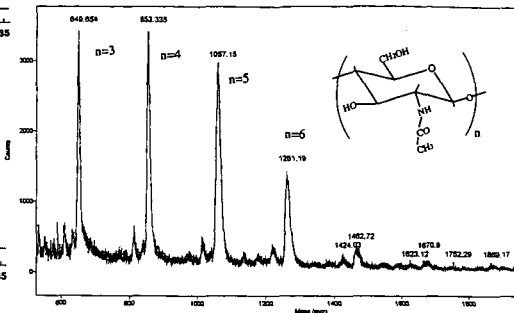


Fig. 2 TOF-MS profile of the WS fraction produced at 300 °C in water

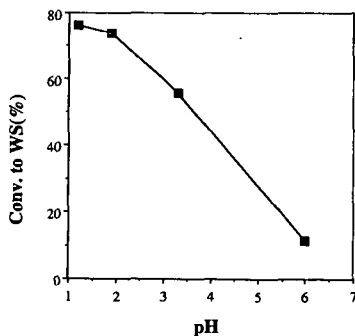


Fig. 3 Effect of pH on the conversion of chitin to WS

[pH; 10% formic acid 1.2
10% acetic acid 1.9
5% acetic acid 3.3
H₂O ca. 6]

KINETICS OF DEUTERIUM EXCHANGE OF RESORCINOL IN D₂O AT HIGH PRESSURE AND HIGH TEMPERATURE

Clement R. Yonker, Shi Bai, and Bruce J. Palmer, Environmental and Energy Sciences Division, Pacific Northwest National Laboratory, Richland WA, 99352

KEYWORDS: High Pressure NMR, Deuterium Exchange

ABSTRACT

The exchange kinetics of deuteration of resorcinol in pure D₂O were studied using a flow-through capillary tubular reactor with *on-line*, proton and deuterium NMR detection at high temperatures and high pressure. The temperatures of these measurements covered a range up to 450°C at a pressure of 400 bar. The hydrogen/deuterium (H/D) exchange in resorcinol (1,3-dihydroxybenzene) under these extreme conditions was easily detected by both proton and deuterium NMR as a function of resorcinol residence time in the capillary tubular reactor, which also served as the high pressure NMR cell. The qualitative NMR results indicate that H/D exchange in resorcinol is observed at 200°C. The kinetics of H/D exchange in resorcinol and the activation energies were extracted from the experimental ¹H and ²H NMR data.

INTRODUCTION

In subcritical (superheated) and supercritical water the hydrothermal oxidation of many organic compounds are enhanced due to the increased reactivity of the substrate and the enhanced solubility of non-polar organic compounds at these high temperatures. The increased reactivity of organic compounds in superheated water has been recognized for its potential in the destruction of toxic and organic wastes via oxidation.^{1,2}

Hydrogen/deuterium (H/D) exchange of some extremely weak organic acids in supercritical water has been investigated.^{3,4} Yao and Evilia³ estimated the equilibrium constant for the acid-base reaction of H/D exchange of benzene with OD⁻ to be three orders of magnitude higher at 400°C than at 25°C. Qualitatively, for substituted benzene compounds (fluorobenzene, 1,2-diphenylhydrazine, and nitrobenzene), the hydrogen in the ortho position was found to be slightly more acidic than those in the para or meta positions when reacted under basic conditions in D₂O at 400°C.³ However, difficulties were encountered when attempting to obtain quantitative chemical kinetic data for these reactions due to the large experimental error in determining temperature, pressure, and heating time when using a batch reactor.

While, NMR has not been widely used for *in situ* investigations of reactions in supercritical water, it has been used to monitor batch reaction products after quenching. The use of NMR detection for the *in situ* study of chemical kinetics generally requires that the NMR data acquisition time for a spectrum be much shorter than the reaction half-life.⁵ An experimental effort using a high pressure, high temperature flow-through capillary tubular reactor with *on-line* NMR detection for the investigation of H/D exchange of resorcinol in superheated and supercritical water will be discussed. The pseudo-first order rate constant for H/D exchange was determined by the disappearance of the α -hydrogens in resorcinol for the first time under these extreme conditions using this micro-volume ¹H NMR technique. In a similar manner, the product of the H/D exchange reaction was monitored *on-line* by ²H NMR. The rates for the resorcinol hydrogen/deuterium exchange reaction and the difference in the reactivity of the α and β hydrogens on resorcinol will be described.

EXPERIMENTAL

Resorcinol (Aldrich Chemical Company, Inc.) was used without further purification. To deoxygenate the solution, D₂O (Cambridge Isotope Laboratories) was boiled for 5 minutes under dry nitrogen and a 20% (w/w) resorcinol-D₂O solution was prepared and purged using dry nitrogen for 10 minutes.

Flow-through Capillary Tubular Reactor

The capillary tubular reactor set-up includes a high pressure syringe pump (ISCO 260D), a tubular piston separator (HIP), a fused silica capillary NMR cell (180 μ m i.d. by 360 μ m o.d., Polymicro Technologies, Inc), and back pressure regulators (Upchurch Scientific). In practice, the resorcinol-D₂O solution was loaded into one side of the piston separator and the other side was filled with water and connected to the syringe pump. The fused silica capillary was bent in a U shape and placed in a 10-mm glass NMR tube so that the bent end did not extend below the bottom edge of the NMR sensitive region along the z-axis. One end of the capillary tube was connected to the solution outlet of the piston separator and the other end of the capillary was connected to the back pressure regulators. When the high pressure syringe pump was operated in a constant flow rate mode, the sample pressure was controlled by the back pressure regulators. Five back pressure regulators (~80 bar each) were used in series so that the sample pressure was maintained between 380 to 400 bar depending on the flow rate.

The detection volume (V) within the NMR sensitive region was estimated from the inner diameter (180 \pm 6 μ m) of the capillary tubular reactor and twice the length of the NMR receiving coil (3.90cm). The volume of the NMR detection region was estimated to be $\sim 9.8 \times 10^{-6}$ ml (0.98

μl). Therefore, the reactor residence time (t_R) may be calculated from the mass flow rate (f) and the solution density (ρ) using equation 1,

$$t_R = V \cdot \rho / f \quad (1)$$

Since the accuracy of the reactor residence time depends on flow rate control and fluid density in the reactor, a system calibration was performed at room temperature and a pressure of 400 bar by collecting and weighing the water eluted from the capillary at specific flow rates over a set time interval. A step profile is assumed for the temperature contour in the reactor region and the density is determined from the Steam Tables⁶. This assumption allows a qualitative determination of the reaction rate under these extreme conditions.

NMR Measurements

All NMR data were obtained on a Varian UnityPlus 300 NMR spectrometer operating at 299.3 and 46.13 MHz for proton and deuterium detection, respectively. A high temperature, high resolution, broad band 10-mm NMR probe (Doty Scientific, Inc.) produces a line width at half-height of 8-10 Hz for proton and 4-8 Hz for deuterium in the resorcinol-D₂O solution in the capillary NMR cell at room temperature. Because of the probe design, there is a region where the tubular reactor temperature is not well controlled. This pre-heated area, before the NMR detection region, could contribute to a overestimation of the deuterated product and a underestimation of the reactant conversion rate. We anticipate solving this problem in future NMR investigations, through redesign of the probe's heated region.

In a typical experiment, the resorcinol-D₂O solution is moving through the capillary high pressure NMR cell⁷ under a constant flow rate at constant temperature and pressure. Concurrent with solution flow, a NMR experiment is running coadding transients until a satisfactory spectrum with an adequate signal to noise ratio is obtained. Since the capillary tubular reactor is an integral part of the NMR capillary cell, a steady state concentration is established in the reactor at constant flow during the experiment. The sample temperature was changed with each flow rate at a constant pressure and the peak integral was used in both the proton and deuterium data analysis.

RESULTS AND DISCUSSION

Proton NMR

The reaction of substituted benzene in basic solutions of D₂O has been discussed by Yao and Evilia.³ The H/D exchange mechanism for resorcinol in pure D₂O is facilitated by the presence of electron-withdrawing groups on the aromatic ring. This activated aromatic ring is deuterated by an electrophilic substitution mechanism, which increases the ease of deuteration under these experimental conditions and eliminates the need of either an acid or base to catalyze the reaction.^{5,8} Resorcinol is an ortho/para director in electrophilic substitution reactions.⁹ Therefore, H/D substitution would be facilitated for the α -hydrogens and not for the β -hydrogen. The α -hydrogen peak area decreased as a function of increasing temperature and reactor residence time. From the H/D substitution reaction rates the pseudo-first order kinetics could be determined for resorcinol under these extreme conditions. The NMR experimental results demonstrate the positional selectivity of the electrophilic substitution during H/D exchange due to the molecular structural information obtained from this technique.

The β -hydrogen in resorcinol can serve as an internal molecular indicator relating to the stability of the molecule to thermolysis reactions under these conditions. Qualitatively, the peak area of the β -hydrogen decreases with increasing reactor residence time, but shows little temperature dependence. Thermolysis of resorcinol at 460°C and 254 bar was reported to produced conversions of ~10%, for residence times of 1 - 7 seconds at 0.01M solution concentration.¹⁰ The NMR results demonstrates the occurrence of a parallel thermolysis reaction of resorcinol under these temperatures and reactor residence times. The thermolysis products could not be identified as they were below the detection limits of the NMR.

Deuterium NMR

At a reaction temperature of 200 °C, the deuterium NMR spectrum shows a new peak with a chemical shift of ~7.2 ppm. The chemical shift difference between this new peak and that of D₂O at 200 °C is ~3.0 ppm, which is the same as the chemical shift difference between the α -hydrogens and water in the ¹H NMR measurement at the same temperature. Therefore, this resonance was assigned to resorcinol deuterated at the α -positions. This qualitative observation demonstrated that H/D exchange did indeed occur for the resorcinol-D₂O solution at 200°C at very long reactor residence times. The intensity of the α -deuterated resorcinol peak increases as a function of temperature and reactor residence time. A pseudo-first order rate constant can be determined from the rate of appearance of the α -deuterium peak and compared with that determined from the ¹H NMR measurements under similar experimental conditions. A β -deuterium peak is not observed under the experimental conditions investigated.

ACKNOWLEDGMENT

Work at the Pacific Northwest National Laboratory (PNNL) was supported by the Office of Energy Research, Office of Basic Energy Sciences, Chemical Sciences Division of the U. S. Departments of Energy, under Contract DE-AC076RLO 1830.

REFERENCES

- (1) Yang, H. H.; Eckert, C. A. *Ind. Eng. Chem. Res.*, **1988**, *27*, 2009-2014.
- (2) Webley, P. A.; Tester, J. W.; Holgate, H. R. *Ind. Eng. Chem. Res.*, **1991**, *30*, 1745- 1754.
- (3) Yao, J.; Evilia, R. F. *J. Am. Chem. Soc.*, **1994**, *116*, 11229-11233.
- (4) Kuhlman, B.; Arnett, M.; Siskin, M. *J. Org. Chem.*, **1994**, *59*, 3098-3101.
- (5) Grimaldi, J.; Baldo, J.; McMurray, C.; Sykes, B. D. *J. Am. Chem. Soc.*, **1972**, *94*, 7641-7645.
- (6) Haar, L.; Gallagher, J. S.; Kell, G. S.; NBS/NRC Steam Tables, Hemisphere Publishing Corp., New York, 1984.
- (7) Yonker, C. R.; Zemanian, T. S.; Wallen, S. L.; Linehan, J. C.; Franz, J. A. *J. Magn. Reson., Ser A*, **1995**, *113*, 102-107.
- (8) Maksić, Z. B.; Kovačević, B.; Kovaček, D. *J. Phys. Chem. A*, **1997**, *101*, 7446-7453.
- (9) Morrison, R. T.; Boyd, R. N. *Organic Chemistry*, 3rd Ed., Allyn and Bacon, Inc., Boston, **1973**, p. 340.
- (10) Martino, C. J.; Savage, P. E. *Ind. Eng. Chem. Res.*, **1997**, *36*, 1385-1390.

HYDROGEN STABLE ISOTOPE RATIOS OF KEROGEN, BITUMEN, OIL, AND WATER IN HYDROUS PYROLYSIS

A. Schimmelmann¹, M. D. Lewan², and R. P. Wintsch¹

¹ Department of Geological Sciences, Indiana University, 1005 East 10th Street,
Bloomington, IN 47405-1403

² U. S. Geological Survey, Box 25046, MS 977, Denver Federal Center,
Denver, CO 80225

INTRODUCTION

Diverse isotopic evidence has been mounting in favor of an active role of water in the chemical transformation of kerogen to bitumen, oil, and gas, and also as an agent promoting hydrogen isotopic exchange with organic hydrogen (e.g., Koepp, 1978; Schoell, 1981; Hoering, 1984; Stalker et al., 1998). At low temperatures, water-hydrogen exchanges quickly with isotopically labile organic hydrogen most of which is bound to organic nitrogen, sulfur, and oxygen (NSO-functional groups; Koepp, 1978; Schoell, 1981). In contrast, most carbon-bound hydrogen does not exchange with water at neutral pH, low temperature, and in the absence of a catalyst, thus conserving the D/H ratios of *n*-alkanes at temperatures well above 150°C (Hoering, 1984; Koepp, 1978). Some aromatic hydrogen and few alkyl hydrogen sites adjacent to branching and carbonyl positions may exchange with water-hydrogen at temperatures as low as 100°C (Alexander et al., 1982; Werstik and Ju, 1989), especially at low pH via carbonium ion mechanisms. At higher temperatures, extensive exchange between water-derived hydrogen and organic hydrogen is attributed to the quenching of free organic radical sites (Hoering, 1984; Lewan, 1997; Stalker et al., 1998). Thermodynamic calculations indicate that reactions of water with alkyl free radicals are highly favorable under experimental and natural maturation conditions (Lewan, 1997, p. 3714-3715).

The determination of meaningful D/H ratios in organic substrates needs to take into account the isotopically labile organic hydrogen that perpetually exchanges with ambient moisture. Only the low concentration of labile NSO-linked hydrogen in oil and bitumen warrants the use of δD of total organic hydrogen. In contrast, kerogens of low to moderate thermal maturity are more hydrophilic because they contain abundant NSO-functional groups that often contain labile hydrogen. In this study we control the isotopic composition of labile hydrogen in kerogen by dual equilibration with isotopic standard water vapors at 115°C, followed by a mass balance calculation to arrive at the isotopic composition of non-labile hydrogen in kerogen (Schimmelmann, 1991). To avoid semantic confusion about different types of exchangeable hydrogen, this study operationally defines "labile organic hydrogen" as the fraction of organic hydrogen that readily exchanges with water vapor at 115°C.

EXPERIMENTAL

We used four thermally immature source rocks that encompass different types of kerogen: Type-I (Mahogany Shale of the Eocene Green River Fm. in Utah), type-II (Clegg Creek Member of the Devonian-Mississippian New Albany Shale in Indiana), type-IIS (Senonian Ghareb Limestone from Jordan), and type-III (Paleocene lignite from Calvert Bluff Fm. of the Wilcox Gp. in Texas).

Hydrous pyrolyses were performed in stainless steel pipe reactors (pipe length 15.1cm, o.d. 1.9cm, internal volume ca. 25.5mL) that were loaded with 5.5 to 10g of rock chips (diameter 2mm to 7mm). The rock was submerged in 10 to 11ml of 0.093 molar aqueous ammonium chloride solution under nitrogen. Three isotopically different aqueous phases were

used with initial δD values of -110, +290, or +1260 per mil. After hydrous pyrolysis and cooling to room temperature, expelled oil or wax on the water surface was collected separately from the water phase. Bitumen was Soxhlet-extracted from dried and powdered rock. Kerogen was prepared by demineralization of bitumen-extracted powdered rock. The isotopic equilibration of aliquots of kerogen at 115°C in isotopic standard water vapors, the conversion of water and organic hydrogen to elemental hydrogen for mass-spectrometric analysis, and the calculation of δD values of non-labile hydrogen in kerogen were described by Schimmelmann (1991). We are aware that water will also continuously exchange with hydrogen in clay minerals and with exchangeable (labile) organic hydrogen.

RESULTS

Waters with strong initial D-enrichment transfer deuterium to organic phases over time, whereas water with an initial δD value of -110 per mil receives organic deuterium. In effect, the directions of isotopic shifts for organic hydrogen in kerogen, bitumen, and oil are opposite to the respective shifts observed for water, depending on the starting δD value of water. Our isotopic choices for water as the dominant hydrogen pool determine the directions of isotopic exchange for all minor, organic hydrogen pools. The converging patterns of isotopic changes of waters and the associated type-II kerogen, bitumen, and oil from 330°C hydrous pyrolysis experiments are shown in Figure 1.

Our D/H data permit a mass balance approach to estimate the fraction of organic hydrogen in kerogen, bitumen, and oil that is derived from water in hydrous pyrolysis experiments. Our calculations are based on hydrous pyrolysis experiments with starting δD values for water of -110 and + 1260 per mil. We cannot discriminate between added hydrogen and hydrogen that was exchanged at temperatures above 115°C, but the calculations are not affected by the presence of labile hydrogen in kerogen. Details of underlying assumptions and algorithms are presented elsewhere (Schimmelmann et al., in review). The percentage P (Table 1) reflects the estimated abundance of water-derived hydrogen in bitumen and oil, and in non-labile organic hydrogen in Kerogen. The isotopic influence of water-hydrogen on type-II kerogen and associated bitumen and oil from New Albany Shale increases over time at 330°C, and with increasing temperature over 72 hours (Table 1a). The four types of source rocks used in this study differ in their content of potentially reactive and exchangeable hydrogen, and therefore in their P values and in their ability to shift δD values of water (Table 1b).

DISCUSSION

Many chemical and physical processes affecting the hydrogen isotopic balance between reactants and phases occur simultaneously and continuously during hydrous pyrolysis of immature source rocks in contact with water. Some bitumen is already present in immature source rocks prior to hydrous pyrolysis, but significant amounts are generated from the kerogen with increasing temperature, along with low-molecular weight compounds (Lewan, 1997). With increasing temperature, the water-saturated bitumen partially decomposes into an immiscible hydrophobic oil that is expelled from the rock (Lewan, 1997). Our D/H data represent time-series of snapshots of this dynamic system of water, kerogen, bitumen, and oil.

Our P values in Table 1b show that hydrogen in type-I kerogen and its associated bitumen and expelled wax is the most isotopically conservative, i.e. with the lowest P values, whereas hydrogen is least isotopically conservative in type-IIS kerogen and its associated bitumen and expelled oil. The decrease in P values in the order of kerogen-types IIS > II \approx III > I can be interpreted in terms of basic chemical structural differences. The strongly aliphatic

type-I kerogen (Tissot and Welte, 1984; Horsfield et al., 1994) has a large isotopically conservative pool of hydrogen in its mostly *n*-alkyl linkages, and can thus be expected to generate the smallest number of free radicals during hydrous pyrolysis and to express the smallest *P* values for kerogen, bitumen, and oil. Type-II kerogen is expected to contain a more branching molecular carbon structure, with larger propensity toward generation of free radical sites and consequently larger *P* values. A similar increase in *P* in type-III kerogen may be the result of a larger abundance of oxygen in lignite, which favors the formation of free radicals. Type-IIS kerogen would form even more free radicals under the same thermal conditions because it contains labile S-S and C-S bonds with low activation energy (Tomic et al., 1995; Lewan, 1998).

CONCLUSIONS

Immature source rocks containing different types of kerogen were heated in hydrous pyrolysis experiments. D/H ratios were monitored in isolated kerogen, extracted bitumen, expelled oil, and ambient water. The isotopic transfer of hydrogen between water and organic hydrogen increases with higher temperature and longer duration of hydrous pyrolysis, via exchange and/or addition, resulting in a convergence of δD values of water and of organic hydrogen. Isotopic mass-balance calculations suggest that, depending on temperature, time, and source rock type, between 35 and 75% of carbon-bound hydrogen is ultimately derived from water-hydrogen. Organic hydrogen in kerogen, bitumen and oil/wax from source rocks containing different types of kerogen rank from least to most isotopically conservative in the order IIS < II \approx III < I, which is consistent with models of chemical reactivity in kerogens through maturation.

The prospect of water-hydrogen becoming available to maturing organic matter may pleasantly revise estimates of oil and gas potentials in sedimentary basins, but its potential D/H isotopic implications may force isotope geochemists to rethink their interpretation of D/H ratios in maturing fossil fuels and associated formation waters. The unresolved controversy about substituting long geologic time in natural maturation with higher temperature in artificial maturation, however, advises to caution when extrapolating our specific isotopic findings from hydrous pyrolysis to D/H ratios in fossil fuels.

ACKNOWLEDGEMENTS

Acknowledgement is made to the donors of The Petroleum Research Fund, administered by the American Chemical Society, for support of this research with grant #31203-AC2, to the U.S. Geological Survey under Energy Resources Project 51564, and to NATO Collaborative Research Programme grant 971381.

REFERENCES

- Alexander, R., Kagi, R. I., and Larcher, A. V., 1982, Clay catalysis of aromatic hydrogen-exchange reactions, *Geochim. Cosmochim. Acta* 46: 219-222.
- Hoering, T. C., 1984, Thermal reactions of kerogen with added water, heavy water and pure organic substances, *Org. Geochem.* 5: 267-278.
- Horsfield, B., Curry, D. J., Bohacs, K., Litke, R., Rullkötter, J., Schenk, H. J., Radke, M., Schaefer, R. G., Carroll, A. R., Isaksen, G., and Witte, E. G., 1994, Organic geochemistry of freshwater and alkaline lacustrine sediments in the Green River Formation of the Washakie Basin, Wyoming, U.S.A., *Org. Geochem.* 22: 415-440.
- Koepp, M., 1978, D/H isotope exchange reaction between petroleum and water: A contributory determinant for D/H-isotope ratios in crude oils? In *Short papers of the Fourth International Conference, Geochronology, Cosmochronology, Isotope Geology.* (ed R.

- E. Zartman), *USGS Open-File Report 78-701*: 221-222. Reston VA, US Geological Survey.
- Lewan, M. D., 1997, Experiments on the role of water in petroleum formation, *Geochim. Cosmochim. Acta* **61**: 3691-3723.
- Lewan, M. D., 1998, Sulphur-radical control on petroleum formation rates, *Nature* **391**: 164-166.
- Schimmelmann, A., 1991, Determination of the concentration and stable isotopic composition of non-exchangeable hydrogen in organic matter, *Anal. Chem.* **63**: 2456-2459.
- Schimmelmann, A., Lewan, M. D., and Wintsch, R. P., (in review), D/H isotope ratios of kerogen, bitumen, oil, and water in hydrous pyrolysis of source rocks containing kerogen types-I, -II, -IIS, and -III, submitted to *Geochim. Cosmochim. Acta*.
- Schoell, M., 1981, D/H-Isotopenverhältnisse in organischen Substanzen, Erdölen und Erdgasen. *BMFT Forschungsbericht T 81-204*, 1-79, Bundesanstalt für Geowissenschaften und Rohstoffe, Hannover, Germany.
- Stalker, L., Larter, S. R., and Farrimond, P., 1998, Biomarker binding into kerogens: evidence from hydrous pyrolysis using heavy water (D₂O), *Org. Geochem.* **28**: 239-253.
- Tissot, B. P., and Welte, D. H., 1984, *Petroleum Formation and Occurrence*. Springer-Verlag.
- Tomic, J., Behar, F., Vandembroucke, M., and Tang, Y., 1995, Artificial maturation of Monterey kerogen (Type II-S) in a closed system and comparison with Type II kerogen: implications on the fate of sulfur, *Org. Geochem.* **23**: 647-660.
- Werstiuk, N. H., and Ju, C., 1989, Protium-deuterium exchange of benzo-substituted heterocycles in neutral D₂O at elevated temperatures, *Can. J. Chem.* **67**: 812-815.

Table 1. Calculated percentage (*P*) of the amount of water-derived hydrogen in the total hydrogen of bitumen and oil, and in the non-labile hydrogen of kerogen, after hydrous pyrolysis experiments in waters with starting δD values of -110 and +1260 per mil. The $\Delta\delta D$ of water is the difference between the final δD values and the starting δD values in water, in per mil.

Hydrous Pyrolysis Experimental Conditions			Kerogen	Bitumen	Oil	$\Delta\delta D$ of Water (per mil)	
Kerogen Type	Temp. (°C)	Time (h)	<i>P</i> (%)	<i>P</i> (%)	<i>P</i> (%)	[starting δD values:]	
						[-110]	[+1260]
a) variations in temperature and time							
II	310	72	47.1	53.1	36.1	10	-115
II	330	12	42.6	48.3	33.9	9	-82
II	330	36	56.6	58.4	43.3	8	-91
II	330	72	61.7	61.9	50.3	11	-104
II	330	144	66.0	70.2	57.7	9	-111
II	350	72	74.5	73.1	58.9	14	-140
b) variations in source rock							
I	330	72	44.4	34.9	39.6	4	-152
II	330	72	61.7	61.9	50.3	11	-104
IIS	330	72	69.7	69.9	68.4	15	-186
III	330	72	69.5	56.9	44.6	22	-262

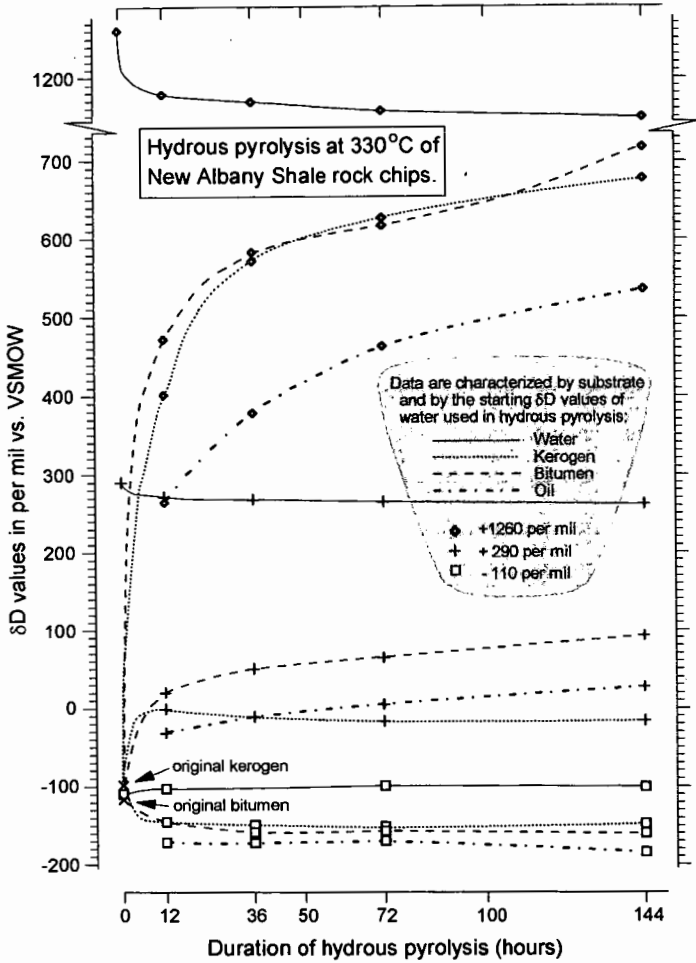


Fig. 1: D/H results from water, kerogen (non-labile hydrogen), bitumen, and oil from hydrous pyrolysis experiments, at 330°C of New Albany Shale. Three isotopically different waters were used, resulting in distinctly converging isotopic shifts of water and organic phases over time for each type of water used, due to isotopic hydrogen transfer between inorganic and organic hydrogen. Connecting lines are drawn to guide the eye. No oil was available before hydrous pyrolysis.

BASE-CATALYZED REACTIONS IN NEAR-CRITICAL WATER FOR ENVIRONMENTALLY BENIGN CHEMICAL PROCESSING

Roger Gläser, James S. Brown, Shane A. Nolen, Charles L. Liotta, and Charles A. Eckert
Schools of Chemical Engineering and Chemistry, and Specialty Separations Center
Georgia Institute of Technology, Atlanta, GA 30332-0100

INTRODUCTION

Water has recently attracted much interest as an environmentally benign solvent for organic syntheses [1,2]. While many of the previous studies have been devoted to water near ambient conditions, it exhibits more favorable characteristics as a medium for organic reactions when it is closer to its critical point (near-critical water) but still in the liquid state. First, the solubility of organic substances in water increases considerably with increasing temperature due to a decrease in dielectric constant. For liquid water at 250 °C the dielectric constant is comparable to that of ambient acetone [3]. Conversely to acetone, product separation from the solvent can occur simply by phase separation upon returning to ambient conditions. Secondly, the ionization constant of near-critical water is several orders of magnitude higher than that of ambient water, thus providing a source of hydronium and hydroxide ions, which can act as catalytically active species in chemical conversions. As shown in previous studies in our group [4,5] acid catalyzed reactions, such as Friedel-Crafts alkylations, can be successfully accomplished in near-critical water with less or even without added catalyst. Thirdly, while reactions in supercritical water have mainly been applied in chemical reactions to break up bonds, e.g., for waste destruction by supercritical water oxidation (SCWO) [6,7], the milder temperature regime of hot liquid water allows for bond formation, i.e., the synthesis of organic compounds.

In this study we aimed at scouting the opportunities to perform organic syntheses in near-critical water that are usually conducted in the presence of base. Based on earlier work by *Katritzky, Siskin et al.* [8], aldol condensations have been chosen as first examples because the reactants are not subject to immediate hydrolysis, and different products can be formed. In the classical preparation methods the selectivity for the products is determined, e.g., by the reaction temperature and by the pH during the work-up procedure. Selectivity for those products might therefore give insight into the effect of water as the reaction medium on product distribution. The aldol condensation of phenylacetaldehyde has been studied in further detail, including different reaction times, reactant concentrations, and in the presence of added acid and base. The scope of this type of reaction has also been explored for some condensations between different reactants. Other synthetically important C-C bond formation reactions involve hydrolyzable compounds, such as esters, and as examples the Dieckmann condensation and typical malonic ester syntheses have been included in the present study to encompass the scope of reactions accessible in near-critical water.

EXPERIMENTAL SECTION

The reactions have been carried out in the batch mode using Titanium vessels (rated to 1 kbar at 500 °C) with an inner volume of 3 ml. After loading, these reactors have been placed in a preheated aluminum block where they reached the desired reaction temperature within ca. 5 min. After stopping the reaction by quenching the reactors in a room temperature water bath, the reactor contents were dissolved in acetone and diluted to a known volume. For determination of product distribution versus time several vessels were loaded in the same manner and have been quenched at different reaction periods. Product analysis was achieved via temperature-programmed capillary GC equipped with an FID or an MS detector and product distribution are given in terms of mole fractions.

All chemicals were ACS grade (Aldrich) and were used as received. Water to be used as reaction solvent was HPLC grade (Aldrich) and was used without further purification. As shown in previous experiments, both deoxygenation of the water and loading under nitrogen atmosphere did not afford a change in the obtained product of more than experimental accuracy.

In a typical run at 275 °C a reactor is loaded at ambient conditions with 1.8 ml liquid reactant/water mixture with a molar ratio of 1/47. Accounting for the expansion of the water with increasing temperature the reactor at 275 °C contains 2.6 ml liquid phase and a small gas phase.

RESULTS AND DISCUSSION

Aldol condensations

The aldol condensation of *n*-butyraldehyde is industrially carried out in the presence of caustic sodium to produce 2-ethyl-2-hexenal. This is later hydrogenated to 2-ethylhexanol which is esterified with phthalic acid to give the plasticizer dioctylphthalate (DOP) [9]. If *n*-butyraldehyde is reacted for 15 hrs at 275 °C in water, essentially complete conversion is obtained without the addition of any catalyst. The main product is, like in the conventional synthesis, 2-ethylhexanal (selectivity 85 %). Some 2-butyl-2-butanone is also formed by double

bond isomerization of the former. Other byproducts with selectivities < 2 % are the dialdolization product, triethylnaphthalene and cis/trans isomers of the formed olefins.

As already pointed out by *Katritzky et al.* [10] phenylacetaldehyde (PAA) is a highly reactive compound and a reaction scheme (Figure 2) has been provided by these authors. The distribution of some key intermediates for the conversion of PAA in water at 275 °C as a function of reaction time is shown in Figure 1. From this Figure it can be clearly seen that products **1** and **2** formed by two aldol reaction steps and subsequent double bond isomerization are intermediate products in the formation of 1,3,5-triphenylbenzene as proposed by the reaction scheme. In addition to the main reaction products observed by *Katritzky et al.* [10] we have also found 2-phenylnaphthalene which can be formed by ring closure of the aldol reaction and subsequent dehydration and isomerization. The presence of small amounts of 2-phenyldihydronaphthalene provides further evidence for the formation of 2-phenylnaphthalene. 2-Phenylnaphthalene is the major reaction product when PAA is converted in the presence of hydrochloric acid (Table 1) and otherwise constant reaction conditions. With added NaOH as a base, however, 1,3-diphenylpropane is the main reaction product and no 2-phenylnaphthalene is observed. Table 1 also shows the influence of the PAA concentration: While higher dilution of the reactant does not afford a considerable change in the product distribution, a higher reactant concentration leads to a lower conversion and lower mole fractions of products formed in subsequent reactions.

Ketones are less reactive in aldol-type reactions than aldehydes. Although acetone is readily converted in near-critical water to mainly mesityloxide, 1-phenyl-2-butanone (PBO) does not undergo any reaction at 275 °C after 24 hrs, and a conversion of only about 15 % is reached in the presence of added NaOH ($n_{\text{PBO}}/n_{\text{NaOH}} = 1/0.5$). Nearly 50 % conversion of PBO is obtained without further addition of base, when it is reacted with benzaldehyde as a more active carbonyl compound. Table 2 summarizes the main products resulting from aldol type C-C bond formations in the conversions of acetone and PBO with benzaldehyde. In accordance with the results reported by *Katritzky, et al.* [11] benzaldehyde alone undergoes primarily Cannizzaro reaction and disproportionation in an overall low conversion (< 5 %) to yield benzoic acid, benzylalcohol, and toluene, respectively.

Dieckmann condensation

Many base catalyzed involve the conversion of hydrolyzable compounds, such as esters in the Claisen condensation [12]. To test whether such reactions can be carried out in near-critical water at 275 °C the Dieckmann condensation of adipic acid and its dimethyl and diethyl ester has been attempted without any added catalyst. Both esters undergo hydrolysis to the monoester and adipic acid, respectively, and, the diethyl ester hydrolyzes slower than the methyl derivative, as expected. It should be noted, however, that even after 16 hrs at 275 °C this hydrolysis is not complete, leaving about a third of the overall adipic acid at the mono- or the diester. Besides hydrolysis the main products were cyclopentanone and benzoic acid. Cyclopentanone is the expected product, if the base-catalyzed ring closure is followed by decarboxylation, which is facilitated at the elevated temperature. More cyclopentanone is formed when the ester hydrolysis is less pronounced, i.e., with diethyl adipate as reactant. With adipic acid the formation of benzoic acid is strongly favored over the formation of cyclopentanone, but the cyclopentanone yield is comparable to the one achieved with the esters. The overall yield of cyclopentanone in all cases is, however, comparably low (< 2 %).

Knoevenagel condensation

The condensation of a carbonyl compound with a malonic ester is a useful tool in the synthesis of substituted organic acids, often referred to as "malonic ester syntheses" [12]. By this method cinnamic acid can be obtained from the conversion of a malonic acid ester with benzaldehyde followed by hydrolysis and decarboxylation. With malonic acid as the reactant, water as the solvent and in the absence of added base, the main product of the conversion is styrene as well as the products arising from self reaction of benzaldehyde (Table 3). Although the desired C-C bond formation has occurred, decarboxylation apparently is the strongly favored reaction under these reaction conditions. In addition to an overall higher conversion than with malonic acid, the use of disodium malonate instead of malonic acid resulted predominantly in an increased formation of benzylalcohol most probably due to the reduction of benzaldehyde, accompanied by the production of carbon dioxide. 2-Methyl-1-propenylbenzene and isobutyric acid were the major products in the conversion of benzaldehyde with dimethyl malonate in near-critical water. The formation of these products involve a series of condensation, hydrolysis, and decarboxylation reactions.

The conversion of benzylaldehyde with diphenylmethane in water at 275 °C did not result in the formation of any detectable condensation product. Presumably the ions from the dissociation of water can neither deprotonate diphenylmethane, nor activate the benzaldehyde carbonyl group to an extent sufficient to bring about the desired reaction.

CONCLUSIONS

Near-critical water is a promising and environmentally benign reaction medium for a number of synthetically important conversions that are conventionally carried out in the presence of base. Due to the high ionization of water these conversions may be accomplished without further addition of base, especially in the when reactive carbonyl compounds and substrates with sufficiently high C-H acidity are involved.

It has been shown that C-C bond formations can be brought about in near-critical water in syntheses that involve hydrolyzable compounds like esters. Decarboxylation, which was indicated to be a limiting factor in these reactions, might be reduced by pressurizing the reaction vessels with carbon dioxide and lowering the reaction temperature. At lower temperature the solubility of the organic reactants might, however, also be considerably reduced. Therefore, more detailed information on the phase behavior of organic substances relevant to chemical synthesis is needed. Investigations are currently underway in our laboratory.

Although the spectrum of prospective reactants might be limited to those thermally stable at temperatures up to ca. 300 °C, the lower cost of the reactants and the solvent, the ease of carrying out the reaction and product separation as well as the opportunity to reduce, if not completely avoid the addition of a catalyst render near-critical water an profitable alternative to many less favorable solvents currently used in chemical processes.

ACKNOWLEDGEMENTS

The authors gratefully acknowledge generous financial support by the U.S. NSF and the U.S. EPA. R.G. thanks the German Research Association (Deutsche Forschungsgemeinschaft) for a research stipend.

REFERENCES

- [1] A. Lubineau, J. Augé and Y. Queneau, *Synthesis*, 741-760 (1994).
- [2] C.-J. Li, *Chem. Rev.* **93**, 2023-2035 (1993).
- [3] M. Siskin and A.R. Katritzky, *Science* **254**, 231-237 (1991).
- [4] K. Chandler, F. Deng, A.K. Dillow, C.L. Liotta, and C.A. Eckert, *Ind. Eng. Chem. Res.* **36**, 5175-5179 (1997).
- [5] K. Chandler, C.L. Liotta, C.A. Eckert and D. Schiraldi, *AIChE J.* **44**, 2080-2087 (1998).
- [6] R.W. Shaw, T.B. Brill, A.A. Clifford, C.A. Eckert and E.U. Franck, *Chem. Eng. News* **69**, 23-39 (1991).
- [7] P.E. Savage, S. Gopalan, T.I. Mizan, C.I. Martino and E.E. Brock, *AIChE J.* **41**, 1723-1778 (1995).
- [8] A.R. Katritzky, M. Siskin et al., series of 18 papers in *Energy & Fuels* **4**, 475-584 (1990).
- [9] K. Weissermel, and H.-J. Arpe: "Industrial Organic Chemistry", 3rd ed., Verlag Chemie, Weinheim, New York (1997).
- [10] A.R. Katritzky, F.J. Luxem and M. Siskin, *Energy & Fuels* **4**, 514-517 (1990).
- [11] A.R. Katritzky, M. Balasubramanian and M. Siskin, *Energy & Fuels* **4**, 499-505 (1990).
- [12] J. March: "Advanced Organic Chemistry, Reactions, Mechanisms, and Structure", J. Wiley & Sons, New York, Chichester, Brisbane, Toronto, Singapore (1985).

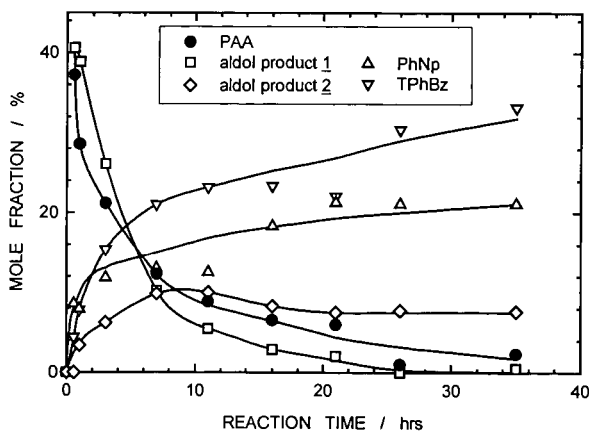


Figure 1: Distribution of major products as a function of reaction time for the conversion of phenylacetaldehyde (PAA) in near-critical water at 275 °C ($n_{\text{PAA}}/n_{\text{H}_2\text{O}} = 1/50$); PhNp: 2-phenylnaphthalene, TPhBz: 1,3,5-triphenylbenzene, aldol product 1 and 2: see Figure 2.

ABIOTIC SYNTHESIS OF ORGANIC COMPOUNDS IN HYDROTHERMAL SYSTEMS:
DEHYDRATION REACTIONS BY SMECTITE CATALYSTS. P.A. O'Day, L.B. Williams,
J.R. Holloway, Arizona State Univ., Tempe, AZ, 85287-1404, and J.R. Delaney, Univ. of
Washington, Seattle, WA 98195

Since the discovery of a diverse, hydrothermally-supported biota at seafloor vents 20 years ago, mid-ocean ridge hydrothermal systems have been postulated as sites in which the abiotic synthesis of simple organic molecules might occur as precursors to the origin of life [1]. Previous work has focused on the role of sulfide catalysts in promoting carbon reduction and hydrocarbon synthesis, primarily by Fischer-Tropsch-type pathways [e. g., 2-3]. Clay minerals and zeolites have also been considered as templates for abiotic synthesis [e.g., 4]. The thermodynamics of a variety of dehydration reactions as a function of temperature and pressure were examined by Shock [5], but few studies have examined specific mechanistic pathways for organic synthesis by mineral catalysts under seafloor hydrothermal conditions.

In a previous study [6], we proposed that formation of C₁-C₄ alcohols may be possible metastable reaction products from seafloor diking events that generate elevated concentrations of CO₂ + H₂. Alcohol formation may be catalyzed by phase separation and reaction with newly precipitated sulfide surfaces in the optimum temperature range of 200-300°C at sub-seafloor pressures (200-500 bars). Solubility of C₁-C₄ alcohols increases with decreasing temperature, allowing for subsequent aqueous reactions with mineral surfaces. Dehydration reactions among short-chain alcohols in the presence of a strong Brønsted-acid catalyst have been shown to produce C₂-C₅ alkenes and C₆-C₈ aromatic compounds [7]. One proposed reaction mechanism is the formation of surface methoxy intermediates from methanol adsorbed at acidic oxygen sites, followed by dehydration and formation of C-C double bonds [8]. Calculations (using SUPCRT92) show that overall methanol dehydration reactions are thermodynamically favored at hydrothermal temperatures (100-375°C) and pressures (100-500 bars) in aqueous solution, and are generally more favored with decreasing temperature. Smectite or other sheet silicates with exchangeable interlayer sites would serve as effective sorbents of alcohols and as strong Brønsted-acid catalysts at low to circum-neutral pH. Recent discovery of significant amounts of smectite within sulfide edifices recovered from MOR vents, in which sulfide minerals are mixed within clay pods, suggests the possibility of natural catalysis by this alcohol-initiated pathway. Results from laboratory experiments of alcohol reaction with smectite under hydrothermal conditions will be discussed.

[1] J. B. Corliss, J. A. Baross, S. E. Hoffman, *Earth. Ocean. Acta* **SP**, 55 (1981).

[2] G. Wächtershäuser, *Prog. Biophys. Molec. Biol.* **58**, 82 (1992).

[3] M. J. Russell, R. M. Daniel, A. J. Hall, J. A. Sherringham, *J. Mol. Evol.* **39**, 231(1994).

[4] A. G. Cairns-Smith, *Genetic Takeover and the Mineral Origins of Life*. Cambridge University Press (1982).

[5] E. L. Shock, *Geochim. Cosmochim. Acta* **57**, 3341 (1993).

[6] P. A. O'Day, J. R. Delaney, M. D. Lilley, J. R. Holloway, *EOS* **78**, F774 (1997).

[7] C. D. Chang, A. J. Silvestri, *J. Catal.* **47**, 249 (1977).

[8] W. W. Kaeding, S. A. Butter, *J. Catal.* **61**, 155 (1980).

ROLE OF WATER IN PREBIOTIC NITROGEN CYCLES

J. A. Brandes, N. Z. Boctor, G. D. Cody, R. M. Hazen, and H. S. Yoder, Jr.

Geophysical Laboratory, Carnegie Institution of Washington, 5251 Broad Branch Rd,
NW Washington, DC 20015-1305

Nitrogen, prebiotic, aqueous chemistry

INTRODUCTION

Hydrothermal systems have been hypothesized as locations for the genesis of life. However, few experiments have been conducted that examine the interplay of biologically important compounds with minerals associated with these systems. One element generally neglected in the study of prebiotic chemistry is nitrogen. Several key questions in the study of the early Earth's nitrogen cycle are: How and under what conditions was reduced nitrogen formed? How was this reduced nitrogen incorporated into organic compounds, and what were the important parameters controlling the stability of these nitrogen containing organic compounds? A series of high pressure-hydrothermal reactions were undertaken to investigate these questions.

EXPERIMENTAL

Experiments were undertaken using a sealed gold tube (Kullerud & Yoder 1959) method. Samples were placed inside prewashed, combusted 99.95% pure Au gold tubes (10mm x 2 mm), followed by freezing and sealing of both ends by arc-welding. The sealed capsules were incubated at known temperature and pressure by use of an internally heated gas pressure device (Yoder 1950). After incubation, samples were frozen in liquid N₂, opened and extracted. Sample analysis for inorganic nitrogen was done by spectrophotometric methods (Strickland and Parsons, 1972), analysis for amino acids was done by ion-exchange HPLC followed by OPAH post-derivatization, and other organic compounds were analyzed by routine GC-MS techniques.

RESULTS AND DISCUSSION

The results for nitrogen gas reduction are shown in Figures 1 & 2. The amount of nitrogen reduction was significantly affected by the amount of water present in the system, with little observable N₂ reduction under hydrothermal conditions in the presence of excess water. This is hypothesized to occur because of the preferential binding of O to the catalytic FeO surface, preventing the binding of N₂ gas.

The role of water in the reductive amination of pyruvic acid, considered an essential step in early biochemical cycles, was investigated. The results (Fig. 3) indicate that the reaction only takes place in high yield at water:pyruvic ratios of 100:1 or greater. Finally, the stability of amino acids in hydrothermal systems was investigated. Our initial results indicate that certain common hydrothermal minerals have the ability to extend the stability of amino acids by many orders of magnitude.

REFERENCES

- Kullerud, G., & Yoder, H. S., Pyrite stability in the Fe-S system *Econ. Geol.*, 54, 534-550, (1959)
Yoder, H. S. High-low quartz inversion up to 10,000 bars. *Trans. Amer. Geophys. Union*, 31, 821-835, (1950)
Strickland, J. D. H., & Parsons, T. R., *A Practical Handbook of Seawater Analysis Fish. Res. Bd of Canada*, (1972)

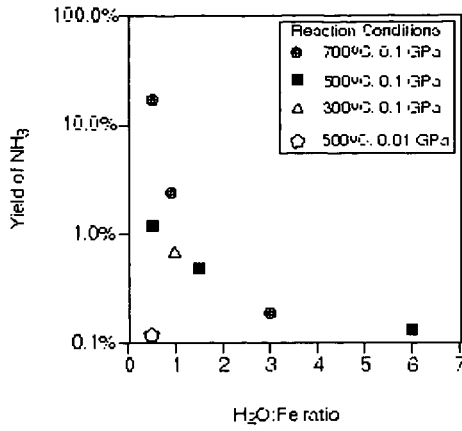


Figure 1. Production of ammonia from N₂ in the Fe:H₂O system

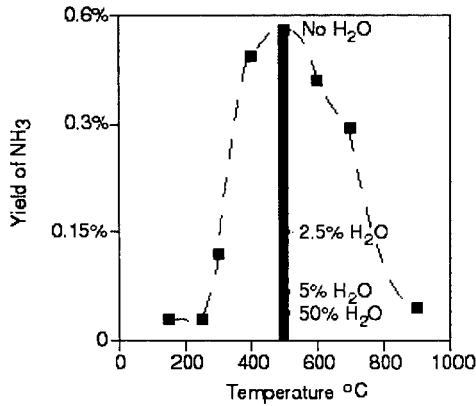


Figure 2. Production of ammonia from N₂ in the Fe₂O₃:H₂CO₂ system

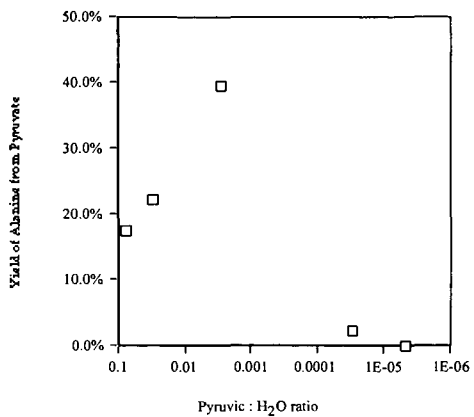


Figure 3. Effect of dilution upon reductive amination of pyruvate to form alanine

A PHYSICAL ORGANIC CHEMIST LOOKS AT HYDROUS PYROLYSIS

John W. Larsen

Department of Chemistry
Lehigh University
Bethlehem, Pennsylvania 18015

Keywords: hydrous pyrolysis, kerogen, water

INTRODUCTION. The invention and development of the hydrous pyrolysis technique by Mike Lewan is an important organic geochemical development and a fascinating reaction system.¹ This paper is a consideration of the reactions between kerogens and water which are a key part of hydrous pyrolysis and is based entirely on data from the literature. We begin with a consideration of the nature of water under hydrous pyrolysis conditions. A special concern here will be the question of contact between water and kerogen. The kerogens are three-dimensionally cross-linked-macromolecular systems and as such do not dissolve in water or any other solvent, but solvents can dissolve in the kerogen.² Another concern here is the possible mechanisms by which water and kerogens might react.

The solution of pentane or other light hydrocarbons in water is an exothermic process.³ These insoluble organic molecules have favorable interactions with water. Their insolubility is due to an enormously unfavorable entropy of solution, the familiar hydrophobic effect.³ As water is heated, its three dimensional hydrogen bonded structure becomes increasingly disarrayed and the entropy driven hydrophobic effect diminishes. The interactions which are responsible for the favorable enthalpy of solution remain so that as water is heated it increasingly becomes a non-polar solvent. This can be seen most easily by looking at the temperature dependence of water's cohesive energy density or its square root, the solubility parameter. These can be calculated as a function of temperature from the data in the Landolt Bornstein Tabellen⁴ and equation 1 where δ is the solubility parameter, ΔE_{vap} and ΔH_{vap} are respectively the energy and enthalpy of vaporization, and V_{mole} is the molar volume. Following Regular Solution Theory and its empirical thermodynamically illegitimate extensions, a liquid having the same δ as a polymer will be the best swelling solvent for it.⁵ As the two δ values (liquid and polymer) diverge, the sorption of the liquid by the polymer will decrease. The δ value for water decreases from 24 cal^{1/2}cm^{-3/2} at temperature to 7.4 cal^{1/2}cm^{-3/2} at 360°C, just below the critical temperature. At 350°C, the temperature used in hydrous pyrolysis, the solubility parameter is 9.1 cal^{1/2}cm^{-3/2}. The solubility for Type I kerogen is approximately 9.75 cal^{1/2}cm^{-3/2} and it is expected that the water will dissolve in and have access to all portions of the kerogen under hydrous pyrolysis conditions. It should also swell the kerogen to whatever extent is permitted by the structure of the surrounding rock.

Equation 1

$$\delta = \left(\frac{\Delta E_{vap}}{V_{mole}} \right)^{1/2} = \left(\frac{\Delta H_{vap} - RT}{V_{mole}} \right)^{1/2}$$

While water probably is soluble in kerogen under hydrous pyrolysis conditions, the situation under geological maturation conditions is not as clear. The oil window occurs at much lower temperatures, temperatures at which the solubility parameter for water is so high as to effectively preclude its dissolution in the kerogen at 200°C, the solubility parameter for water is 19 cal^{1/2}cm^{-3/2}. Only if the kerogen is inhomogeneous on the molecular level might water gain access to polar regions. This "first order" consideration of the solubility of water in Type I kerogen raises a concern about using hydrous pyrolysis as a model for geological kerogen maturation. Type II kerogen will probably be similar to Type I.

If temperature were the only variable, the situation would be simple, but we also need to consider pressure effects and salt effects. Lithostatic pressures between 800 bar and 1000 bar are commonly encountered during kerogen maturation.⁶ These pressures and the temperatures encountered in petroleum kitchens can have significant effects on the solubility of organic molecules in water.⁷ This can be seen most easily in Figure 1 which shows the effect of temperature and pressure on the miscibility of water and 4-methylpiperidine.⁷ The addition of salt

can complicate the situation enormously as shown in Figure 2. The situation is sufficiently complicated so that I am unwilling to reach a conclusion as to the solubility of water in kerogen under the conditions existing in petroleum kitchens. This is an important point for understanding not only what is going on in hydrous pyrolysis, but also its use to model kerogen maturation.

The next concern is the mechanisms by which the kerogens and water react. There are three strong indications that this reaction does not occur by radical pathways. As pointed out by Dave Ross, at 330°C β -scission of an alkyl radical is 300 times faster than hydrogen abstraction from water so olefin formation will greatly exceed saturates formation.⁸ Formation of large amounts of olefin in hydrous pyrolysis has not to my knowledge been reported and olefins are rare components of crude oils.⁶ Lewan has carried out hydrous pyrolysis in the presence of added H₂ and did not observe any significant change in the product distribution.¹ The bond in water at 119.1 kcal/mole is much stronger than the bond in H₂ at 104.2 kcal/mole.⁸ A radical that can abstract H from water will abstract H from H₂ much more rapidly so a significant change in the product distribution is expected when hydrogen is added to the hydrous pyrolysis system if it is undergoing a radical reaction with water. The only thing which might affect this would be inaccessibility of hydrogen to the reacting centers and this seems unlikely. Finally, there has been one study of pure compounds under hydrous pyrolysis conditions using simulated oil field brine.¹⁰ n-Hexadecane cracked to give alkanes and olefins in reactions that were inhibited by a radical hydrogen donor. These results are best explained using radical reactions. There was no evidence of hydrogen abstraction from or oxidation by water. These three lines of evidence lead to the conclusion that the reactions between kerogen and water are not occurring by a radical process.

Direct reaction between water and some functional groups is possible, but it is hard to envision hydrocarbon formation from kerogens based solely on water-kerogen reactions of the type so thoroughly studied by Siskin and Katritsky.¹¹ Both Ross and Helgeson et al have argued for involvement of mineral matter in reactions between organics and water.^{12,13} Ross argued for the possibility of a mineral matter catalyzed oxidation of hydrocarbons by water and Helgeson et al argued that in oil reservoirs, hydrocarbons, water, minerals, carboxylic acids and CO₂ had reached thermodynamic equilibrium. In both cases, mineral matter is involved in the oxidation of hydrocarbons by water. This is shown most directly using the scheme below taken directly from a paper by Dave Ross. In it, a hydrocarbon is cleaved and oxidized to CO₂ by a metal oxide, for example an iron oxide which is reduced in the process. In the second step of the reaction, the reduced metal oxide is reoxidized by water generating a pair of hydrogen atoms which are added to an organic molecule. The net reaction is the oxidation of the organic material, kerogen, by water catalyzed by mineral matter. The thermodynamics of this are favorable as long as the end products are carboxylic acids or carbon dioxide. The thermodynamics are not favorable for the formation of intermediate carbon oxidation states such as alcohols or aldehydes. There is some evidence for this chemistry occurring. Eglinton studied the hydrous pyrolysis of several immature kerogens and measured, among other things, the formation of carboxylic acids.¹⁴ The addition of limonite to Kimmeridge kerogen tripled the amount of carboxylic acids formed. The limonite was not altered (XRD analysis). It seems that limonite catalyzes carboxylate formation from Kimmeridge kerogen during hydrous pyrolysis. This is in general agreement with Ross's scheme and Helgeson et al observations.

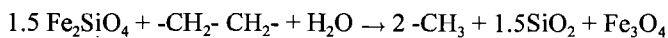
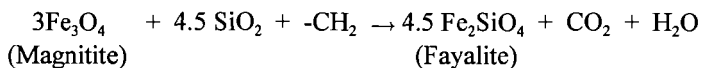
The hydrous pyrolysis reaction system is intriguing both physically and chemically. It is an excellent entree to the chemistry responsible for kerogen maturation and has the advantage that it can be studied in our lifetimes. It is a major step forward and worthy of very careful scrutiny.

ACKNOWLEDGMENTS: Acknowledgment is made to the Donors of the Petroleum Research Fund, administered by the American Chemical Society, for the partial support of this research. I would like to thank Drs. Raymond Michels and Patrick Landais and the CNRS for three wonderful months in Nancy during which time many of the ideas in this paper were initially developed.

REFERENCES

1. Lewan, M. *Geochim. Cosmochim Acta* **1997**, *61*, 3691-3723 and references therein.
2. Larsen, J. W.; Li, S. *Organic Geochem* **1997**, *26*, 305-309.
3. Tanford, C. *The Hydrophobic Effect: Formation of Micelles and Biological Membranes* Krieger Publishing Co., Malabar, FL: **1991**
4. Landolt-Bornstein Tabellen, Band IV, 4 Teil, Springer-Verlag, Berlin **1967**, pp. 426-439.
5. Hildebrand, J. H.; Prausnitz, J. M.; Scott, R. L. *Regular and Related Solutions* Van Nostrand Reinhold Co., New York: **1970**.
6. Hunt, J. M. *Petroleum Geochemistry and Geology* W. H. Freeman and Co., New York: **1996**.
7. Schneider, G. M. *Water. A Comprehensive Treatise, Vol. 2*, F. Franks, Ed., Plenum Press, New York, **1973** Cp. 6.
8. Ross, D. S. *Prepr. Pap. Am. Chem. Soc. Fuel Div.* **1992** 1555-1566.
9. Lide, D. R. Ed., *CRC Handbook of Chemistry and Physics* 72nd Ed., **1991**.
10. Weres, O.; Newton, A. S.; Tsao, L. *Org. Geochem.* **1988**, *12*, 433-444.
11. Katritzky, A. R.; Allin, S. M.; Siskin, M. *Acci. Chem. Res.* **1996**, *29*, 399-406.
12. Ross, D. S., *4th Intl. Symp. On Hydrothermal Reactions*, Nancy, France, **1992**.
13. Helgeson, H. C.; Knox, A. M.; Owens, C. E.; Shock, E.L. *Geochim Cosmochim. Acta*, **1993**, *57*, 3295-3339.
14. Eglinton, T. I.; Curtis, C. D.; Rowland, S. J. *Mineral Mag.* **1987**, *51*, 495-503

Scheme 1 (from reference 12)



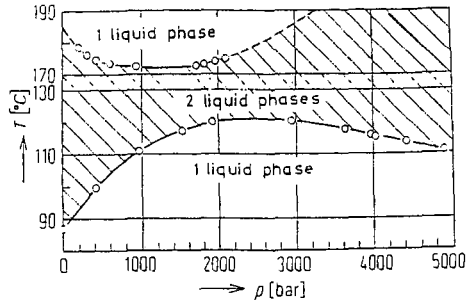


Fig. 1. Pressure influence on liquid-liquid immiscibility in the system 4-methylpiperidine-H₂O for $\chi = \text{const.} \approx \chi_c^{\text{lcst}}$ at 1 bar (from ref. 7).

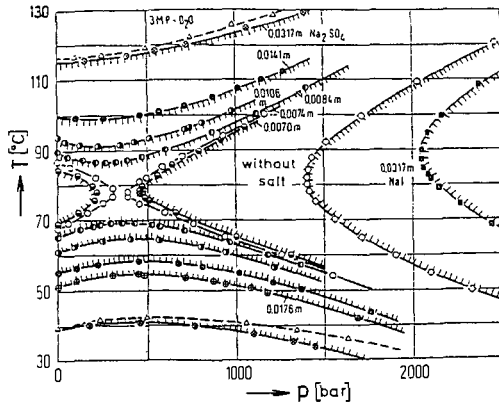


Fig. 2. Salt and pressure effects on liquid-liquid immiscibility in the system 3-methylpyridine-H₂O wt.% water/wt% 3-methylpyridine = const. = 7/3; (from ref. 7).

PROCESSES LEADING TO INCREASE OF ALKYL CHAIN LENGTHS UNDER HYDROUS PYROLYSIS CONDITIONS

Tanja Barth and Birthe G. Hansen
Department of Chemistry, University of Bergen,
Allégaten 41, N-5007 Bergen, Norway

KEYWORDS:

Hydrous pyrolysis, polymerisation, short-chain carboxylic acids

INTRODUCTION

In the last decades, various kinds of pyrolysis procedures have been used to simulating petroleum generation from source rocks or kerogen, and the effect of water on the saturated hydrocarbon yields has been a matter of debate. Pyrolysis processes tend to give a larger proportion of both unsaturated compounds and polar compounds than in natural petroleum, where the aliphatic hydrocarbon fraction is normally the major constituent. Confined system pyrolysis with excess water present during pyrolysis results in a more hydrocarbon-rich product with a composition more similar to natural petroleum than products from unconfined and dry pyrolysis (Lewan, 1997). Confined pyrolysis in gold tubes, with a compressed gas phase and some excess water produced in the initial reactions, also give a high proportion of aliphatic products (Michels *et al.*, 1995).

The generally accepted model for hydrocarbon generation assumes that a given quantity of aliphatic chains is present in the polymeric kerogen material, and is released in the thermal cracking of the polymer. In this model, water functions as a hydrogen donor and increases the amount of saturated products after an initial cracking step. In confined systems with less water, other constituents, including hydrogen gas produced during pyrolysis, may function in a similar way. However, both models imply that the total amount of aliphatic compounds possible to generate is limited by the amount of alkyl units initially incorporated in the starting material.

However, pyrolysis experiments with simple compounds show that polymerisation type reactions producing liquid phase products also occur. Investigations on the thermal stability of organic acids in formation waters (Andresen *et al.*, *in press*) and gases in hydrothermal systems (Berndt *et al.*, 1996) show the generation of larger hydrocarbon molecules from small reactants. To explain such observations, polymerisation reactions of gaseous molecules with water involved in the reaction seem the most relevant pathway.

In this presentation, observations of alkyl chain generation in "classical" hydrous pyrolysis of simple compounds will be shown to reproduce the series of homologous organic acids found in waters in the vicinity of oil, and also contribute to the long-chain hydrocarbon compounds that are found in the petroleum phases. The possibility of a Fischer-Tropsch mechanism for the polymerisation step will be discussed.

EXPERIMENTAL

Hydrous pyrolysis of simple organic compounds has been performed in stainless steel autoclaves. In one series of experiments, formic acid (HCOOH) is used as the organic reactant. The gaseous, aqueous and extractable products have been analysed for an experimental design on the experimental conditions, varying the parameters in the following range: *Reactors*: Parr 71 ml(=L), SS tubes 10 ml (S); *Temperatures*: 300-380 °C; *Head-space to liquid volume ratios(subcritical)*: 0.1-0.9; *Water/formic acid ratio*: 0 - 9; *Presence of mineral phase (goethite)*: present/absent; *Oil phase (cyclohexane)*: present/absent. All experiments have had a duration of 72 hours. After the experiment, quantitative analyses were made of the generated gas phase for hydrocarbon gases including hydrogen and carbon monoxide in some cases, the aqueous phase was analysed for content of dissolved organic compounds and the oil phase products were extracted, quantified gravimetrically and analysed by GC.

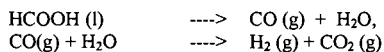
For comparison, the results from similar experiments are given for a Kimmeridge source rock.

RESULTS AND DISCUSSION

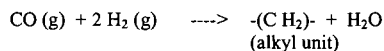
Products with increased alkyl chain length were consistently found both in the gas phase and aqueous products. In the experiments using the small reactors, wax profiles were observed in the extractable organic fraction (Figure 1). Selected experimental results are summarised in Table 1.

The results confirm observations from previous experiments with acetate cracking in gold tubes, which gave generation of a wide spectrum of longer-chain products, including C₃-C₆ hydrocarbon gases and C₇+ hydrocarbons with chain lengths up to C₃₂ (Andresen *et al.*, *in press*). Considerable levels of carbon monoxide was also found in the gas phase, while hydrogen was not analysed.

In the new experiments with formic acid (HCOOH) as the starting material, polymerisation reactions is the only possibility for generation alkyl chains. Formic acid rapidly decomposes and reacts with water upon heating:



and the products can polymerise by a surface catalysed Fischer-Tropsch mechanism:



Carboxylic acids are a well-known product from such reactions. The distribution of homologues expected from this mechanism correspond to the distribution generally observed in oil-field waters, with an exponential reduction of concentration relative to acetic acid with increasing carbon number. This distribution has also been observed in all hydrous pyrolysis experiments performed at this laboratory, and it seems to be

completely independent of the type of organic starting material (single compounds, biomass or sedimentary organic material).

As shown by the results given in Table 1, there is a considerable effect from variations in the reaction conditions with regards to the product composition. The choice of reactor is one major factor. n-Alkanes in the wax range, as shown in the chromatogram in Figure 1, were found in higher than trace amounts only in the experiments using the small stainless steel reactors. This can be caused either by differences in the catalytic activity of the reactor surfaces, or by the relatively higher loading in the small reactors, which will give higher concentrations of reactive gas phase species. At present it is not clear what is the limiting factor for the alkane formation.

REFERENCES

- Andresen, B., T.Barth, I.Johansen and K. Vagle (1998) Thermal stability of aqueous acetate *Organic Geochemistry*
- Barth, T., Borgund A.E. and Hopland A.L. (1989) Generation of organic compounds by hydrous pyrolysis of a Kimmeridge Oil shale - bulk results and activation energy calculations. *Organic Geochemistry*, **14**, 69-76.
- Berndt, M.E., Allen, D.E. and Seyfried, W.E. (1996) Reduction of olivine at 300 degrees C and 500 bar. *Geology*, **24**, 351-354
- Lewan, M.D. Experiments on the role of water in petroleum formation. *Geochimica et Cosmochimica Acta*, **61**, 3691-3723.
- Michels, R., Landais, P., Torkelson, B.E. and Philp, R.P. (1995) Effects of effluents and water pressure on oil generation during confined pyrolysis and high-pressure pyrolysis. *Geochimica et Cosmochimica Acta*, **59**, 1589-1604.

Table 1. Composition of products from selected pyrolyses

Reaction conditions	Gas phase (% of initial C)				Aqueous acids (mM)			HC chains ?	
	CO ₂	CO	CH ₄	H ₂	C ₁	C ₂	C ₃		
Formic acid									
S/330 /-w	Not measured				0.75	17.10	4.92	C ₇ -C ₂₅	
S/330 /-w,+min.	Not measured				0.60	10.28	2.34	C ₈ -C ₂₈	
S/300 /-w (Fig.1)	Not measured				3.03	3.34	0.63	C ₈ -C ₃₁	
S/380 /-w	Not measured				0.50	3.39	1.91	C ₉ -C ₃₂	
S/380 /+w,+C C ₁₄ -C ₃₂	Not measured					3.30	7.26	1.18	
S/380 /+w,	Not measured				2.96	3.93	0.89	C ₁₉ -C ₃₁	
L/330 /+w,+min.	46.5	n.m.	0.18	n.m.	0.82	0.76	0.56	-/trace	
L/380 /+w,+C /trace		43.8	n.m.	0.28	n.m.	6.28	1.21	0.10	
L/380 /+w,+min.+C	70.4	n.m.	0.07	n.m.	0.51	0.50	0.004	-/trace	
L/380 /+w	18.6	n.m.	0.02	n.m.	0.49	0.12	0.09	-/trace	
L/330 /+w	23.6	0.76	0.02	n.m.	0.98	0.09	0.05	-/trace	
L/330 /+w,+min	16.3	0.26	0.02	n.m.	0.58	0.74	0.15	-/trace	
Kimmeridge source rock -standard hydrous pyrolysis (Barth et al. 1989)									
L/300 to >C ₂₉		4.8	n.m.	0.4	0.06	tr	13.15	2.45	up
L/330		7.8	n.m.	1.3	1.84	tr	14.26	2.71	
L/350 C ₁₀ -C ₃₀		10.4	n.m.	1.5	1.75	tr	12.38	2.80	

n.m.: Not measured

-: Below detection level

Figure 1.

Gas chromatogram of the alkane profile from experiment 3, Table 1.

Column: HP-5, 25m; Temperature program: 40°C*1 min, 6°C/min to 290°C *5 min., FID detector.

IMPORTANCE OF THE POLARS AS INTERACTION MEDIUM WITH WATER DURING HYDROUS PYROLYSIS OF WOODFORD SHALE.

V. Burkle¹, R. Michels¹, E. Langlois¹, P. Landais¹ and O. Brevart²

¹ UMR7566/CREGU Universite Henri Poincare BP239 54506 Vandoeuvre les Nancy, France

² Elf Exploration Production CSTJF 64018 Pau, France

Keywords: hydrous pyrolysis, shale, petroleum generation

INTRODUCTION

The thermal degradation of kerogen leads to the formation of a complex system in which gases, water, free hydrocarbons, polars and the residual kerogen are in close contact. The simulation of the formation of the bitumen wetted kerogen during artificial maturation allows to study the close interactions between the various phases formed. Previous studies have compared the influence of the reaction medium on the generation of hydrocarbons in hydrous pyrolysis conditions (where water is added to the sample) and confined pyrolysis (no water is added to the sample)^{1,2}. These experiments could account for the effect of an external phase on the thermal evolution of type II kerogen. Other studies, (using a combination of pyrolysis and selective extractions) have focused on the role of internal media (free hydrocarbons, polars, residual kerogen) in the maturation processes and interactions with water during the maturation of type III organic matter^{3,4}. The comparison between the two types of studies allows to precise the respective role of the organic reactants versus water in the chemical control of the organic system.

Although the role of liquid water is capital in hydrous pyrolysis, the role of the organic phases generated, the interactions between themselves and their interactions with water need still to be clarified. The following study aims to describe the reactivity of the organic system and its interactions with water in relation to the generation of hydrocarbons during hydrous pyrolysis of Woodford shale.

EXPERIMENTAL

The sample used is Woodford shale (WD26; 22%TOC; HI=401mgHC/gTOC, Tmax=427°C), collected in the Anadarko basin, Oklahoma. Powdered shale aliquots (10g) were loaded in stainless steel reactors (30cm³ internal volume) pyrolyzed in the presence of 100 weight% water at temperatures between 260°C and 365°C for 3 days (temperature measurements were performed through an internal thermocouple in contact with the sample). Several maturation series were performed: 1) a reference series, called HP 2) a series called HPEC in which a same shale aliquot was treated the following way: pyrolysis at temperature T1, subsequent chloroform extraction; pyrolysis of the extracted sample at T2, subsequent chloroform extraction. This process was performed until 365°C. 3) a series called HPEP in which a same shale aliquot was treated the same way as for the HPEC series, but the extracting solvent was pentane.

In the HPEC and HPEP series, the same shale aliquot was repyrolyzed several times. Therefore, the pyrolysis time-temperature pair was compensated by TTI calculations in order to obtain maturation series that have reached TTI values identical to the reference series. However, for convenience, maturation scales are indicated in temperature and not in TTI, as far as the effective pyrolysis temperatures are not much different for all the series.

The samples were extracted either by hot chloroform or pentane for 45 minutes. No distinction was made between the expelled phase and the bitumen.

In order to quantify the polars yields and for further analysis of the solid residue, the samples of the HPEP series were also extracted by chloroform.

The asphaltenes were precipitated in hot heptane for 15 minutes and filtered. The maltene fraction was fractionned on alumina and silica micro-columns in resins, aromatics and saturates. All fractions were quantified.

PyGCMS was performed on chloroform extracted residues with a Pyroprobe CDS2000 connected to a HP5980 Series II Plus gas chromatograph coupled with a HP5972A mass spectrometer. The GC was equipped with a 60m DB-5 ms column initially held at 0°C for 5 min, then heated to 300°C at 5°C/min and held at 300°C for 15min.

RESULTS

Figure 1 shows the polars and aliphatics cumulated yields obtained for each series as well as the non cumulated values for the HPEC series. The yields obtained with the experimental procedures used have different meanings and therefore, some values must be mathematically cumulated in order to allow comparisons. The data for the reference series are always cumulative values, as far as the reactor is loaded with a new shale aliquot at each pyrolysis step, and no mathematical treatment needs to be done. For the HPEP series, the resins yields have been cumulated and added to the non cumulated asphaltene yields of each experiment (asphaltenes are not removed from the sample at each pyrolysis step).

Up to $T=300^{\circ}\text{C}$, Figure 1 shows similar values for the polars yields of the reference and the cumulated HPEP series. The cumulated HPEC series on the contrary are far stronger at $T>300^{\circ}\text{C}$. The secondary cracking of the polars during hydrous pyrolysis can be estimated from these data. The values for the reference series decrease at $T>300^{\circ}\text{C}$, while the polars generation potential of the kerogen is not totally exhausted (there is a difference of about 55mg/g of rock between the reference series and the cumulated HPEC series at 330°C). Therefore, it seems that the « real » maximum bitumen generation occurs at 350°C and not 300°C as shown by the maximum non cumulated yield of the HPEC series (occurring at 350°C) and the flattening of the HPEC cumulated curve. However, additional experiments at 310°C would be necessary in order to confirm this aspect. The removal of the hydrocarbons and part of the resins by pentane extraction does not modify the polars yields in the $260\text{-}300^{\circ}\text{C}$ range as shown by Figure 1.

Figure 1 also shows the aliphatics yields for the reference series and the cumulated values for the HPEC-HPEP series as well as the non cumulated values for the HPEC series. At $T>330^{\circ}\text{C}$, the cumulated aliphatic yields are far higher for the HPEC series than for the others. In addition, the non cumulative aliphatic yield for the HPEC series decreases, indicating that the kerogen alone is not able to generate additional hydrocarbons. The HPEP series shows always the lowest yields, even when cumulated.

As for the polars, the maximum aliphatic yield observed at 330°C is only apparent. The HPEC series shows that the kerogen is able to generate hydrocarbons up to 350°C . The low values for the HPEP series indicate that the removal of the maltenes has a deleterious effect on the capacity of the kerogen+asphaltenes assemblage to generate hydrocarbons.

It is difficult to estimate the secondary cracking of the aliphatics as far as 1) the reference series includes the aliphatics generated by the kerogen and the polars, while the HPEC series includes only the generation from the kerogen 2) the generation of aliphatics from the kerogen+asphaltenes assemblage is modified by the removal of the maltenes.

Table I and Figure II are respectively the Rock-Eval data and the PyGCMS chromatograms of the chloroform extracted samples. Despite the different pyrolysis conditions, these data are identical for all maturation series. This shows that the kerogen itself is not much influenced by the removal of either the polars+hydrocarbons or the maltenes.

DISCUSSION AND CONCLUSION

The use of the successive extraction-maturation series (HPEC and HPEP series) allows to investigate the role of the bitumen as well as the maltenes on the maturation of kerogen in hydrous conditions. The removal of the bitumen or the maltenes at each maturation step does not influence the generation of the polars from kerogen. It seems therefore that the polars and the hydrocarbons do not have a great influence on the initial thermal breakdown of Woodford kerogen in hydrous pyrolysis. As far as Lewan⁵ reached similar conclusions through his anhydrous versus hydrous pyrolysis conditions, it may be concluded that neither the polars+hydrocarbons nor water influence the initial thermal breakdown of the kerogen. This may support the idea that this stage resembles a « depolymerization » process⁶.

The situation is somewhat different when the generation of aliphatic hydrocarbons is considered. The removal of the bitumen (HPEC series) at each maturation step does not influence the aliphatic generation from the kerogen. However, the data show that the aliphatic generation from the kerogen is almost exhausted at $T \geq 350^\circ\text{C}$. On the contrary, the aliphatic yield is strongly lowered in the HPEP series (removal of the maltenes) whatever the temperature: the kerogen+asphaltenes assemblage yields less aliphatics than the kerogen alone (HPEC). This might be surprising as far as the polars content of the system decreases. However, the decrease in polars is not counterparted by the generation of C_{15} aliphatics. For Mahakam coal^{4,5}, such behavior has been attributed to crosslink reactions between the asphaltenes and the kerogen in the absence of the maltenes. However, the effect must be less important for Woodford kerogen in the conditions described here, as far as the Rock-Eval Tmax and the pyGCMS chromatograms are not modified (these parameters were strongly influenced in the experiments using Mahakam coal^{4,5}).

These results suggest that the presence of liquid water is not the only necessary condition to allow the generation of aliphatics from the type II kerogen+asphaltenes assemblage. Indeed, water and the maltenes need to be present together in order to allow good conditions for aliphatics generation. As far as the kerogen alone yields higher amounts than the kerogen+asphaltenes assemblage, it is suggested that the maltenes in addition to water avoid the crosslink reactions of the asphaltenes with the kerogen during maturation

ACKNOWLEDGEMENTS The authors wish to thank Elf EP for financial support and M. D. Lewan for providing the Woodford samples.

REFERENCES

- 1 Michels R., Landais P., Philp R. P., and Torkelson B. E. (1994) *Energy Fuels*, 8, 741-754.
- 2 Michels R., Landais P., Torkelson B.E. and Philp R.P. (1995) *Geochim. Cosmochim. Acta*, 59, 1589-1604.
- 3 Mansuy L. and Landais P. (1995) *Energy Fuels*, 9, 809-821.
- 4 Mansuy L., Landais P. and Ruau O (1995) *Energy Fuels*, 9, 691-703.
- 5 Lewan M. D. (1998) *Geochim. Cosmochim. Acta*, 61, 3691-3723
- 6 Larsen J. W. and Li S. (1997). *Energy Fuels*, 11, 897-901

TABLE I Rock-Eval data on raw Woodford Shale and on pyrolyzed samples HP. Hydrous pyrolysis reference series. HPEC successive pyrolysis- chloroform extraction series. HPEP successive pyrolysis- pentane extraction series. All samples chloroform extracted prior to Rock-Eval pyrolysis.

Pyrolysis Temperature ($^\circ\text{C}$)	HP		HPEC		HPEP	
	Tmax ($^\circ\text{C}$)	HI mgHC/gC	Tmax ($^\circ\text{C}$)	HI mgHC/gC	Tmax ($^\circ\text{C}$)	HI mgHC/gC
Raw Woodford Shale	427	401				
278	440	349	438	390	438	371
298	442	305	441	319	442	287
329	453	126	453	109	454	101
346	461	57	468	38	466	50
358	554	21	540	19	-	-

FIGURE 1 Polars and C₁₅⁺ aliphatics yields for the HP, HPEC and HPEP series. Cumulated and non cumulated values as indicated. The reference series (HP) values are intrinsic cumulative data as far as a new shale aliquot is loaded in the reactor at each pyrolysis temperature.

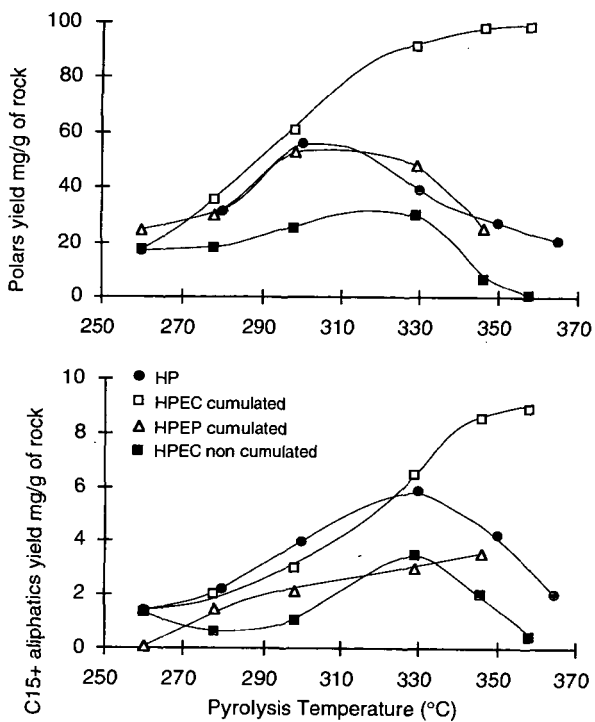
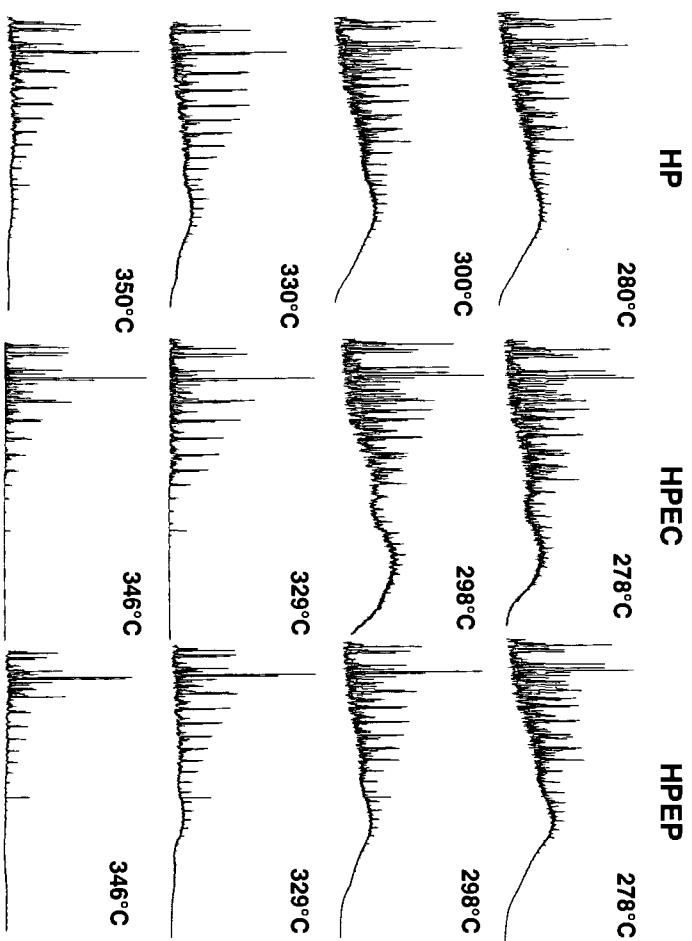


FIGURE 2 PyGCMS chromatograms of the chloroform extracted residue for each pyrolysis series



COMPETITION BETWEEN THE ORGANIC MATTER AND WATER IN THE HYDROGEN TRANSFER REACTIONS DURING ARTIFICIAL MATURATION.

R. Michels¹, V. Burkle¹, L. Mansuy¹, E. Langlois¹, P. Landais¹ and O. Brevart².

¹ UMR7566/CREGU UHP BP239 54506 Vandoeuvre les Nancy, France

² Elf Exploration Production CSTJF 64018 Pau, France

Keywords: artificial maturation, coal, kerogen

INTRODUCTION

The quantity, quality and timing of oil generation from source rock is directly dependant upon the type of organic present in the sediment. Type II are considered as oil prone, while type III is rather considered as gas prone, although some coals are sources of economic oil fields. The initial nature of the kerogen being significantly different in type II and III kerogens, it is important to study the similarities or differences of the chemical reactions taking place in both during maturation. Water is considered as an important parameter in the generation of hydrocarbons and is suspected to act as a source of hydrogen. However, coals are known to contain significant amounts of hydronaphthalenics able to efficiently provide hydrogen to organic reactions. Also, type III kerogens are richer in aromatics than type II kerogens and undergo more readily aromatization reactions which provide abundant hydrogen to the surrounding medium.

The following experiments compare the role of the free hydrocarbons, polars and water in the maturation and oil generation capabilities of type II kerogen (Woodford) and type III coal (Mahakam). The aim of the study is to identify the interactions between organic moieties (residual kerogen, polars, free hydrocarbons) and of these moieties with water. It is suspected that the dominant hydrogen sources and transfer mechanisms are different depending on the availability of specific hydrogen sources and on the stages of maturation of each kerogen type.

EXPERIMENTAL AND ANALYTICAL

The samples used are Woodford kerogen (Devonian Type II, Anadarko basin, Oklahoma, USA; T_{max}=422°C, HI=534mgHC/gOC) and Mahakam coal (Tertiary Type III, Mahakam delta, Kalimantan, Indonesia; T_{max}=418°C HI=258mgHC/OC). Experiments were performed by confined pyrolysis¹ (250-370°C, 24 and 72 hours, 700 bars). The experiments using successive pyrolysis of a same sample aliquot were adjusted to the reference series using temperatures adjusted by Time Temperature Index calculations². Several experimental series were performed: 1) standard pyrolysis (CP) in which the gold cell is loaded with fresh sample at each maturation stage 2) EC series in which a unique sample aliquot is isothermally heated from 250 to 370°C and chloroform extracted (removal of the bitumen) after each pyrolysis step. 3) EP series using the same procedure as for the previous series, but chloroform is replaced by pentane (removal of the free hydrocarbons and part of the resins after each pyrolysis step). 4) these series were also performed in the presence of 100 weight percent water (ECO and EPO series).

Hot chloroform and pentane extraction were performed on powdered samples during 45 minutes. For the CPEP series, the aliquots of the residual solid obtained after pentane extraction were extracted by chloroform for the quantitation of the asphaltenes. In such experiments, pentane yields values must be cumulated in order to be comparable to the CP and CPEC series, while the values for asphaltenes are not (they are intrinsic cumulative values as far as they remain in the reactor at each maturation step). Therefore, the cumulative pentane extraction yields are summed with the asphaltenes yields obtained at each temperature in order to obtain the cumulative bitumen yields. The residual kerogen (chloroform extracted) were analyzed by Rock-Eval pyrolysis and Py-GCMS (Pyroprobe CDS2000 connected to a HP5980 Series II Plus gas chromatograph coupled with a HP5972A mass spectrometer. The GC was equipped with a 60m DB-5 ms column initially held at 0°C for 5 min, then heated to 300°C at 5°C/min and held at 300°C for 15min).

RESULTS AND DISCUSSION

Figure 1 compares the effect of the removal of the bitumen, of the absence of the resins+free hydrocarbons and of the presence of water on the capacity of the residual kerogen (EC-ECO series) and kerogen+asphaltenes assemblage (EP-EPO series) to generate bitumen. General trends of the behavior for both kerogens appear: the cumulative bitumen yields for the EC and ECO series give values close to the maximum bitumen yield of the reference series. The removal of the resins+free hydrocarbons (EP series) lead to a deficit in the generation of bitumen. However, the effects are stronger for the coal than for the type II kerogen.

The addition of water to the sample in the chloroform extracted series (ECO experiments) does not change much the results for type II kerogen, while the effect is stronger for type III. In the pentane extraction series, the addition of water (EPO series) clearly improves the yields for both kerogens.

The removal of specific organic phases and the addition of water can also be followed through the analyses obtained on the residual kerogen. T_{max} values increase faster with maturation in the EC and EP series (Figure 2). The removal of the resins+hydrocarbons has strongest effect on the coal. For type II kerogen, the fastest T_{max} increase occurs in the EC series. In general, the extraction of the bitumen (EC) or resins+hydrocarbons (EP) has a smoother effect on the type II kerogen than on type III.

The addition of water retards the increase of T_{max} with maturation. With Mahakam coal, the effect is clear in the ECO series while the strongest retardation is noticed with the EPO series. For type II kerogen, the ECO is not much different from the EC series, while the EPO series shows the strongest effect (as for the coal).

The impact of the extractions on the structure of the residual kerogen were followed by PyGCMS (Figure III). For type III, the removal of the bitumen (EC series) or of the resins+hydrocarbons (EP series) leads to the destruction of the hydrocarbon potential (no free hydrocarbons are generated to counter part the loss of hydrocarbons in the coal). The presence of water in the ECO series allows a better preservation of the hydrocarbon potential of the coal. The effect is much stronger in the EPO series (kerogen+asphaltenes assemblage). This potential is also well preserved in the reference series.

For type II kerogen, the removal of the bitumen (EC series) leads to a PyGCMS chromatograms containing less aliphatics than the reference. For the EP series the results are fairly similar to the reference. The addition of water (comparison of the EC and EP chromatograms with the ECO and EPO series) has not much effect on the Py-GCMS chromatograms.

DISCUSSION AND CONCLUSION

In both types of kerogen, the removal of the bitumen does influence the yields, but the effects are rather limited. On the contrary, the removal of the resins+free hydrocarbons strongly decreases the bitumen yields, especially for the coal. The thermostability of the kerogen (T_{max} in the EC series) and the kerogen+asphaltenes (EP series) increases faster than for the reference series. This effect is related to an increasing aromaticity of the residue and a loss of the aliphatic potential of the sample (as followed by Py-GCMS and Mansuy et al.). This effect is however far stronger for the coal than for type II kerogen. These experiments show that the resins+hydrocarbons play a crucial role in the generation of hydrocarbons from kerogen. The kerogen+asphaltenes assemblage needs the presence of the resins+hydrocarbons in order to generate the bitumen. The presence of the resins+hydrocarbons avoids the crosslink of the kerogen+asphaltenes during maturation, which leads to the loss of the hydrocarbons potential in the kerogen^{2,3}

For the coal, the addition of water improves the yields in presence of the kerogen alone (ECO series) and in the presence of the asphaltenes (EPO). At the same moment, the thermostability of the residue (Table I) increases later in the maturation profile while the hydrocarbons potential in the kerogen is better preserved, especially in the EPO series (Figure III). For type II kerogen, water does not modify the behavior of the kerogen alone (EC and ECO series). A clear improvement is however noticed on the bitumen yields in the EPO series. Water also retards the increase of the Rock-Eval T_{max} with maturation (the effect is moderate in the ECO series for type II kerogen, but significant for the EPO series). The PyGCMS chromatograms are however not very conclusive concerning the preservation of the aliphatic potential in the residual kerogen

These data suggest that in the kerogen and especially in the kerogen+asphaltenes assemblage, chemical functions allowing the interaction with water are present. These interactions allow a better preservation of the oil potential in the kerogen and improve the generation of the bitumen from the kerogen+asphaltenes assemblage. It must however be noticed that the addition of water to the kerogen+asphaltenes (EP and EPO series) never totally restores the generation capability of the kerogen (either reference series or EC+ECO series). Therefore, it can be concluded that the full capacity of the organic matter to generate the bitumen needs the presence of the resins, the free hydrocarbons and water. In the reference series, these conditions are reached as far as the sample generates all of these ingredients during confined pyrolysis. The kerogen alone, as shown by the EC and ECO series behave fairly closely to the reference series. This shows that the crucial chemical interactions leading to good conditions of the generation of bitumen avoid crosslink reactions between the asphaltenes and the kerogen and allows a good preservation of the hydrocarbons potential.

The close contact between the kerogen, the asphaltenes, the resins, the hydrocarbons and water are therefore responsible for proper generation of bitumen. Specific oxidation of the polars by water during hydrous pyrolysis could be evidenced on Woodford Shale⁴. These results strongly suggest that water preferentially interacts with the polars (through oxidation-reduction reactions) during maturation. The fact that the addition of water in the EPO series never completely restores the generation capabilities as seen in the reference series suggests that other compounds are acting in the chemical network.

A closer analysis of the polars and kerogen from Mahakam coal (for which the removal of the resins+hydrocarbons has the most drastic effect) lead to identify the presence of significant amounts of hydronaphthalenics. These compounds are known to be very effective in the radical hydrogen transfer reactions during the pyrolysis of coal. Also, the strong abundance of naphthalenes in the aromatics generated by the coal during maturation is a good marker of hydronaphthalenic precursors. The removal of the polars by pentane extraction would remove this source of hydrogen and contribute to the destruction of the hydrocarbon potential in the kerogen by crosslink reactions.

Therefore, two types of hydrogen transfer reactions can be considered prior to aromatization reactions (which occur later in the maturation profile): 1) the polars+water interactions through oxidation-reduction reactions 2) the radical hydrogen transfer between hydronaphthalenics and the organic system.

Both systems are certainly active during maturation and are in competition, one taking advantage of the other depending on the composition of the medium. This composition is dependant either on the maturation stage (as in the reference series) or on the modifications induced by the chemical treatment during the EC, EP, ECO and EPO series.

ACKNOWLEDGEMENTS The authors wish to thank Elf EP for financial support, TOTAL and M. D. Lewan for providing the Mahakam and Woodford samples respectively.

REFERENCES

- 1 Landais P., Michels R. and Poty B. (1989) J. of Anal. and Appl. pyrolysis, 16, 103-115.
- 2 Mansuy L. and Landais P. (1995) Energy Fuels, 9, 809-821.
- 3 Mansuy L., Landais P. and Ruau O (1995) Energy Fuels, 9, 691-703.
- 4 Michels R., Langlois E., Ruau O., Mansuy L., Elie M., and Landais P. (1996). Energy Fuels, 10, 39-48.

TABLES AND FIGURES

TABLE I: ROCK-EVAL Tmax (°C) for the chloroform extracted residual kerogen obtained after confined pyrolysis of Woodford kerogen and Mahakam coal. CP: reference series EC: chloroform extracted series EP: pentane extracted series ECO: chloroform extracted series with addition of water EPO: pentane extracted series with addition of water.

	WOODFORD KEROGEN					MAHAKAM COAL				
	CP	EC	ECO	EP	EPO	CP	EC	ECO	EP	EPO
Raw	422					418				
260	-	440	440	439	439	-	-	-	-	-
278	432	444	-	441	441	437	439	437	437	437
300	436	449	450	445	445	444	446	445	455	449
323	-	-	-	-	-	451	463	455	544	453
330	445	461	456	455	456	454	538	486	553	455
346	-	564	550	540	464	-	-	-	-	-
350	496	-	560	-	-	457	564	542	574	521
358	-	580	-	560	553	-	-	-	-	-
365	521	-	-	-	-	514	582	556	579	531
375	-	580	585	573	569	561	-	-	-	-
400	541	-	-	-	-	579	-	-	-	-

FIGURE 1: Bitumen yields obtained after confined pyrolysis of Mahakam coal and Woodford kerogen. Pyrolysis series as in Table I. The yields are cumulative for the EC, EP, ECO and EPO series. The yields are not cumulated for the reference series (CP), however, they are intrinsic cumulative values (see text).

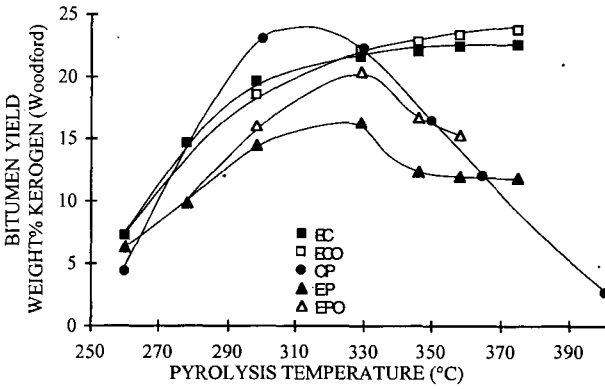
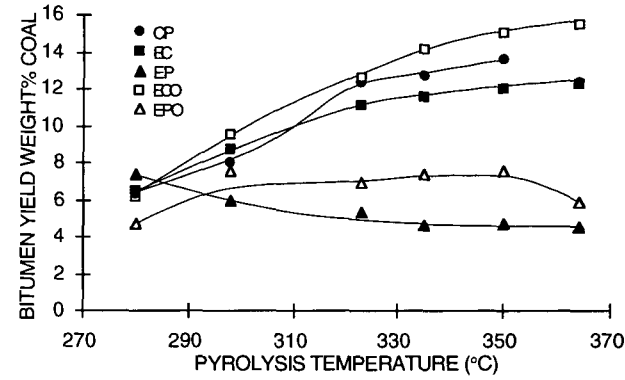
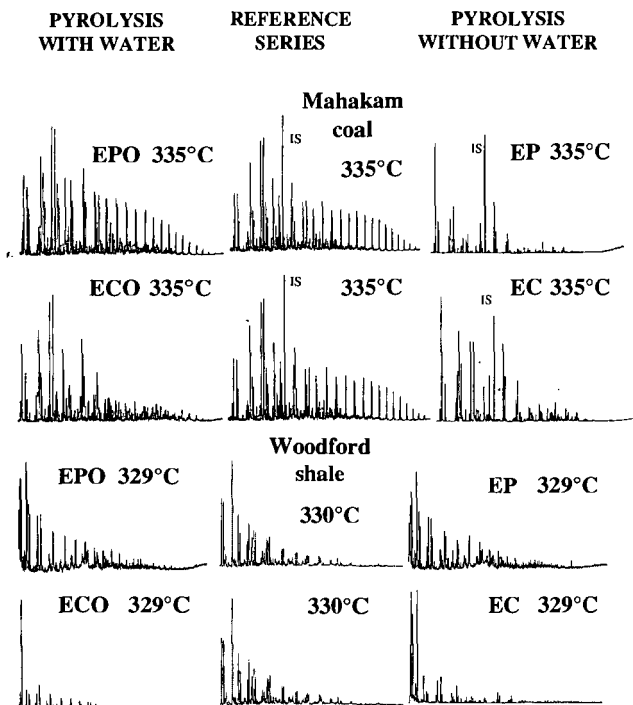


FIGURE II: PyGCMS chromatograms of the chloroform extracted kerogens obtained after confined pyrolysis at 335°C (Mahakam coal) and 330°C (Woodford kerogen). EC, EP, ECO, EPO as in text. IS: internal standard



THE EFFECT OF SUPERCRITICAL WATER ON VITRINITE REFLECTANCE AS OBSERVED IN CONTACT METAMORPHISM AND PYROLYSIS EXPERIMENTS

Charles E. Barker and M.D. Lewan, U.S. Geological Survey, Box 25046, Denver, Colorado, USA.

Introduction

Natural thermal maturation of sedimentary organic matter (SOM), which includes both coal and dispersed organic matter, increases with heating. In particular, dike contact metamorphic zones are widely studied because within the narrow sampling range near the dike, SOM composition changes little along a well-exposed sample plane while thermal maturation increases markedly as temperature increases from ambient to as high as 700°C (Bostick, 1979; Clayton and Bostick, 1986; Bishop and Abbott, 1994; Galushkin, 1997, and Barker et al., 1998; among others). These studies indicate contact metamorphism typically increases thermal maturity as measured by vitrinite reflectance, Rock-Eval parameters, as well as affecting SOM, petroleum and biomarker compositions. In this study, mean vitrinite reflectance in oil (mean or maximum parameter both annotated as R_0 for this general discussion) is used because it is widely reported in dike studies as an index of heating relative to petroleum generation (i.e., the thermal maturation process). R_0 is a physical measure of the degree of aromaticity in the SOM. During thermal maturation, the degree of aromaticity in vitrinite increases with the continuing condensation of aromatic clusters (van Krevelen, 1981; Wilson, 1987).

Given the change in host-rock temperature from ambient to those produced by contact with a magma, a surprising aspect of these studies is that R_0 does not always continue to increase as a dike is closely approached. Next to some dikes R_0 increase is retarded or R_0 may even decrease. This is true whether R_0 is measured next to dikes as discussed above or next to sills as well as whether maximum or random reflectance of vitrinite is measured (Raymond and Murchison, 1989). Fluid inclusion evidence indicates that the zone of retarded or reduced R_0 roughly corresponds to a zone where water vapor or supercritical-water phases evolve during contact metamorphism by the dike (Barker, 1995). In particular, the limited range of physical and chemical conditions that lead to the evolution of supercritical fluids may explain the retarded or reduced R_0 found near dikes. The development of water vapor is thought less important because it typically forms during contact metamorphism (Jaeger, 1959; Delaney, 1982; 1987) at the shallow to moderate crustal depths prevalent in sedimentary basins and its effects should be widely expressed next to dikes. Although there are other possible causes of retarded or reduced R_0 near dike contacts, the purpose of this paper is to investigate the effect of supercritical water on thermal maturation by hydrous pyrolysis experiments.

Contact Metamorphism

The sample selected for hydrous pyrolysis study is a bituminous coal (mean random $R_0 = 0.6\%$), taken from a site not locally affected by contact metamorphism even though from an area where a mid-Cretaceous age dike swarm intrudes the Upper Jurassic-Lower Cretaceous Strzelecki Group, western onshore Gippsland Basin, Victoria, Australia. This sample was collected about 50 meters below the surface in the State coal mine near Wonthaggi, Victoria. The Strzelecki Group banded coals contain mostly normal vitrinite (i.e., not suppressible by the definition of Barker et al., 1996). Thermal history reconstruction suggests that at the time of dike swarm intrusion the host rock was at a temperature of 100-135°C while fracture-bound fluid inclusions in the host rocks next to thin dikes (< 3.4 m thick) suggest temperature increases to at least 450°C at the dike contact (Fig. 1). Burial history reconstruction indicates that when intrusion occurred the host rocks were near two km depth and at about 20 MPa pressure using a fresh water hydrostatic gradient (Barker et al., 1998). Fresh water boils at about 300°C at this depth. The critical point of fresh water is near 374°C, 22 MPa. Thus, the temperature and pressure near the dike contact, along with the low to moderate salinity fluids (Barker, 1995) are conditions close to those required for the development of water vapor or supercritical fluids (Roedder, 1984; Bodnar and Vityk, 1994).

Pyrolysis Experiments

The development of supercritical fluids next to these dikes was simulated by heating aliquots of the Strzelecki Group coal in closed-system experiments using pyrolysis techniques developed by Lewan (1993) and a small stainless steel reactor described by Barker et al. (1996). The initial series of pyrolysis experiments was held at temperatures of 300°C, 330°C, 365°C and 380°C for 72 hours. The 380°C experiment was then run again for 24 hours. Experiments at 365°C or lower temperature were designed to keep liquid water in contact with the sample. Experiments at 380°C introduced supercritical water to the sample.

These experiments showed an increase in vitrinite reflectance as long as pyrolysis temperatures were held to subcritical liquid-water conditions. The runs at 380°C, with supercritical-water conditions in contact with the sample, showed a reduced R_0 (Fig. 2). Increasing time from 24 to 72 hours at 380°C produced a further reduction in R_0 .

Discussion

During contact metamorphism R_0 increase sometimes is retarded or even reduced close to the dike contact, even though fluid inclusion homogenization data indicates that temperatures were still increasing. Fluid inclusion evidence also indicates that the evolution of water vapor or supercritical

water in the rock pores roughly corresponds to the zone where R_0 is retarded or reduced. This relationship infers that the generation of water vapor or supercritical water near the dike contact may change vitrinite evolution reactions. The limited range of conditions in sedimentary basins that allow supercritical fluids to exist may explain why a retarded or reduced R_0 is not always observed near dikes. Because water vapor and supercritical water have a limited range of occurrence in sedimentary basins, there may be other causes of retarded or reduced R_0 next to dikes. Some of these causes are hydrothermal overpressuring next to the dike, catalytic effects, advection, convection, groundwater flow across the dike, and the presence of suppressible SOM.

The physical and chemical basis for a retarded R_0 with increasing temperature remains speculative. For example, is it that condensation reactions in SOM are inhibited causing a retardation of R_0 or is condensation destroyed causing a reduction of R_0 . What is known is that within the zone of retarded or reduced R_0 , molecular disorder is increasing (Khavari-Khorasani et al., 1990); and the fraction of aromatic carbon increases and then may fluctuate (Barker, 1995). Further, as the dike is approached, ^{13}C CP MAS nuclear magnetic resonance (NMR) data suggest that phenol and carbonyl contents initially decrease but that there is slight increase in phenol and carbonyl content in the zone of retarded R_0 (Barker, 1995). Along with these changes, the total organic carbon (TOC) content is lowered (Degens, 1965; Barker, 1995). The loss in TOC as the dike is approached is partially attributable to petroleum generation and migration as shown by a corresponding decrease in Rock-Eval hydrogen index (HI) and S_1 (Fig. 3). Next to some dikes, HI and the oxygen index (OI) may both stop decreasing or start to increase in the zone where R_0 increase is retarded. This change in HI and OI may be caused by the addition of phenol and carbonyl radicals to the residual SOM. These geochemical data suggest that in the presence of water vapor or supercritical water, hydrogen and oxygen are being introduced into the coal during reactions like those observed in liquid-water pyrolysis experiments (Stalker et al., 1994; Lewan, 1997).

A fraction of the TOC, however, also appears to directly react with the pore water and is in part mobilized as CO_2 (Lewan, 1992; Price, 1994). Given the exceptional solubility of SOM in supercritical fluids, SOM may be directly dissolved in the supercritical water (Lewan, 1993). The strong loss of TOC indicates the presence of a supercritical fluid rather than a vapor phase. SOM is thought to have a far lower solubility in a water vapor. A mesh-like porous structure observed in the Strzelecki Group vitrinite after supercritical pyrolysis also may be a reflection of a selective dissolution process.

Conclusions

1. The evidence suggests several reaction mechanisms producing a reduction or a retardation of condensation in SOM caused by the development of water vapor or supercritical water: a) After high temperature condensation reactions, the substitution of oxygen- and hydrogen-bearing radicals destroy aromatic carbon bonds in the highly condensed SOM; b) further condensation of the SOM may be retarded by the early reaction of phenolic and carbonyl radicals with the aromatic carbon clusters in a less mature vitrinite; and c) simultaneous thermal maturation and dissolution of the condensed structures at the surface of the vitrinite leaving residual SOM with a retarded aromaticity.
2. Experimental, geochemical and petrographic evidence indicate direct SOM reactions with water are a major factor during contact metamorphism near the dike contact.
3. The atypical occurrence of retarded R_0 near dike contacts is attributed to the limited range of physical conditions and pore-water chemistry under which supercritical water can exist in sedimentary basins.
4. Because water vapor and supercritical fluids have a limited range of occurrence, there may be other causes of retarded or reduced R_0 next to dikes in sedimentary basins.

References

- Barker, C.E., 1995, Physical and chemical conditions of organic metamorphism next to selected dikes, Victoria, Australia. Ph.D. thesis, University of Adelaide, 293 p. + appendices.
- Barker, C.E. and Pawlewicz, M.J., 1994. Calculation of vitrinite reflectance from thermal histories and peak temperature: a comparison of methods, in P.K. Mukhopadhyay and W.G. Dow (Editors), Vitrinite Reflectance as a Maturity Parameter. Am. Chem. Soc. Symp. Series no. 570, p. 216-229.
- Barker, C.E., Lewan, M.D., and Pawlewicz, M.J., 1996, A simple hydrous pyrolysis technique to detect suppressed vitrinite reflectance: Abstracts and Program, The Soc. for Org. Petrol., v. 13, p. 36-38.
- Barker, C.E., Bone, Y. and Lewan, M.D., 1998, Fluid inclusion and vitrinite reflectance geothermometry compared to heat flow models of maximum paleotemperature next to dikes, western onshore Gippsland Basin, Australia: International J. Coal Geol., v. 37, p. 73-113.
- Bishop, A.N. and Abbott, G.D., 1994, Vitrinite reflectance and molecular geochemistry of Jurassic sediments: the influence of heating by Tertiary dykes (northwest Scotland): Org. Geochem., v. 22, p. 165-177.
- Bodnar, R.J. and Vityk, M.O., 1994, Interpretation of microthermometric data for $\text{H}_2\text{O-NaCl}$ fluid inclusions, in De Vito, B. and Frezzotti, M.L., eds., Fluid Inclusions in Minerals: methods and applications: Short Course, International Mineralogical Association Working Group "Inclusions in Minerals", p. 117-130.
- Bostick, N.H., 1979, Microscopic measurement of the level of catagenesis of solid organic matter in sedimentary rocks to aid exploration for petroleum and to determine former burial temperatures--a review, in Scholle, P. A., and Schluger, P. R., eds., Aspects of Diagenesis: Society of Economic Paleontologists and Mineralogists Special Publication, No. 26, p. 17-44.

- Clayton, J.L., and Bostick, N.H., 1986, Temperature effects on kerogen and molecular and isotopic composition of organic matter in Pierre Shale near an igneous dike: *Org. Geochem.*, v. 10, p. 135-143.
- Degens, E.T., 1965, *Geochemistry of Sediments-A Brief Survey*: Prentice-Hall, New Jersey, 346 p.
- Delaney, P.T., 1982, Rapid intrusion of magma into wet rock: groundwater flow due to pore pressure increases: *J. Geophysical Research*, v. 87, p. 7739-7756.
- Delaney, P.T., 1987, Heat transfer during emplacement and cooling of mafic dykes. In: H.C. Halls and W.F. Fahrig (Editors), *Mafic Dyke Swarms*. Geol. Assoc. of Canada Special Paper 34, pp. 31-46.
- Galushkin, Y.I., 1997, Thermal effects of igneous intrusions of maturity of organic matter: A possible mechanism of intrusion: *Org. Geochem.* v. 26, p. 645-658.
- Khavari-Khorasani, G.K., Murchison, D.G. and Raymond, A.C., 1990, Molecular disordering in natural cokes approaching dyke and sill contacts: *Fuel*, v. 69, p. 1037-1045.
- Jaeger, J.C., 1959, Temperatures outside a cooling intrusive sheet: *Rev. of Geophysics*, v.2, p. 443-466.
- Lewan, M.D., 1992, Water as a source of hydrogen and oxygen in petroleum formation by hydrous pyrolysis: *Am. Chem. Soc., Division of fuel Chemistry*, preprints, vol. 37, no. 4, p. 1643-1649.
- Lewan, M.D., 1993, Laboratory simulation of petroleum formation: hydrous pyrolysis, in, M.H. Engel and S.A. Macko (Editors), *Organic Geochemistry*. Plenum Press, New York, p. 419-442.
- Lewan, M.D., 1997, Experiments on the role of water in petroleum formation: *Geochim. Cosmochim. Acta*, v. 61, p. 3691-3723.
- Price, L. C., 1994, Metamorphic free-for-all. *Nature*, v. 370, p. 253-254.
- Raymond, A.C. and Murchison, D.G., 1989, Organic maturation and its timing in a Carboniferous sequence in the central Midland Valley of Scotland: comparisons with northern England: *Fuel*, v. 68, p. 328-334.
- Roedder, E., 1984, *Fluid Inclusions*: Min. Soc. Am., *Reviews in Mineralogy*, v. 12, 644p.
- Stalker, L., Farrimond P. and Larter, S.R., 1994, Water as an oxygen source for the production of oxygenated compounds (including CO₂ precursors) during kerogen maturation: *Org. Geochem.* v. 22, p. 477-486.
- van Krevelen, D.W., 1981, *Coal*: Elsevier, Amsterdam, 514 p.
- Wilson, M.A., 1987, *NMR Techniques and Applications in Geochemistry and Soil Chemistry*: Pergamon Press, Oxford, 353 p.

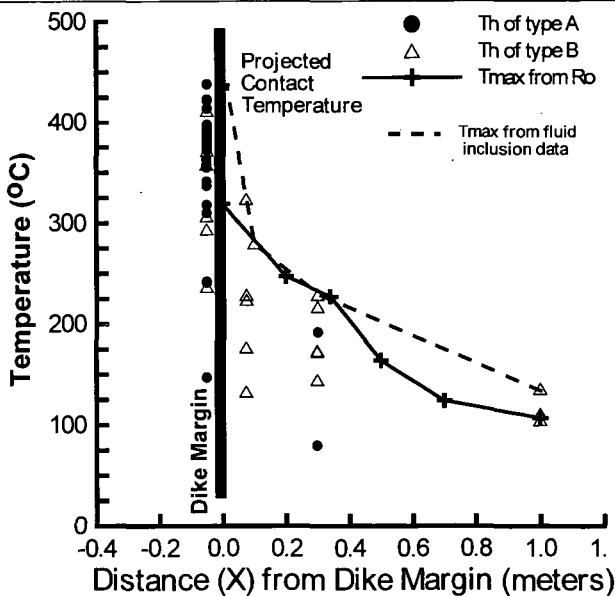


Figure 1. Measurements and calculated maximum host rock temperatures reached next to the 0.6 m thick San Remo-1 dike, western onshore Gippsland Basin, Australia. Figure from Barker (1995). T_h = homogenization temperature of a fluid inclusion. Type A and B refer to types of fracture-bound fluid inclusions. Projected contact temperature is estimated from fluid inclusion measurements on a host rock xenolith partially imbedded in the dike. T_{max} from R_o refers to a temperature estimate made using the hydrothermal geothermometer of Barker and Pawlewicz (1994). A reassessment of the position of the xenolith sample used to determine the projected contact temperature indicates it was taken a few centimeters from the dike contact rather than 20 cm away as reported by Barker (1995).

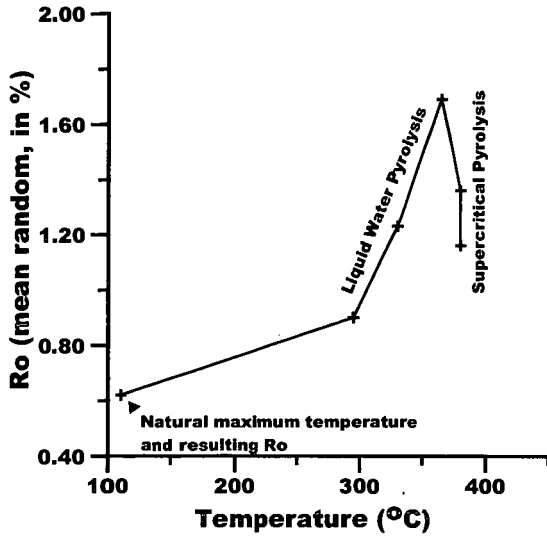


Figure 2. Vitrinite reflectance of Strzelecki Group coal after natural diagenesis, liquid water and supercritical water pyrolysis.

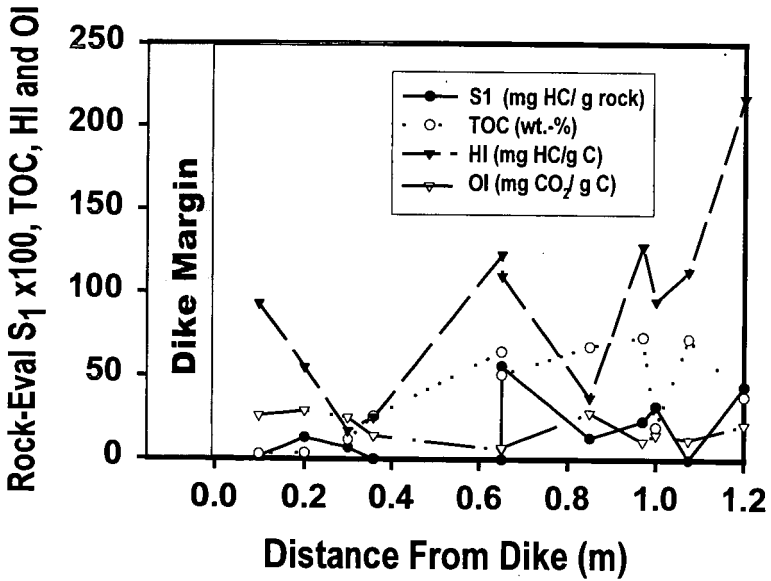


Figure 3. Rock-Eval pyrolysis assay results from coaly rocks in the Strzelecki Group next to the San Remo-1 dike, western onshore Gippsland basin, Australia. Data from Barker (1995)

THERMODYNAMIC CONSTRAINTS ON THE GENERATION AND MATURATION OF PETROLEUM IN SEDIMENTARY BASINS

Harold C. Helgeson, Laurent Richard, William F. McKenzie, and Denis L. Norton
 Department of Geology and Geophysics
 University of California
 Berkeley, CA 94720

KEYWORDS: Hydrolytic disproportionation, oxidation of kerogen, chemical evolution of petroleum

ABSTRACT

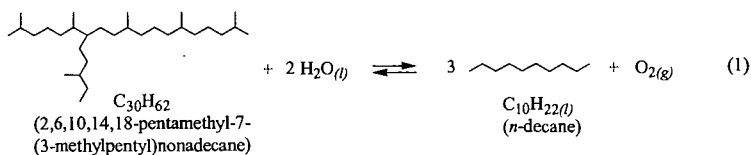
Preliminary Gibbs free energy minimization calculations indicate that high molecular weight compounds in kerogen may be in metastable equilibrium with hydrocarbon species in petroleum during the incongruent partial melting process responsible for the generation and maturation of petroleum, which is accompanied by progressive oxidation of kerogen with increasing depth of burial. It appears that H₂O plays a crucial role in the process, which may be driven by escape from the system of methane as the ultimate product of the irreversible hydrolytic disproportionation of the light paraffins.¹

INTRODUCTION

Although the overall process responsible for the generation of bitumen from kerogen and the chemical evolution of high molecular weight compounds in bitumen to the lower molecular weight species that predominate in petroleum is irreversible (Tissot and Welte, 1984; Béhar *et al.*, 1992; Helgeson *et al.*, 1993; Planche, 1996), thermodynamic calculations indicate that metastable equilibrium states probably prevail among liquid hydrocarbon species with carbon numbers $\geq 6-15$ and carbon-bearing aqueous species such as CO₂ and CH₃COOH at the oil-water interface (Helgeson *et al.*, 1993). In addition, it appears from the results of recent calculations that mature kerogen may be in metastable equilibrium with maturing crude oil in hydrocarbon source rocks. Thermodynamic calculations lead to the conclusion that the maturation process may be driven by the extent to which methane escapes from the system as the ultimate product of the irreversible hydrolytic disproportionation of hydrocarbons with carbon numbers $\leq 6-15$. The large chemical affinities of these reactions are an attractive energy source for thermophilic microbes, which may then mediate the maturation process if the system is open at the hydrocarbon-water interface (Helgeson *et al.*, 1993).² It follows that irreversible hydrolytic disproportionation reactions among the light hydrocarbons should perturb to the right reversible reactions representing hydrolytic reduction of the higher molecular weight compounds to form lighter species.

HYDROLYTIC OXIDATION/REDUCTION AND DISPROPORTIONATION REACTIONS

To illustrate the hydrolytic oxidation/reduction process in a maturing source rock, reversible reaction of the highly branched isoprenoid liquid species corresponding to 2,6,10,14,18-pentamethyl-7-(3-methylpentyl)nonadecane (C₃₀H₆₂) in kerogen or bitumen to form a light paraffin species such as liquid decane (C₁₀H_{22(l)}) in petroleum can be described in terms of the overall reaction represented by

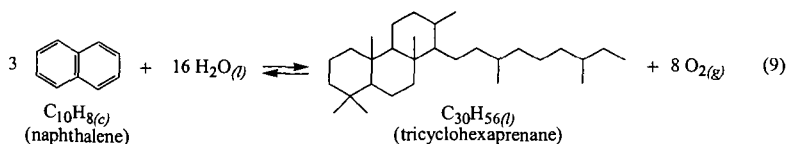
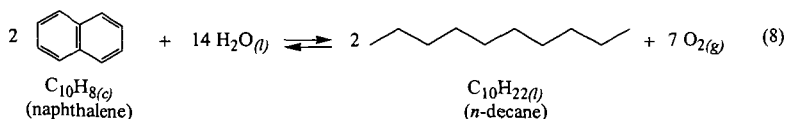
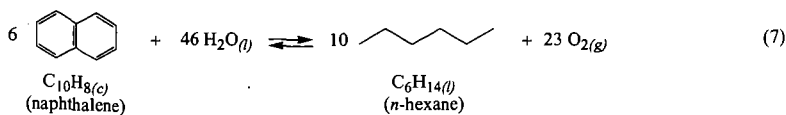


¹ The term hydrolytic disproportionation refers to reaction of a given hydrocarbon with H₂O to form a lighter hydrocarbon and oxidized carbon-bearing species.

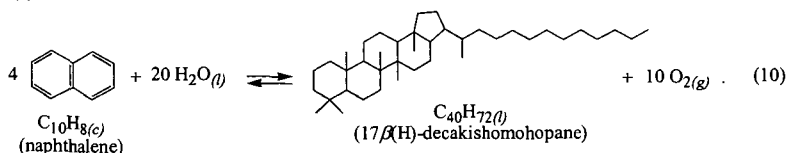
² The chemical affinity of the *r*th irreversible reaction (*A_r*) can be expressed as $A_r = 2.303RT \log(K_r / Q_r)$, where *A_r* stands for the chemical affinity of the *r*th reaction, *R* refers to the gas constant, *K_r* represents the equilibrium constant for the reaction, and *Q_r* designates the activity quotient for the subscripted reaction, which is given by

$$Q_r = \prod_i a_i^{\hat{n}_{i,r}}$$

where *a_i* denotes the activity of the *i*th species in the system and $\hat{n}_{i,r}$ stands for the reaction coefficient of the *i*th species in the *r*th reaction, which is positive for products and negative for reactants. Although *K_r* is computed from the standard molal thermodynamic properties of the species in the reaction, *Q_r* is evaluated from compositional data. Hence, if $Q_r = K_r$, *A_r* = 0 and the reaction is reversible. Otherwise, $A_r d\xi_r > 0$ where ξ_r stands for the progress variable for the *r*th reaction.



and



The logarithmic analogs of the law of mass action for these reactions can be written for unit activity of crystalline naphthalene as

$$\log a_{\text{C}_6\text{H}_{14}(l)} = (\log K_{(7)} - 23 \log f_{\text{O}_2(a)}) / 10 \quad (11)$$

$$\log a_{\text{C}_{10}\text{H}_{22}(l)} = (\log K_{(8)} - 7 \log f_{\text{O}_2(a)}) / 2 \quad (12)$$

$$\log a_{\text{C}_{30}\text{H}_{56}(l)} = \log K_{(9)} - 8 \log f_{\text{O}_2(a)} \quad (13)$$

and

$$\log a_{\text{C}_{40}\text{H}_{72}(l)} = \log K_{(10)} - 10 \log f_{\text{O}_2(a)} \quad (14)$$

where $K_{(7)}$, $K_{(8)}$, $K_{(9)}$, and $K_{(10)}$ stand for the equilibrium constants for the subscripted reactions. Equations (10)-(14) represent the curves shown in Fig. 2, where it can be seen that the curves in each of the four diagrams cross each other over narrow temperature intervals at log activity values which are slightly below zero. It follows that the liquid hydrocarbons represented by these curves can coexist with appreciable concentrations in a single liquid phase in metastable equilibrium with crystalline naphthalene at the temperatures and fugacities of oxygen corresponding to those of the curve-crossings in Fig. 2. A $\log f_{\text{O}_2(a)}$ - temperature profile consistent with this observation is depicted in Fig. 3, where it can be compared with the profile in the hydrocarbon reservoirs of the Texas Gulf Coast (Helgeson *et al.*, 1993). It can be seen in Fig. 3 that the two curves are separated by only 2 log units or $\sim 10^\circ\text{C}$.

Calculated changes in speciation are depicted in Fig. 4 for maturation of the hypothetical hydrocarbon liquid represented by the curve-crossings in Fig. 2 and the upper temperature - $\log f_{\text{O}_2(a)}$ profile in Fig. 3. The curves shown in this figure were generated from Eqns. (11)-(14) and the relation $\sum_i X_i = 1$ (where X_i stands for the mole fraction of the i th species in the liquid) assuming in a first approximation ideal mixing of the four hydrocarbon species in the hypothetical liquid.³ It can be deduced from Fig. 4 that increasing burial of naphthalene in kerogen coexisting with this liquid along the upper temperature - $\log f_{\text{O}_2(a)}$ profile in Fig. 3 would be accompanied by "maturation" of the liquid from ~ 90 mole percent tricyclohexaprenane ($\text{C}_{30}\text{H}_{56}(l)$) and 17 β (H)-decakishomohopane ($\text{C}_{40}\text{H}_{72}(l)$) at low temperatures to ~ 80 mole percent *n*-hexane ($\text{C}_6\text{H}_{14}(l)$) and *n*-decane ($\text{C}_{10}\text{H}_{22}(l)$) at 125°C . Preliminary calculations indicate that similar, but much more complex behavior can be expected in actual bitumen and

³ The mole fraction of the i th hydrocarbon species (X_i) in bitumen or petroleum is related to its activity (a_i) by $X_i = a_i / \lambda_i$

where λ_i stands for the rational activity coefficient of the subscripted species, which is unity in the case of ideal mixing.

petroleum during burial of hydrocarbon source rocks along profiles like those depicted in Fig. 1. Although the incongruent partial melting of kerogen in source rocks may not occur to an appreciable extent at low temperatures, the metastable equilibrium calculations represented by the curves shown in Figs. 2, 3, and 4 indicate that the incongruent partial melting of kerogen species and the maturation process are simultaneous interrelated processes.

CONCLUSIONS

The fact that the curves in each of the diagrams in Fig. 2 cross each other over narrow temperature ranges is a consequence of the actuality that hydrocarbon species are members of closely related homologous series. However, the observation that they cross each other at log activities corresponding to appreciable concentrations at geologically reasonable values of $\log f_{O_2(a)}$ and temperature is a manifestation of the physical, chemical, and thermodynamic reality of metastable equilibrium states among many (but not all) hydrocarbon species in kerogen, bitumen and petroleum in the Earth. Under these circumstances, if hundreds of curves were drawn in Fig. 2 representing reversible hydrolytic reduction reactions for the multitude of hydrocarbon species found in bitumen and petroleum, all of them would be expected to cross in approximately the same narrow temperature - $\log f_{O_2(a)}$ interval shown in Fig. 3. A similar result would be expected for metastable equilibrium among these species in the liquid phase and other hydrocarbon compounds in kerogen. Gibbs free energy minimization calculations are currently being carried out to explore the extent to which these metastable equilibrium states may obtain in hydrocarbon source rocks. Preliminary results of these calculations indicate that oxidized kerogen may coexist in metastable equilibrium with crude oil in source rocks during progressive burial and maturation of the oil. Furthermore, the maturation process may persist at temperatures in excess of 200°C. Because the composition and speciation of both the kerogen and maturing oil generated in the Gibbs free energy minimization calculations are consistent with geologic reality, it appears that the process is not controlled by chemical kinetics, but instead by the thermal gradient, rate of burial, availability of H₂O, and the degree to which methane can escape from the system.

ACKNOWLEDGEMENTS

The research described above was supported by the United States Department of Energy (DOE Grant DE-FG03-85ER-13419) and the National Science Foundation (NSF Grants EAR 8606052, EAR 9117395, and EAR 9613753), together with funds received from the donors of the Petroleum Research Fund, administered by the American Chemical Society (ACS-PRF Grants 23026-AC2, 26237-AC2, and 28550-AC2), and the Committee on Research at the University of California, Berkeley. Support was also contributed in the form of a postdoctoral grant to Laurent Richard by Elf Aquitaine Production. We are indebted to Leigh Price, Jan Amend, Christine Owens, Allen Young, and Everett Shock for helpful discussions during this research.

REFERENCES

- Béhar, F.; Kressmann, S.; Rudkiewicz, J.-L.; Vandenbroucke, M. *Org. Geochem.* **1992**, *19*, 173.
- Helgeson, H.C.; Knox, A.M.; Owens, C.E.; Shock, E.L. *Geochim. Cosmochim. Acta* **1993**, *57*, 3295.
- Helgeson, H.C.; Owens, C.E.; Knox, A.M.; Richard, L. *Geochim. Cosmochim. Acta* **1998**, *62*, 985.
- Planche, H. *Geochim. Cosmochim. Acta* **1996**, *60*, 447.
- Richard, L.; Helgeson, H.C. *Geochim. Cosmochim. Acta* **1998** (in press).
- Tissot, B.P.; Welte, D.H. *Petroleum Formation and Occurrence*; Springer-Verlag: Berlin, 1984.

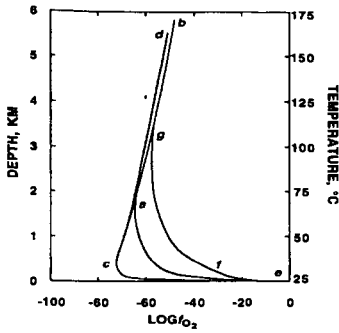


Fig.1 Temperature - $\log f_{O_{2(l)}}$ - depth profiles in hydrocarbon source rocks and reservoirs (see text). The profiles were generated for a nominal temperature gradient of 25°C/km. Curves *ea* and *ec* represent idealized profiles drawn to connect curves *ab* and *cd* at *a* and *c*, respectively, with atmospheric $f_{O_{2(a)}}$ at 25°C. Curve *efg* is a hypothetical profile representing more oxidized conditions at greater depths than those along *ea* and *ec*. Curves *cab* and *cad* are consistent with the temperature - $\log f_{O_{2(l)}}$ profiles in hydrocarbon reservoirs calculated by Helgeson *et al.* (1993).

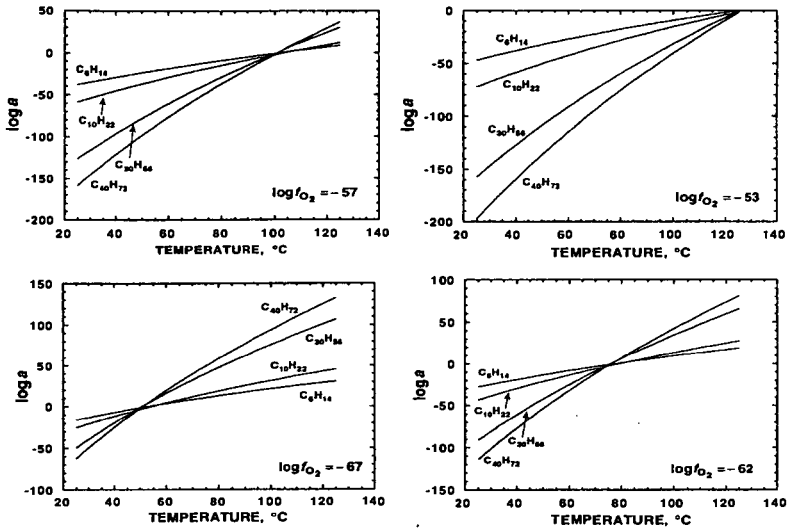


Fig.2 Graphic representation of Eqns. (11) - (14) as a function of temperature at constant pressure and $\log f_{O_{2(l)}}$ (see text).

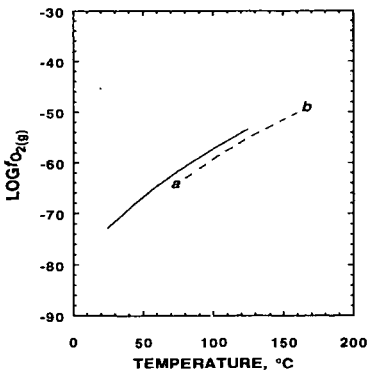


Fig. 3 Temperature - $\log f_{O_{2(l)}}$ profile consistent with the curve-crossings in Fig. 2 (upper curve) and profile *ab* in hydrocarbon reservoirs in the Texas Gulf Coast taken from Helgeson *et al.* (1993).

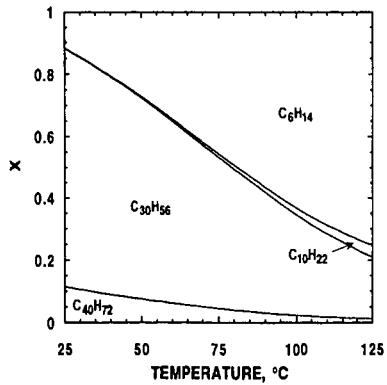


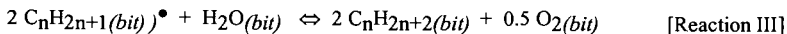
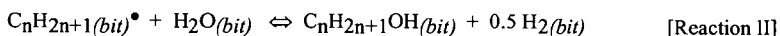
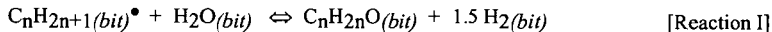
Fig. 4 Mole fraction (*X*) - temperature maturation diagram for the hypothetical hydrocarbon liquid represented by the upper curve in Fig. 3 coexisting with naphthalene in kerogen (see text).

THEMODYNAMICS OF REACTIONS INVOLVING H₂O AND HYDROCARBON RADICALS BETWEEN 27 AND 374°C

Michael D. Lewan
U. S. Geological Survey
Box 25046, MS 977
Denver Federal Center
Denver, CO 80225

Hydrous pyrolysis experiments at temperatures between 300 and 360°C for 72 hours have shown that H₂O is a source of oxygen and hydrogen in the generation of oil from petroleum source rocks. Oxygen mass-balance calculations indicate that the only source of the calculated excess oxygen in the form of CO₂ is H₂O (Lewan, 1992; Seewald, 1994). Experiments with D₂O instead of H₂O show that generated hydrocarbons are highly deuterated (Hoering, 1984), which is interpreted as being the result of D₂O-derived deuterium quenching free-radical sites as the organic matter in a petroleum source rock thermally decomposes (Lewan, 1997).

Hydrous pyrolysis experiments are typically conducted with crushed gravel-sized (0.5 to 2.0 cm) source rock, which is heated in contact with liquid H₂O at subcritical temperatures (<374°C). Initially, the maturing source rock gravel is impregnated with polar-rich bitumen that partially decomposes with increasing thermal stress to yield an expelled saturate-rich oil. As demonstrated by Lewan (1997), the reaction of H₂O with the organic matter occurs within the hydrophobic bitumen-impregnated rock and not in the liquid H₂O that surrounds the rock gravel. Therefore, the reaction involves dissolved H₂O in the bitumen of the rock and not aqueous organic species in the surrounding liquid water. It has been proposed that the H₂O dissolved in the bitumen (H₂O_(bit)) of a source rock reacts with free radical sites to generate aldehydes, alcohols, alkanes, hydrogen, or oxygen. The model reactions include the following:

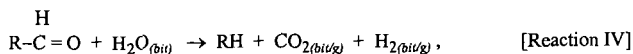


Although it is uncertain whether these model reactions have kinetic energy barriers to overcome, the first concern is whether they are thermodynamically possible within the experimental conditions. Unfortunately, thermodynamic data on alkyl radicals, H₂O, and the proposed products in a bituminous phase are not currently available. However, a first approximation of the thermodynamic feasibility of these model reactions can be obtained by considering the reactions in a gaseous phase for which thermodynamic data are available.

Gibbs free energies for these reactions in the gaseous phase where $n = 2$ were calculated from tabulated standard-state (25°C at 100 kPa) heat capacities given by Benson (1976) and Gurvich et al. (1994) for temperatures between 27 and 374°C. As shown in Figure 1, the resulting Gibbs free energy of reaction between 0 and 400°C at 100 kPa for Reactions I, II, and III are -10.5 to -13.5 kcal/mol, -18.8 to -11.9 kcal/mol, and -27.3 to -17.8 kcal/mol, respectively. These negative values indicate that the model reactions for $n = 2$ are thermodynamically favorable in this temperature range at hydrogen or oxygen fugacities of 100 kPa or less.

Reaction I involves oxygen from a water molecule reacting with an unpaired electron at an alkyl radical site to form an aldehyde and hydrogen. The hydrogen would be available to react with other free radical sites and the aldehyde would react with other water molecules to form a carboxylic acid and through subsequent decarboxylation form CO₂. Each molecule of water that reacts with a free radical site by this reaction,

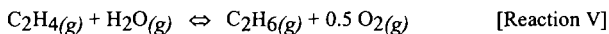
generates three atoms of hydrogen that can terminate or initiate additional free radical sites. A subsequent reaction of the resulting aldehyde with other water molecules yields two additional hydrogen atoms by the reaction



where R is an alkyl or aryl group in macromolecules of the organic matter. The interaction of water with carbonyl groups has been suggested to be responsible for increased CO₂ yields associated with the weathering of coal in water vapor at low temperatures (150°C; Peitt, 1991) and the noncatalytic liquefaction of water-treated coals at 350°C (Song et al., 1994). As a result, reactions I and IV may collectively generate 5 water-derived hydrogen atoms for every water-derived oxygen that reacts with a free radical site.

Alcohols have not been reported in the products of hydrous pyrolysis experiments as prescribed by reaction II. However, Stalker et al. (1994) have reported the generation of phenols from water-derived oxygen in H₂¹⁸O-experiments with kerogen at 300°C after 72 hours. Smith et al. (1989) observed that hydrous pyrolysis of n-octadecanol in the presence of coal completely reacts to form n-alkanes at 330°C after 72 hours. Therefore, it is reasonable to tentatively suggest that alcohols derived from reaction II may be ephemeral intermediates in the formation of alkanes.

Reaction III is the most thermodynamically favorable reaction of the three model reactions. Molecular oxygen generated from this reaction would be highly reactive and prone to generate or terminate other free-radical sites. Eventually, this oxygen would occur as a carbonyl, carboxyl, or CO₂ through a series of subsequent reactions. The significance of the thermodynamic favorability of reaction III is demonstrated by comparing its low Gibbs energy of reaction with that of the thermodynamically unfavorable reaction of H₂O with ethene to form an ethane (Figure 1):



It is not the intent of this discussion to suggest that reactions I, II, and III are specific reactions that occur in petroleum formation, but rather they simply serve to demonstrate that reactions between alkyl free-radical sites and water in gaseous phases are thermodynamically favorable between 27 and 374°C at 100 kPa. A more specific thermodynamic evaluation of the feasibility of these model reactions requires obtaining thermodynamic parameters on H₂O as a dissolved species in bitumen or oil solvents. Once these parameters have been determined, the competition between H₂O_(bit) and H₂(bit) for alkyl free-radical sites can be properly assessed.

REFERENCES CITED

- Benson, S. W., 1976, *Thermochemical Kinetics*, John Wiley & Sons, New York.
- Gurvich, L. V., Iorish, V. S., Yungman, V. S., and Dorofeeva, O. V., 1994, Thermodynamic properties as a function of temperature, in Lide, D. R., ed., *CRC Handbook of Chemistry and Physics*, 75 th Edition, CRC Press, Boca Raton, Section 5, p. 48-71.
- Hoering, T. C., 1984, Thermal reactions of kerogen with added water, heavy water and pure organic substances: *Organic Geochemistry*, v. 5, p. 267-278.
- Lewan, M. D., 1992, Water as a source of hydrogen and oxygen in petroleum formation by hydrous pyrolysis: *ACS, Div. Fuel Chemistry Preprints*, v.37, No. 4, pp. 1643-1649.
- Lewan, M. D., 1997, Experiments on the role of water in petroleum formation: *Geochimica et Cosmochimica Acta*, v. 61, p. 3691-3723.

- Peitt, J. C., 1991, A comprehensive study of the water vapour/coal system: application to the role of water in the weathering of coal: *Fuel*, v. 70, pp. 1053-1058.
- Seewald, J. S., 1994, Evidence for metastable equilibrium between hydrocarbons under hydrothermal conditions: *Nature*, v. 370, p. 285-287.
- Smith, J. W., Batts, B. D., and Gilbert, T. D., 1989, Hydrous pyrolysis of model compounds: *Organic Geochemistry*, v. 14, pp. 365-373.
- Song, C., Saini, A. K., and Schobert, H. H., 1994, Effects of drying and oxidation of Wyodak subbituminous coal on its thermal and catalytic liquefaction. Spectroscopic characterization and product distribution: *Energy & Fuels*, v. 8, pp. 301-312.
- Stalker, L., Farrimond, P., and Larter, S. R., 1994, Water as an oxygen source for the production of oxygenated compounds (including CO₂ presursors) during kerogen maturation: *Organic Geochemistry*, v. 22, nos. 3-5, p. 477-486.

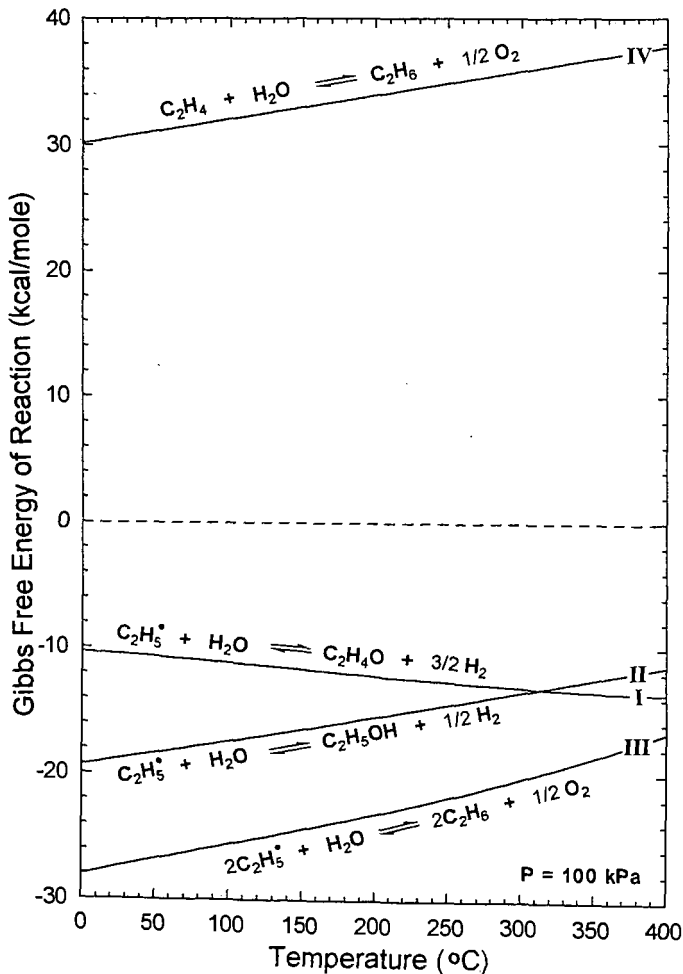


Figure 1. Gibbs free energy of reaction for model reactions I, II, III, and IV for various temperatures at 100 kPa.